Terms and Conditions of Use of Digitised Theses from Trinity College Library Dublin

Copyright statement

All material supplied by Trinity College Library is protected by copyright (under the Copyright and Related Rights Act, 2000 as amended) and other relevant Intellectual Property Rights. By accessing and using a Digitised Thesis from Trinity College Library you acknowledge that all Intellectual Property Rights in any Works supplied are the sole and exclusive property of the copyright and/or other IPR holder. Specific copyright holders may not be explicitly identified. Use of materials from other sources within a thesis should not be construed as a claim over them.

A non-exclusive, non-transferable licence is hereby granted to those using or reproducing, in whole or in part, the material for valid purposes, providing the copyright owners are acknowledged using the normal conventions. Where specific permission to use material is required, this is identified and such permission must be sought from the copyright holder or agency cited.

Liability statement

By using a Digitised Thesis, I accept that Trinity College Dublin bears no legal responsibility for the accuracy, legality or comprehensiveness of materials contained within the thesis, and that Trinity College Dublin accepts no liability for indirect, consequential, or incidental, damages or losses arising from use of the thesis for whatever reason. Information located in a thesis may be subject to specific use constraints, details of which may not be explicitly described. It is the responsibility of potential and actual users to be aware of such constraints and to abide by them. By making use of material from a digitised thesis, you accept these copyright and disclaimer provisions. Where it is brought to the attention of Trinity College Library that there may be a breach of copyright or other restraint, it is the policy to withdraw or take down access to a thesis while the issue is being resolved.

Access Agreement

By using a Digitised Thesis from Trinity College Library you are bound by the following Terms & Conditions. Please read them carefully.

I have read and I understand the following statement: All material supplied via a Digitised Thesis from Trinity College Library is protected by copyright and other intellectual property rights, and duplication or sale of all or part of any of a thesis is not permitted, except that material may be duplicated by you for your research use or for educational purposes in electronic or print form providing the copyright owners are acknowledged using the normal conventions. You must obtain permission for any other use. Electronic or print copies may not be offered, whether for sale or otherwise to anyone. This copy has been supplied on the understanding that it is copyright material and that no quotation from the thesis may be published without proper acknowledgement.

The Role of S1P Receptors and their Interacting Proteins in Krabbe Disease

Thesis submitted for the degree of Doctorate of Philosophy at the University of Dublin, Trinity College

Catherine O'Sullivan
2015

Supervisor: Prof. Kumlesh Dev
Molecular Neuropharmacology,
Department of Physiology, School of Medicine,
Trinity College Dublin, Ireland

Declaration and Statement of Plagiarism

I declare that this thesis has not been submitted as an exercise for a degree at this or any other university and it is entirely my own work.

I agree to deposit this thesis in the University's open access institutional repository or allow the library to do so on my behalf, subject to Irish Copyright Legislation and Trinity College Library conditions of use and acknowledgement.

Date

3.05.16

Acknowledgements

I am very grateful to my supervisor, Prof. Kumlesh Dev, for his continuous support and much valued advice and guidance. I am particularly grateful for his hands on approach in the lab and appreciate the time spent writing papers. Many thanks to Solange Vidal from Novartis Institutes for Biomedical Sciences, Basel, Switzerland for providing the S1PR1 and PEX14-v5 constructs. I would also like to thank the current and former lab members who provided advice and experimental support: Dr. Adam Pritchard, Dr. Ola Rutkowska and Sinead O'Sullivan.

My gratitude goes to my funding body, PRTLI, for enabling me to carry out this research and to the PRTLI course co-ordinators for organising many useful workshops and journal clubs.

Finally, I would also like to thank my friends and family, in particular the PRTLI PhD gang, David Tiernan and my mother. Without her unwavering believe and high expectations I would not be where I am today.

Table of Contents

List of Figures & Tables

Chapter 4. The dual S1PR1/5 drug BAF312 (Siponimod) attenutes psychosine induced demyelination in organotypic slice cultures.

Chapter 5. Discovery of novel S1PR interacting proteins.

Chapter 6. Discussion

Appendices

List of Abbreviations

AC	Adenylate Cyclase
BBB	Blood brain barrier
BSA	Bovine serum albumin
cAMP	Cyclic adenosine monophosphate
CNS	Central Nervous System
CSF	Cerebrospinal fluid
DMSO	Dimethyl sulfoxide
EAE	Experimental autoimmune encephalomyelitis
EDG-1	Endothelial differentiation gene-1
EDTA	Ethylenediaminetetraacetic acid
EGTA	Ethyleneglycoltetraacetic acid
ERK	Extracellular-signal-regulated kinase
FBS	Fetal bovine serum
GFAP	Glial fibrillary acidic protein
GPCR	G protein coupled receptor
HEK	Human embryonic kidney
KD	Krabbe disease
LPC	Lysophosphatidylcholine
LPS	Lipopolysaccharide
LPA	Lysophosphatidic acid
MAPK	Mitogen activated protein kinase
MBP	Myelin basic protein
MOG	Myelin oligodendrocyte glycoprotein
MS	Multiple sclerosis
MSC	Mesenchymal stem cell
NPC	Neural precursor cells
NSC	Neuronal stem cells
OPC	Oligodendrocyte precursor cell
pFTY720	Phosphorylated FTY720
Pi3K	Phosphoinositide 3-kinase
PKC	Protein kinase C
PLC	Phospholipase C
PLP	Proteolipid protein
S1P	Sphingosine 1-phosphate
S1PR	Sphingosine 1-phosphate receptor
SphK	Sphingosine kinase
TNFα	Tumour necrosis factor alpha

Scientific Abstract

Globoid cell leukodystrophy (Krabbe disease, KD) is a rare autosomal recessive neurodegenerative disorder that presents within the first six months of life and is usually fatal by the age of two years. KD is caused by a deficiency in the lysosomal enzyme galactocerebrosidase (GALC), which results in the accumulation of the toxic metabolite psychosine in the brain. Here we investigated the ability of psychosine to directly induce hallmarks of KD, in vitro, focusing on increased levels of glial cell death, mitochondrial dysfunction, pro-inflammatory cytokines and demyelination. Importantly we also demonstrate reversal of these effects by the sphingosine 1-phosphate receptor (S1PR) agonist pFTY720 (Fingolimod) (**Results 1**). We additionally investigated effects of an S1PR1/S1PR5 agonist called BAF312 on psychosine-induced toxicity in isolated astrocyte and microglia cultures as well as in slice culture models of demyelination. Treatment of human and mouse astrocytes with this S1PR1/S1PR5 dual agonist modulated pERK, pAKT and Ca^{2+} signaling pathways as well as inducing S1PR1 internalization. In organotypic slice cultures, BAF312 reduced LPC-induced levels of IL6, and more importantly attenuated LPC-mediated demyelination. In addition, BAF312 attenuated psychosine-induced demyelination (**Results 2**). Finally we aimed to identify novel S1PR1 interacting proteins, with the purpose to further understand S1PR1 trafficking and internalization, and perhaps identify novel methods to regulate S1PR1. Here, we report a previously unknown interaction between the peroxisomal matrix protein Pex14 and the intracellular loop (ICL) 3 and C-terminus (CT) of S1PR1. While the function of this Pex14/S1PR1 interaction remains elusive, we find that Pex14 did not block S1PR1 internalisation in HEK293 or astrocyte cells nor does it affect S1PR1 modulation of cytokine release or pERK and pAKT signaling (**Results 3**). Overall, this current study suggests that pFTY720 and BAF312 can modulate glial cell function and attenuate demyelination, highlighting S1PRs as potential drug targets for the devastating childhood illness KD.

Lay Abstract

There are four main cell types in the brain: (i) nerve cells, which process information via electrical signals, (ii) oligodendrocytes, which form the insulating layer (myelin) around nerve cells, (iii) microglia, which provide immune defence in the brain and (iv) astrocytes that communicate with other cells, provide support and ensure proper nerve cell functioning. Krabbe Disease (KD) is a disorder of the brain that affects children within the first three to six months of life and is usually fatal by the age of two years. Currently there is no cure for this disease. KD is caused by a deficiency in an enzyme, which leads to the build-up of a toxic compound called psychosine. Psychosine is damaging to the brain and causes the oligodendrocyte cells to die. A drug used to treat Multiple sclerosis (MS) called Gilenya (pFTY720) can act on brain cells to protect them from damage in MS. In this study we used drugs like Gilenya and showed they were beneficial in the treatment of KD. We used cultures of astrocytes and brain slices from mice to investigate the damaging effects of psychosine and the protective effects of pFTY720 and BAF312. From this we demonstrate that psychosine can cause astrocyte cell death and demyelination (damage to the insulating myelin layer that surrounds the axon of a neuron). Importantly, pFTY720 and BAF312 protected against this damage.

Brain cells, and all living cells, have a large number of proteins on their surface called receptors. Receptors are activated by specific molecules which result in a message being sent to other cells that can have a wide range of effects. Many drugs have been developed that bind to and activate particular receptors. Gilenya binds to receptors called sphingosine-1 phosphate receptors (S1PRs) and can have a therapeutic effect in MS patients. In this study we further investigated the function of the S1PR1 and discovered that this receptor binds to a protein called Pex14.

Hypothesis and Aims

We hypothesise that inflammation and astrocyte damage contributes to the demyelinating phenotype of Krabbe disease, and SIPR agonists will therefore, by reducing inflammation and protecting astrocytes, be therapeutic.

The aims of the study to investigate this hypothesis are as follows:

1. To generate cell culture and cerebellar slice cultures of Krabbe disease based on psychosine exposure and to use these to;
    - investigate the effect of psychosine on astrocyte survival and to demonstrate the protective effect of pFTY720.
    - study the effect of psychosine on pro-inflammatory cytokine levels in mouse astrocytes.
    - investigate the effect of psychosine on myelination state in cerebellar slices and explore the protective effects of pFTY720.

2. To demonstrate that SIPR agonists activate pro-survival signaling pathways and are protective of astrocytes and myelin by;
    - investigating the effect of the S1PR1/5 agonist, BAF312, on ERK and AKT phosphorylation in human and mouse astrocytes.
    - determine whether the S1PR1/5 selective agonist, BAF312, induces Ca^{2+} signalling and internalisation of the S1PR1 in human astrocytes.
    - determine if BAF312 is protective against LPC and psychosine induced demyelination.

3. To investigate if the putative interacting protein, PEX14, plays a role in SIPR signalling and/or trafficking by;
    - Investigating the site of interaction of Pex14 on the S1PR1
    - Determine if Pex14 alters S1PR1 trafficking +/- pFTY720
    - Determine if Pex14 overexpression influences pFTY720 modulation of LPS-induced cytokine release.

Value of Research

The pleiotropic mediator, S1P, plays a role in many physiological and pathophysiological processes within the immune, cardiovascular and central nervous systems. Understanding of the structure of the S1PR1 subtype has benefited in designing new specific agonists and antagonists. The uses of such selective compounds will likely help to further elucidate the role of S1PRs in normal and disease states. In particular, the S1PR modulator, pFTY720 (Gilenya®), has received a great deal of attention as it is currently used as a therapy for relapsing remitting MS. However, it is thought that this drug may be beneficial in a number of diseases that exhibit a range of neuroinflammatory and neurodegenerative features. Therefore, investigating this S1P/S1PR signalling pathway in a demyelinating disorder such as KD could prove therapeutically worthwhile. In addition, elucidation and understanding of the interaction of S1PR1 with its putative interacting proteins may provide additional strategies for the development of novel therapeutic agents.

Outputs

Papers

O'Sullivan C. and Dev. K.K. The dual S1PR1/S1PR5 drug BAF312 (Siponimod) attenuates psychosine induced demyelination in organotypic slice cultures Journal of Neuroinflammation *(accepted)*

O'Sullivan C. and Dev K.K. Galactosylsphingosine (psychosine) induced demyelination is attenuated by sphingosine 1-phosphate signalling. 2015, Journal of Cell Science *(accepted)*

O'Sullivan C. and Dev.K.K. The structure and function of the S1P1 receptor. 2013, Trends in Pharmacological Sciences, 34, 401-412

Kelly RJ, Minoque AM., Lyons A, Jones RS, Browne TC, Costello DA, Denieffe S, **O'Sullivan C,** Connor TJ, Lynch MA. Glial Activation in AβPP/PS1 Mice is Associated with Infiltration of IFNγ-producing Cells. 2013. Journal of Alzheimers Disease. 37(1), 63-75.

Kilbride SM, Gluchowska SA, Telford JE, **O'Sullivan C**, Davey GP. 2011. High-level inhibition of mitochondrial complexes III and IV is required to increase glutamate release from the nerve terminal.6(1)

Invited Talks

O'Sullivan C. and Dev. K.K. Psychosine induced demyelination is attenuated by sphingosine 1 phosphate signalling. Frontiers in Neurology Ireland Conference Nov. 2015.

Presented Posters

O'Sullivan C. and Dev. K.K. Psychosine induced demyelination is attenuated by sphingosine 1 phosphate signalling. Glia Conference, Bilbao Spain, Jul. 2015.

O'Sullivan C. and Dev. K.K. Activation of S1P receptors attenuates psychosine-induced demyelination and astrocyte dysfunction**,** Frontiers in Neurology Ireland Conference Nov. 2014.

O'Sullivan C. and Dev. K.K. Psychosine-induced astrocyte cell deficits are attenuated by S1P receptor activation, 9th FENS Forum of Neuroscience, Jul. 2014.

O'Sullivan C. and Dev. K.K. S1P receptor activation attenuates psychosine-induced astrocyte cell death, Astrocytes in Health and Neurodegenerative Disease, University College London Apr. 2014.

O'Sullivan C. and Dev. K.K. The protective effects of S1P receptor activation on psychosine-induced astrocyte cell death, Neuroscience Ireland UCC Sept. 2013.

O'Sullivan C. and Dev. K.K S1P receptor activation attenuates psychosine-induced astrocyte cell death**,** Postgraduate Research Day, TCD Nov. 2013.

O'Sullivan C. and Dev. K.K. Psychosine-induced astrocyte cell deficits are attenuated by S1P receptor activation: possible implications for Krabbe Disease. Young Life Scientist Symposium, UCC Sept. 2013.

O'Sullivan C. and Dev. K.K. Molecular mechanisms governing S1PR1 trafficking in astrocytes. School of Medicine Postgraduate Research day, TCD, Dec. 2012.

O'Sullivan C., Denieffe S., Lynch M**.** Investigation of the effects of Aβ peptide on microglial activation states. Neuroscience Ireland, RCSI Sept. 2012.

O'Sullivan C., Denieffe S., Lynch M. Characterisation of microglial activation states in the presence of Aβ peptide. 2nd Annual Meeting Block-MS, May 2012.

Awards

Best poster prize: 4th Annual Meeting Frontiers in Neurology Ireland, Dublin Ireland, Nov 2014 (350EUR).

FENS/IBRO travel grant: 9th FENS Forum of Neuroscience in Milan Italy, July 2014 (750EUR).

Biochemical Society Student Bursary: to attend Astrocytes in Health and Neurodegenerative Disease conference in London Apr 2014 (300GBP).

Trinity Travel Grant: Astrocytes in Health and Neurodegenerative Disease Conference London (295EUR).

Chapter 1. Introduction

1. Introduction to Sphingosine 1-phosphate receptors

1.1 G-protein coupled receptors

Cellular activity is regulated by a plethora of plasma membrane receptors which recognise, decode and transduce extracellular signals into intracellular messages. G protein coupled receptors (GPCRs) represent the largest family of signal transduction molecules with over 800 unique members **(Pham et al., 2008)**. These receptors can interact with a diverse range of bioactive molecules, including amino acids, lipids, peptides, proteins and nucleotides. Thus, this family of proteins regulates a myriad of essential biological processes such as cell growth, differentiation, metabolism, defence, secretion and neurotransmission. Of the 13,779 proteins whose functions have been predicted, 616 (>4%) are members of the rhodopsin, secretin or metabotropic glutamate receptor class of GPCR **(Venter et al., 2001)**. With such crucial roles in almost every aspect of cell physiology, it is no surprise that over 50% of drugs and a huge number of drug candidates still under development, target GPCRs **(Zhu and Li, 2012)**. The overwhelming potential of GPCR ligands as therapeutics highlights the important need to accurately characterise GPCR structure, functions and pharmacology. Bovine rhodopsin (deposited in the Protein Data Bank under the identifier 1F88), was the first highly resolved GPCR to be experimentally characterized and has since been used as the primary template in GPCR model development **(Zhu and Li, 2012)**.

Thanks to homology models, mutagenesis data and low resolution structural studies, various characteristic features common to GPCRs have been identified **(Zhang et al., 2006)**. A common feature for GPCRs is the seven hydrophobic transmembrane α-helices (TM1-TM7), which span the lipid bilayer creating a polar internal tunnel **(Hanson et al., 2012)**. In addition, the N-terminus and three interconnecting loops, (ECL1 between helices II and III, ECL2 between helices IV and V, and ECL3 between helices VI and VII), are exposed to the exterior. Moreover, the C-terminus and three interconnecting loops, (ICL1 between helices I and II, ICL2 between helices III and IV, and ICL3 between helices V and VI), are exposed to the interior **(Hanson et al., 2012)**. Different classes/families of GPCRs (from A to F) have been identified through sequence analysis. These include the rhodopsin-like family (class A), the secretin-like family (class B), the metabotropic glutamate and pheromone family (class C), the fungal pheromone receptors (class D), the cAMP receptors (class E) and the frizzled/smoothened family (class F) **(Fanelli and De Benedetti, 2011)**.

Here, we will focus on the structure and function of the family of sphingosine 1-phosphate receptors (S1PRs), in particular S1PR1. The role of S1PRs in autoimmune illnesses has received a great deal of attention since the clinical approval of the drug Fingolimod (Gilenya®). This compound targets S1PRs and has been approved as the first oral therapy for multiple sclerosis (MS) **(Kappos et al., 2006)**. The functional roles of modulating S1PRs by its natural ligand, sphingosine 1-phosphate (S1P), as well as newly designed pharmacological compounds, are also the subject of intense research activity in academic, clinical and pharmaceutical sectors.

1.2 Sphingosine 1-phosphate

Sphingosine 1-phosphate (S1P) is a zwitterionic lysophospholipid that has been implicated as a crucial regulator in many physiological and pathophysiological processes. S1P is derived from the related sphingolipid ceramide, which is itself synthesised either via the actions of

sphingomyelinases in the membrane or via *de novo* pathways initiated in the endoplasmic recticulum (Figure 1.1). Deacylation of ceramide by ceramidase results in release of sphingosine ((2*S*,3*R*,4*E*)-2-amino-4-octadecen-1,3-diol), which is subsequently phosphorylated in an ATP-dependent manner by sphingosine kinases (SphK1 or SphK2) to form S1P **(Podbielska et al., 2011)**. Thus, sphingolipid turnover yields different potent signalling molecules including ceramide and sphingosine, both of which promote cell-cycle arrest and apoptosis. The phosphorylated form, ceramide 1-phosphate, antagonises the pro-apoptotic effects of ceramide, is mitogenic, and promotes inflammation **(Nixon, 2009)**. On the other hand, S1P enhances cell proliferation and has pro-survival, pro-inflammatory, and pro-motility characteristics. Together, these sphingolipids perform a vital balancing act which regulates survival, trafficking and function of many cells **(Nixon, 2009)**. Not surprisingly, therefore, tight control is kept over S1P production. SphKs catalyse formation of its substrate; sphingosine while S1P-phosphatases, three lipid phosphate phosphatases and S1P lyase catalyse its degradation (Figure 1.1) **(Maceyka et al., 2012)**.

1.3 Discovery of Fingolimod

The actions of S1P are primarily mediated via S1P receptors (S1PRs). These receptors are known drug targets for multiple sclerosis, where the oral therapy Gilenya® (Fingolimod, FTY720) has been approved for clinical use **(Kappos et al., 2010)**. This formulation contains fingolimod hydrochloride which is converted *in vivo* to the active metabolite fingolimod-phosphate (pFTY720). After enantiospecific mono-phosphorylation by SphK2, pFTY720 binds with high affinity to S1PRs and results in sequestration of lymphocytes into secondary lymphoid tissues. This sequestration subsequently modulates the recirculation of lymphocytes between blood and lymphoid tissues **(Adachi and Chiba, 2008)**. pFTY720 was first synthesised through structural simplification of ISP-I (a natural immunosuppressive product), leading to discovery of a nonchiral symmetric 2-substitued-2-aminopropane-1,3-diol framework and subsequently, discovery of pFTY720 **(Kiuchi et al., 2000)** (Table 1.1). pFTY720 contains a prochiral quarternary carbon atom bearing two hydroxylmethyl groups (CH_2-OH). Substitution of one CH_2-OH group with an alkyl group (such as methyl) generated a racemate mixture of the pFTY720 analog **(Kiuchi et al., 2000)**. Pharmacological evaluation of each enantiomer revealed a biologically critical role for the pro-(*S*)-CH_2-OH group, in which only the (*S*)-enantiomer of pFTY720 binds all S1PRs (except S1PR2) **(Kiuchi et al., 1998, Albert et al., 2005)**. In contrast, the pro-(*R*)-CH_2-OH group generating the (*R*)-enantiomer appears inactive on S1PRs, however may have chemical and physicochemical important roles in improving the solubility of the molecule **(Adachi and Chiba, 2008, Chiba and Adachi, 2012)**.

Since the development of pFTY720 a number of S1PR agonists and antagonists have been synthesised. The structure and use of these compounds are shown in Table 1.1. Early suggestions, though over simplistic, have proposed the clinical benefits of pFTY720 are attributed to regulation of S1PR1, while side effects of this drug are linked to S1PR3 activation **(Pan et al., 2013, Forrest et al., 2004)**. Thus, as a group, these pharmacological agents have become more selective, with the development of S1PR1 drugs being favoured over S1PR3. The lack of commercially available selective S1PR3 compounds has limited an understanding of how S1PR3 plays a role in the efficacy and side effects of pFTY720. Noteworthy compounds among these structures are those preferably used as tool compounds and those currently in

clinical trials Table 1.2. These include the pharmacological tool compounds AUY954, a selective S1PR1 agonist, and the newly developed S1PR1 antagonist NIBR-0213. Of more importance are the S1PR modulators currently in clinical trials. These include BAF312 (a S1PR1/S1PR5 dual agonist), presently in clinical trials for secondary progressive MS **(Kappos et al., 2014)** and the compound KRP203 (a S1PR1 agonist), in phase II clinical trials for active subacute cutaneous lupus erythematosus. The structure and use of these compounds are shown in Table 1.1.

1.4 The S1PR family and signalling pathways

The first S1PR identified, namely, S1PR1 was discovered in 1990 by the isolation of clones induced by phorbol 12-myristate 13-acetate (PMA) **(Hla and Maciag, 1990)** and later deorphanised in 1998 **(Postma, 1996, Zondag, 1998)**. Since then a total of five S1PRs (S1PR1-5) formally known as endothelial differentiation genes, Edg-1 (S1PR1), -5 (S1PR2), -3 (S1PR3), -6 (S1PR4) and 8 (S1PR5) respectively have been identified **(Yamazaki, 2000, Im et al., 2000, Songzhu et al., 1997, Okamoto et al., 1999).** The Edg family of receptors also includes the lysophosphatidic acid (LPA) receptor family, which comprises Edg 2 (LPA1), Edg 4 (LPA2), and Edg 7 (LPA3). In addition, the orphan receptors OGR1, GPR3, GPR4, GPR6 GPR12 and G2A are also know to share some homology with S1PRs **(Meyer zu Heringdorf and Jakobs, 2007)** (Figure 1.2). The genes encoding S1PR2, 4 and 5 are located on chromosome 19, with S1PR2 and S1PR5 located closely together on 19p13.2. S1PR3 and S1PR1 however, are located at disparate locations from the other three receptors and can be found on chromosomes 9q22.2 and 1p21 respectively **(Rosen et al., 2009)**.

The S1PR1 subtype couples exclusively with the Gi/o alpha subunit of heterotrimeric G proteins and hence inhibits adenylyl cyclase resulting in a reduction in cAMP production (Figure 1.3). The S1PR1 subtype also causes an increase in intracellular calcium concentration, can stimulate the Ras/ERK pathway to enhance proliferation and can activate the PI3K/Akt pathway to inhibit apoptosis. Moreover, this receptor subtype activates the PI3K/Rac pathway to promote cytoskeletal rearrangement and cellular migration **(Hannun and Obeid, 2008)**. Similar to S1PR1s, the S1PR2-R5s couple with Gi/o and can also couple to G12/13 to enhance Rho activation and hence inhibit Rac. The S1PR2 and S1PR3 couple additionally with Gq to activate PLC **(Obinata and Hla, 2012)**. Given that S1PRs couple to a wide range of intracellular signalling pathways, this receptor family can elicit many cellular responses in a temporal and spatial manner that is dependent on the receptor expression pattern, cell type and signalling pathways present (Figure 1.3). The roles of S1PRs in the immune, cardiovascular and central nervous systems have been extensively reviewed in a number of recent articles **(Dev et al., 2008, Hla and Brinkmann, 2011, Mann, 2012, Nixon, 2009, Iwasaki, 2011)**. Briefly, in T cells, S1PRs play a role in the transmigration of T cells and egress from lymphoid tissues. In addition, the activation of S1PRs on endothelial cells tightens the endothelial barrier, further restricting T cell movement. S1PR activation also regulates cytokine release and antibody production from immune cells, which likely too contributes to their role as drug targets in multiple sclerosis **(Hla and Brinkmann, 2011)**. We and others have also shown that S1PRs play roles in (i) astrocyte migration, (ii) oligodendrocytes myelination state and (iii) neurite outgrowth and neurogenesis **(Dev et al., 2008)**.

1.5 S1PR1 internalisation and persistent signalling

The binding of pFTY720 to S1PR1s causes receptor internalisation and is thought to result in either functional antagonism **(Choi et al., 2011)** and/or persistent signalling (Figure 1.4 and 1.5) **(Mullershausen et al., 2009)**. Agonist binding of S1PR1s results in phosphorylation of its serine rich C-terminus and subsequent internalisation via β-arrestin-mediated clathrin coated vesicles. While S1P stimulation mostly results in internalisation and consequent recycling of the S1PR1s back to the membrane (Figure 1.4), binding of pFTY720 to S1PR1s internalises the receptor with subsequent WWP2 (ubiquitin E3 ligase)-dependent polyubiquitinylation and degradation (**Figure 5**) **(Obinata and Hla, 2012, Oo et al., 2007, Oo et al., 2011)**. Interestingly, pFTY720-induced internalised S1PR1s have also been suggested to continue to signal in a process known as persistent S1PR1 signalling **(Mullershausen et al., 2009)**. This persistent signalling induced by treatment of pFTY720 was found to be dependent on the alkyl chain length of the compound. Specifically, the sustained S1PR1 signalling observed in response to pFTY720, as well as the FTY720 analog AFD-R (containing the same alkyl chain length), was reduced when the alkyl chain was shortened by one carbon and eliminated when further shortened by two carbons **(Mullershausen et al., 2009)**. These findings support a hypothesis in which the length of the aliphatic chain is essential in inducing S1PR1 to adopt a distinct conformation when bound to pFTY720, enabling persistent receptor signalling **(Mullershausen et al., 2009)**. To date, it remains unclear how internalisation, degradation and sustained signalling collectively regulate S1PR1 function. In addition, further studies to fully elucidate the molecular mechanism governing S1PR1 internalisation and degradation are still required.

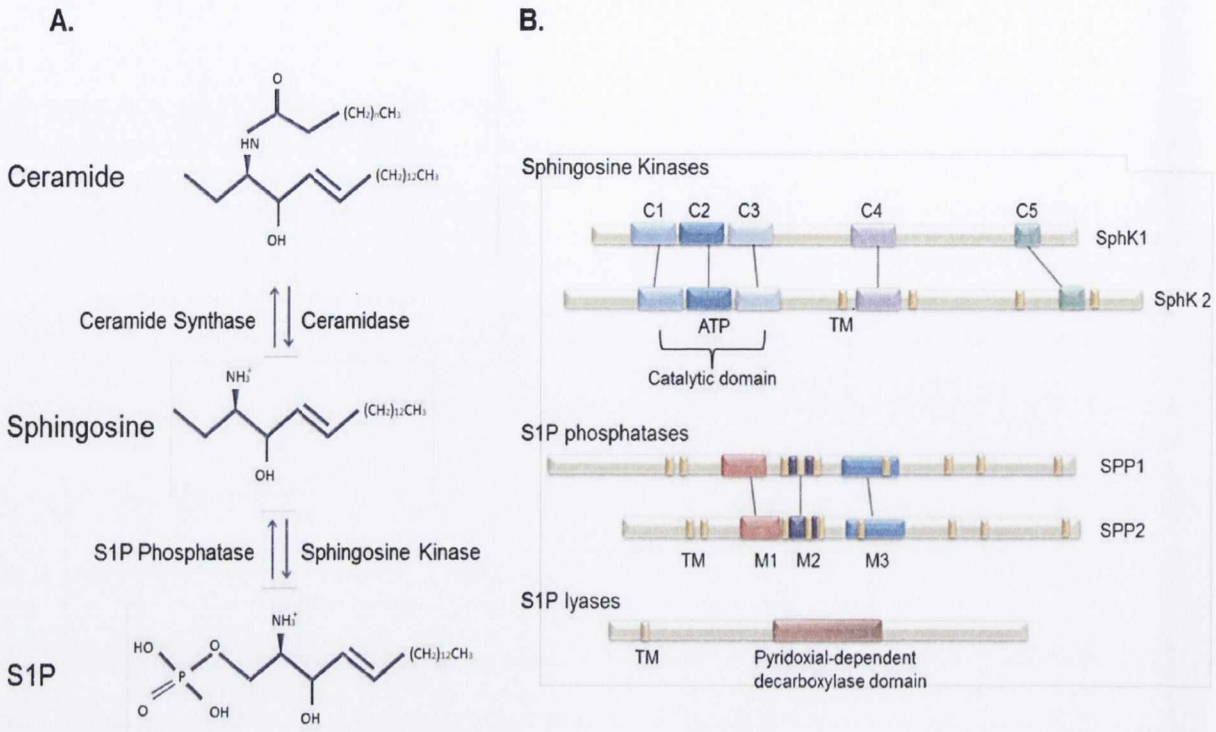

Figure 1.1 S1P synthesis and the S1P-related enzymes. (A). *De novo* synthesis of sphingolipids produces ceramide. *N*-deacetylatation of ceramide yields sphingosine which is converted to S1P via sphingosine kinases. S1P can be recycled to sphingosine and then ceramide by S1P phosphatase and ceramide synthase, respectively. **(B)** SphK1 and SphK2 possess five conserved domains (C1–C5) with a unique catalytic domain contained within C1–C3. The ATP-binding site (SGDGX(17–21)K(R)) is located within C2. There are two mammalian S1P phosphatases; SPP1 and SPP2, all containing three conserved motifs. Both possess similar enzymatic activity but have different expression patterns (SPP1 highest in kidney and placenta, SPP2 highest in brain, lung, heart and small intestine). S1P lyase contains one TM near the N-terminal and a conserved pyridoxal-dependent decarboxylase. **(Spiegel and Milstien, 2003)**. TM transmembrane domain, M1; motif 1, M2; motif 2, M3; motif 3, C; catalytic domain, SphK; sphingosine kinase.

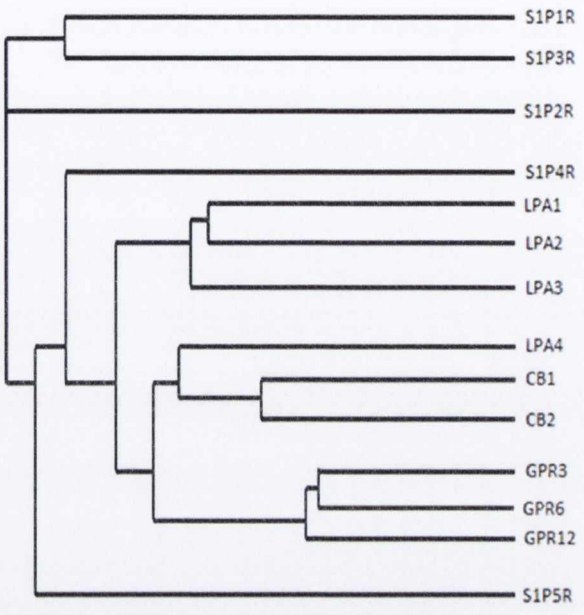

Figure 1.2 Phylogenetic tree of S1PRs. This phylogenetic tree was constructed from protein sequences of human phospholipid receptors. The tree was constructed using ClustalW2 software from http://www.ebi.ac.uk. S1PR; sphingosine-1 phosphate receptor, LPA; lysophospholipid receptor, CB; cannabinoid receptor, GPR; orphan G protein coupled receptor.

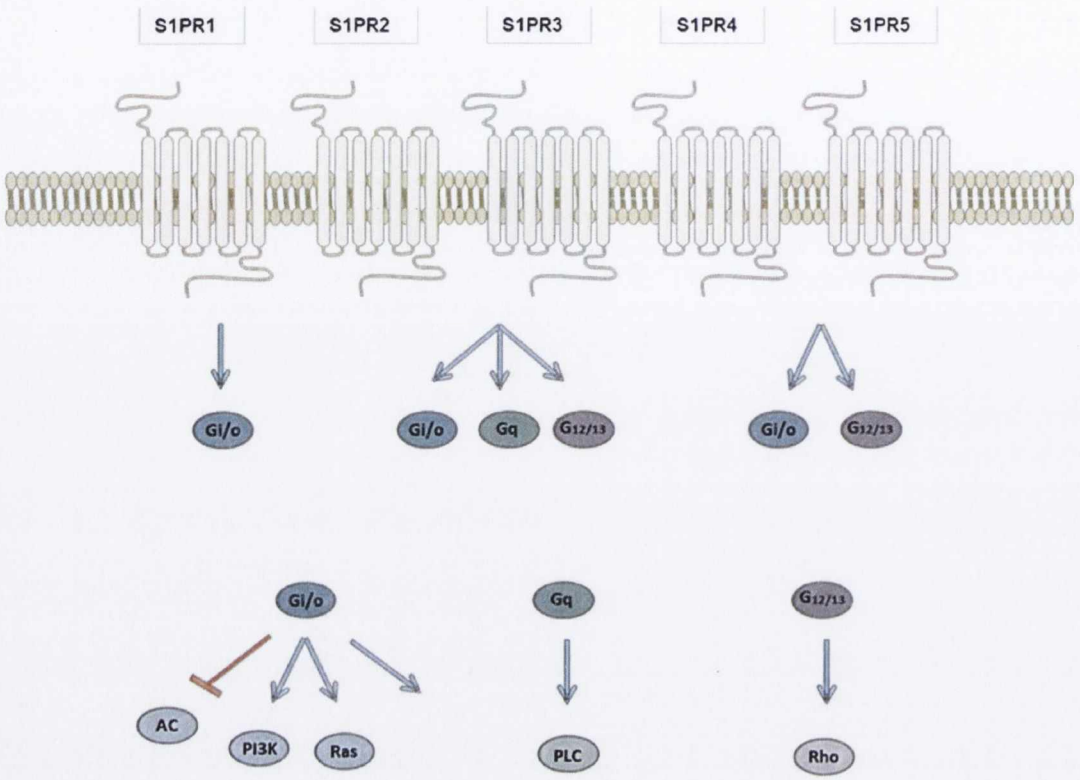

Figure 1.3 S1P Receptor Signalling Pathways. Coupling of S1P receptors with their G proteins and the resultant activation or inhibition of downstream second messengers are illustrated. AC; adenyl cyclase, PI3K; phosphoinositol 3-kinase, PLC; phospholipase C, Gi/o, Gq, $G_{12/13}$; G alpha subunit subtype, Ras, Rho; family of small GTPases.

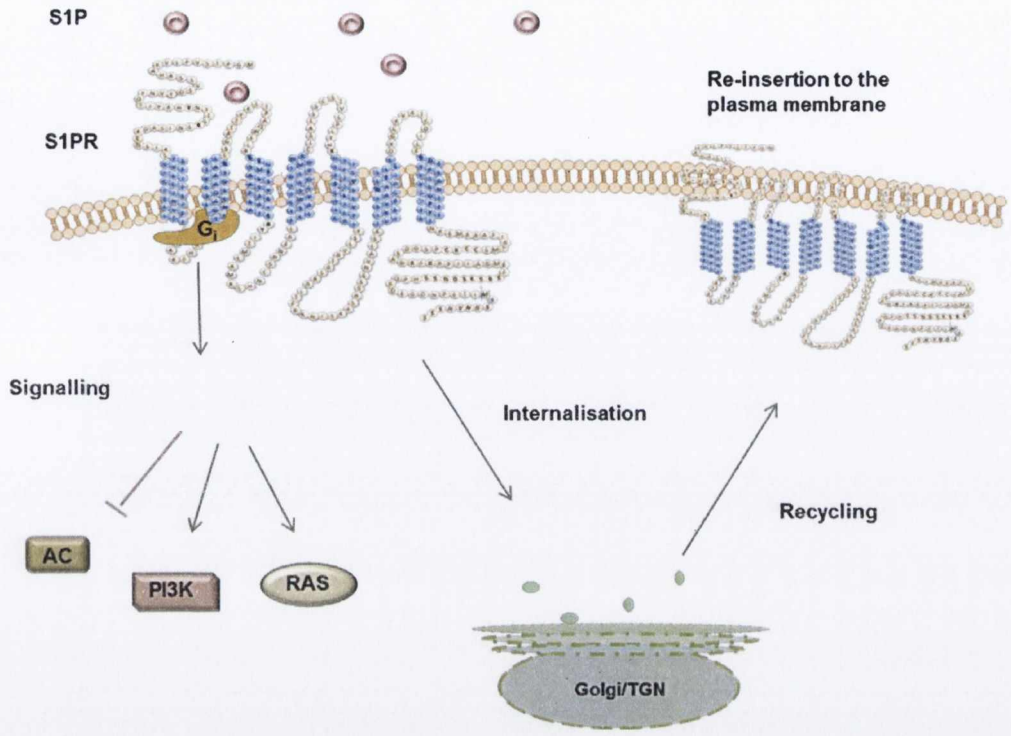

Figure 1.4 Schematic of S1P signalling at S1PR1. Binding of the endogenous ligand S1P to S1PR1 results in signalling via the G_i G-protein, receptor internalisation and consequent recycling of the S1PR1 and insertion back into the membrane. AC; adenyl cyclase, PI3K; phosphoinositol 3-kinase, Ras; family of small GTPases, TGN; trans golgi network.

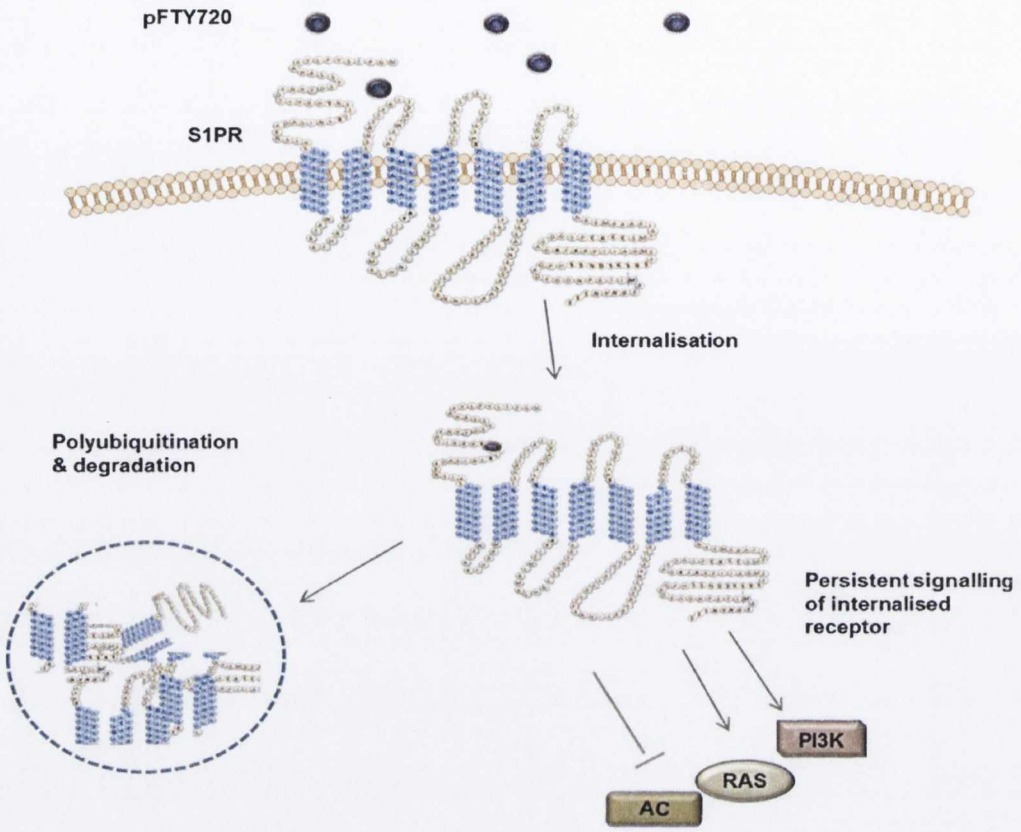

Figure 1.5 Schematic of pFTY720 signalling at S1PR1. Binding of pFTY720 to S1PR1 results in signalling via the G_i G-protein, receptor, internalisation accompanied by persistent internalised signalling, before subsequent WWP2 (ubiquitin E3 ligase)-dependent polyubiquitinylation and degradation. AC; adenyl cyclase, PI3K; phosphoinositol 3-kinase, Ras; family of small GTPases.

Name	Structure	Primarily used as	Refs
S1P	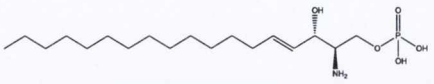	S1PR1-5 Agonist	[1]
pFTY720	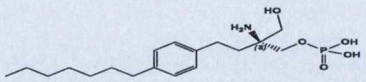	S1PR1,3,4,5 Agonist	[2]
Phosphonate	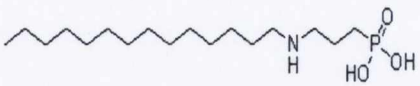	S1PR1,3,4,5 Agonist	[3] [4]
AFD(R)	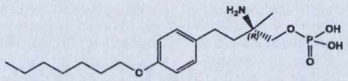	S1PR1 Agonist	[10] [11]
Benzimidazole	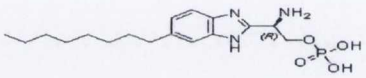	S1PR1,4,5 Agonist	[7] [8]
CYM5442	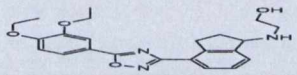	S1PR1 Agonist	[13]
Azetidine	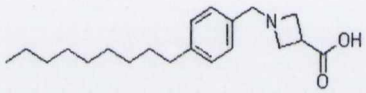	S1PR1, 5 Agonist	[5] [6]
SEW2871	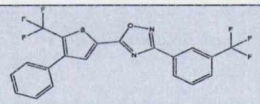	S1PR1 Agonist	[12]
BAF312	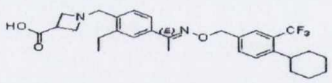	S1PR1, 5 Agonist	[9]
KRP203	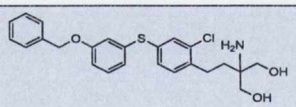	S1PR1 Agonist	[14]

Name	Structure	Primarily used as	Refs
AUY954	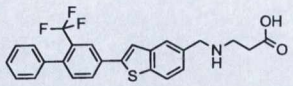	S1PR1 Agonist	[15]
NIBR0213	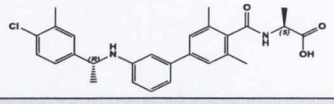	S1PR1 Antagonist	[16]
W146/ML056	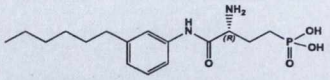	S1PR1 Antagonist	[17]
VPC44116	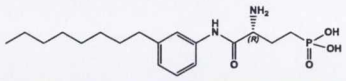	S1PR1 Antagonist	[18] [19], [20]
VPC23019	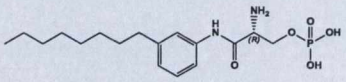	S1PR1, 3 Antagonist	[21]
JTE013	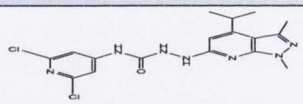	S1PR2 Antagonist	[22] [23]

Table 1.1: S1PR agonists and antagonists.
Please see Appendix 1 for references.

Drug	Target receptor	Clinical Use	ClinicalTrials.gov	Phase/out come
pFTY720 fingolimod	pan S1PR	Relapsing-remitting MS (RRMS)		Approved
		Primary progressive MS	NCT00731692	III
		RRMS with depression & antidepressants	NCT01436643	IV (Terminated)
		Kidney transplant	NCT00099801	III
		inflammatory demyelinating polyradiculoneuropathy	NCT01625182	III
		ALS	NCT01786174	II
		Children with Rett Syndrome	NCT02061137	I/II
		Acute stroke	NCT02002390	II
		Acute demyelinating optic neuritis	NCT01757691	II (Terminated)
		Acute, non-infectious intermediate, posterior and pan-uveitis	NCT01791192	II (Withdrawn)
		Schizophrenia	NCT01779700	II
		pFTY720 with radiation and Temozolomide in high grade glioma	NCT02490930	0
BAF312 Siponimod	S1PR1 & S1PR5	Secondary progressive MS	NCT01665144	III
		Primary progressive MS	NCT000731692	III
		RRMS	NCT01185821	II
		Active dermatomyositis	NCT02029274	II
		Polymyositis	NCT01801917	II
		Hepatic impairments	NCT01565902	I
KRP203	S1PR1	Ulcerative colitis	NCT01375179	II (Terminated)
		Sub-acute cutaneous lupus erythematosus	NCT01294774	II (Terminated)
RPC1063	S1PR1	RRMS	NCT02294058	III
		Ulcerative colitis	NCT02435992	III
ACT-128800 Ponesimod	S1PR1	RRMS	NCT01006265	II
		Plague psoriasis	NCT00852670	II
		Psoriasis	NCT01208090	II
GSK2018682	S1PR1	RRMS	NCT01466322	I

Table 1.2:S1PR modulators in clinical trials.

2 Structure of the S1PR1 Subtype

2.1 Elucidation of the structure of S1PR1

S1PRs are each roughly 400 amino acids in length. The common features for GPCRs include (i) the seven hydrophobic transmembrane α-helices (TM1-TM7), which span the lipid bilayer creating a polar internal tunnel, (ii) the N-terminus and three extracellular loops (ECL1-ECL3) exposed to the exterior and (iii) the C-terminus and three intracellular loops (ICL1-ICL3) exposed to the interior. Early studies have reported homology models of the S1PR1 on the basis of comparisons with the structure of bovine rhodopsin. These models have been refined by manual optimisation of the interhelical network of hydrogen bonds at conserved positions followed by energy minimization **(Parrill et al., 2000)**. From this, the S1PR1 has been observed to possess a similar interhelical hydrogen bonding network to that found in the crystal structure of bovine rhodopsin. Upon energy minimisation, hydrogen bonds connecting the amino acids Asn^{63} to Asp^{91} (TM1 and 2), Asn^{86} to Ser^{134} (TM2 and 3), Asn^{86} to Trp^{168} (TM2 and 4), Asp^{91} to Ser^{304} (TM2 and 7), Ser^{131} to Ser^{304} (TM3 and 7), and Trp^{182} to His^{201} (TM4 and 5), were found to be retained **(Parrill et al., 2000)**. Notably, in this model, the TM6 did not participate in the interhelical network of hydrogen bonds created in the S1PR1 **(Parrill et al., 2000)**. Continuing efforts to identify the structural determinants of S1P binding to the S1PR1 has led to the formulation of a dual site binding model. In this model, interactions between the polar head group of S1P with charged amino acid side chains of the receptor is accredited as one binding site, while interactions between the acyl-chain of S1P with domains in the hydrophobic binding pocket constitutes the other (Figure 1.6 and Figure 1.7) **(Rosen and Goetzl, 2005)**.

More recently, x-ray diffraction data processing methods along with a microdiffraction data assembly method has been used to obtain the crystal structure of S1PR1 complexed with the selective antagonist ML056 (Table 1.1) to a resolution of 2.8Å **(Hanson et al., 2012)**. The S1PR1 was found to share many of the common features characteristic of class A GPCRs including TM1-TM7 helices and the highly conserverd D(E)RY (TM3) and NPXXY (TM7) domains. These domains are known to be important in transformation of the receptor from an inactive to a G protein coupled conformation **(Hanson et al., 2012, Palczewski, 2006)**. Particular features in the receptor structure were noted that where likely due to a highly amphipathic ligand-binding pocket and the hydrophobic-zwitterionic nature of the agonist. Folding of the N-terminus over the receptor was suggested to allow it to contribute to binding interactions, while also limiting access to the binding pocket by forming a helical cap **(Hanson et al., 2012)**. Tight packing of the ECL1 and ECL3 against the N-terminus was also found to occlude access of the ligand to the receptor. This may, in part, explain why ligands of the S1PR1 exhibit slow receptor binding saturation despite excess ligand being present **(Hanson et al., 2012)**. Another key feature noted was the intraloop disulfide bonds within ECL2 and ECL3, which constrain these helices and contribute interactions to the binding pocket. Development of this structural S1PR1 model also uncovered a putative mechanism through which S1P gains entry to the receptor binding pocket. The structural evidence available indicated that ligand binding occurs by initial delivery of S1P to the exterior portion of the cell membrane, subsequent lateral diffusion into the binding pocket and entry between TM1 and TM7 (Figure 1.6 and Figure 1.7) **(Parrill et al., 2012)**.

2.2. The Ligand Binding Site

Analysis of the interaction between S1PRs and the stereoisomers and derivatives of S1P, revealed that D-erytho and dihydro- forms of S1P possess higher affinities than other synthesised stereoisomer forms **(Lim et al., 2004)**. This indicated that the 3D orientations of the C2-amino and C3-hydroxyl groups of S1P are essential for specific binding. Various mutagenesis studies have identified particular amino acids that perform critical roles in ligand recognition, binding and receptor activation. In particular, the three amino acids Arg^{120} (TM3), Glu^{121} (TM3) and Arg^{292} (TM7) of S1PR1 are all required for recognition of S1P (Figure 1.6 and Figure 1.7) **(Hanson et al., 2012, Rosen and Goetzl, 2005)**. It is predicted that the cationic Arg^{120} (TM3) and Arg^{292} (TM7) both bind with the anionic phosphate moiety of S1P, and that the anionic Glu^{121} (TM3) interacts with the S1P protonated amino group, via a salt bridge or hydrogen bond **(Hanson et al., 2012, Rosen and Goetzl, 2005)**. Interestingly, the Glu^{121} (TM3) residue is conserved in the S1PR family and found to be replaced with a glutamine (Gln) in LPA receptors. This Glu-Gln shift has been suggested to account for specificity of S1PRs towards S1P as opposed to LPA **(Wang et al., 2001)**, where it has been shown that mutation of Glu to Gln in the S1PR1 alters specificity from S1P to LPA **(Holdsworth et al., 2004)**. While some discrepancies exist, the Arg^{292} (TM7) residue of the S1PR1 has been suggested to only make direct interactions during agonist binding **(Hanson et al., 2012, Parrill et al., 2012)**. This Arg^{292} (TM7) residue may also serve as a 'cationic lure', coaxing phospholipids towards the receptor **(Parrill et al., 2012)**. Adding to the complexity of S1PR1-ligand interactions, the agonists themselves can be classified into two separate groups depending on their differential receptor interactions. Class I ligands can either be lipid-like compounds such as pFTY720 or non-lipid like molecules that possess polar head groups such as SEW2871, which mimic the sphingophospholipid head group interactions. In contrast, class II ligands such as CYM5442, do not require polar-head group interactions, and it appears that compounds like CYM5442 do not utilise the Arg^{120} (TM3) or Glu^{121} (TM3) residues for binding to the S1PR1 **(Hanson et al., 2012)**. A conserved Trp residue located in TM6 of numerous GPCR's is crucial for ligand induced GPCR activation as well as controlling ligand induced conformational states. In S1PR1, this residue Trp^{269} (TM6), has been shown to contribute to the stabilisation and binding of different S1PR1 ligands (Figure 1.6 and Figure 1.7) **(Parrill et al., 2012)**.

2.3 Hydrophobic Binding Pocket

Theoretical modeling predicts that a number of residues residing in TM3, TM5 and TM6 of the S1PR interact with the hydrophobic tail of S1P **(Fujiwara et al., 2007)**. When compared to the S1PR1, this hydrophobic binding pocket appears most well conserved with S1PR3, moderately with S1PR2 and S1PR4, and least well with the S1PR5 **(Fujiwara et al., 2007)**. The position of the S1P hydrophobic tail has been described as pointing downwards into the intracellular face of the S1PR1 binding pocket formed by the TM helices **(Fujiwara et al., 2007)**. The conformation adopted by the hydrophobic tails of the ligands is suggested to be dependent on the geometric shape of the binding pocket. S1PR1 has a higher affinity for unsaturated ligands which dock into S1PR1 and S1PR5 in an extended conformation **(Fujiwara et al., 2007)**. In contrast, due to a 4Å shorter binding pocket, S1PR4 prefers saturated ligands which bind in a folded conformation **(Pham et al., 2008)**.

The number of strong interactions between the ligand and the complementary sites in S1PR1 determines the binding affinities of the ligand. Ligand potency for S1PR1 have been reported in the order of pFTY720 > S1P > phosphonate > azetidine > SEW2871 (Table 1.1) **(Pham et al., 2008)**. Complementary polar interactions are seen between the nitrogen atoms in Arg^{120} (TM3), Glu^{121} (TM3) and Arg^{292} (TM7) residues of the S1PR1 and fluorine atoms in SEW2871, as well as oxygen atoms in phosphate/carboxylate groups of most other agonists (Figure 1.6 and Figure 1.7). In addition, complementary interactions are measured between the ammonium nitrogen and oxygen atoms of Glu^{121} (TM3), the centroid of the five membered ring of Trp^{182} (TM4) and the centroid of the phenyl ring of Phe^{125} (TM3) **(Pham et al., 2008)**. Ligands such as pFTY720 and S1P have phosphate head groups and hence a -2 charge. Docking studies show these ligands possess strong ion-pair interactions with the positively charged residues in TM3, 5 and 7. In comparison, ligands with a -1 charge (as seen in carboxylate head group containing ligands such as azetidine) display relatively weaker interactions **(Pham et al., 2008)**. Studies also suggest that the binding pocket lengths of S1PR1 and S1PR3 are key determinants of ligand binding selectivity **(Pham et al., 2008)**. Moreover, the Leu^{276} (TM6) in S1PR1 and the Phe^{263} in S1PR3 are reported to play important roles in altering the ligand binding properties of these receptor pockets (Figure 1.6 and Figure 1.7) **(Schurer et al., 2008)**. pFTY720 is known to have a higher affinity than S1P at the S1PR1 subtype. This stronger receptor-ligand interaction is likely due to additional hydrogen bonding between the hydroxyl group of pFTY720 and the oxygen atom at Glu^{121} (TM3) **(Pham et al., 2008)**. Benzimidazole, a heterocyclic aromatic organic compound, activates S1PR1, S1PR4 and S1PR5 but not S1PR2 or S1PR3 (Table 1.1). The receptor selectivity of this ligand is likely due to an interaction between the aromatic rings of benzimidazole and Phe^{125} (TM3) of the S1PRs as well as interactions between the ammonium nitrogen benzimidazole and aromatic rings of Phe^{125} (TM3) and Trp^{269} (TM6). These interactions are substantially weaker in benzimidazole binding of S1PR2 and S1PR3 **(Pham et al., 2008)** .

The tetraaromatic compound SEW2871 has proven to be a useful tool in investigating S1PR1. Significant overlap between the interactions of S1PR1 with this compound and S1PR1 with its endogenous ligand, such as volume and length of hydrophobic interactions, has been noted **(Jo et al., 2005)**. Selectivity of SEW2871 for S1PR1 but not S1PR2-R5 is thought to be, in part, due to the Arg^{292} (TM7) in S1PR1, as this residue is not present in the four remaining receptors. As SEW2871 is chemically unequipped to form salt bridges with the receptor, interactions involving the SEW2871 trifluoromethyl group (CF_3) on ring A are also suggested to be important **(Jo et al., 2005)**. The S1PR1 hydrophobic residues Phe^{125} (TM3), Trp^{269} (TM6) and Phe^{296} (TM7), in addition, make close contact with the aromatic rings of SEW2871, which likely contribute to the potency of SEW2871 at S1PR1 **(Pham et al., 2008)**. Mutational studies in which residues of Arg^{120} (TM3), Glu^{121} (TM3) and Arg^{292} (TM7) were replaced with an alanine revealed a reduction in S1P and SEW2871 triggered phosphorylation of Akt and ERK2. A substitution of CF_3 on ring D of SEW2871 with a methyl group also reduced Akt and ERK2 responses in the alanine mutants, highlighting this as an important functional group for SEW2871 signalling **(Pham et al., 2008)**.

Also important in ligand binding are the residues Tyr^{29} (TM1), Lys^{34} (TM1) and Asn^{101} (TM2), which are involved in binding sphingosine-like head groups (Figure 1.6 and Figure 1.7) **(Hanson et al., 2012)**. The residues Leu^{135} (TM3), Leu^{136} (TM3), Leu^{214} (TM5), Val^{261} (TM6) and Phe^{265}

(TM6) are also reported to make van der Waals contact with each other, as well as, with the alkyl chain of S1P **(Fujiwara et al., 2007)**. In addition, mutational analysis has shown that the Phe^{210} (TM5) residue is important for receptor activation. Residues with particularly important roles in signalling have also been suggested such as Phe^{125} (TM3), Phe^{272} (TM6), and especially Trp^{269} (TM6). The Trp^{269} (TM6) residue is favorably positioned to make edge-to-face interactions with Phe^{265} (TM6). Activation of S1PR1 involves formation of contact between these two residues **(Fujiwara et al., 2007)**.

2.4 S1PR1 interacting proteins

The increased understanding of the structure of S1PR1 has benefited in designing new, more specific agonists and antagonists. Knowledge of the structure and physiochemical properties of this receptor will also be essential in the elucidation of the mechanisms involved in S1PR1 internalisation and trafficking, which are presently unclear. Although not yet determined, it is reasonable to assume that S1PR1 must interact with a range of other proteins, proteins that help the insertion and removal of S1PR1 in the membrane and also scaffolding proteins that stabilise the receptor are just a couple of putative roles these S1PR1 interacting proteins may possess.

The classically accepted form of GPCR signalling in which GPCRs transduce information into intracellular second messengers via the exchange of GDP for GTP on a Gα subunit leading to the dissociation of Gα from Gβγ and subsequent regulation of downstream effectors **(Neer, 1995)** is now no longer the only mechanism of GPCR signal transduction. This classic model is rather oversimplified as GPCRs have now been demonstrated to be able to signal via G-protein independent mechanisms, such as the β-arrestin mediated signalling through Src, mitogen activated kinase (MAPKs), NFκB and PI3K pathways **(Luttrell, 2008, Rajagopal et al., 2010)** and via GPCR interacting proteins **(Bockaert et al., 2004, Kamal et al., 2011)**. The former is believed to mediate cell signalling through the recruitment of GPCR interacting proteins (cytosolic or transmembrane) to the GPCR which now acts as a scaffold. The association of the GPCR interacting proteins with the GPCRs modulates the GPCR function and signal transduction **(Bockaert et al., 2004)**. These interacting proteins can have a variety of effects on the function of GPCRs including important roles in regulating (i) receptor endocytosis (β-arrestins, phospholipase D2, Arf6), (ii) receptor ligand specificity (receptor activity modulating proteins) (iii) receptor recycling (synapse-associated protein 97, (SAP97) and (iv) expression at the cell surface (post-synaptic density protein 95, PSD95) **(Ferguson, 2007, Bockaert et al., 2004, Bhattacharya et al., 2004, Magalhaes et al., 2012)**. GPCR interacting proteins thus have the ability to modulate GPCR localisation and form multiprotein scaffold complexes, referred to as 'signalsomes' in specific intracellular membrane compartments **(Magalhaes et al., 2012)**. Therefore, interaction of S1PR1 with accessory proteins may also have roles in modulating its G-protein coupling, endocytosis, desensitisation and subcellular localisation. Importantly, interaction with these proteins may also have the capacity to form new signal transduction complexes that can alter cellular function **(Magalhaes et al., 2012)**. Full elucidation and understanding of the interaction of S1PR1 with its putative interacting proteins may provide new insights into the pharmacology, signalling and subcellular localisation of the S1PR1. Development of mechanisms to either promote or block this may then also allow for the development of novel therapeutic agents.

The expression of S1PR1s at the plasma membrane is likely controlled by a range of interacting proteins that regulate receptor recycling. In support of this idea, the Rac guanine nucleotide exchange factor, P-Rex1 contains a PDZ (PSD95-disc large-Zonula occludens) domain and has been suggested to interact with S1PR1s **(Li et al., 2005)**. Given that the last 3 residues of the C-terminus of S1PR1 are composed of a triple serine sequence (Figure 1.7) and thus do not represent a typical PDZ motif, the interaction between S1PR1 and P-Rex1 likely employs the use of an internal PDZ motif located intracellularly in S1PR1. Of interest, studies have also shown that the type II transmembrane protein, CD69, directly interacts with TM4 of S1PR1 resulting in internalisation of the receptor and hence inhibition of S1PR1 function **(Bankovich et al., 2010, Cyster and Schwab, 2012)**. Protein-protein interactions among S1PRs forming homodimers and with GPR4, LPA and OGR1 receptors forming heterodimers have also been reported previously **(Zaslavsky et al., 2006)**. It has been suggested that Cys^{184} and Cys^{191} in ECL2 and Cys^{281} and Cys^{286} in ECL3 may play a role in S1PR1 dimersation **(Van Brocklyn et al., 2002)** (Figure 1.7).

2.5 S1PR1 post-translational modifications

A number of post-translational modifications have also been reported for the S1PR1 (Figure 1.7). These have been suggested to regulate ligand binding, internalisation and degradation of S1PR1. For example, the conserved serine rich region located in the C-terminus of S1PR1 is phosphorylated by GRK2 and protein kinase C **(Thangada et al., 2010, Oo et al., 2007)**. Studies have also showed that the E3 ubiquitin ligase WWP2 can polyubiqutinylate multiple lysine residues in the C-terminal tail of S1PR1, including Lys^{330} Lys^{339} Lys^{341} Lys^{354} **(Oo et al., 2011)**. In addition, S1PR1s are palmitoylated at three Cys residues, Cys^{327}, Cys^{328} and Cys^{330} in the cytoplasmic tail **(Ohno et al., 2009)**. Moreover, N-glycosylation of Asp^{30} in the extracellular amino terminal of S1PR1 **(Kohno et al., 2002)** as well as tyrosine O-sulfation of Tyr^{19} and Tyr^{20} in S1PR1 have also been identified **(Fieger et al., 2005)** (Figure 1.7).

2.6. S1PR dimerisation

In recent years, it has become widely accepted that many GPCR's exist as homodimers and/or heterodimers, although the functional importance and ratio of monomeric, homodimeric and heterodimeric receptor forms on the cell surface remain somewhat ambiguous **(Somvanshi and Kumar, 2012)**. Multiple S1PR subtypes are co-expressed on the same cell allowing the possibility of receptor dimerisation, both in homomeric and heteromeric forms **(Van Brocklyn et al., 2002, Zaslavsky et al., 2006)**. The mechanism of S1P homo-dimerization has been noted to most resemble M3 muscarinic receptor dimerisation. It has been suggested that Cys^{184} and Cys^{191} in ECL2 and Cys^{281} and Cys^{286} in ECL3 of S1PR1 may play a role S1PR1 dimersation **(Van Brocklyn et al., 2002)**. Mutation of either the ECL2 or ECL3 pair however did not abolish the ability to dimerise indicating these residues are either not essential in the process or a possible degree of redundancy between these residues exists. The formation of homodimers among S1P receptors and heterodimers between S1P receptors and GPR4, LPA and OGR1 receptors has been previously reported **(Zaslavsky et al., 2006)**. These results imply a crosstalk between S1P and LPA signalling pathways and suggest that one ligand may affect the signalling of several receptor subtypes **(Zaslavsky et al., 2006)**. Although the implications surrounding S1PR homo- and hetero-dimer formation still require much study, dimerisation of GPCR's in general

have proven to be important in ligand affinity, efficacy, specificity of signal transduction and trafficking **(Zaslavsky et al., 2006)**.

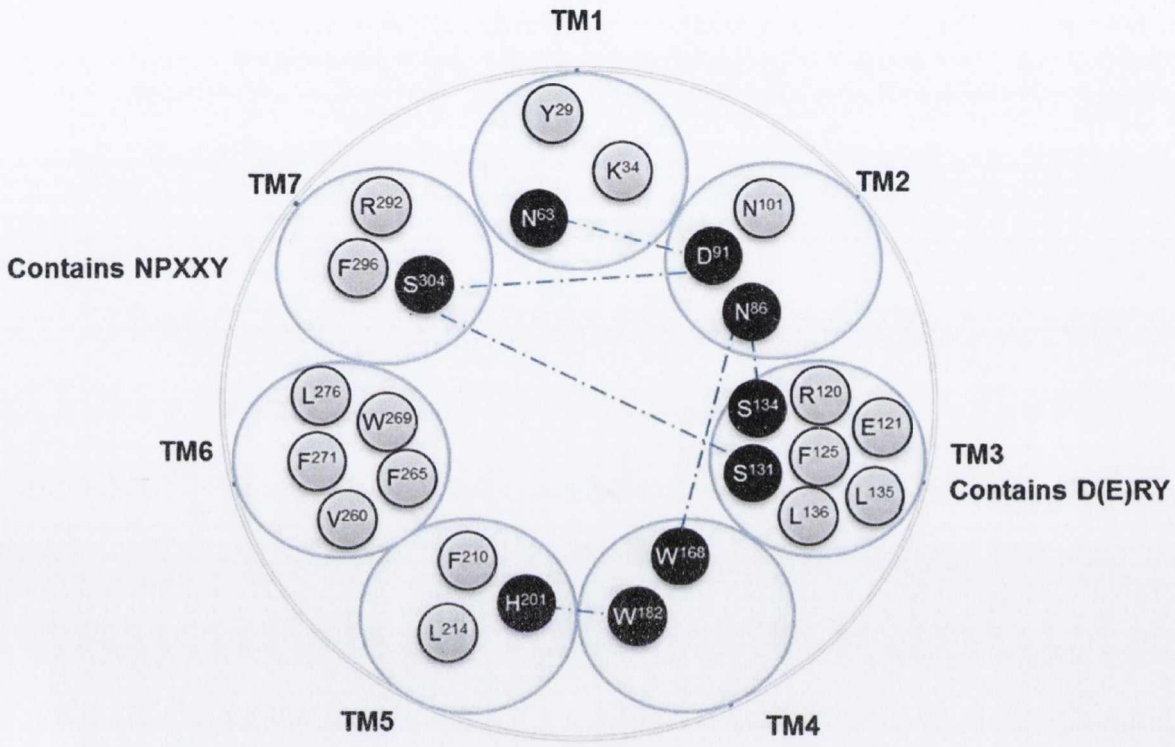

Figure 1.6. Interactions between Transmembrane Domains. Above illustrates the transmembrane domains (TM) 1-7 of the S1PR1 and the important amino acids contained in each. Amino acids in black denote hydrogen bonded amino acids while those in grey denote important amino acids for various interactions, ligand binding and post translational modifications (see text).

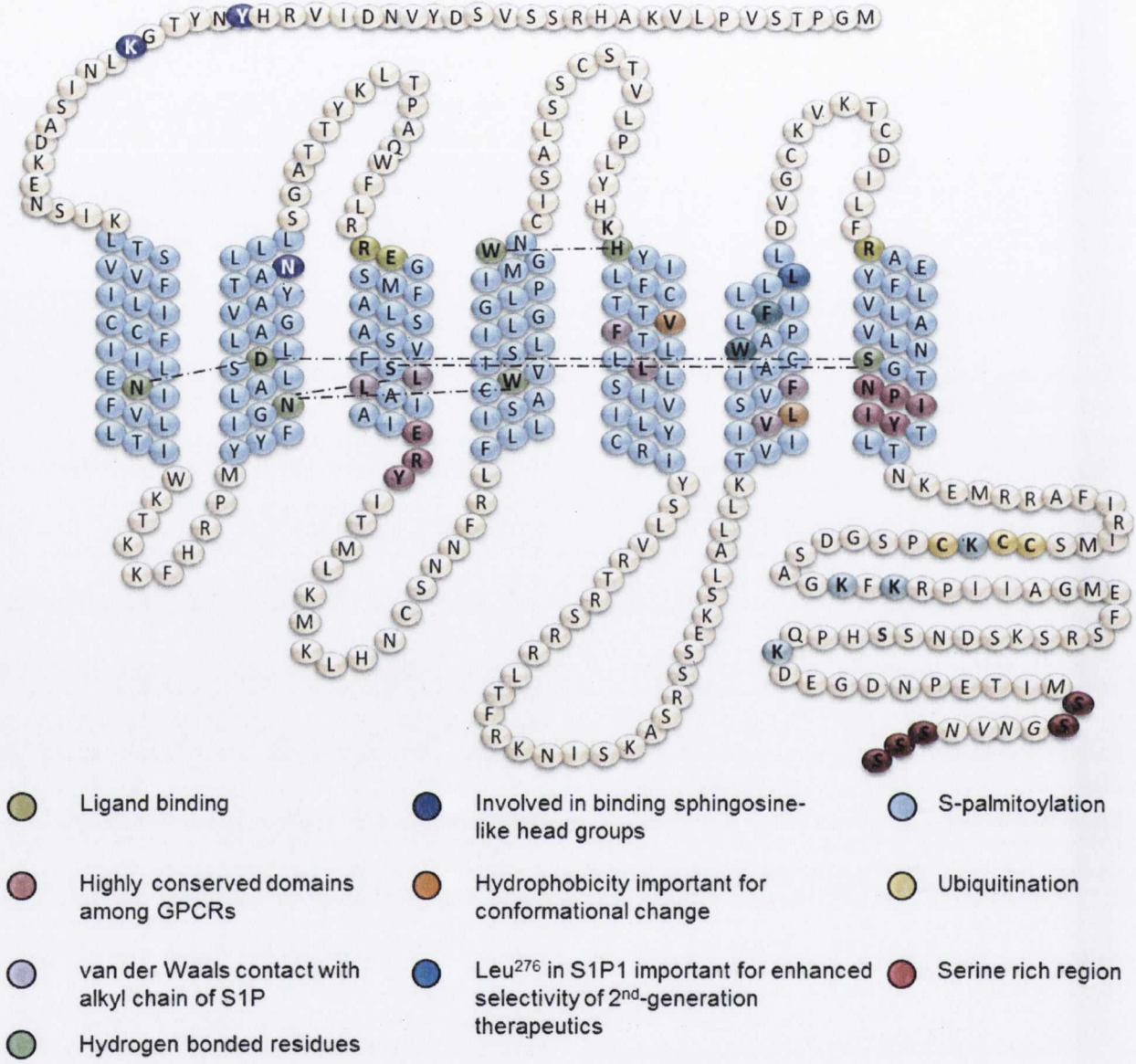

Figure 1.7. The amino acid structure of S1PR1. The 382 amino acid structure of the GPCR, S1PR1 is shown above. Highlighted are the amino acids within this receptor which play more prominent roles in ligand binding, receptor activation and cell signalling, as well as post-translationally modified residues.

3. S1PR expression and function in the CNS

Glia, derived from the Greek word gliok, (commonly translated as glue), is the collective name given to brain cells other than neurons. Many prominent histologists greatly advanced the field of glial biology, in particular, Camillo Golgi (1843), Gustav Retzius (1842-1919), Santiago Ramon Cajal (1852-1934) and Pio Del Rio Hortega (1882-1945). These cells which include astrocytes, oligodendrocytes, microglia and the less commonly known NG-2 cell all function to maintain homeostasis in the nervous system. The simplistic view of them as idle support cells however has changed in the past 20 years and the functional significance of these cells are finally beginning to be appreciated. The homeostatic function of glial cells includes body and organ homeostasis, cellular homeostasis, morphological homeostasis, molecular homeostasis, metabolic homeostasis, long-range signalling homeostasis and defensive homeostasis **(Verkhratsky and Butt, 2013)**.

Expression of S1PR1, S1PR2 and S1PR3 is widespread throughout many systems in the body and can be found on cells of the immune, cardiovascular and central nervous systems, amongst others. S1PR4 and S1PR5 however have been reported to have more selective expression patterns as S1PR4 has been found mainly to reside in lymphatic tissues while S1PR5 is believed to be primarily located on Natural Killer cells and on oligodendrocytes of the CNS **(Walzer et al., 2007, Dev et al., 2008, Hla and Brinkmann, 2011, Nixon, 2009, Mann, 2012, Iwasaki, 2011, Groves et al., 2013)**. The relative S1PR expression within the CNS also varies from cell type to cell type. Astrocytes have an S1PR expression pattern of S1PR3 > S1PR1 > S1PR2 > S1PR5 **(Rao et al., 2003)**. Neurons have an expression pattern of , S1PR3 > S1PR1 ≈ S1PR2 > S1PR5 ≈ S1PR4 **(Kays et al., 2012)**. Microglia's relative expression of the S1PRs is S1PR1 > S1PR3 > S1PR2 > S1PR5 **(Tham et al., 2003)** and oligodendrocytes have the following relative expression of S1PRs, S1PR5 > S1PR1 ≈ S1PR2 > S1PR3 **(Yu et al., 2004)** (Figure 1.8).

3.2 S1PR function in Astrocytes

Astrocytes express a variety of S1PRs of which their activation can have a range of disparate intracellular effects (Figure 1.8 and Table 1.3). These include calcium influx, phosphoinositide hydrolysis, ERK1/2 phosphorylation and [3H]-arachidonic acid (AA) release **(Rao et al., 2003)**. Inhibition of sphingosine kinase or pre-treatment with PTX was found to inhibit these downstream signalling events to varying degrees hence implicating both Gi and Gq-coupled GPCRs in S1P signalling in astrocytes **(Rao et al., 2003)**. S1P treatment of astrocytes has been shown to induce neuronal differentiation of neuronal progenitor cells (NPC) via the increase of laminin (a major protein of the basement membrane) **(Spohr et al., 2012)**. Cerebellar astrocytes have also been found to release S1P in response to basic fibroblast growth factor (bFGF). This can then induce the proliferation of astrocytes via Gi coupled GPCRs **(Bassi et al., 2006)**. As both bFGF and S1P are involved in the maintenance of endothelial tight junction and astrocyte growth, this S1P/bFGF induced proliferation of astrocytes is likely to be beneficial in decreasing blood brain barrier (BBB) permeability **(Abbott et al., 2006)**. S1P has also been demonstrated to strongly inhibit gap junction communication by a mechanism that involves both G_i and Rho/ROCK signalling (the former probably mediated by $G_{12/13}$) **(Rouach et al., 2006)**. There are several reports in the literature that suggest suppression of gap junction communication correlates with enhanced mitogenesis and that the S1P induced Rho/ROCK pathway is involved in reorganization of the actin cytoskeleton **(Rouach et al., 2006)**. S1P

activation of astrocytic S1PRs however does not always result in beneficial effects. Injection of S1P into the striatum of mice was seen to induce astrogliosis **(Sorensen et al., 2003)**. In addition, S1PR3 and SphK1 have been demonstrated to be up-regulated in MS lesions and that activation of astrocytes by LPS up-regulated the SphK1/S1PR3 signalling axis **(Fischer et al., 2011).**

While S1P is a full agonist and activates S1PR1 and S1PR3 on astrocytes, **(Fischer et al., 2011, Osinde et al., 2007)**, pFTY720 mainly activates S1PR1 and only partially activates S1PR3 **(Mullershausen et al., 2007)**. As mentioned previously, activation of S1PR1 by pFTY720 does not result in the same physiologic responses seen when the receptor is activated by S1P (Figure 1.4 and Figure 1.5). The binding of pFTY720 to S1PR1 causes receptor internalisation and is thought to result in either functional antagonism **(Choi et al., 2011)** and/or persistent signalling **(Mullershausen et al., 2009)**. Agonist binding of S1PR1s results in internalisation via β-arrestin-mediated clathrin coated vesicles. While S1P stimulation mostly results in internalisation and consequent recycling of the S1PR1s back to the membrane, binding of pFTY720 to S1PR1s internalises the receptor and can result in persistent S1PR1 signalling and subsequent polyubiquitinylation and degradation **(Obinata and Hla, 2012, Oo et al., 2007, Oo et al., 2011).** Treatment of cultured astrocytes with pFTY720 was seen to stimulate ERK phosphorylation and induce cell migration **(Mullershausen et al., 2007, Osinde et al., 2007)** and to inhibit the production of proinflammatory cytokines and chemokines **(Van Doorn et al., 2010)**. In an *in vivo* study performed on EAE mice, proinflammatory cytokine levels and disease-associated increases in S1P levels were reduced in the animals lacking astrocytic S1PR1 **(Choi et al., 2011)**. This report highlighted the important role of astrocytes in the efficacy of pFTY720. The mutants which lacked S1PR1 on GFAP positive glial cells exhibited reduced severity of EAE in comparison to littermate controls **(Choi et al., 2011)**. This study also supported functional antagonism of S1PR1 as the main receptor mechanism by which pFTY720 exerted its efficacy in the CNS **(Choi et al., 2011)**.

3.4 S1PR signalling in Microglia

Microglia express all S1PR subtypes found in the CNS, that is all except S1PR4 **(Noda et al., 2013)** (Figure 1.8). The relative levels of expression of each S1PR subtype by microglia depends, to a significant degree, on the activation state of the cells **(Tham et al., 2003)**. For example, in activated microglia, S1PR1 and S1PR3 are notably down-regulated while S1PR2 is upregulated **(Tham et al., 2003)**. As a principal cell type for neuroinflammation, S1PR expression on microglia may be an important target that requires further assessment. Signalling via S1PR1 and 5 have been suggested to contribute to microgliosis, while S1PR3 signalling may attenuate this response **(Miron et al., 2010)**. Furthermore, activated microglia present during EAE are histologically diminished by the genetic deletion of S1PR1 in the CNS or by pFTY720 treatment **(Choi and Chun, 2013)**. pFTY720 activation of S1PR1 has also been reported to inhibit the production of pro-inflammatory cytokines such as IL6, TNFα and IL1β from LPS-activated microglia and enhance the expression of the neurotrophic factors BDNF (brain-derived nerve factor) and GDNF (glial-derived nerve factor) **(Noda et al., 2013)**. In LPC-induced demyelination in a rat CNS spheroid cell culture model (contains microglia but is devoid of blood-bourne immune cells), partial inhibition of microglial activation correlated with increased remyelination **(Jackson et al., 2011a)**. Therefore, if pFTY720 can promote the

neuroprotective effects of microglia, then this may represent a potential therapeutic opportunity as microglial activation is now believed to contribute to the progression of many neurological disorders including MS, Alzheimer's disease, stroke and spinal cord injury **(Giunti et al., 2014)**.

3.6 S1PR signalling in Oligodendrocytes

Human oligodendrocytes have been reported to express S1PR transcripts in the relative abundance of S1PR5>S1PR1=S1PR2>S1PR3, with undetectable levels of S1PR4 **(Yu et al., 2004)** (Figure 1.8). It is not surprising then that in oligodendrocytes, S1PRs have been reported to regulate a wide range of signalling molecules related to Gi, Gq and G12/13 pathways. These include adenylate cyclase (AC), phospholipaseC (PLC), extracellular signal-regulated kinase 2 (ERK2), protein kinase C (PKC), phosphoinositide 3-kinase (Pi3K), cAMP-response elementbinding protein (CREB), pAKT and Ras homolog A (Rho A) **(Hida et al., 1999, Saini et al., 2005, Yu et al., 2004)**. S1P activation of S1PR5 is reported to play a role in inhibiting oligodendrocyte precursor cell (OPC) migration. This inhibition was found to enlist the G12/13 coupled Rho/ROCK signalling pathway **(Novgorodov et al., 2007)**. In addition, S1PR5 activation on $O4^+$ pre-oligodendrocytes induces process retraction via the Rho kinase/collapsing response-mediated protein signalling pathway **(Jaillard et al., 2005)**. Interestingly, this process retraction is not observed at later developmental stages and therefore, this S1PR5-mediated process modulation appears to be exclusive to immature cells **(Jaillard et al., 2005).** Moreover, S1PR1 activation has been linked to process extension **(Miron et al. 2008)** and pFTY720 has been shown to inversely modulate the mRNA expression of S1PR1 and S1PR5 thereby regulating the pattern of process retraction and elaboration in a concentration and time dependent manner **(Miron et al. 2008)**. S1P also induces preferential activation of ERK2 on oligodendrocytes **(Hida et al. 1999)** and the reported improved survival of neonatal rat oligodendrocytes treated with pFTY720 during serum withdrawal is associated with the phosphorylation of ERK1/2 and Akt **(Jung et al., 2007)**.

S1P and pFTY720 have been shown to promote the differentiation of neural precursor cells (NPCs) towards an oligodendroglial lineage indicated by the expression of OPC markers, Olig2 and O4. In addition, activation of S1PR1 protects NPCs from ceramide induced apoptosis **(Bieberich, 2011)**. pFTY720 has been demonstrated to regulate OPC differentiation into mature oligodendrocytes in a concentration-dependent manner **(Jung et al. 2007)** and in particular, a selective S1PR5 compound (Compound 1L, BAF312), has been shown to induce a significant increase in the number of MBP-positive mature oligodendrocytes **(Mattes et al., 2010)**. As well as regulating oligodendrocyte differentiation, S1PRs also play a role in the survival of mature oligodendrocytes. For example, pFTY720 has been demonstrated to rescue mature oligodendrocytes from serum and glucose deprivation-induced apoptosis **(Miron et al., 2008a)**. These pro-survival effects have been attributed in part to pERK1/2 and pAKT signalling **(Coelho et al., 2007, Miron et al., 2008b)**.

Loss of the myelin sheath due to the presence of auto-reactive T-cells is the main pathological feature of MS. Therefore, understanding of the roles of S1PR modulation on myelination of the CNS is of relevance. Organotypic slice cultures are an established *in vitro* assay for the study of myelin development and maintenance and represent an excellent compromise between single

cell cultures and *in vivo* animal studies. Unlike single cell cultures, organotypic slice cultures preserve the architecture of the brain regions that they originate from and can more accurately represent the complex processes and interactions that occur between cells and their microenvironment. Such slice cultures have been an invaluable tool in the study of CNS S1PRs and their roles in myelination. Treatment of organotypic slices with the demyelinating agent lysophosphatidylcholine (LPC) has been used as an *in vitro* model to study the effects of S1PRs on demyelination **(Miron et al., 2010, Sheridan and Dev, 2012)**. pFTY720 treatment of LPC-induced demyelination in organotypic cerebellar slice cultures was seen to enhance remyelination and process extension by OPCs and mature oligodendrocytes **(Miron et al., 2010)**. Interestingly, pFTY720 and the S1PR1/5 selective agonist BAF312, but not AUY954 (S1PR1 specific agonist) significantly augment MBP expression in the remyelination phase following LPC-induced demyelination in the rat telencephalon **(Jackson et al., 2011a)**. Organotypic cerebellar slices treated with pFTY720 and SEW2871 (S1PR1 specific agonist) have also been shown to attenuate LPC-induced demyelination **(Sheridan and Dev 2012)**. These studies implicate S1PR3/5 in the promotion of remyelination and S1PR1 in the attenuation of demyelination; however it is likely these roles are not mutually exclusive. A reduction in the production of pro-inflammatory factors such as TNFα, IL-1, LIX, MIP-1α and MIP-3α and in signalling molecules such as nitric oxide metabolites and the apoptotic effectors caspase 3 and 7 have all been suggested to preserve myelination state after treatment with S1PR modulators **(Jackson et al. 2011, Sheridan and Dev 2012)**. In addition to highlighting the influence of S1PRs in regulating the myelination state, these results also implicate inflammation as an important factor when considering demyelination.

3.7 Inflammation and demyelination

Inflammation is a common feature in demyelinating disorders and indeed, in most neurological disorders. A number of possibilities exist for the relationship between inflammation and demyelination: (i) that inflammation induces demyelination; (ii) that demyelination causes inflammation; (iii) other factors contribute to the development of inflammation and/or demyelination; (iv) inflammation and demyelination participate in a cycle in which they augment one another; and (v) that inflammation can protect against demyelination.

To investigate the direct effect of inflammation on demyelination, focal inflammatory lesions can be induced by LPS or cytokine injection into the CNS of mice and rats. One such study injected LPS into the rat spinal white matter and reported a large demyelinating lesion developed after 5-7 days **(Felts et al., 2005)**. However, direct injection of killed bacillus Calmette–Guérin (BCG) into the hippocampus produced an acute inflammatory response but did not result in myelin loss **(Matyszak and Perry, 1995)**, and furthermore, an injection of TNFα into white matter *in vivo* also does not result in demyelination **(Hall et al., 2000)**. Therefore, it is not yet clear if an acute focal injection of an inflammogen is sufficient to induce demyelination and perhaps chronic inflammation is required to initiate demyelination *in vivo*. In MS and EAE, inflammatory mechanisms such as autoantibodies, T cells and macrophages lead to demyelination in the majority of patients, lending further support to the assumption that inflammation and demyelination are closely related. In some scenarios however it has been suggested that oligodendrocyte and myelin damage are in fact the primary events. This is then followed by microglia activation and proliferation and later by the invasion of peripheral

inflammatory cells **(Stadelmann et al., 2011)**. Axonal injury and subsequent demyelination can also occur in the absence of inflammation as demonstrated by a number of non-inflammatory demyelination animal models. In shiverer mice and mice with deficient PLP, cyclic nucleotide phosphodiesterase (CNP-1) and/or MAG, the metabolic function and integrity of the myelin sheath is disrupted often resulting in demyelination in the absence of inflammation **(Brück, 2005)**.

During primary demyelination, microglial cells, the resident immunocompetent cells in the CNS, are reported to increase in number through proliferation as well as by recruitment of progenitors from blood **(Remington et al., 2007)**. One of the initial functional outcomes of microglial activation is induction of the pro-inflammatory phase of an innate immune response and is termed 'classical activation'. This activation state leads to the production and secretion of pro-inflammatory cytokines (such as interleukin 1β (IL-1β), interleukin-6 (IL-6), tumor necrosis factor-α (TNFα), reactive oxygen-nitrogen species (for example, N2O3, NO2) and proteases (e.g., matrix metalloproteinase-9) **(Colton and Wilcock, 2010)**. These agents are released during classical activation to defend tissue and promote the destruction of pathogens; however, if not kept under tight control they can induce inflammotoxicity of the tissue. In LPC-induced demyelination in a rat CNS spheroid cell culture model (contains microglia but is devoid of blood-bourne immune cells), partial inhibition of microglial activation correlated with increased remyelination **(Jackson et al., 2011a)**. Astrocytes also have a role in the regulation of inflammation and many now believe that astrocytes and microglia play a prominent role in myelin dysfunction **(Chew et al., 2013, Yeo et al., 2012)**. Other factors such as zinc metallothioneins have been suggested to have a role in preventing demyelination and decreasing inflammation during MS and EAE **(Peterson and Fujinami, 2007)**. Influx of extracellular Ca^{2+} has also been shown to be involved in demyelination, however, calcium channel inhibitors appear to only be effective if given before the onset of inflammation **(Brand-Schieber and Werner, 2004).** In addition, sodium channels have been reported to be involved in the activation of macrophages and microglia and as well as play a role in phagocytosis of myelin debris. Inhibition of sodium channels therefore was seen to reduce inflammation and axonal damage in the EAE animal model **(Craner et al., 2005)**.

It is typically thought that demyelination and inflammation act in a 'vicious cycle' where demyelination can induce inflammation which then leads to further demyelination. In a model where the axon is injured, microglia can become activated and the damage can spread to oligodendrocytes either through induction of apoptosis or disruption of cross-talk, potentially resulting in demyelination. Damaged myelin, oligodendrocytes and axons are then phagocytosed and can result in further microglial activation and a perturbation of the inflammatory response which in turn leads to additional demyelination. Demyelination can then lead to axonal damage and thus the cycle continues. It is important to note that the inflammatory response is a mechanism used to protect the body. It is only when the inflammation goes unchecked that it itself induces damage. Therefore, alternative activation of microglia may help protect against demyelination as well as enhance remyelination (Figure 1.9) **(Olah et al., 2012)**. Anti-inflammatory cytokines such as IL-4, IL-13, IL-10 and transforming growth factor-β (TGFβ) are released from microglia, accessory immune cells such as astrocytes or from T_H2 regulatory T cells in an autocrine manner and

trigger the down regulation of the pro-inflammatory phase and induce tissue repair **(Colton and Wilcock, 2010)**.

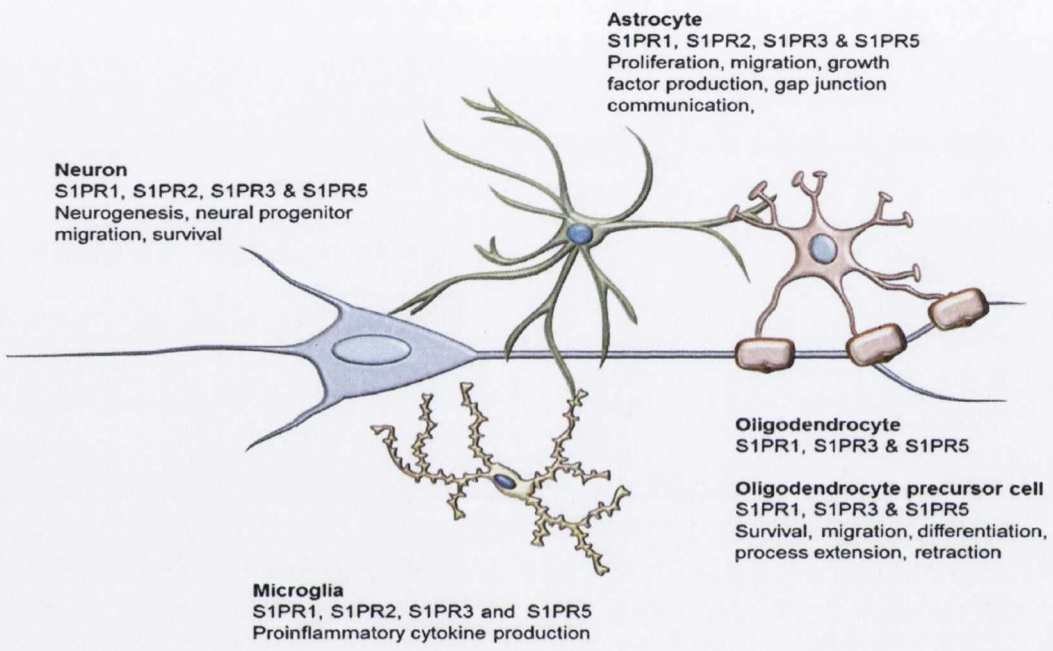

Figure 1.8. S1PR's and the cells of the CNS. Distribution and summary of functions of S1PR subtypes in cells resident in the CNS.

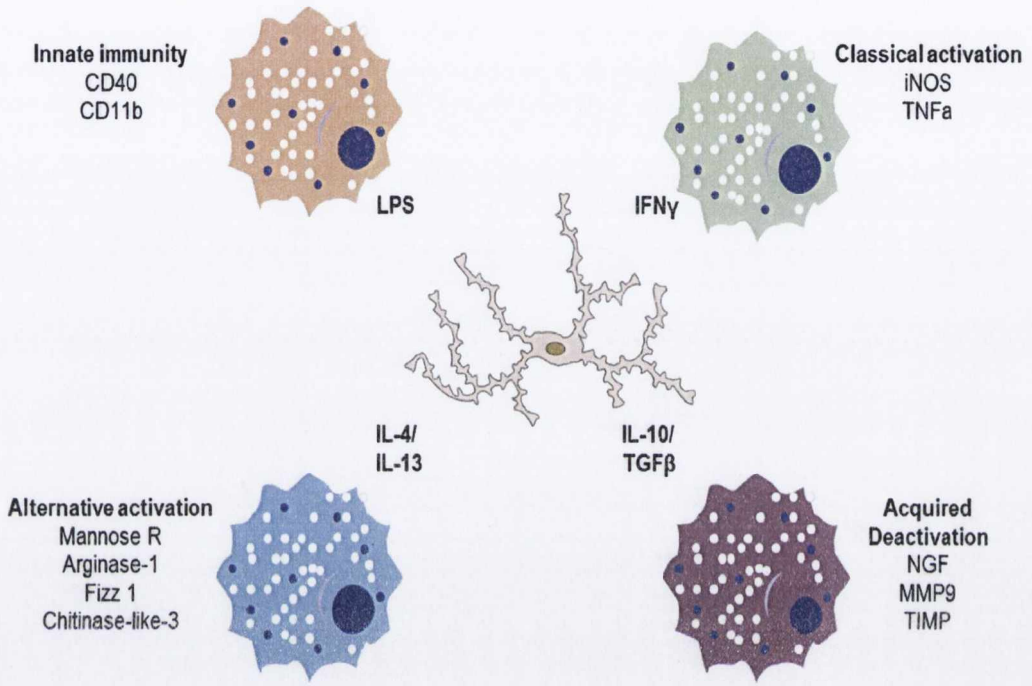

Figure 1.9. Microglia activation states. Four main microglial activation states have been described based on the expression of certain characteristic markers. CD40; cluster of differentiation 40, CD11b; cluster of differentiation 11b, iNOS; inducible nitric oxide synthase, TNFα; tumor necrosis factor α, Mannose R; mannose receptor, NGF; nerve growth factor, MMP9; matrix metalloproteinase 9, TIMP; tissue inhibitor of metalloproteinase, LPS; lipopolysaccharide, IFNγ; interferon γ, IL-; interleukin.

Astrocyte subtype	Description
Protoplasmic	Grey matter astrocytes, morphologically heterogeneous, occupy discrete territorial domains, can form perivascular endfeet and subpial endfeet.
Fibrous	White matter astrocytes, long processes (up to 300μm), show high degree of overlap, diverse morphology,
Surface-associated	Astrocytes associated with the cortical surface in the posterior pre-frontal cortex and amygdaloid cortex
Velate	Subtype of protoplasmic astrocytes, occur in brain regions densely packed with small neurons
Interlaminar	Found in cerebral cortex of higher primates, extend 1 or 2 long unbranched processes that terminate in button masses that contain a single mitochondria
Polarised	Found in deep cortical layers near white matter, possess 1 or 2 long processes (up to 1mm)
Varicose projection	Appear to only be found in humans, characterised by several long (up to 1mm) unbranched processes that extend to deep cortical layers
Radial glia	Bipolar cells common to the developing brain, form a scaffold to assist neuronal migration, after maturation radial glia can disappear from many regions and transform into stellate astrocytes
Müller cells	Specialised radial glia cells found in the retina, each Müller cell forms contacts with a clearly defined group of neurons (a single Müller cell supports ~16 neurons).
Bergmann glia	Specialised radial glia cells found in cerebellum, elaborate processes, several Bergmann glia surround a Purkinje neuron and form close contact with synapses
Tanycytes	Bipolar astrocytes found in periventricular organs, hypothalmus and hypophysis, form BBB by forming tight junctions with capillaries
Perivascular & Marginal	Localised close to pia matter, form endfeet with blood vessels, form the pia and perivascular glia limitans barrier
Ependymocytes	Line the ventricles and subretinal space, secretory epithelial cells produce a stream of CSF

Table 1.3. Astrocyte subtype

3.8 The role of astrocytes in myelination

Astrocytes are now accepted to significantly contribute to the development and maintenance of CNS myelin as well as to the pathology of demyelinating disorders (Barnett and Linington, 2013). Initial experiments to investigate the influence of astrocytes on myelination *in vivo,* demonstrated that transplanted type 1 cortical astrocytes enhanced remyelination of ethidium bromide-induced demyelinating lesions in the spinal cords of animals **(Blakemore and Crang, 1989)**. It has since been demonstrated that astrocytes can influence oligodendrocyte differentiation through the production of extracellular matrix (ECM) molecules that impact on oligodendrocyte maturation **(Wiese et al., 2012)**. In particular fibroblast growth factor 2 (FGF2) and platelet derived growth factor α (PDGF α) are released from astrocytes and work in combination to promote self-renewal of the OPC population **(Barnett and Linington, 2013)**. In addition, astrocytes are also reported to promote myelination in response to electrical impulses. This involves a cross-talk between neurons, astrocytes and oligodendrocytes whereby ATP liberated from axons during an action potential stimulates astrocytes to release leukemia inhibitory factor (LIF) which then in turn promotes myelination **(Ishibashi et al., 2006).** In chronic myelin lesions in MS, astrocytes have been identified as a source of tenascin-c which is an inhibitory ECM substrate for oligodendrocyte progenitor cells (OPCs) **(Gutowski et al., 1999).** Expression of another ECM, fibronectin by astrocytes has been shown to be induced in models of immune-mediated myelin injury and to be upregulated in astrocytes in response to inflammatory mediators such as LPS **(Stoffels et al., 2013)**. This production of fibronectin by astrocytes has also been reported to attenuate the differentiation of OPCs *in vitro* and to impair remyelination of LPC induced white matter lesions **(Stoffels et al., 2013)**. Accumulation of another astrocytic protein called hyaluronan in inflammatory lesions has also been demonstrated to impair remyelination and the hyaluronan receptor, CD44, is expressed on reactive astrocytes **(Sosunov et al., 2013).**

Therefore, astrocyte phenotype is likely to have a significant role in the outcome of CNS repair and myelination. Depending on the nature of the factors secreted (inhibitory or promoting) astrocytes can have either a negative or positive effect on myelination. Furthermore, these factors can directly affect OPC proliferation, differentiation and myelin ensheathment, or, indirectly via effects on microglia or neurons. A focus on astrocytes as a modulator of myelination in the future may reveal targets for research and aid in the development of astrocyte-specific strategies aimed to enhance lesion repair demyelinating diseases.

4. S1PRs as potential drug targets for Krabbe Disease

The effect of S1PR1 down regulation in the immune system has been well documented. Internalisation of S1PR1 renders B and T cells unresponsive to the S1P gradient and prevents these cells from exiting the lymph nodes and entering the lymphatic circulation **(Kappos et al., 2006)**. This 'functional antagonism' of the S1PRs is the basis attributed for pFTY720's efficacy in the treatment of the autoimmune disease MS. MS is the most commonly diagnosed neurological disorder in people aged 18-50 **(Compston and Coles, 2008).** Pathologically this disease is characterised by inflammation and demyelination of neuronal axons due to the presence of auto-reactive T-cells. Demyelination is usually centred in various foci and these

lesions, or scleroses, can occur in any region of the brain and spinal cord containing white matter **(Compston and Coles, 2008)**. In addition to the immunomodulatory effects of pFTY720 on lymphocytes in the periphery, increasing evidence now suggests an important role for pFTY720 acting on S1PRs in the CNS. Indeed, many research groups are now beginning to investigate the modulation of S1PRs as potential therapies for a diverse range of disorders both in the periphery and CNS (see Table 1.4). Of the CNS based disorders, the putative protective effect of pFTY720 is being investigated in **(Di Pardo et al., 2014, Hemmati et al., 2013, Deogracias et al., 2012, Estrada-Bernal et al., 2012, Gao et al., 2012)**. Here we have focused on the role of S1PRs in the childhood demyelinating disorder: Krabbe disease (KD).

4.1 Krabbe Disease

KD is a rare autosomal recessive neurodegenerative disorder affecting 1:100,000 live births in the United States **(Wenger et al., 1997)**. Typically this is an early onset, rapidly progressing and invariably fatal disease in infants. It can be characterised into four clinical subtypes depending on the age of onset. These include infantile (from 3- 6 months), late infantile (from 6 months - 3 years), juvenile (from 3 - 8 years) and adult (8+ years) **(Suzuki, 2003)**. The vast majority (85-90%) of cases are of the infantile form, with the juvenile and adult onset forms being considered extremely rare **(Wenger et al., 1997)**. Hallmark symptoms of the classic infantile form include irritability, hypersensitivity, psychomotor arrest and hypertonia. This is followed by rapid mental and motor deterioration, seizures, optic atrophy and elevated protein levels in the cerebrospinal fluid (CSF). Death usually occurs within the first two years of life and there is currently no cure **(Davenport et al., 2011)**. KD is caused by a deficiency in the lysosomal enzyme galactosylceramidase (GALC) **(Suzuki, 2003)**. This results in the accumulation of a toxic lipid metabolite; psychosine (also known as galactosylsphingosine). Another substance, β-galactosylceramide also accumulates within cells of the myeloid lineage to form the characteristic globoid cells seen in the KD brain, however the accumulation of psychosine relative to galactosylceramide is greater as galactosylceramides are also hydrolyzed by GM1ganglioside β-galactosidase **(Giri et al., 2002)**. Progressive accumulation of psychosine is now believed to be the critical pathogenetic mechanism of cell death in the KD brain as concentrations of this molecule are estimated to be increased more than 100-fold in KD patients **(Svennerholm et al., 1980)** with reports of psychosine's cytotoxicity seen both *in vitro* and in intracranial-injection experiments **(Giri et al., 2006)**.

Pathological features of this disease include profound demyelination and almost complete loss of oligodendrocytes in the white matter, reactive astrocytosis and infiltration of numerous multinucleated macrophages termed 'globoid cells'. These globoid cells are a unique feature of KD and are seen to accumulate around blood vessels and in the regions of demyelination **(Suzuki, 2003)**.

4.2 Galactosylceramidase is mutated in KD

GALC, located on chromosome 14q23.3–32.1, is composed of 16 introns (ranging from 247 bp to 12 kb in size) and 17 exons (39 to 181 bp in size) encoding a 669 amino acid glycoprotein **(Luzi et al., 1995)**. The first 26-amino acids encode for a signal peptide which targets it to the endoplasmic recticulum where it is produced, glycosylated and then trafficked, via the mannose-6-phosphate (M6P) pathway, to the lysosome **(Nagano et al., 1998)**. The remaining

643 amino acids contain six potential glycosylation sites **(Wenger et al., 1997)**. Similar to genes of other lysosomal proteins, the 5' untranslated region of GALC is GC-rich and does not contain any definitive TATA or CAAT sequences **(Uniprot)**. The GALC enzyme displays specificity for glycolipids that possess a terminal galactose moiety in the β anomeric configuration **(Suzuki, 2003)**. GALC hydrolyses the galactose ester bonds of its major natural substrate, Galactosylceramide (mainly localized in the myelin sheath) with it also acting on monogalactosyldiglyceride, psychosine and the seminolipid precursor 1-alkyl,2-acyl-,3-galactosyl glycerol **(Suzuki, 2003)**. Structurally, GALC possess 3 main domains; a triosephosphate isomerase barrel at the centre containing the active site, a β-sandwich domain and a ~30-kDa C-terminal domain with a lectin fold **(Lieberman, 2011)**.

Common mutations of the GALC gene have been reported for this disease including the 502T/del mutation (present in about 40% of KD patients of European ancestry) and the T513M mutation (a C>T change at 1538 in Northern European ancestry) **(Wenger et al., 1997)**. Many more mutations have also been found including missense mutations (G>A at 284, A >T at 301), nonsense mutations (G>T transversion at 1105), six single base deletions (382delA, 805delG, 906delT, 964delG, 1424delA, 1852delT) and a single base insertion (1675insT) **(Wenger et al., 1997)**. In addition to GALC, a small, heat-stable nonenzymatic glycoprotein; saposin A, (sphingolipid activator protein) is also crucial for the *in vivo* degradation of galactosylceramide **(Kolter and Sandhoff 2005)**. Saposin A belongs to a family of four homologous glycoproteins, (saposin A, B, C and D), which are essential for normal lysosomal degradation and range from 8-11 kDa in size **(Kishomoto et al., 1992)**. A genetic sapsoin A deficiency may also be associated with chronic late onset KD in human patients **(Matsuda et al., 2001)**.

4.3 The Krabbe disease twitcher mouse

The twitcher (twi/twi) mouse is a naturally occurring, enzymatically authentic model of human KD resulting from a spontaneous mutation in the *Galc* gene **(Kobayashi et al., 1980)**. Like the *Galc* mutation seen in KD, the twi/twi mutation is also inherited in an autosomal recessive fashion. Furthermore, the clinical and pathological course of the disease in twi/twi mice closely resembles the disease course observed in humans **(De Gasperi, 2004)**. Clinically, twi/twi mice are normal until around 20 days of age. After this they begin to grow slower, develop tremors and progressive muscular weakness, especially in the hind limbs which soon after become paralysed **(Davenport et al., 2011, De Gasperi, 2004)**. As in humans, disease progression is rapid and twi/twi mice rarely life above 40 days of age **(De Gasperi, 2004)**. Demyelination can be detected in the peripheral nervous system (PNS) of the twi/twi mice by day 10, spinal cord by day 20 and thereafter in the cerebellum and cerebrum **(Suzuki and Taniike, 1995)**. The pathological hallmark of the disease, globoid cells, also form in twi/twi mice by day 25 **(Takahashi and Suzuki, 1984)**. The twi/twi mouse has proven to be an invaluable research tool in both the effort to elucidate of the pathogenesis of KD and also in aiding the effort to develop therapeutic strategies to tackle this disease. Like all animal models however there are some discrepancies between the disease in humans and in the twi/twi mice. For example, in the twi/twi mice the CNS pathology is milder and the PNS more severely affected in comparison to KD pathology **(Duchen et al., 1980)**. In addition, twi/twi mice don not exhibit seizures and deceberate rigidity as seen in the KD patients **(Suzuki and Taniike, 1995)**.

4.4 Physiochemical properties of psychosine

Galactosylsphingosine was first obtained in 1884 by the alkaline hydrolysis of galactolipid in the brain and was given the name psychosine **(Thudichum, 1884)**. Psychosine is synthesized by the transfer of the galactose residue from UDP-galactose to sphingosine bases via the action of UDP-galactose ceramide galactosyl transferase (CGT) then itself reacts with fatty acid-Coenzyme A to form the cerebroside **(Cleland and Kennedy, 1960, Won et al., 2013)** (Figure 1.10). The microsomal enzyme CGT is approximately 50-70kDa in weight and is primarily expressed by oligodendrocyte cells in the brain **(Schulte and Stoffel, 1993)**. Studies of the mouse genome revealed the CGT gene is located to the E3-F1 region on chromosome 3 and is composed of 6 exons, the first of which is non-coding with the remaining five exons containing the coding sequence and the 3' UTR region **(Coetzee et al., 1996)**. To date, the physiochemical properties of psychosine have received little to no attention and there is very limited information available regarding properties such as pKa value. One group however, have attempted to characterise psychosine's physiochemical properties using 1H nuclear magnetic resonance (NMR) and electron microscopy (EM) and are the only group to have reported the pKa of the protonated amine group of psychosine to be 7.18 ± 0.05 **(Orfi et al., 1997)**. Using this technique they also give insight into the disparate molecular interactions of psychosine at different pH values and report that it is the free amine group that is necessary for psychosine to mediate it's toxic effects **(Orfi et al., 1997)**. Psychosine is normally enzymatically broken down in the acidic environment of the lysosome (~4.5 pH). In KD however, unmetabolised psychosine escapes from lysosomes and dying cells into the cytoplasm/extracellular milieu which has a pH of ~7.4. From these NMR and EM studies, psychosine was seen to form larger, more unstable aggregates at a neutral pH than at an acidic pH **(Orfi et al., 1997)**. The explanation given for this concerns the amine group. In the protonated state, the amine group is raised above the hydrophobic layer of carbon chains, allowing the acyl chains to form an orderly, stable array. The deprotonated state of psychosine has also been suggested to destabilise/disrupt the organisation of cellular membranes **(Orfi et al., 1997)**.

4.5 Activation of caspases by psychosine

The cytotoxic actions of psychosine have been attributed to several different mechanisms. Increasing evidence now suggests that the wide spread demyelination and loss of oligodendrocytes seen in KD is due to apoptotic processes. A TUNEL assay to detect apoptosis was performed on cultured oligodendrocyte cells incubated with psychosine **(Zaka and Wenger, 2004)** and DNA fragmentation, a marker of apoptosis was detected in glial derived MOCH-1 cells in response to psychosine treatment **(Tohyama et al., 2001)**. Psychosine induced apoptosis has also been found to involve activation of the initiator caspases 9 and 8 and the effector caspase 3, all of which are known to play central roles in apoptosis **(Giri et al., 2006, Giri et al., 2008, Zaka and Wenger, 2004, Haq et al., 2003)**. In order to activate caspase 9 from its inactive zymogen state it must first bind to the protein co-factor Apaf-1 in the presence of cytochrome *c* **(Li et al., 1997)** and psychosine treatment *in vitro* has been found to result in mitochondrial cytochrome *c* release **(Haq et al., 2003)**. Activated caspase 9 can then activate caspase 3 by proteolytic cleavage which in turn executes apoptosis by cleaving proteins following specific aspartate residues **(Taylor et al., 2008)**. Activation of caspase 8 involves the binding of extracellular death receptors such as type 1 tumor necrosis factor receptor (TNF-R1)

and the FAS receptor. Activated caspase 8 can then also proteolytically cleave and activate caspase 3 **(Taylor et al., 2008)** (Figure 1.11).

4.6 Psychosine inhibits protein kinase C (PKC)

Another mechanism by which psychosine induces toxicity involves the molecules preferential accumulation in lipid rafts **(White et al., 2009)**. This accumulation is also associated with regional cholesterol increases and alterations in the distribution of the lipid raft markers: flotilin-2 and caveolin-1 **(White et al., 2009)**. This disruption of the architecture and composition of lipid rafts has also been suggested as a putative mechanism by which psychosine inhibits protein kinase C (PKC) activity **(Davenport et al., 2011, Yamada et al., 1996, Hannun and Bell, 1987)**. PKC is an important signaling molecule that has many biological functions including regulation of cell differentiation and proliferation as well as roles in regulating membrane structure modification **(Davenport et al., 2011)**. PKC isozymes are lipid raft dependent and hence the psychosine induced lipid raft disruption may lead to reduced PKC function resulting in altered cell signaling and downstream effects such as demyelination and oligodendrocyte cell death **(White et al., 2009)** (Figure 1.11).

4.7 Psychosine up-regulates JNK signalling

The mitogen activated protein kinases (MAPKs) are a superfamily of kinases that regulate an extensive array of cellular process by relaying extracellular signals to rapid intracellular responses. In mammals, three main branches of the MAPK pathway have been identified. These are the extracellular signal-regulated kinases (ERKs), the c-Jun N-terminal kinases (JNK) and the p38 protein kinases **(Haq et al., 2003)**. There is much evidence implicating the JNK signalling pathway in apoptosis **(Liu and Lin, 2005)**. Psychosine treatment of oligodendrocyte cells has been shown to increase the DNA binding activity of a downstream signalling molecule of the JNK pathway: activator protein-1 (AP-1) **(Haq et al., 2003)**. This suggests psychosine up-regulates JNK signalling resulting in activation of c-Jun (which in combination with c-Fos), forms the AP-1 early response transcription factor, leading to apoptosis **(Haq et al., 2003)**. The same study also report a decrease in the nuclear translocation and DNA binding of nuclear factor kappa-B (NFκB) in response to psychosine treatment **(Haq et al., 2003)**. NFκB is known to be a suppressor of TNFα induced apoptosis **(Van Antwerp et al., 1996)** and in the absence of NFκB activation, JNKs have been found to promote TNFα induced apoptosis **(Karin and Lin, 2002)**.

4.8 Psychosine and its effects on inflammation

Inflammatory molecules, such as AMP-activated protein kinase (AMPK), prostaglandin D, inducible nitric oxide synthase (iNOS), pro-inflammatory cytokines and phospholipase A2 (PLA2) have all been implicated in KD. AMPK is a metabolic sensor enzyme that becomes activated under stressful conditions that deplete cellular ATP supplies such as low glucose, hypoxia and ischemia **(Giri et al., 2008)**. It is also believed to possess anti-inflammatory properties **(Salt and Palmer, 2012)**. Psychosine treatment of oligodendrocytes and astrocytes was shown to down-regulate AMPK activity leading to lipid alterations in both of these cell types **(Giri et al., 2008)**. The use of the AMPK activator AICAR proved insufficient to rescue oligodendrocytes from cell death, however, it did down-regulate psychosine-potentiated LPS-

induced expression of pro-inflammatory cytokines and reduced nitric oxide (NO) production in astrocytes **(Giri et al., 2008)**.

ukThe expression of pro-inflammatory cytokines and chemokines such as IL-6, TNFα, MCP-1, MIP-1α, IP-10 and RANTES in the twi/twi mouse has further strengthened the belief that inflammation plays a role in the pathogenesis of KD **(LeVine and Brown, 1997)**. Psychosine has also been seen *in vitro* to markedly potentiate the LPS-induced production of the cytokines IL-6, TNFα and IL-1ß in primary rat astrocyte cultures **(Giri et al., 2002)**. Interestingly, in these studies, psychosine treatment has not been sufficient to induce the increase of pro-inflammatory cytokines or NO production and instead appears to only potentiate the LPS-induced levels of these pro-inflammatory mediators **(Giri et al., 2002, Giri et al., 2008)**. Enhanced modulation of the nuclear translocation of AP-1 (plays a role in regulating cytokine-mediated iNOS induction) by psychosine, compared to the modulation of AP-1 by cytokine alone, may be one mechanism by which it potentiates cytokine-mediated iNOS induction **(Marks-Konczalik et al., 1998, Giri et al., 2002)**. In addition, psychosine was also shown to potentiate the cytokine-induced nuclear translocation of C/EBP-δ, another transcription factor which is induced by IL-1ß and promotes iNOS expression **(Kolyada and Madias, 2001, Giri et al., 2002)**. This excessive production of NO under such inflammatory conditions may lead to oligodendrocyte cell death and hence be a major factor in the pathogenesis of KD **(Giri et al., 2002).**

Increases in the levels of inflammatory cytokines in turn can induce the sPLA2 enzyme system. The products of sPLA2 include lysophosphatidylcholine (LPC), known to induce demyelination and arachidonic acid which can lead to increases in reactive oxygen species (ROS) **(Giri et al., 2006)**. Psychosine treatment of oligodendrocytes has been shown to induce the generation of LPC and arachidonic acid and furthermore, a sPLA2 inhibitor attenuated the psychosine-induced increase in both LPC and arachidonic acid as well as inhibited psychosine-induced cell death **(Giri et al., 2006)**. This implicates activation of the sPLA2 pathway and subsequent increases in LPC and arachidonic acid as mediators of psychosine-induced cell death.

4.9 Peroxisomal dysfunction in KD

Peroxisomes are dynamic, multifunctional organelles found in all eukaryotes (excluding Archaezoa) and participate in the metaolism of ROS and β-oxidation of fatty acids, particularly very-long-chain fatty acids (VLCFA) in animals **(Brown and Baker, 2008, Bharti et al., 2011)**. VLCFAs play structural roles in cellular membranes and are also suggested to have metabolic and signalling roles, such as being components or precursors of ceramide, sphingolipid and glycosylphosphatidyl-inositol anchor **(Chen et al., 2010)**. Two peroxisomal enzymes, acyl-CoA oxidase and alkyl-DHAP synthase, have both been reported to decrease in twitcher brains over time compared with age-matched controls **(Haq et al., 2006)**. In addition, psychosine treatment of primary oligodendrocyte cultures reduced alkyl-DHAP synthase levels while β-oxidation was also seen to be reduced in twitcher brains **(Khan et al., 2005)**. Peroxisome proliferator-activated protein α (PPAR-α), involved in the regulation of peroxisomal enzyme transcription, was also found to be decreased in twitcher brains **(Haq et al., 2006)**. Furthermore, peroxisomal dysfunction in the twitcher mice has been suggested to be due to

psychosine-mediated activation of sPLA2 as inhibition of sPLA2 reduced the degree of down-regulation of PPAR-α in psychosine treated oligodendrocytes **(Haq et al., 2006)**. Given the important role of many peroxisomal enzymes in ROS synthesis and degradation, dysfunction of these organelles could lead to alterations in the expression of these enzymes and result in a net increase ROS as supported by depleted levels of glutathione in both psychosine treated oligodendrocytes and in the twitcher brain **(Haq et al., 2003, Khan et al., 2005)**.

4.10 Astrocytes in KD

Very little is known about the role of astrocytes in KD as the majority of studies have mainly been focused on the myelin producing oligodendrocyte cells. Remarkably, when oligodendrocytes from twi/twi mice were transplanted into a different mouse model of demyelination, (referred to as the shiverer mice), the transplanted oligodendrocytes from twi/twi mice were capable of myelinating the shiverer axons **(Kondo et al., 2005)**. This indicates that demyelination in KD cannot be solely attributed to oligodendrocyte dysfunction and that given a different environment, the oligodendrocytes may function normally. The exact contribution of astrocytes in the pathogenesis of KD however still needs to be defined. We suspect that astrocytes may have an influential role in the initiation, progression and perhaps the resolution of KD, and have focussed a large part of our studies herein to address this idea.

4.11 Existing therapies for KD

The only therapy currently available for the treatment of KD is hematopoietic stem-cell transplantation (HSCT), which at best, provides only modest improvements if initiated before symptom onset **(Escolar et al., 2006)**. This in itself is a problem as most countries do not routinely screen newborns for this disease. Therefore, as these therapies are not curative, further elucidation into the mechanisms driving the pathogenesis and the development of more efficacious therapeutic regimens are of the utmost importance. In this regard the twi/twi mouse has become an indispensable tool to aid in the development of treatments. This twi/twi mouse appears to be a biochemically faithful model of human KD that occurs naturally from the spontaneous mutation of the GALC gene at position 1017. This creates a premature stop codon that results in nonsense-mediated decay of the mRNA **(Lee et al., 2006)**. This mouse model is being used to test single and combination experimental therapies.

4.11.1 Bone marrow transplantation, mesenchymal stem cells and neuronal stem cell treatments

One such single therapy involves bone marrow transplantation (BMT) from normal donor mice in an attempt to provide the enzyme-deficient cells from the host with functioning enzyme from the transplanted cells in a process known as cross-correction **(Hoogerbrugge et al., 1988)**. This method was not overly successful however as only a 15% increase in CNS GALC levels were recorded after complete engraftment with no significant improvement in limb strength **(Hoogerbrugge et al., 1988, Lin et al., 2007)**. Mesenchymal stem cell (MSC) transplantation decreased neuroinflammation in the twi/twi mice however did not increase GALC activity in the brain and had only minimal improvements in disease progression **(Ripoll et al., 2011)**. One particularly interesting experiment used neuronal stem cells (NSCs) transduced with a recombinant GALC-encoding viral vector with the aim that overexpression of GALC

would allow for cross-correction of the GALC deficient host cells while the NSCs can replace damaged neurons. Notably, twi/twi mice treated with nontransduced NSCs experienced a similar increase in life span as the GALC transduced NSCs **(Neri et al., 2011)**. These results indicate that GALC overexpression is not the only therapeutic route warranting investigation and highlights the need to further study other untargeted aspects of the disease that may be limiting the efficacy of GALC overexpression.

4.11.2 Viral-mediated gene therapy and substrate reduction therapy

Directly addressing the GALC deficiency in KD through enzyme replacement therapy is currently unavailable due to the inability of GALC to penetrate the BBB and the impracticality of repeated intracranial delivery of the enzyme. Viral-mediated gene therapy to deliver GALC cDNA however has the potential to mediate long term expression of this enzyme. Intravenous injection with the recombinant adeno-associated virus (AAV): AAVrh10-GALC increased the life span of twi/twi mice to 120 days and is to date the best single therapy for treatment of twi/twi mice **(Rafi et al., 2012)**. Substrate reduction therapy has also been attempted. For this, L-cycloserine, an irreversible inhibitor of an enzyme required for psychosine synthesis, 3-ketohidrosphingosine synthase, was administered to twi/twi mice and moderately increased the mean life span. L-cycloserine however also inhibits the synthesis of other cerebrosides and so will unlikely ever be used in a clinical setting **(LeVine et al., 2000)**.

4.11.3 Combination therapy for KD

The use of these therapies singularly in twi/twi mice has proven to have limited therapeutic effect, however, combinations of treatments that target different aspects of the disease may demonstrate increased efficacy. Combination of BMT with intravenous VEGF, known to render the neonatal BBB temporarily more permeable, lead to a significant increase in twi/twi life span **(Young et al., 2004)**, as did a combination of BMT with L-cycloserine **(Biswas and Le Vine, 2002)**. Furthermore, BMT in combination with intracranial and intrathecal administration of recombinant AAV resulted in a synergistic effect with the median life span of treated twi/twi mice reaching ~123 days. Remarkably, some mice even lived to 282 days **(Reddy et al., 2011)**.

In the current study we investigated the protective effect of the S1PR modulators, pFTY720 and BAF312, against psychosine-induced astrocyte toxicity and demyelination of cerebellar slice cultures.

System	Disease	Notes	Ref
CNS	Alzheimer's Disease	S1P increases BACE proteolytic activity	[1]
		S1P levels reduced in brain samples of Alzheimer's disease	[2]
	Ischemia	S1P levels increased in ischemic brain of a mouse model of middle cerebral artery occlusion	[3]
	Stress	S1P levels increased in rats model of stress	[4]
	Pain	S1P levels decreased in the CSF of rat models of pain	[5]
	Multiple Sclerosis	S1P levels elevated in CSF (but not blood) from MS patients	[6]
PNS	Peripheral Neuropathy & Pain	S1P induces hyperalgesia via S1PR1	[7]
Eye	Retinal inflammation	Retinal neovascularization retarded by S1PR2 KO	[8]
	Diabetic neuropathy	Role of S1P in VEGF-induced retinal EC migration and proliferation and reduced retinal vascular leakage	[9]
	AMD	Role of S1P in AMD-associated neovascularization, inflammation and fibrosis	[10]
Ear	Deafness	Loss of S1PR2 and S1PR3 display cochlear and vestibular defects resulting in deafness	[11]
Lung	Asthma	S1P levels elevated in the BAL fluid of asthmatics.	[12]
	COPD	S1P levels decreased in lungs of patients with cystic fibrosis and COPD; reduced S1PR5 levels in COPD	[13]
	Anaphylaxis	Anaphylactic responses attenuated S1PR2 antagonist JTE-013 and in S1PR2 KO mice	[14,15]
Vasculature	Sepsis	TLR4 signaling activates SphK1 causes S1P production and sepsis-induced inflammation	[16]
	Atherosclerosis	pFTY720 limits atherosclerosis in apoE KO mice on high-cholesterol diet (suppression of monocyte/macrophages)	[17]
	Coronary Artery Disease	S1P levels elevated in coronary artery disease and considered predictor of occurrence and severity of coronary stenosis	[18,19]
Heart	Myocardial Infarction & ischemia	S1P protects heart against ischemia reperfusion injury. Treatment with pFTY720 improves recovery during reperfusion	[20]
	Heart rate	S1PR3 implicated in sinus bradycardia	[21,22]
Liver	Hepatitis	S1P levels reduced in chronic hepatitis C with liver fibrosis	[23]
	Portal hypertension	S1PR2 activation of Rho kinase plays a role in portal hypertension, S1PR2 antagonists may aid portal hypertension	[24]
Pancreas	Diabetes	S1P (via S1PR1) prevent interaction of monocytes with type 1 diabetic endothelium	[25]
	Insulin resistance	S1PR2 KO mice have increased plasma insulin levels and polymorphisms in S1PR2 show association with onset of diabetes	[26]
		SphK activity and S1P levels are suggested to be critical for glucose-stimulated insulin secretion	[27]
		pFTY720 treatment of diet-induced obese mice prevent weight gain and improve insulin sensitivity	[28]
Skin	Atopic dermatitis	Linked to increased release of S1P from mast cells and Th2 immune response, where pFTY720 may prove useful	[29,30]
	Acne vulgaris	S1P down-regulate keratinocytes proliferation and has been considered for use in psoriasis vulgaris and acne vulgaris.	[31]
	Lupus erythematosus	Increased concentration of serum S1P in JSLE. pFTY720 treatment was effective in SLE.	[32]
Skeleton	Rheumatoid arthritis	Altered S1P levels in arthritis	[33]
	Osteoporosis	S1PR1-S1PR3 regulate synoviocytes survival, migration, cytokine production. Antagonists of SphK and S1PR may be useful	[34,35]
		pFTY720 reduces osteoclast number and osteoporosis in an ovariectomized mouse model of postmenopausal osteoporosis	[36]
Cancer	Cancer	Cancer cells promote production of S1P via up-regulation of SphK1. This promotes infiltration of mast cells, ECs, platelets, fibroblasts and neutrophils, resulting in an inflammatory response and tumour angiogenesis.	[37,38-40]

Table 1.4: Association of S1P/S1PR signalling with disease.
Please see Appendix 2 for references.

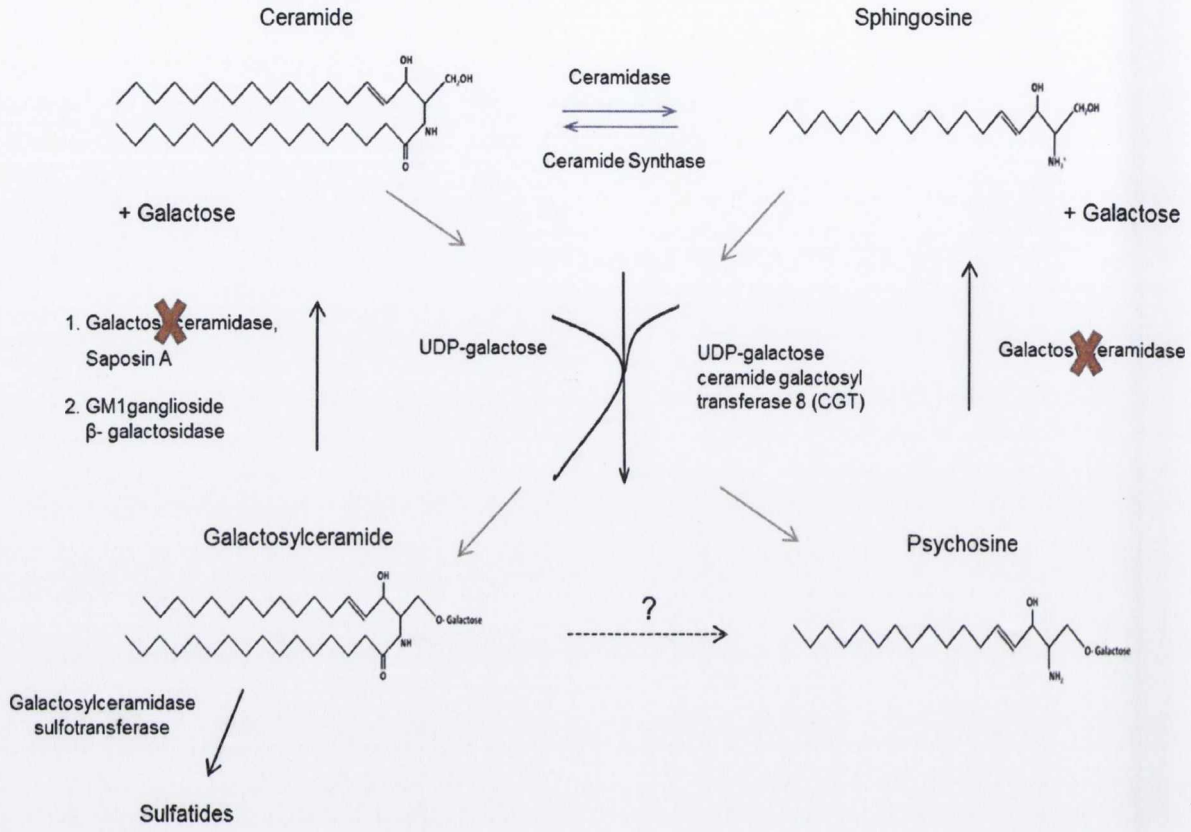

Figure 1.10. Psychosine synthesis. The biosynthesis pathway of psychosine is not well understood. It is believed that psychosine is synthesized by the transfer a galactose residue from UDP-galactose to sphingosine bases via the action of UDP-galactose ceramide galactosyl transferase 8 (CGT). Psychosine is then broken down by the action of galactosylceramidase, which is the deficient enzyme in Krabbe disease (denoted as deficient in diagram by an X).

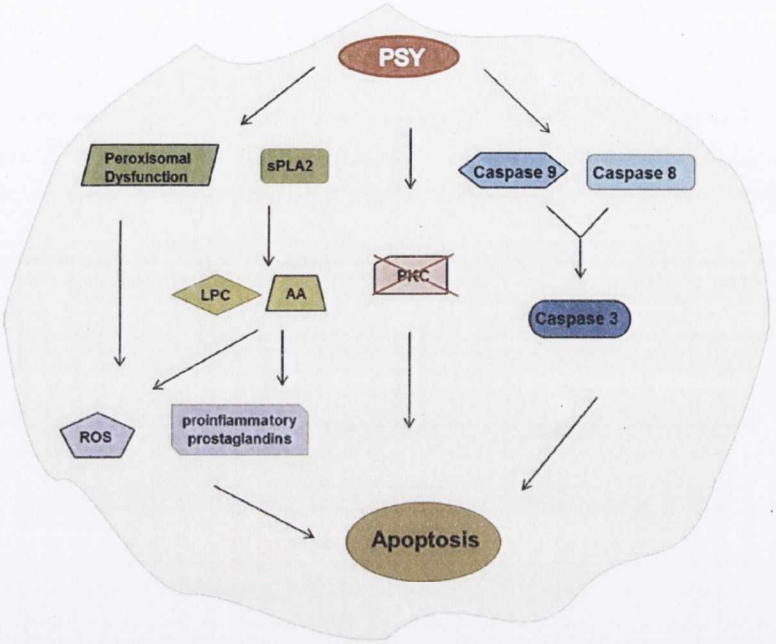

Figure 1.11. Mechanisms of psychosine cytotoxicity in oligiodendrocytes. The above schematic depicts some of the proposed mechanisms by which psychosine exerts its toxic effects on oligodendrocytes. AA: Arachidonic acid, LPC: lysophosphatidylcholine, PSY: psychosine, sPLA2: secreted phospholipase A2, cPLA2: cytosolic phospholipase A2, ROS: reactive oxygen species.

5. Conclusion

The pleiotropic mediator, S1P, plays a role in many physiological and pathophysiological processes within the immune, cardiovascular and central nervous systems. Crystallisation of the first member of the S1PR family **(Hanson et al., 2012)** has now highlighted many of the key interactions between S1PR1 and its ligands. Understanding the structure of the S1PR1 subtype has benefited in designing new, more specific agonists and antagonists and perhaps, in the future, development of allosteric modulators. The uses of such selective compounds will likely also help to further elucidate the role of S1PRs in normal and disease states. Given that (i) aberrant S1P levels and S1PR signalling has been reported in a range of diseases, (ii) Gilenya® has proven useful in the clinic, and (iii) novel selective S1PR1 agonists and antagonists are in development, investigating this S1P/S1PR signalling pathway in other autoimmune and demyelinating disorders like KD could now prove therapeutically worthwhile. In addition, elucidation and understanding of the interaction of S1PR1 with its putative interacting proteins may provide additional strategies for the development of novel therapeutic agents that regulate the function of these receptors.

Chapter 2. Materials and Methods

1. Materials

1.1 Chemicals

The following chemicals and reagents were used: Agar (Fisher Scientific, Ireland), Agarose (Fisher Scientific, Ireland) , Ampicillin (Sigma-Aldrich, Ireland), BamH1 (Roche Applied Science, UK) Calcium chloride ($CaCl_2$, $2H_2O$) (Sigma-Aldrich, Ireland), D-(+)-glucose (Sigma-Aldrich, Ireland), DH5α chemically competent cells (Invitrogen, Ireland), EcoR1 (Roche Applied Science, UK), Ethanol (Sigma-Aldrich, Ireland), exACTgene 1 kb DNA ladder (Fisher Scientific, Ireland), GelRed (Biotium, Ireland), Glycerol (Sigma-Aldrich, Ireland), Luria Bertani (LB) Broth Miller (Fisher Scientific, Ireland), Magnesium chloride ($MgCl_2$, $6H_2O$) (Sigma-Aldrich, Ireland), Magnesium sulfate ($MgSO_4$) (Sigma-Aldrich, Ireland), 2-mercaptoethanol (Gibco, Ireland), One shot BL21 competent cells (Invitrogen, Ireland), Plasmid Maxi kit (Qiagen, UK), 2-propanol (Sigma-Aldrich, Ireland), Sodium chloride (NaCl) (Sigma-Aldrich, Ireland), SuRE/Cut buffer A (Roche Applied Science, UK), Acetic acid (Sigma-Aldrich, Ireland), Acrylamide 30% / bis solution 37.5 (Bio-Rad, Ireland) 6-aminohexanoic acid (Sigma-Aldrich, Ireland), Ammonium persulfate (Sigma-Aldrich, Ireland), B27 supplement (Invitrogen, Ireland), Bovine serum albumin (BSA) (Sigma-Aldrich, Ireland), Brilliant blue R-250 (Coomassie blue) (Fisher Scientific, Ireland), Dimethylsulfoxide (DMSO) (Sigma-Aldrich, Ireland), Dulbecco's modified Eagle medium (DMEM/F12) (Fisher Scientific, Ireland) DMEM high glucose (Biosera, UK), Dulbecco's Phosphate buffered saline (1x) (Invitrogen, Ireland), Ethylenediaminetetraacetic acid (EDTA) (Sigma-Aldrich, Ireland), Fetal bovine serum (FBS) heat inactivated (Biosera, UK), Formaldehyde 37% solution (Sigma-Aldrich, Ireland), Glutamax (Invitrogen, Ireland), Glycine (Fisher Scientific, Ireland), HEK293T cells (ATCC, UK), HEPES (Invitrogen, Ireland), Hydrochloric acid (HCl) (Sigma-Aldrich, Ireland), Isopropyl β-D-1-thiogalactopyranoside (IPTG) (Sigma-Aldrich, Ireland), L-glutamine (Sigma-Aldrich, Ireland), Laemmli buffer (Bio-Rad, Ireland), Lipofectamine transfection reagent (Invitrogen, Ireland), Lysozyme (Roche Applied Science, UK), Methanol (Fisher Scientific, Ireland), Neurobasal A medium (Invitrogen, Ireland), N,N,N',N'-tetramethylethylenediamine(TEMED) (Sigma-Aldrich, Ireland) Normal goat serum (Vector Laboratories, UK) Optimem I reduced serum medium (Invitrogen, Ireland), Penicillin/streptomycin (Sigma-Aldrich, Ireland), Phosphate buffered saline (PBS) (Invitrogen, Ireland), PlusReagent (Invitrogen, Ireland), Poly-L-lysine hydrobromide (Sigma-Aldrich, Ireland), Potassium chloride (KCl) (Sigma-Aldrich, Ireland), Potassium phosphate (K_2HPO_4, $3H_2O$) (Sigma-Aldrich, Ireland), Precision Plus Protein Dual color standard (Bio-Rad, Ireland), Sodium chloride (NaCl) (Sigma-Aldrich, Ireland), Sodium dodecyl sulfate (SDS) (Sigma-Aldrich, Ireland), Sodium hydroxide (NaOH) (Sigma-Aldrich, Ireland), Sodium phosphate (Na_2HPO_4, $7H_2O$) (Sigma-Aldrich, Ireland), Sodium phosphate (NaH_2PO_4, H_2O) (Sigma-Aldrich, Ireland), Sodium pyruvate (Sigma-Aldrich, Ireland), Tris base (Fisher Scientific, Ireland), Triton X-100 (Sigma-Aldrich, Ireland), Trypan blue solution (0.4%) (Sigma-Aldrich, Ireland), Trypsin-EDTA solution (0.25%) (Sigma-Aldrich, Ireland), Tween-20 (Sigma-Aldrich, Ireland), Vectashield mounting medium (Vector Laboratories, UK), Water, Hyclone cell culture grade (Thermo Scientific, Ireland), Western Chemiluminescent HRP substrate (Millipore, Ireland).

1.2 Compounds

All experiments used the pure active (S)-enanotiomer of pFTY720 (2-amino-2-[2-(4-octylphenyl)ethyl] propane-1,3-diol)prepared as a 10mM stock solution in 90% DMSO and 20mM HCL. S1PR3 agonist and antagonist, CYM5541 (Tocris bioscience, 4897) and TY52156

(Tocris bioscience, 5328) were prepared as a 10mM stock solution in DMSO. Psychosine was prepared as a 10mM stock solution in DMSO. Lysolecithin from egg yolk (L-α-Lysophosphatidylcholine, LPC, Sigma, L4129) was prepared as a 25mg/ml stock in serum free media. LPS was prepared as a 1mg/ml stock solution in sterile water (Sigma, L2630). The cytokines used were interleukin 17A (IL17A) (R&D Systems, 17-ILB) and tumor-necrosis factor α (TNFα) (R&D Systems, 210-TA). All the above compounds were stored in aliquots at -20°C.

1.3 Antibodies

All primary antibodies used in study are listed in Table 2.1. Primary rabbit polyclonal antibodies were: anti-glial fibrillary acidic protein (GFAP, Abcam, ab7260), anti-myelin basic protein (MBP, Abcam, ab40390), anti-S1PR1 (Santa-Cruz, sc-25489), anti-Pex14 (Millipore, ABC142), anti-phospho-Akt (Cell Signalling, S473), anti-Myc tag (Santa-Cruz, sc-789) anti-Iba1 (Wako, 019-19741). Primary mouse monoclonal antibodies used were: anti-vimentin (Santa Cruz, sc-373717), anti-V5 tag (Abcam, ab27671), anti-myelin oligodendrocyte glycoprotein (MOG, Millipore, MAB5680), anti-Myc tag (Millipore, 05-419), anti-S1PR1 (Millipore, MABC94), anti-actin (Abcam, ab3280), anti-ERK (Millipore, 05-1152) and anti-NG2 (Millipore, 05-710). The other antibodies used were: chicken polyclonal anti-neurofilament heavy chain (NFH, Millipore, AB5539) and anti-βIII tubulin (Millipore, AB9354) and rabbit polyclonal antibody anti-phospho-ERK1/2 (Millipore, (05-797R).

All secondary antibodies used in study are listed in Table 2.2. Secondary antibodies used for immunocytochemistry were: anti-mouse 488 (Invitrogen Alexa, A28175), anti-mouse 633 (Invitrogen A-21126), anti-mouse Dylight 549 (Jackson ImmunoResearch, 715-505-020), anti-rabbit 488 (Invitrogen Alexa, A27034), anti-rabbit 633 (Invitrogen Alexa, A21070), anti-chicken 633 (Invitrogen Alexa, A21103), biotinylated anti-rabbit (Vector, BA-1000) and avidin-alexa 488 coupled secondary antibody (Invitrogen, S-11223). Secondary antibodies used for Western blotting and conjugated to horse-radish peroxide (HRP) were: donkey anti-rabbit IgG (GE Healthcare, NA934) and goat anti-mouse (Sigma, A8924).

1.4 Stains

Dyes and chemicals used for cellular staining were: nuclear staining Hoechst 34580 (Invitrogen, H21486), Fluo-4 (Invitrogen, F-14127), 3-(4,5-Dimethylthiazol-2-yl)-2,5—Diphenyltetrazolium bromide (MTT, Invitrogen, M6494) and 5,5",6,6"-tetrachloro-1,1",3,3"-tetraethylbenzimidazolcarbocyanine iodide (JC-1, Fisher, T-3168).

2. Methods

2.1. Cell Culture

2.1.1 Aseptic technique

All *in vitro* cell culture procedures were carried out under strict aseptic technique. All instruments used were thoroughly sterilised before and after use using an autoclave and sprayed with 70% ethanol before being placed in the laminar flow hood (Mason Technologies, Ireland). The interior of the laminar flow hood including all equipment were exposed to a germicidal UV lamp which emits ultraviolet radiation at 253.7nm to ensure sterility. The tissue culture preparation took place under the laminar flow hood and all cells were kept in an incubator and the temperature and CO^2 concentration was maintained at a constant rate of 37°C and 5% respectively. A cell culture laboratory coat was worn at all times and gloved hands were sprayed with 70% ethanol before entering the hood or the incubator to ensure sterility.

2.1.2 Preparation of coverslips

For the application of immunocytohistochemistry cells were grown on borosilicate glass coverslips with a diameter of 13mm (VWR, Ireland). These coverslips first had to be sterilized prior to use by immersion in 70% ethanol followed by exposure to UV light overnight. Sterile poly-L-lysine solution (40µg/ml in sterile H_20: Sigma-Aldrich, UK) was then coated onto glass coverslips and incubated overnight at 37°C and 5% CO_2. The solution was aspirated using pasteur pipettes and each glass slide washed with sterile dH_2O (Invitrogen, USA). The H_2O was then removed and the coverslips subsequently laid out in the laminar flow hood to dry.

2.1.3 Preparation of mixed cortical glia

Primary cortical mixed glial cultures were prepared using postnatal one day old female Wistar (Harlan, UK) rats or postnatal one day old (P0) C57BL/6 mice (supplied by the Bioresources Unit, Trinity College Dublin). Aseptic technique was strictly adhered to throughout the procedure. Using a sterile dissection kit the pups were sacrificed by decapitation in accordance with The Animals Act 1986 (Scientific Procedures) Schedule I guidelines. The skull was exposed by cutting the skin from the base of the skull down to the tip of the nose. The skull was removed by making a sagittal cut along the level of the medial longitudinal fissure and two horizontal cuts along each side of the skull at the level of the ears. Using a curved forceps, the skull was peeled back revealing the cortex which was pinched off from both hemispheres. The hemispheres were then placed in a petri dish with pre-warmed Dulbeco's Modified Eagle Medium F12 (DMEM/F12; Fisher, SH30023.01) which was supplemented with 10% heat inactivated foetal bovine serum (FBS) (Labtech, FB-1090) and 1% penicillin/streptomycin (Sigma, P4333). The meninges were peeled off from the cortices using a fine straight forceps and disposed of. The cortices were then transferred into fresh supplemented DMEM/F12 pre-warmed to 37°C. With a sterile disposable scalpel, the cortices were cross chopped. The chopped tissue was triturated and passed through a sterile nylon mesh cell strainer (40µM; BD Biosciences, USA). Additional astrocyte media was added to the tissue (~10ml) and the mixture was transferred to a sterile 50ml falcon tube. The cells were suspended in the solution by gently pipetting up and down. The mixture was then centrifuged at 3,000rpm for 5 min. The resulting cell pellet was re-suspended in 40mls pre-warmed astrocyte media. This 40ml suspension was then split between four poly-L-lysine coated T75 flasks (Cat #83.1813.002, Sarstedt AG, Nümbrecht, Germany). Cells were left to attach in the incubator for 4 h at 37°C

and 5% CO_2 followed by the addition of 10mls of media. The media was subsequently changed every 3 days for ~ 12 days.

2.1.4 Preparation of astrocyte and microglia cultures

Mixed glial cultures were first prepared exactly as described above. Due to the differential adhesion properties of glial cells, astrocytes and microglia can be separated by a 'shake-off' method. Once the cells reached confluency the neck and caps of the T75 flasks were made air tight with parafilm and shaken for 3 h at 37°C and 200 RPM in an orbital shaker (Excella E24, New Brunswick Scientific, Boulevard Enfield, CT, USA). Each flask then receives a few hard taps and the media containing the microglia was collected and centrifuged at 3000rpm for 3 min at room temperature. The microglia were then re-suspended in supplemented DMEM/F12, counted and plated into 24 well plates. Astrocytes strongly adhere to the bottom of the culture flasks and hence require trypsin-EDTA to detach the cells. For this the astrocytes were washed in sterile water and incubated for 10 min with 2ml of 0.1% trypsin-EDTA (Sigma-Aldrich, UK) until the astrocyte layer lifted. FBS (contains alpha-1-antitrypsin) supplemented DMEM/F12 was then added to the T75 flasks to inhibit the action of the trypsin. The media and free astrocytes were removed and centrifuged at 3000rpm for 5 min at room temperature. The resulting pellet was re-suspended in supplemented DMEM/F12, cells were counted and then plated into the required 96 well, 24 well or 6 well plates.

2.1.5. Preparation of Human Astrocyte Cultures

Human astrocytes from a male fetal brain (cerebal cortex) at 21 weeks gestation were purchased from ScienCell Research laboratories US (1800, Lot No. 9063) as previously described **(Healy et al., 2013)**. Each vial contained 1 mL of cryopreserved cells (>5 x 10^{x6}) at passage one and were delivered frozen. To culture these cells, 1ml aliquots of human astrocyte cells were removed from -80°C storage and thawed quickly (1-2 min) in a water bath at 37°C. The cells was added to a T25 cm^2 flask containing 9 mL of DMEM/F12, supplemented with 10% heat-inactivated FBS, 1% penicillin/streptomycin and 1% astrocyte growth supplement (ScienCell, 1852), named supplemented media hereafter. Cells were mixed by gently swirling the flask and then incubated overnight at 37°C and at 5% CO_2. The next day, the media was replaced with 10 mL of pre-warmed supplemented media and were maintained in supplemented media until they reached a confluency of approximately 90%, at which stage the cells were split. Briefly, the old media was removed and cells washed once with pre warmed sterile PBS. Following this, 1 mL of trypsin-EDTA was added for 2 min to allow cells to detach. To stop trypsinisation, 9 mL of supplemented media was added and cells were re-suspended by gentle pipetting. Depending on the concentration of cells needed, an appropriate volume of this solution was transferred into a T75 cm2 flask containing pre-warmed supplemented media. Cells were then incubated at 37°C, 5% CO_2 until used or further split.

2.1.6. HEK293T and BV2 cell culture

The human embryonic kidney (HEK293T) cell line stably and constitutively expresses the temperature sensitive gene for simian virus 40 (SV40) large T antigen. This cell line is ideal for transfection studies as it displays high efficiency of transfection and protein production. To culture these cells, 1ml aliquots of HEK293T (ATCC) were removed from -80°C storage and thawed quickly (1-2 min) in a water bath at 37°C. The 1ml of HEK293T cells was added to a T25

cm^2 flask containing 9 mL of pre-warmed high glucose Dulbecco's modified Eagle's medium (DMEM) , supplemented with 10% heat-inactivated FBS and 1% penicillin/streptomycin, named supplemented media hereafter. Cells were mixed by gently swirling the flask and then incubated overnight at 37°C and at 5% CO_2. The next day, the media was replaced with 10 mL of pre-warmed supplemented media and were maintained in supplemented media until they reached a confluency of approximately 80%, at which stage the cells were split. BV2 microglia were obtained from Prof. Veronica Campbell (School of Medicine, Trinity College Dublin) and cultured in DMEM supplemented with 2% FBS (Labtech) and 1% penicillin/streptomycin (Sigma) at 37°C and 5% CO_2. When 80% confluent cells were split into 24 well plates to be treated.

2.1.7. Cryogenic Preservation of HEK293T

For long term storage, HEK293T cultures at an early passage number (typically PN=3 or PN=4) were frozen in liquid nitrogen. For cryogenic preservation cells were grown in a T75 flask until 90% confluent. These were then split and thoroughly re-suspended with 9 mL of pre-warmed supplemented media (without antibiotics) and 20% dimethylsulfoxide (DMSO). Cells were counted with a haemocytometer and aliquots of 1 mL were prepared in cryogenic vials. Tubes were transferred immediately at -20°C for 1.5 h before being moved to liquid nitrogen for long-term storage.

2.1.8. Cerebellar Slices

Organotypic slice cultures are an established *in vitro* assay for the study of myelin development and maintenance and represent an excellent compromise between single cell cultures and *in vivo* animal studies. Unlike single cell cultures, organotypic slice cultures preserve the architecture of the brain regions that they originate from and can more accurately represent the complex processes and interactions that occur between cells and their microenvironment.

Organotypic cerebellar slices were prepared using tissue isolated from postnatal day 10 (P10) C57BL/6 mice of either sex (Bioresources Unit, Trinity College Dublin). The cerebellar slice culture method was based on protocols previously published (**Birgbauer et al., 2004**). Briefly, the pups were sacrificed by decapitation in accordance with The Animals Act 1986 (Scientific Procedures) Schedule I guidelines. The skull was exposed and carefully removed. The cerebellum was then separated from the cerebrum and cut into parasagittal slices (400µm) using a McIlwain tissue chopper. Four slices were grown on each cell culture insert (Millicell PICMORG50). Slices were cultured using an interface method with 1mL of medium per 35mm well. For the first three days *in vitro* (DIV) the slices were grown in serum-based media (50% Opti-Mem, 25% Hanks' buffered salt solution (HBSS), 25% heat-inactivated horse serum and supplemented with 2mM Glutamax, 28mM D-glucose, 100U/mL penicillin/streptomycin and 25mM HEPES) at 35.5°C and 5% CO_2. After three DIV the slices were transferred to serum-free media (98% Neurobasal-A and 2% B-27 (Invitrogen), supplemented with 2mM Glutamax, 28mM D-glucose, 100U/mL penicillin/streptomycin and 25mM HEPES).

2.1.9 Treatments

Cells were plated out into appropriate sized plates (96, 24 or 6 well plates) or onto poly-L-lysine coated coverslips, depending on the assay involved. Before all treatments the cells were serum starved for 3-4 h. For this the supplemented media was completely removed from the wells and the cells washed once in sterile PBS. The cells were then incubated in serum-free DMEM/F12 at 37°C and 5% CO_2. Specific treatment details are indicated in the figure legends.

2.2 Cellular and Biochemical Analysis

2.2.1 Cell Membrane Preparation

To examine the expression of endogenous or transfected proteins, a cell membrane preparation containing both soluble and insoluble cell fractions was prepared. Astrocytes and HEK293T cells to be harvested were removed from the wells by scraping with a cell scraper directly in their own media on ice. The now free floating cells were transferred into 2 mL microtubes and centrifuged at 13,000 x g for 5 min at 4°C. The supernatant was discarded and the cell pellet was lysed in 50-500 µL ice-cold PTxE (PBS containing 1% Triton X-100 and 0.1 mM EDTA) depending size of pellet. The cell membrane preparation obtained was either used immediately for immunoblotting studies or stored at -20°C until further use. Cerebellar slices were scraped from the culture membrane and suspended in ice-cold PTxE buffer using sonication and mechanical homogenization.

2.2.2 SDS-PAGE and Western Blot

Samples were mixed with an equivolume of sample buffer (1:20 β-mercaptoethanol in laemmli buffer (Bio-Rad, 161-0737) and boiled for 5 min at 95°C to denature the proteins. Following this, proteins were separated by sodium dodecyl sulfate polyacrylamide gel electrophoresis (SDS-PAGE) which separates proteins according to their molecular weight (Laemmli, 1970). A 10% poly-acrylamide gel (0.38M Tris, 10% acrylamide, 0.1% SDS, 0.005% APS, 0.01% TEMED) and a 4% stacking gel (0.38 M Tris, 4% acrylamide, 0.1% SDS, 0.005% APS, 0.01% TEMED) were prepared. The samples (15 µL) were loaded into separate lanes and one well was loaded with 4-5 µL of protein marker. The gels were run in running buffer (25 mM Tris, 0.19 M glycine, 0.1% SDS, pH 8.3) at 100 V until they reached the top of the resolving gel and then the voltage was increased to 150 V and allowed to run until the proteins had reached the bottom of the gel. The proteins resolved by SDS-PAGE were then transferred using a semi-dry blotting system, onto an Immobilon-P polyvinylidene difluoride (PVDF) membrane (Millipore, IPVH00010). The PVDF membrane was first activated in methanol and then immersed in solution C (25 mM Tris base, 40 mM 6- aminohexanoic acid, 0.02% SDS, 20% methanol, pH 9.4) for 30-60 min. To transfer, the apparatus was set up as follows; anode, two Whatman filter papers soaked with solution A (0.3 M Tris base, 0.02% SDS, 20% methanol, pH 10.4), two Whatman filter papers soaked in solution B (25 mM Tris base, 0.02% SDS, 20% methanol, pH 10.4), PVDF membrane, SDS-gel, two Whatman filter papers soaked in solution C and cathode. The transfer was run for 90 min at 50 mA. The membrane was then blocked for 1 h at room temperature with blocking buffer (5% milk in PBS-T: PBS, 0.05% Tween-20) to prevent non-specific background binding. Primary antibodies were diluted in blocking buffer and incubated with the membrane overnight at 4°C. The blots then received 3 x 15 min washes in PBS-T before HRP-conjugated secondary antibodies were diluted in blocking buffer and incubated with the membrane for up to 2 h at room temperature. The blots were then washed

thoroughly with at least 3 x 15 min washes in PBS-T. To develop the blot, equivolumes of Luminol reagent and HRP substrate peroxide solution were mixed and incubated with the blot for 5 min before they were imaged at different exposure times in a digital dark room.

2.2.3 Immunocytochemistry and Image Analysis

Post transient transfection or post-treatment cells were carefully washed once with 1mL PBS (Sigma Aldrich, UK) and then fixed by incubation for 5 min with ice cold PFA buffer (3.7% formaldehyde in PBS (pH7.4). This was followed by 2 x 5 min washes in PBS. Cells were then permeabilised with PTx buffer (0.1% Triton X-100 in PBS (pH7.4) for 5 min followed by 2 x 5 min washes in PBS. Non-reactive sites were blocked by incubating cells in blocking buffer (2% bovine serum albumin (BSA; Sigma Aldrich, UK) in PBS for 1 h at room temperature. The blocking buffer was then removed and the cells were incubated in primary antibody(s) diluted to their optimum concentration in blocking buffer and left to incubate for 1 h at room temperature or overnight at 4°C. Once the primary antibody was removed the cells received a 1 x 5 min wash in PBS, a further 1 min was in PTx buffer, followed by another 1 x 5 min was in PBS. The cells were then incubated with the appropriate secondary antibody(s), also diluted to their optimum working concentration in blocking buffer, for 1 h. Cell were then washed another 3 x 5 min in PBS. For nuclear staining the cells were incubated with Hoescht (1:1000 in PBS) for 15 min at room temperature, washed 3 x 5 min in 1ml PBS and then left in PBS for mounting. The coverslips were inverted and carefully lowered onto a drop of vectorshield on a glass slide and sealed with nail polish. Cells were visualized using a confocal microscope (Carl Zeiss Axioplan 2 with LSM 510 software or an Olympus FV1000 scanning confocal).

Immunocytochemistry for organotypic slice cultures was performed by first washing the slices in PBS x 2. The slices were then fixed with 4% PFA for 10 min and washed again in PBS. Slices were incubated overnight in TxBN buffer (PBS, supplemented with 0.5% Triton-X100, 10% BSA) to reduce non-specific binding. The slices were then incubated overnight with primary antibodies diluted in PBS supplemented with 0.1% Triton-X100 and 2% BSA, washed twice and incubated in secondary antibodies overnight. The slices received a final 3 washes and were mounted on glass slides with vectorshield and sealed with nail polish. They were then visualised with a Zeiss LSM 700 confocal microscope or an Olympus FV1000 scanning confocal. A total number of 5-6 slices were used per condition and the fluorescence of each cerebellar slice was captured using 5-10 independent regions of interest (ROI). The ROI were selected randomly to cover the whole slice and the mean fluorescence was then calculated using two separate methods. Method 1; for the initial cerebellar slice experiments (Figure 3.5) a total of 25-36 independent ROI observations were made of each 10x slice image and the mean fluorescence was then calculated for each independent experiment. Method 2; for the later experiments (all other slice figures), 9-10 independent regions of the full slice were captured at 20x. The whole fluorescence of the resulting images were then taken and averaged to give the mean fluorescence of that slice. The second method became the standard for analysis of all slice images as it removed the need to select ROIs and hence reduced bias.

2.2.4. Enzyme-linked immunosorbent assay (ELISA)

Supernatants from cell culture were kept and their cytokine content analysed according to manufacturer's instructions using the following ELISA kits from R&D systems: human IL6

(DY206), mouse IL6 (DY406), mouse TNFα (DY410) and mouse IL-1β (DY401). Briefly, 96 well plates were coated with the appropriate capture antibody diluted in PBS and incubated overnight at room temperature. The plates were washed 4 times in wash buffer (PBS, 0.05% Tween-20) and incubated for 1 h at room temperature in blocking buffer (1% BSA, PBS). Standards and samples were added to the plate and incubated at room temperature for 2 h. Plates were washed 4 times with wash buffer and incubated with detection antibody for 2 h at room temperature. Plates were again washed 4 times and incubated with horseradish peroxidase-conjugated streptavidin (Strep-HRP) in the dark at room temperature for 20 min. Plates were washed 4 times in wash buffer and incubated with substrate solution until colour developed. The reaction was stopped using ELISA stop solution (1M H_2SO_4) and the absorbance was read using Labsystem Genesis v3.03 at 450nm. A standard curve was made. Cytokine concentration was assessed by reference to the standard curve and analysed using Graph Pad Prism v5.0.

2.2.5 MTT Assay

Rat astrocytes were plated in 96-well plates and cultured for 24 h until 80% confluent. The cells were first serum starved for 3 h and pre-treated for 1 h with pFTY720 (1 μM). The cells were then treated with increasing concentrations of psychosine (5 μM, 10 μM, 15 μM and 20 μM) for 2 h. After the treatments, media with compounds was removed and replaced with 100 μl of fresh media supplemented with 10 μl of 12 mM MTT (Invitrogen, M6494). The cells were incubated with MTT for 4 h at 37°C. Next, 85 μl of media was removed and 50 μl of DMSO per well was added for 10 min and incubated at 37°C. The samples were then mixed and absorbance read at 540nm. Bar graphs show mean and SEM of the values obtained from the reader.

2.2.6 JC-1 Assay

JC-1 dye (5,5‟,6,6‟-tetrachloro-1,1‟,3,3‟-tetraethylbenzimidazolcarbocyanine iodide can be used as an indicator of mitochondrial membrane potential as it exhibits potential-dependent accumulation in mitochondria. At depolarized (-100 mV) membrane potentials JC-1 exists as green monomers with emission peak at 527 nm. As the membrane is hyperpolarized (-140 mV) JC-1 dye forms aggregates (fluorescence in red, 590 nm). Thus, the quotient between green and red JC-1 fluorescence provides an estimate of membrane potential. Mouse astrocytes were plated in 96-well plates and cultured for 24 h until 80% confluent. The cells were serum starved for 3 h and pre-treated for 1 h with pFTY720 (1 μM). The cells were then treated with increasing concentrations of psychosine (5 μM, 10 μM, 15 μM and 20 μM) for 2 h. The cells were then incubated with a final concentration of 2 μM JC-1 for 15 minutes at 37°C. The plate was centrifuged for 5 min at 400 x g and the media replaced with HBSS (HEPES buffered salt solution). The plate was centrifuged again and the supernatant replaced with 100 μl of fresh HBSS. The fluorescence was then measured in a Spectramax Gemini XS plate reader at an excitation spectrum of 490 nm and emission spectra of 535 and 560nm.

2.2.7 Calcium signalling

Human astrocytes were plated on glass bottom, 35 mm FluoroDishes (World Precision Instruments) and grown until 80% confluent. Cells were washed twice in serum free media and left in fresh serum free media for 3 h. Cells were then washed once with 1 mL 37°C HBSS

(Invitrogen) supplemented with 20 mM HEPES buffer (Invitrogen) and 5.5 mM glucose (Sigma Aldrich). Cells were loaded with 2 µM Fluo-8 AM (Invitrogen) in supplemented 37°C HBSS for 30-40 min at 37°C and 5% CO2. Fluo-8 AM dye was removed and cells were washed with 37°C supplemented HBSS for 20 min in the dark. After the 20 min wash, the buffer was removed and replaced with 1 ml fresh supplemented HBSS. Stimulation of cells was performed by adding BAF312 or glutamate in supplemented HBSS with a manual pipette. Changes in calcium concentration were recorded with an Olympus FV1000 confocal microscope.Baseline recordings were taken for 30 s, test reagents were then added and changes in $_{i}Ca^{2+}$ levels were recorded for a further 120 s. After 150 s, 30 µM glutamate (Sigma Aldrich) was added and recording was continued for a further 90 s. Recordings were terminated at 240 s. Images were obtained at a rate of 1 frame/2 sec for a total of 320 sec at a 512 x 512 pixel resolution and exported as .tiff files. Images were then analysed using the Olympus Fluoview viewer software. Fluorescence was normalised to mean baseline fluorescence (0-30 sec) (ΔF/F0). GraphPad Prism 4 software was used to generate calcium response traces presented as ΔF/F0 over time.

Primary Antibodies				
Antibody	**Host**	**Manufacturer**	**Dilution**	**Purpose**
anti-S1PR1	Rabbit	Santa Cruz	1/200	IHC/CO-IP
anti-S1PR1	Mouse	Millipore	1/200	IHC
anti-myc tag	Rabbit	Santa Cruz	1/200	IHC
anti-myc tag	Mouse	Millipore	1/200	IHC
anti-v5 tag	Mouse	Abcam	1/500 1/5000	IHC/WB/CO-IP
anti-Pex14	Rabbit	Abcam	1/1000	IHC/CO-IP
anti-pERK	Rabbit	Millipore	1/3000	WB
anti-ERK	Mouse	Millipore	1/3000	WB
anti-pAkt	Rabbit	Millipore	1/3000	WB
anti-MOG	Mouse	Millipore	1/3000	IHC/WB
anti-GFAP	Mouse	Millipore	1/10,000	WB
anti-Tubulin	Mouse	Abcam	1/8000	WB
anti-Actin	Mouse	Abcam	1/10,000	WB
anti-MBP	Rabbit	Abcam	1/1000	IHC
anti-NFH	Chicken	Millipore	1/1000	IHC
anti-Iba1	Rabbit	Wako	1/500	IHC
anti-NG2	Mouse	Millipore	1/1000	IHC
anti-βIII Tubulin	Chicken	Millipore	1/1000	IHC
Anti-PLP	Mouse	Millipore	1/1000	IHC

Table 2.1. List of primary antibodies

Secondary Antibodies				
Antibody	**Host species**	**Manufacturer**	**Dilution**	**Purpose**
anti-Rabbit HRP	Donkey	GE Healthcare	1/10,000	WB
anti-Mouse HRP	Goat	Sigma	1/10,000	WB
anti-rabbit Alexa 488	Goat	Invitrogen	1/1000	IHC
anti-Mouse Alexa 488	Goat	Invitrogen	1/1000	IHC
anti-Mouse Dylight 549	Goat	Jackson ImmunoResearch	1/1000	IHC
anti-Rabbit Alexa 633	Goat	Invitrogen	1/1000	IHC
anti-Mouse Alexa 633	Goat	Invitrogen	1/1000	IHC
anti-chicken Alexa 633	Goat	Invitrogen	1/1000	IHC
Biotinylated anti-rabbit	Goat	Vector	1/500	IHC

Table 2.2 List of secondary antibodies

2.3 Molecular Biology Methods

2.3.1 Plasmids used

All cloning was performed by standard molecular techniques and confirmed by sequence analysis by Novartis. Full length mouse S1PR1 (n-terminal myc tagged) (Figure 2.1) was cloned into pLL4.0 **(Osinde et al., 2008)** and human Pex14 (c-terminal v5-tagged) (Figure 2.2) was cloned into pcDNA3.1 (Invitrogen V790-20). The individual intracellular loops (ICL) of S1PR1, ICL1, ICL2, ICL3, C-terminus (CT) and the last 10 amino acids of the C-terminus (CT-10) (Figure 2.3) were cloned into pGEX4T1 (GE Healthcare Life Sciences, 28-9545-49).

2.3.1 Preparation of Competent Cells

A 50 µL aliquot of DH5α Escherichia coli (E.coli) or BL21 E.coli was removed from -80°C storage and streaked directly onto a fresh Luria-Bertani (LB) agar plate (1% tryptone, 0.5% yeast extract, 1% NaCl, 1.5% agar, pH 7.5, autoclaved). The plate was inverted and incubated for 12-14h at 37°C. A single E.coli colony was then picked and inoculated in 5 mL of LB (1% tryptone, 0.5% yeast extract, 1% NaCl, pH 7.5, autoclaved) and incubated at 37°C in an orbital shaker set to 200 rpm for 12-14h. Following this, 2mL of the bacterial culture was aseptically transferred into a flask containing 100 mL LB and incubated with shaking at 200 rpm for 2-3h at 37°C. Optical density (OD) was measured at 595 nm. If the OD was comprised between 0.6-1.0, the incubation was stopped. If inferior to 0.6, the bacterial culture was incubated for a further 30 min and OD measured again. The culture was then aseptically transferred into two sterile pre-chilled 50 mL tubes and centrifuged at 1,000 x g for 15 min at 4°C. The medium was decanted and the pellet resuspended in 20 mL of ice-cold 100 mM $MgSO_4$ and centrifuged at 1,000 x g for 15 min at 4°C. The pellet was finally resuspended in 2 mL of a 100mM ice-cold $CaCl_2$ solution containing 15% glycerol. The resuspension was aliquoted (50 µL) in 1.5 mL microtubes pre-chilled in the -80°C. Tubes were stored at -80°C until needed for bacterial transformation and molecular cloning.

2.3.2 Heat Shock Bacterial Transformation

DNA transformation is a process by which foreign DNA is taken up by a host cell and the genes encoded on it are expressed. For bacterial transformation, the foreign DNA must penetrate the protective membrane so that the intracellular machinery can decode the DNA sequence and express the desired biomolecules. The current methods to increase the permeability of the cell membrane to facilitate such a process include electroporation using an externally applied electrical field and heat shock by a rapid increase in temperature. Electroporation may be undesirable for bacterial transformation because of the high cell mortality rate at these voltages. Heat shock, on the other hand, is a milder procedure and is a viable alternative. Competent *E.coli* (strain DH5α; 50µl) were stored at -80°C in 50µl aliquots. One aliquot of competent *E.coli* was thawed and 1µg of plasmid DNA added. The *E.coli* and DNA were incubated on ice for 30 min and then placed in a water bath at 42°C for 1 min. After 1 min in the water bath the mixture was quickly transferred back to ice for a further 2 min to reduce damage to the E. coli cells. LB broth (450µl) was then added to the competent cells and shaken at 200rpm for 1 h at 37°C. The resultant culture (100µl) was spread on LB agar plates containing 100µg/mL ampicillin (if plasmids contain an Ampicillin resistant gene, AMP^R) and also on a LB plate containing Kanamycin to act as a negative control. This was left to grow for 12-16 h. A single, isolated colony of transformed *E.coli* was selected from the LB agar plate and

inoculated into 5mL of LB broth containing ampicillin. This was then shaken overnight at 200rpm at 37°C. After 12–14 h of the bacteria multiplying, the starter culture appears cloudy. 1ml of this is then aseptically transferred to a large autoclaved flask containing 500mL of LB broth and ampicillin. This too was left to shake (200rpm), for 12-16 h at 37°C. As the bacteria multiply exponentially this larger culture also turns a thick cloudy appearance after 12-16 h. The bacterial cells were then harvested by centrifugation at 6000 x g for 15 min at 4°C and stored at -20°C.

2.3.3 Plasmid DNA Extraction; QIAGEN Plasmid Purification

The principle underlying the QIAGEN plasmid purification protocol is based on a modified alkaline lysis step followed by binding of the plasmid DNA to the positively charged Diethylaminoethyl (DEAE) groups on the surface of the QIAGEN Anion-Exchange Resin. Whether the DNA remains bound or is eluted from the column is determined by the salt and pH conditions. Impurities such as RNA, proteins, dyes, and carbohydrates are removed by a medium-salt buffer while plasmid DNA is eluted in a high-salt buffer.

RNase A and LyseBlue reagent were added to Buffer P1 and the bottle shaken before use to ensure LyseBlue particles were completely resuspended. The bacterial pellet was then resuspended in 10ml of Buffer P1 by pipetting up and down until no cell clumps remained. 10 ml of Buffer P2 was added (turning the cell suspension blue) and mixed thoroughly by vigorously inverting the sealed tube until a homogeneously coloured suspension was achieved. This was incubated at room temperature (15–25°C) for 5 min and 10 ml of pre-chilled Buffer P3 was added. This was mixed immediately by vigorously inverting until all trace of blue was gone and a fluffy white precipitate containing genomic DNA, proteins, cell debris and KDS was left and incubated on ice for 20 min. In order to remove the precipitate, the suspension was centrifuged at 20,000 x g for 30 min at 4°C and the supernatant containing the plasmid DNA was promptly collected and centrifuged again at 20,000 x g for 15 min at 4°C. Next the QIAGEN-tip 500 was equilibrated by adding 10ml of Buffer QBT to the column and allowing it to flow through by gravity. Once the column was equilibrated the supernatant from the second centrifuge step was applied to the column and allowed to flow through. The QIAGEN-tip was then washed through with 2 x 30 ml of supplied Buffer QC (in order to remove contaminants from the plasmid DNA preparation) and the DNA eluted with 15ml of pre-warmed (65°C) Buffer QF. Addition of room temperature isoproponal (10.5ml) followed by immediate centrifugation at ≥15,000 x *g* for 30 min at 4°C precipitated out the DNA. The supernatant was carefully decanted and the pellet washed with 5 ml of room-temperature 70% ethanol, and centrifuged at ≥15,000 x *g* for 10 min. Again the supernatant was carefully decanted and the pellet air dried. Once dry, the DNA was re-dissolved in EB buffer, pH 8.0 and stored at -20ºC. To determine the yield, DNA concentration was determined spectrophotometrically at 260nm and quantitatively analysed on an agarose gel. For list of buffers used see **Table 2.3.**

2.3.4 Restriction Digest

Digestion of DNA is carried out with restriction enzymes, also referred to as restriction endonucleases. These enzymes recognize short, specific (often palindromic) DNA sequences, usually in the range of 4-base (tetramer), 5-base (pentamer) or 6-base (hexamer) long sites located on the incoming DNA, and make double-stranded cuts. Physiologically, their main role

appears to be in protecting cells from invading foreign DNA's, especially bacteriophage DNA. These sites however can be found randomly in the DNA of the organism that produces the restriction endonuclease and hence all organisms possess a methyl transferase that recognizes and methylates the same site that the endonuclease cuts, in order to protect its own sites from restriction. To digest the purified plasmid DNA, the correct restriction enzymes needed to cleave the DNA at the required sites (1 µl), 10xBuffer (2 µl) suitable for the restriction enzymes used, DNA (1 µg) and H_2O were pipetted together in order to achieve a final volume of 25 µl. The digestion reaction was then left to proceed for 2 h at 37°C before 5 µl of the digested sample was added to loading buffer (30% glycerol and 0.25% bromophenol blue) and ran on an agarose gel. See Table 2.4 for list of restriction enzymes used.

2.3.5. Gel Electrophoresis

After restriction digest, DNA can then be analysed using gel electrophoresis. Agarose gel electrophoresis was carried out essentially as described by Shambrook and Russel **(Sambrook and Russel, 2001)**. A 1% agarose gel was prepared by mixing agarose powder with Tris/borate/EDTA (TBE) buffer and then heated in a microwave oven until completely melted. Gel-red, (nucleic acid gel stain), was supplemented in the agarose gel for visualising DNA using a UV transilluminator in a long wave length (302nm). The solution was then poured into a casting tray containing a sample comb and allowed to solidify at room temperature. After the gel solidified the comb was removed and the gel, still in its plastic tray, was inserted into the electrophoresis chamber and covered with TBE buffer. Samples of cut and uncut DNA were mixed with 2x loading buffer (30% glycerol and 0.25% bromophenol blue) and then pipetted into the sample wells. A constant current of 100 V was applied until the DNA had migrated three quarters of the way down the agarose gel towards the positive electrode, (bromophenol blue dye migrates through agarose gels at roughly the same rate as double-stranded DNA fragments allowing for the distance the DNA had migrated to be monitored.

2.3.6 Lipofectamine Trasnfection of Cells

Cells for transfection were plated out into 6 well plates or onto poly-L-lysine coated on glass slides at approximately 30-50% confluency and allowed to recover in a 37°C incubator with 5% CO_2 overnight. The culture media was then aspirated off and replaced with pre-warmed Opti-MEM and returned to the incubator. Two microfuge tubes (A and B) were set up for each well to be transfected and 500µl of Opti-MEM placed in each. The DNA (1µg) to be transfected into the cells was added to microfuge tube A. LipofectAMINE 2000 reagent (4µl) (Invitrogen, USA) was then added to each microfuge tube B, mixed gently and left to sit for 5 min. The contents of tubes A were slowly pipetted into the corresponding tubes B, mixed gently by slow pipetting and incubated at room temperature for 15 min. The Opti-MEM was then removed from the cells to be transfected and replaced with 1 ml of the reaction mix. This was left in the 37°C incubator with 5% CO_2 for 4-6 h. After this incubation time, supplemented media was added to the Opti-MEM/DNA and returned to the incubator overnight. The next morning the media was replaced by pre-warmed supplemented media and the cells were let to incubate for a further 30-40 h.

2.3.7. Preparation of large scale bacterial sonicates

BL21 *E. coli* were transformed using the heat shock method previously described in 2.4.2 A single colony of transformed BL21 *E. coli* was inoculated into 10 mL LB broth, supplemented with 100µg/mL of ampicillin, and left to shake at 200 rpm for 12-16 h at 37°C. Following this, 1 mL of the overnight culture was inoculated into 100 mL of LB broth and left to shake at 200 rpm for 90 min at 37°C. A 1 mL sample of the culture was taken and stored at -20°C before induction with lactose analoge isopropyl β-D thiogalactoside (IPTG). IPTG was aseptically added to the rest of the culture (1 mM final concentration) and shaken 200 rpm at 37°C. After 1 h, 2 h and 4 h, 1 mL samples were taken from the culture and kept at -20°C for further analysis. The IPTG induced culture was centrifuged for 20 min at 1,000 x g at 4°C in 2 x 50 mL tubes. The pellets were then re-suspended in a final volume of 5 mL PBS and rotated with 1 mg/mL lysozyme (Sigma-Aldrich, UK) for 1 h at 5rpm and 4°C, to lyse the bacterial cell wall. Following this, the bacterial cells were sonicated 6 x 10 seconds at 20% amplitude. Triton X-100 (1%) and 0.1mM EDTA were added to the samples and the samples rotated again for 1 h at 5rpm and 4°C to ensure solubilisation. This solubilised cell suspension was then stored in 1 mL aliquots at -20°C until required.

2.3.8. GST pull-down assay

GST fusion proteins (GST-ICL1, GST-ICL2, GST-ICL3 GST-CT and GST-CT10 proteins) (**Figure 2.4**) were purified from *E. coli* strain BL21. Lysates of bacterial cultures (OD_{600} of 0.4–0.5) were prepared by sonication and solubilisation in ice cold PTxE buffer (PBS, 1% Triton X-100, 0.1 mM EDTA, pH 7.4) and lysates were stored in 1 ml (~1 mg total protein) aliquots at -20°C. Pex14-V5 was obtained from transiently transfected HEK293T cells. Cell pellets were thawed on ice and resuspended in 650µl ice cold PTxE. Both GST and GST-fusion protein bacterial lysates (1ml) and Pex14-V5 cell lysates (650µl) were sonicated for 6x10s. Sonicates were solubilised by rotation for 1 h at 4°C in ice-cold PTxE buffer and then centrifuged at 10,000 x g for 20 min in a microfuge. Supernatants of GST and GST-fusion proteins were rotated with 20 µl glutathione Sepharose 4B (GE Healthcare Life Sciences,17-0756-01) in the presence of 1 mg/ml bovine serum albumin (BSA, Sigma) for 30 min at 4°C, after which the coupled Sepharose was washed with 2x1 ml aliquots of PTx buffer (PBS, 0.1% Triton X-100, pH 7.4). Pellets were resuspended in 200 µl PTx buffer and incubated with 300 µl Pex14-V5 (~0.1 mg protein, in PTxE buffer) in the presence of 2 mg BSA. After rotation for 5 h at 4°C, the suspensions were washed with 4 x 1 ml aliquots of PTx buffer. Pellets were finally resuspended in 30 µl PTx buffer and SDS-PAGE was performed. For immunoprecipitation studies, cell sonicates from astrocytes transiently transfected with Pex14-V5 or HEK293T cells transiently co-transfected with Pex14-V5 and myc-S1PR1 were prepared as described above. Aliquots of 500µl cell lysate (~1 mg/ml protein), 20µl of protein G Sepharose beads (Invitrogen) and either 5µg of anti-V5 mAb, anti-Pex14 rAb or anti-S1PR1 rAb were rotated for 2 h at 4°C. The beads were then washed 3 x 1 ml aliquots of PTx buffer and processed for Western blotting.

Buffer	Use	Ingredients
Buffer 1	Resuspension buffer	50mM Tris-Cl ph 8.0 10mM EDTA 100µg/ml RNase A
Buffer 2	Lysis buffer	200mM NaOH 1% SDS (w/v)57yu
Buffer 3	Neutralisation buffer	3.0 M potassium acetate pH 5.5
Buffer QC	Wash buffer	1.0M NaCl 50mM MOPS, pH 7.0 15% isopropanol (v/v)
Buffer QF	Elution buffer	1.25 M NaCl 50 mM Tris·Cl, pH 8.5 15% isopropanol (v/v)

Table 2.3 List of buffers used in QIAGEN plasmid purification

Enzyme	Organism	Recognition sequence	Cut site
Eco R1	Escherichia coli	5'GAATTC 3'CTTAAG	5'---G↓AATTC---3' 3'---CTTAA↑G---5'
Bam H1	Bacillus amyloiiquefaciens	5' GGATCC 3' CCTAGG	5'---G↓GATCC---3' 3'---CCTAG↑G---5'
Pst1	Providencia stuartii	5'CTGCAG 3'GACGTC	5'---CTGCA↓G---3' 3'---G↑ACGTC---5'

Table2.4. List of restriction enzymes.

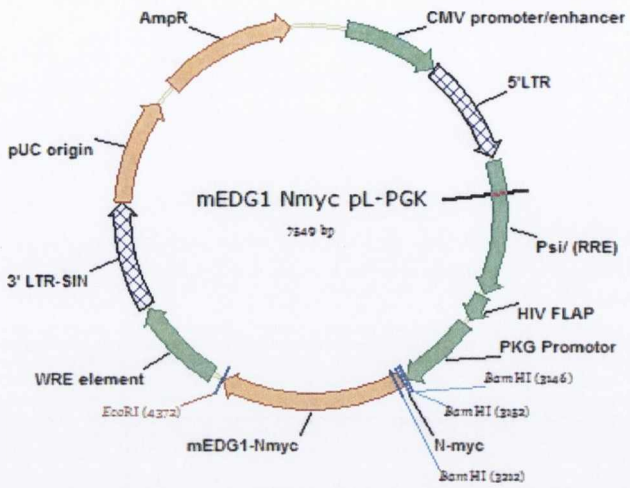

Myc-S1PR1 nucleotide sequence

atggagcagaagctgatctccgaggaggacctgggatccgtgtccactagcatcccggaggttaaagctctccgcagc
tcagtctctgactatgggaactatgatatcatagtccggcattacaactacacaggcaagttgaacatcggggcggag
aaggaccatggcattaaactgacttcagtggtgttcattctcatctgctgcttcatcatcctagagaatatatttgtc
ttgctaactatttggaaaaccaagaagttccaccggcccatgtactatttcataggcaacctagccctctcggaccta
ttagcaggcgtggcttacacagctaacctgctgttgtctggggccaccacttacaagctcacacctgcccagtggttt
ctgcgggaagggagtatgtttgtggctctctctgcatcagtcttcagcctccttgccatcgccattgagcgctacatc
accatgctgaagatgaaactacacaacgggagcaacagctcgcgctcctttctgctgatcagcgcctgctgggtcatc
tccctcatcctgggggcctgcccatcatgggctggaactgcatcagctcgctgtctagctgctccaccgtgctcccg
ctctaccacaagcactatattctcttctgcaccaccgtcttcactctgctcctgctttccatcgtcatcctctactgc
aggatctactccttggtcaggactcgaagccgccgcctgaccttccgcaagaacatctccaaggccagtcgcagttct
gagaagtctctggccttgctgaagacggtgatcattgtcttgagtgtcttcattgcctgctgggcccctctcttcatc
ctactactgttagatgtgggctgcaaggcgaagacctgtgacatcctgtacaaagcagagtacttcctggttctggct
gtgctgaactcaggtaccaaccccatcatctacactctgaccaacaaggagatgcgccgggccttcatccggatcgta
tcttgttgcaaatgccccaacggagactctgctggcaaattcaagaggcccatcatcccaggcatggaatttagccgc
agcaaatcagacaactcctctcacccccagaaggacgatggggacaacccagagaccattatgtcgtctggaaacgtc
aattcttcttcctaa

Myc-S1PR1 amino-acid sequence

M E Q K L I S E E D L G S V S T S I P E V K A L R S S V S D Y G N Y D I I V R
H Y N Y T G K L N I G A E K D H G I K L T S V V F I L I C C F I I L E N I F V
L L T I W K T K K F H R P M Y Y F I G N L A L S D L L A G V A Y T A N L L L S
G A T T Y K L T P A Q W F L R E G S M F V A L S A S V F S L L A I A I E R Y I
T M L K M K L H N G S N S S R S F L L I S A C W V I S L I L G G L P I M G W N
C I S S L S S C S T V L P L Y H K H Y I L F C T T V F T L L L L S I V I L Y C
R I Y S L V R T R S R R L T F R K N I S K A S R S S E K S L A L L K T V I I V
L S V F I A C W A P L F I L L L L D V G C K A K T C D I L Y K A E Y F L V L A
V L N S G T N P I I Y T L T N K E M R R A F I R I V S C C K C P N G D S A G K
F K R P I I P G M E F S R S K S D N S S H P Q K D D G D N P E T I M S S G N V
N S S S Stop

Figure 2.1 myc-S1PR1 vector map, nucleotide sequence and amino acid sequence.

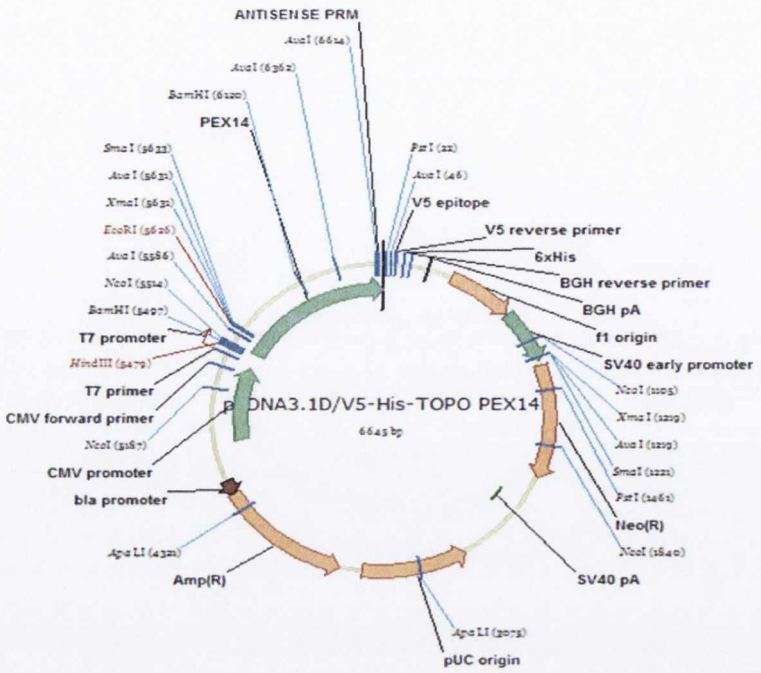

Pex14-v5 nucleotide sequence

atggcgtcctcggagcaggcagagcagccgagccagccaagctctactccaggaagtgaaaatgtgctgcctcgagag
ccgctgattgccacggcagtgaagtttctacagaattcccgggtccgccagagcccacttgcaaccaggagagcattc
ctaaagaagaaagggctgacagatgaagagattgatatggccttccagcagtcgggcactgctgccgatgagccttcg
tccttgggcccagccacacaggtggttcctgtccagccccctcacctcatatctcagccatacagtcccgcaggctcc
cgatggcgagattacggcgccctggccatcatcatggcaggcattgcatttggctttcaccagctctacaagaaatac
ctgctcccccctcatcctgggcggccgagaggacagaaagcagctggagaggatggaggccggtctctctgagctgagt
ggcagcgtggcccagacagtgactcagttacagacgaccctcgcctccgtccaggagctgctgattcagcagcagcag
aagatccaggagcttgcccacgagctggccgctgccaaggccaccacatccaccaactggatcctggagtcccagaat
atcaacgaactcaagtccgaaattaactccttgaaagggcttcttttaaatcggaggcagttccctccatccccatca
gccccgaagatcccctcctggcagatcccagtcaagtcaccgtcaccctccagccctgcggccgtgaaccaccacagc
agcagcgacatctcacctgtcagcaacgagtccacgtcgtcctcgcctgggaaggagggccacagccccgagggctcc
acggtcacctaccacttgctgggcccccaggaggaaggcgaggggtggtggacgtcaagggccaggtgcggatggag
gtgcaaggcgaggaggagaagagggaggacaaggaggacgaggaggatgaggaggatgatgatgtgagccatgtggac
gaggaggactgcctgggggtgcagagggaggaccgccggggcggggatgggcagatcaacgagcaggtggagaagctg
cggcggcccgagggcgccagcaacgagagtgagcgggac

Pex14-v5 amnio-acid sequence

M A S S E Q A E Q P S Q P S S T P G S E N V L P R E P L I A T A V K F L Q N S
R V R Q S P L A T R R A F L K K K G L T D E E I D M A F Q Q S G T A A D E P S
S L G P A T Q V V P V Q P P H L I S Q P Y S P A G S R W R D Y G A L A I I M A
G I A F G F H Q L Y K K Y L L P L I L G G R E D R K Q L E R M E A G L S E L S
G S V A Q T V T Q L Q T T L A S V Q E L L I Q Q Q Q K I Q E L A H E L A A A K
A T T S T N W I L E S Q N I N E L K S E I N S L K G L L L N R R Q F P P S P S
A P K I P S W Q I P V K S P S P S S S P A A V N H H S S S D I S P V S N E S T S
S S P G K E G H S P E G S T V T Y H L L G P Q E E G E G V V D V K G Q V R M E
V Q G E E E K R E D K E D E E D E E D D D V S H V D E E D C L G V Q R E D R R
G G D G Q I N E Q V E K L R R P E G A S N E S E R D

Figure 2.2 Pex14-v5 vector map, nucleotide sequence and amino acid sequence.

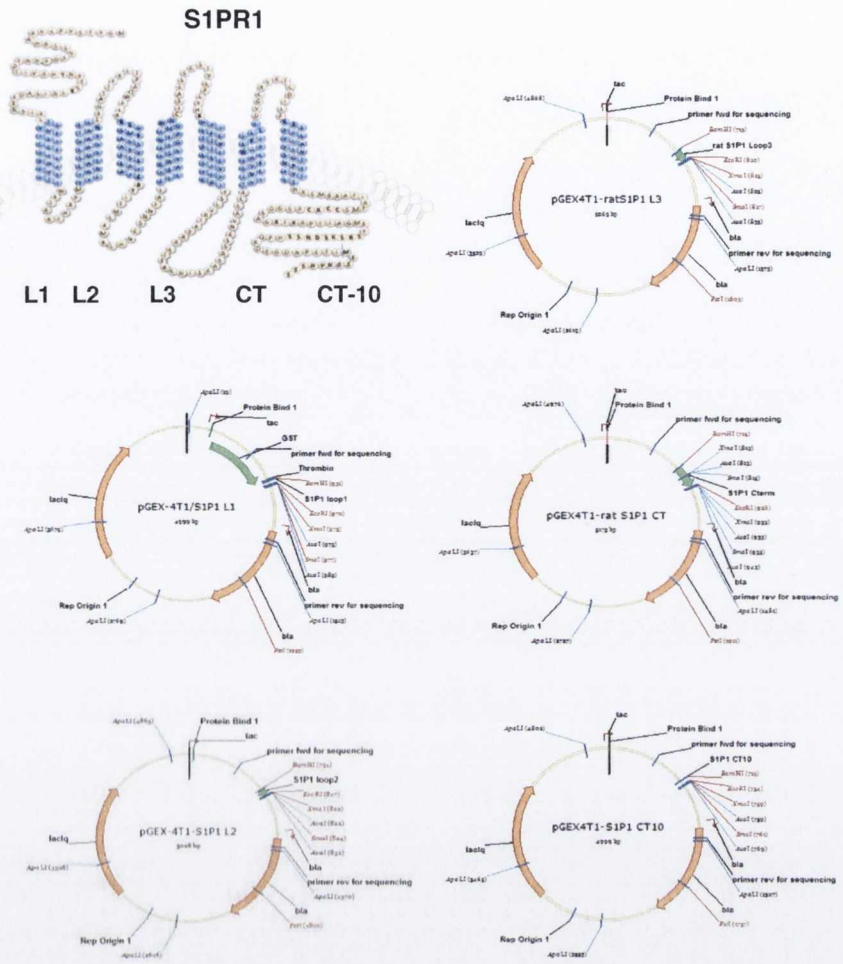

S1PR1 ICL	Nucleotide Sequence	Amino acid sequence
L1	tggaaaaccaagaagttccaccggcccatgtaa	WKTKKFHRPM
L2	gatcccgctacatcaccatgctgaagatgaaactacaca acggcagcaacagctcgcgctcctaag	RYITMLKMKLHNGSNSSRS
L3	gatcctactccttggtcaggactcgaagccgccgcctga ccttccgcaagaacatctccaaggccagccgcagttccg agaagtctctggccttgctgaagtaag	YSLVRTRSRRLTFRKNISK ASRSSEKSLALLK
CT	gatccaacaaggagatgcgccgggccttcatcaggatca tatcttgttgcaaatgccccaacggagactccgctggca aattcaagaggcccatcatcccgggcatggaatttagcc gcagcaaatcagacaactcctcccacccccagaaggatg atggggacaatccagagaccattatgtcttctggaaacg tcaattcttcttcctaag	NKEMRRAFIRIISCCKCPN GDSAGKFKRPIIPGMEFSR SKSDNSSHPQKDDGDNPET IMSSGNVNSSSstop.
CT-10	gatcctcgtctggaaacgtcaattcttcttcctaataag	SSGNVNSSSstop

Figure 2.3 S1PR1 intracellular loop (ICL) constructs. S1PR1 intracellular loop vector maps and nucleotide sequences for L1-CT10. L1= ICL 1, L2 = ICL2, L3 = ICL3, CT = C-terminus and CT10 = the last 10 amino acids of the C-terminus.

A.

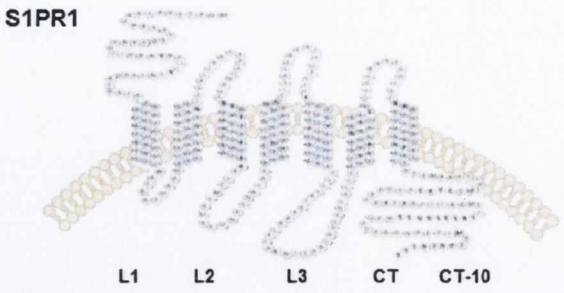

B.

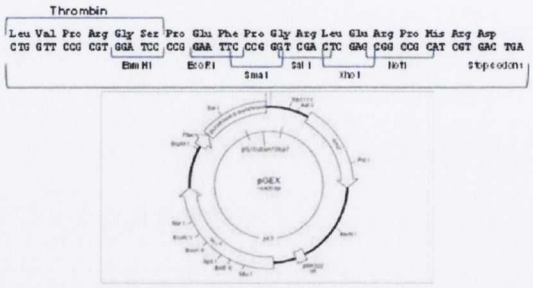

C.

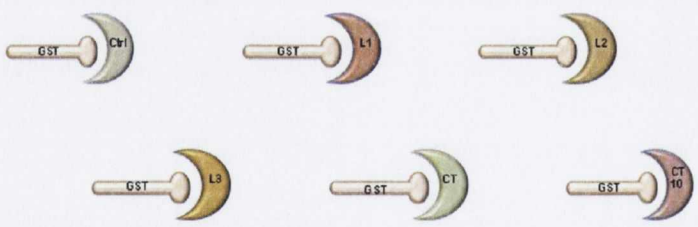

Figure 2.4. S1PR1 GST fusion proteins. GST fusion proteins were constricted by cloning the individual S1PR1 ICL's **(A)** into the multiple cloning site of the pGEX4T-1 vector **(B)**. Diagram of S1PR1 GST fusion proteins **(C).**

Chapter 3. Galactosylsphingosine (psychosine) induced demyelination is attenuated by sphingosine 1-phosphate signalling.

Chapter Aims:

- To investigate the effect of psychosine on astrocyte survival and demonstrate the protective effects of pFTY720 against psychosine-induced cell toxicity.
- To determine the effect of psychosine on astrocyte mitochondrial membrane potential.
- To study the effect of psychosine on pro-inflammatory cytokine release from mouse astrocytes.
- To investigate the effect of psychosine on myelination state in cerebellar slices and explore the protective effects of pFTY720.

Abstract

Globoid cell leukodystrophy (Krabbe disease, KD) is a rare infantile neurodegenerative disorder. KD is caused by deficiency in the lysosomal enzyme galactocerebrosidase (GALC) resulting in brain accumulation, in the micromolar range, of the toxic metabolite galactosylsphingosine (psychosine). Here we find psychosine induces human astrocyte cell death likely via an apoptotic process in a concentration- and time-dependent manner (EC50 ~15μM at 4h). We show these effects of psychosine are attenuated by pre-treatment with the sphingosine 1-phosphate receptor (S1PR) agonist pFTY720 (Fingolimod) (IC50 ~100nM). Psychosine (1μM, 10μM) also potentiates LPS-induced (EC50 ~100ng/ml) production of pro-inflammatory cytokines in mouse astrocytes, which is also attenuated by pFTY720 (1μM). Most notably, for the first time, we show that psychosine, at a concentration found in the brains of patients with KD (EC50 ~100nM) directly induces demyelination in mouse organotypic cerebellar slices in a manner that is independent of proinflammatory cytokine response and that pFTY720 (0.1nM) significantly inhibits. These results support the idea that psychosine is a pathogenic agent in KD and suggest that sphingosine 1-phosphate signalling could be a potential drug target for this illness.

.

1. Introduction

Globoid cell leukodystrophy (Krabbe disease, KD) is a rare autosomal recessive neurodegenerative disorder affecting 1:100,000 live births in the United States **(Wenger et al., 1997)**. This lysosomal disorder typically has an early onset, is rapidly progressing and invariably fatal in infants. The vast majority (85-90%) of cases are of the infantile form, with the juvenile and adult onset forms being considered extremely rare **(Wenger et al., 1997)**. The hallmark symptoms of the infantile form include irritability, hypersensitivity, psychomotor arrest and hypertonia. This is followed by rapid mental and motor deterioration, seizures and optic atrophy. Death usually ensues within the first two years of life and there is currently no cure **(Davenport et al., 2011)**. KD is caused by a mutation in the lysosomal enzyme galactosylceramidase (GALC) **(Suzuki, 2003)**. This GALC deficiency results in the accumulation of a toxic lipid metabolite psychosine (galactosylsphingosine) and to a lesser extent, β-galactosylceramide **(Giri et al., 2002)**. Pathological features of KD include profound demyelination and almost complete loss of oligodendrocytes in the white matter, reactive astrocytosis and infiltration of numerous multinucleated macrophages termed 'globoid cells'. These globoid cells accumulate around blood vessels and in the regions of demyelination and are a unique feature of KD **(Suzuki, 2003)**. Progressive accumulation of psychosine, in the brains of KD patients is thought as the critical pathogenic mechanism of this illness **(Davenport et al., 2011)**. In some cases the levels of psychosine rise more than 100-fold, from sub-nanomolar concentrations to those in the micromolar range **(Svennerholm et al., 1980)**. In KD, the high levels of psychosine escape from lysosomes and dying cells forming aggregates **(Orfi et al., 1997)**. Several reports have demonstrated that psychosine causes direct cellular cytotoxicity by mechanisms that include mitochondrial dysfunction **(Haq et al., 2003)**, caspase activation , alteration of lipid rafts, and modulation of PKC, JNK and NFκB signaling pathways **(Davenport et al., 2011, Yamada et al., 1996, Haq et al., 2003)**. Inflammation is also now accepted to play an important role in the pathogenesis of KD **(LeVine and Brown, 1997)**. Inflammatory molecules, such as AMP-activated protein kinase (AMPK), prostaglandin D, inducible nitric oxide synthase (iNOS) and pro-inflammatory cytokines have all been implicated in KD as well as in the twi/twi mouse animal model of this disease **(Giri et al., 2008)**. Taken together, this increasing evidence now suggests that the loss of oligodendrocytes and wide spread demyelination seen in KD is due to apoptotic processes as well as aberrant inflammatory response **(Tohyama et al., 2001, Giri et al., 2006, Giri et al., 2008, Haq et al., 2003)**.

The GALC enzyme, mutated in KD, is involved in the complex pathway of sphingolipid metabolism, which includes bioactive lipids such as ceramide, sphingosine and sphingosine 1-phosphate (S1P), all of them particularly important in regulating neural cell function. In particular, the family of S1P receptors (S1PRs) are G-protein coupled and expressed in a range of cells, including those of the immune, cardiovascular and central nervous systems **(Dev et al., 2008, Fyrst and Saba, 2010)**. These receptors are drug targets for the drug fingolimod, which is the first oral therapy for relapsing remitting multiple sclerosis (MS) **(Kappos et al., 2010)**. The proposed mechanism of action for fingolimod is reported as being dependent on internalisation of S1PR1s in T cells limiting their S1P-mediated egress from lymph nodes and thus the attenuation of inflammatory response in the brains of MS patients **(Adachi and Chiba, 2008)**. Importantly, a number of studies have now demonstrated that compounds such as

fingolimod can also regulate neuronal and glial cell function **(Fischer et al., 2011, Osinde et al., 2007, Choi et al., 2011, Balatoni et al., 2007)**. Indeed, we and others have shown that S1PRs regulate a number of intracellular signalling pathways in astrocytes and promote astrocyte migration **(Mullershausen et al., 2007, Mullershausen et al., 2009).** In addition, modulation of S1PRs also promotes oligodendrocyte differentiation and survival **(Miron et al., 2008b, Dev et al., 2008)**. S1PRs have also been shown to limit events of demyelination and promote remyelination, which are likely mediated by the dampening of pro-inflammatory cytokine levels **(Sheridan and Dev, 2012, Miron et al., 2010)**. Overall, therefore, S1PRs represent an important drug target that can be exploited for use in neuroinflammatory, demyelinating and neurodegenerative diseases as documented by a growing body of literature **(Asle-Rousta et al., 2013, Deogracias et al., 2012)**. Here we investigate whether regulation of S1P signalling alters psychosine-induced astrocyte dysfunction, pro-inflammatory cytokine release and demyelination.

2. Results

2.1 Psychosine induced human astrocyte cell death is attenuated by pFTY720

The modulation of psychosine on astrocyte cell function is less well studied in KD. We therefore first investigated the effects of this toxin on human astrocyte survival and also demonstrated the protective effects of pFTY720. Cultured human astrocytes were serum starved for 4 h and then pretreated with pFTY720 for 1 h before treatment with psychosine, at the timepoints and concentrations indicated (Figure.3.1A). Psychosine reduced human astrocyte numbers in a concentration dependent manner, where psychosine treatment for 4 h significantly reduced astrocyte cell survival (10 μM, 55.4+/-3.8%; 15 μM, 44.3+/-2.7%; and 20 μM, 39.8+/-1.8%, compared to control). Importantly, pre-treatment with 1μM pFTY720 significantly attenuated the psychosine-induced cell death (reduced by 9.8+/-4.1%, 21.1+/-2.5% and 18.4+/-2.2%, respectively) (Figure.3. 1B). The psychosine (10 μM) induced decrease in survival of human astrocytes was also observed to be time dependent (2 h, 79.2+/-3.2%; 4h, 63.5+/-2.4%; 6 h, 37.1+/-3.3%) and again significantly attenuated in the presence of pFTY720 (reduced by 17.4+/-4.6% at 4 h and 23.1+/-4.3% at 6 h) (Figure. 3.1D). These effects of pFTY720 were also concentration-dependent, where 1 μM pFTY720 significantly increased cell survival by 34.3+/-3.2%, compared to 10 μM psychosine treatment alone (Figure. 3.1E). During the course of our experiments demonstrating psychosine-induced astrocyte cell death and reversal by pFTY720 (Figure. 3.1A-E), we noted these effects were also dependent on the density of cultured astrocytes. To quantify these observations, human astrocytes were seeded at densities ranging from $1.2x10^5$ to $6x10^5$. The cells were then pre-treated with 1 μM pFTY720 followed by 10 μM psychosine treatment for 2 h and imaged (Figure. 3.2A). Human astrocytes seeded at low densities of $1.2x10^5$ and $2.4x10^5$ were most sensitive to psychosine insult, with 81.5+/-6.2% and 68.5+/-5.1% cell death occurring after 2 h treatment. Astrocytes seeded at a density of $3.9x10^5$ displayed 39.4+/-5.3% cell death for psychosine treatment alone, which was significantly attenuated to 20.6+/-3.6% in the presence of pFTY720 (Figure. 3.2B). At the two highest densities, $4.8x10^5$ and $6x10^5$, 10 μM psychosine treatment for 2 h did not induce overt astrocyte toxicity, with cell densities of 94.4+/-3.7% and 99.9+/-5.4%, respectively (Figure. 3.2C).

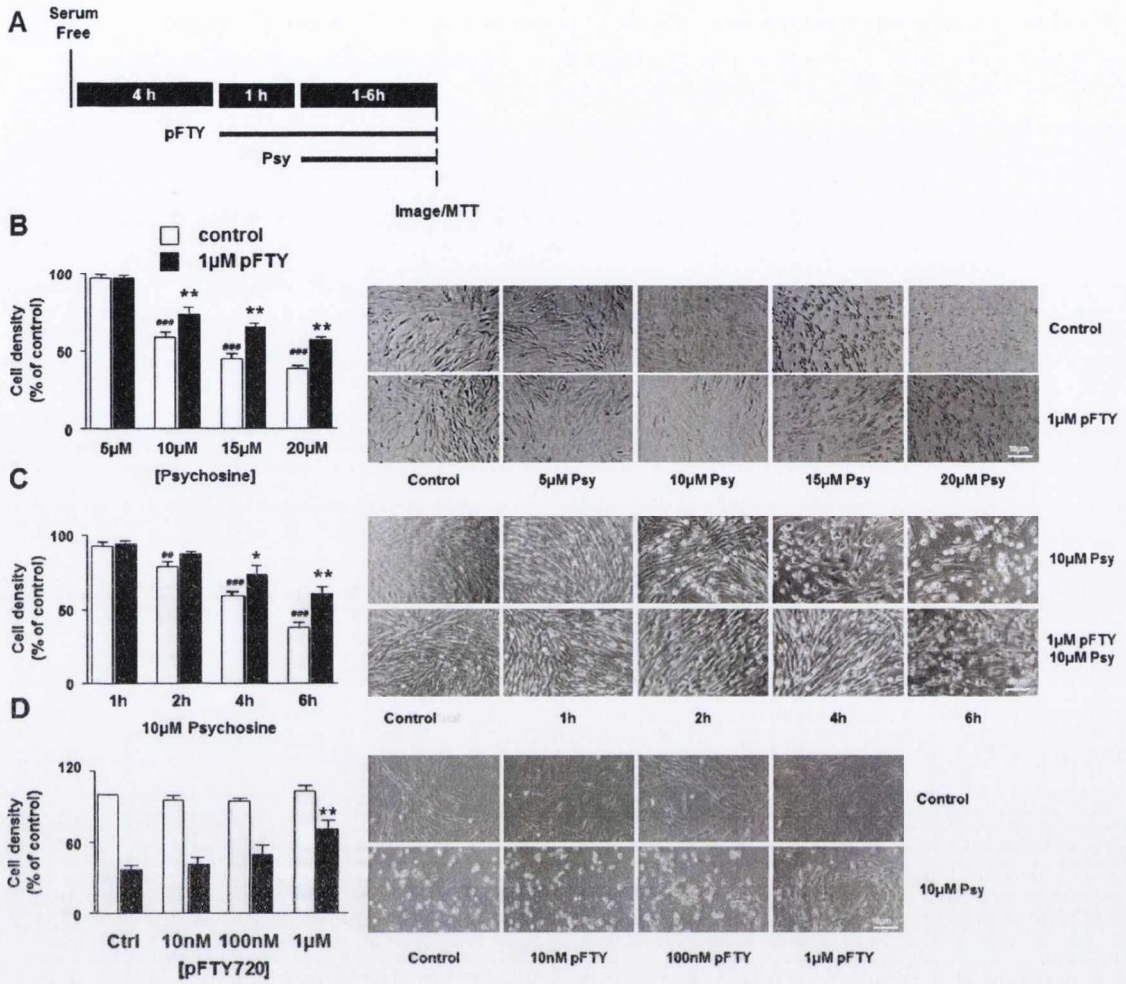

Figure 3.1: pFTY720 attenuates psychosine-mediated astrocyte cell death. (A) Diagram of experimental timeline and treatments. Human astrocytes were pre-treated with 1 μM pFTY720 (pFTY) for 1 h followed by 5 μM, 10 μM, 15 μM and 20 μM psychosine (Psy) for 1-6 h. Cells were imaged under light microscopy. **(B)** Concentration-dependent psychosine induced cell death is attenuated by pFTY. Human astrocytes were treated with 5 μM, 10 μM, 15 μM and 20 μM psychosine for 4 h +/- pFTY. **(C)** Time-dependent psychosine induced cell death is attenuated by pFTY. Human astrocytes were pre-treated with 1 μM pFTY for 1 h followed by 10μM psychosine for 1, 2, 4 and 6 h. **(D)** pFTY attenuates psychosine-induced astrocyte cell death in a concentration-dependent manner. Human astrocytes were pre-treated with 10 nM, 100 nM and 1 μM pFTY for 1 h followed by 10 μM psychosine for 2 h. In all cases, image analysis was performed using Image J software and graphical data is presented as mean +/- SEM (n=3-6). Representative images are also shown. Statistical analysis was performed using one-way ANOVA and Newman-Keuls multiple comparison post-test *p < 0.05, ** p < 0.01 compared to pFTY; ## p <0.01, ### p <0.001 compared to control.

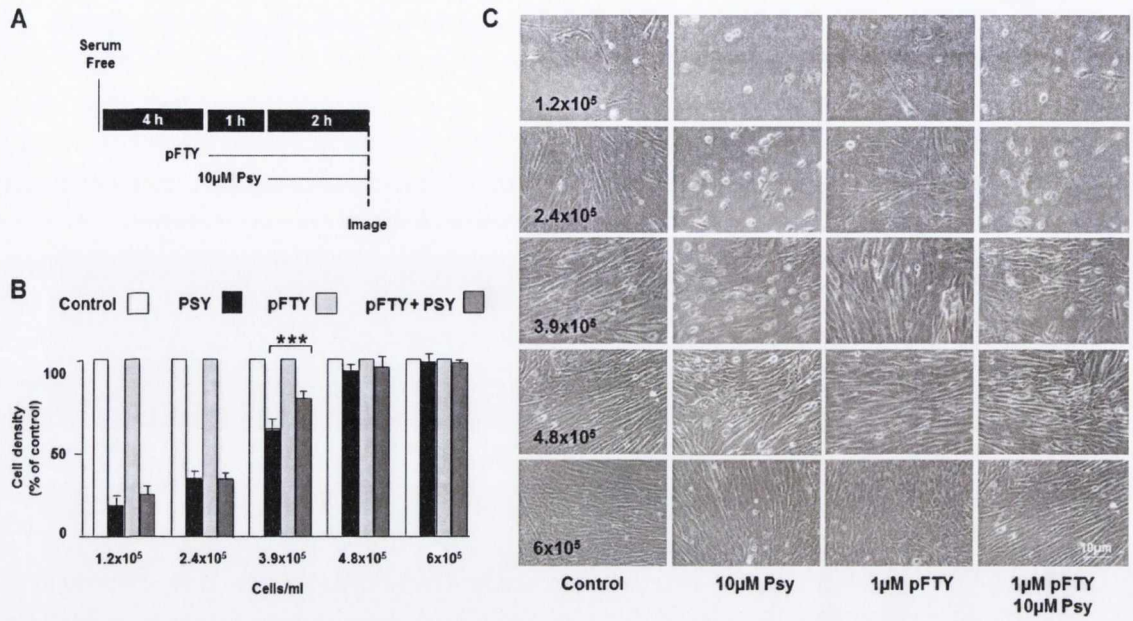

Figure 3.2: Psychosine induced cell toxicity is dependent on astrocyte cell density. (A) Human astrocytes were seeded at densities ranging from $1.2x10^5$ to $6x10^5$, pre-treated with 1 μM pFTY for 1 h followed by 10 μM psychosine for 2 h. **(B)** Image analysis was performed using Image J software. Data presented as mean +/- SEM (n=4), one-way ANOVA and Newman-Keuls multiple comparison post-test *** $p < 0.001$. **(C)** Representative images showing psychosine induced cell loss, with or without pFTY treatment.

2.2 pFTY720 attenuates psychosine-induced decrease of mitochondrial membrane potential in astrocytes

Increasing evidence now suggests the involvement of apoptosis as a mechanism underlying oligodendrocyte cell death seen in KD, where mitochondrial cytochrome *c* release, alterations in electron transport and loss of mitochondrial membrane potential (ΔΨm) occurs **(Haq et al., 2003)**. Here, the ΔΨm was measured using the membrane-permeant dye tetraethylbenzimidazolylcarbocyanine iodide (JC-1), which exhibits potential-dependent accumulation in mitochondria. At high ΔΨm this dye forms aggregates yielding an emission at 590 nm (red) whereas at low ΔΨm JC1 is primarily in monomeric form yielding an emission at 530 nm (green) (Figure. 3A). Cultured astrocytes were serum starved and pre-treated for 1 h with pFTY720 (1 μM) before treatment with psychosine (5 μM, 10 μM, 15 μM, 20 μM). Cells were then loaded with 1 μM JC-1 and after 30 min the emission spectra was measured. Psychosine treatment of mouse astrocytes decreased the aggregate:monomer ratio of JC-1, indicating loss of ΔΨm compared to control (Figure. 3B). Notably, treatment with pFTY720 attenuated the psychosine-induced decrease in aggregate:monomer ratio of JC-1 returning the ΔΨm close to control levels. These findings were supported by use of the MTT colorimetric cell viability assay (based on the reduction of MTT into formazan crystals by metabolically active cells), which showed psychosine caused a significant concentration-dependent reduction of rat astrocyte viability (10 μM, 73.3 +/-2.7%; 15 μM, 63.5+/-3.6%; and 20 μM, 49.9+/-1.7%, compared to control). In agreement, pFTY720 significantly attenuated this psychosine induced cell death by 14.4+/-1.7% and 17.3+/-2.5% at 10 μM and 20 μM psychosine concentrations, respectively (Figure. 3.3C).

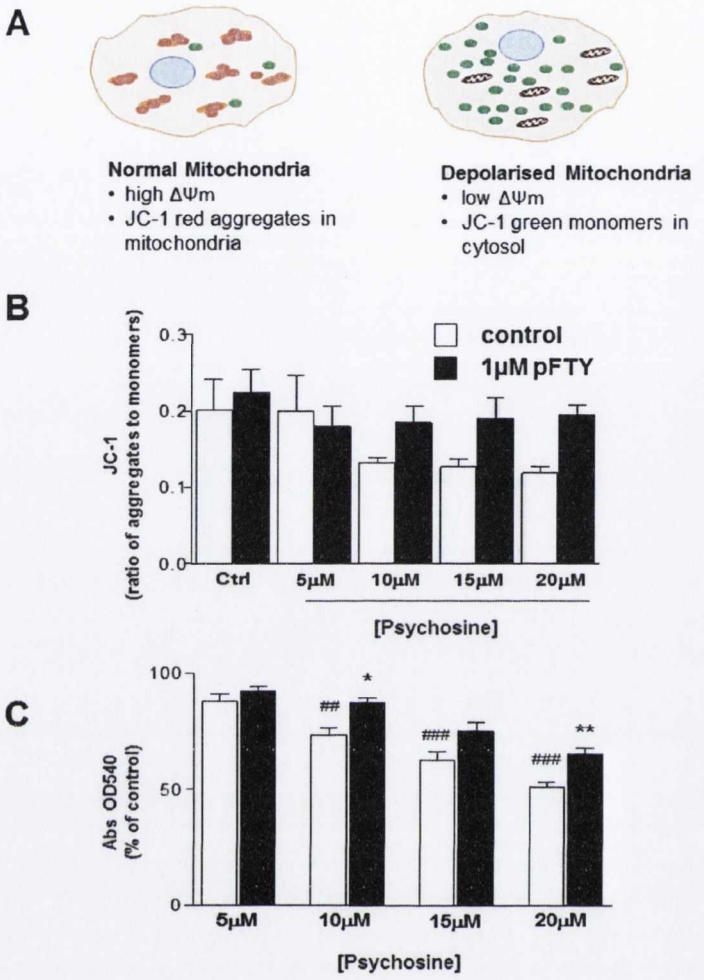

Figure 3.3. pFTY720 attenuates psychosine-induced decrease of mitochondrial membrane potential in astrocytes. (A) Schematic shows that at high mitochondrial membrane potentials JC-1 forms red aggregates (590 nm) in mitochondria while at low mitochondrial membrane potentials the JC-1 is predominately found as a green monomer (535 nm) in the cytosol. **(B)** Treatment of mouse astrocytes with psychosine (2 h) resulted in a decrease in the ratio of red aggregates to green monomers to ~75% of controls, while pre-treatment with pFTY (1 μM, 1 h before addition of pyschosine) attenuated this decrease. Data presented as mean +/- SEM (n=3), unpaired student t-test *$p < 0.05$, ** $p < 0.01$ comparing psychosine +/- pFTY. **(C)** Graph shows MTT assays performed on rat astrocytes treated with psychosine for 2 h +/- pFTY. MTT absorbance read at 540 nm. Data presented as mean +/- SEM (n=3), one-way ANOVA and Newman-Keuls multiple comparison post-test *$p < 0.05$, ** $p < 0.01$ comparing psychosine +/- pFTY; ## $p < 0.01$, ### $p < 0.001$ comparing control +/- psychosine.

2.3 Psychosine potentiates lipopolysaccharide (LPS)-induced levels of pro-inflammatory cytokines in mouse astrocytes

The expression of several pro-inflammatory cytokines and chemokines has been observed in the *twi/twi* mouse model **(LeVine and Brown, 1997)**. Psychosine has also been seen *in vitro* to markedly potentiate the LPS-induced production of pro-inflammatory cytokines in primary rat astrocyte cultures **(Giri et al., 2002)**. Here, we investigated the effect psychosine on the levels of IL6, TNFα and IL1ß in mouse astrocytes in the presence and absence of LPS. Firstly, LPS (1 ng/ml to 10 µg/ml) was shown to induce a concentration dependent increase in the levels of IL6 (Figure. 3.4A), TNFα (Figure.3.4B) and IL1ß (*data not shown*), where 100 ng/mL LPS was selected as the optimal concentration for use in further experiments. Next, cultured mouse astrocytes were serum starved, pre-treated with pFTY720 (1 µM for 1 h) and then treated with LPS (100 ng/mL) and/or psychosine (1 µM and 10 µM) for 3 h, 6 h and 12 h. No discernible release of IL6, TNFα or IL1ß was observed after 3 h treatment with LPS and/or psychosine (*data not shown*). In contrast, the treatment of astrocytes for 6 h with LPS induced at least a 2-fold increase in the levels of IL6 (5.1+/-0.9 pg/ml vs. 31.5+/-4.3 pg/ml) (Figure. 3.4C), TNFα (19.4+/-3.4 pg/ml vs. 48.3+/-2.1 pg/ml) (Figure.3.4D) and IL1ß (1.1+/-0.5 pg/ml vs. 14.3+/-5.5 pg/ml) (*data not shown*), compared to control. Moreover, psychosine (10 µM), while having little effect alone, significantly augmented the LPS induced production of IL6 (31.5+/-4.3 pg/ml vs. 44.8+/-4.2 pg/ml) (Figure. 3.4C) and TNFα (48.3+/-2.1 pg/ml vs. 59.1+/-2.8 pg/ml) (Figure. 3.4D) (Unpaired Student's T test #$p<0.05$). Importantly, pFTY720 treatment significantly attenuated the increased levels of IL6 (44.8+/-4.2 pg/ml vs. 25.6+/-4.9 pg/ml) (Figure. 3.4C) and TNFα (59.1+/-2.8 pg/ml vs. 42.4+/-4.4 pg/ml) (Figure. 3.4D) induced by LPS and/or psychosine (10 µM). Similar findings were observed at 12 h, where pFTY720 attenuated the LPS and/or psychosine (10 µM) mediated increase in levels of IL6 (132.0+/-3.4 pg/ml vs. 56.4+/-21.3 pg/ml) (Figure 3.4E) and TNFα (183.8+/-88.9 pg/ml vs. 78.8+/-25.3 pg/ml) (Figure.3.4F). Collectively, these findings suggest that psychosine may enhance the LPS-induced levels of pro-inflammatory cytokines in astrocytes as previously reported **(Giri et al., 2002)**, and that pFTY720 attenuates these effects.

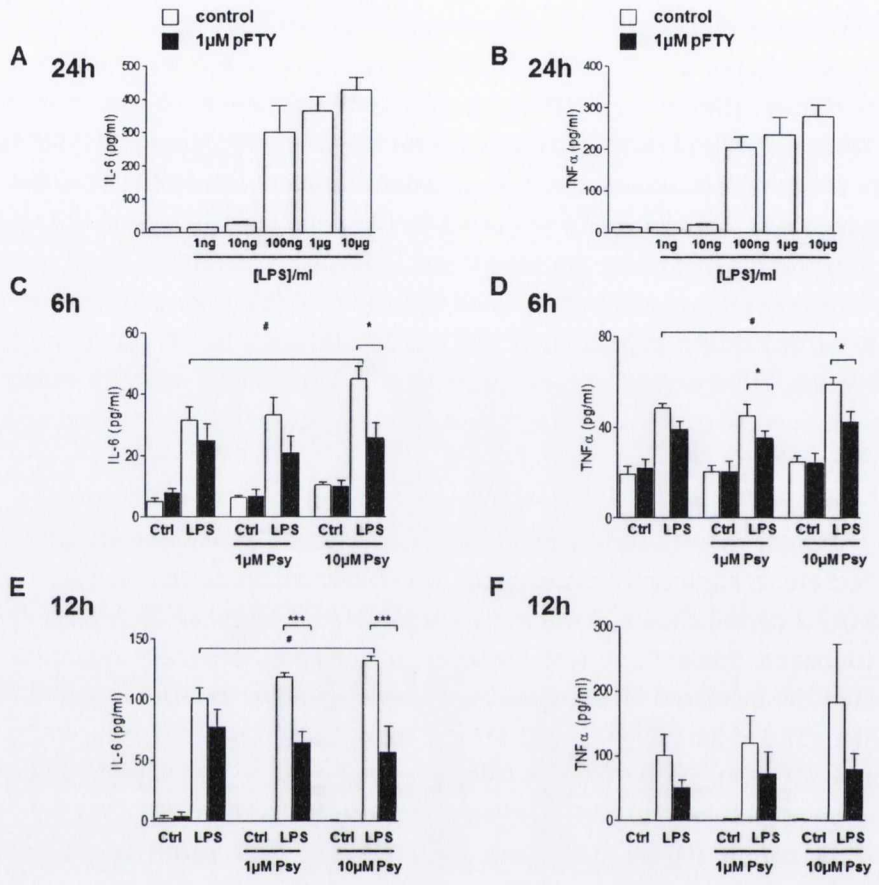

Figure 3.4. Psychosine potentiates LPS-induced production of proinflammatory cytokines in primary mouse astrocytes. Mouse astrocytes were serum starved for 4 h and pre-treated for 1 h with 1 μM pFTY before treatment with LPS and/or 1 μM or 10 μM psychosine. The supernatant was collected and an ELISA performed. Treatment of mouse astrocytes with LPS (1 ng/ml - 10 μg/ml) induced a concentration-dependent increase in levels **(A)** IL6, **(B)** TNFα. Mouse astrocytes treated with 100 ng/ml LPS +/- psychosine treatments for **(C,D)** 6 h or **(E,F)** 12 h showed an increase in **(C,E)** IL6, **(D,F)** TNFα, that was attenuated by pre-treatment with 1 μM pFTY. Data is presented as mean +/- SEM (n=3-4), one-way ANOVA and Newman-Keuls multiple comparison post-test *p < 0.05, *** p < 001; unpaired student t-test # p<0.05 compared to LPS alone.

2.4 Psychosine treatment did not alter GFAP expression in organotypic cerebellar slices.

Psychosine treatment was seen to induce wide-spread cell death in our single cell astrocyte cultures. Unlike single cell cultures, organotypic slice cultures preserve the architecture of the brain regions that they originate from and can more accurately represent the complex processes and interactions that occur between cells and their microenvironment. Therefore, we investigated the effect of psychosine treatment on astrocytes in organotypic cerebellar slices. Organotypic cerebellar slices were exposed to psychosine (20 μM) in the presence or absence of pFTY720 (1nM) for 18 h and treated for a further 30 h with pFTY720 (1nM). The slices were then stained for GFAP (and NFH), as alterations in the levels of GFAP expression can indicate astroglial activation and gliosis. Treatment of these slice cultures with psychosine or with pFTY720 did not alter the levels of GFAP expression.

2.5 pFTY720 inhibits psychosine induced demyelination in organotypic cerebellar slices

Rapid and complete loss of myelin and the myelin forming oligodendrocytes is one of the main pathological features of KD **(Davenport et al., 2011)**. Of interest, pFTY720 promotes remyelination as well as limit demyelination induced by the bioactive lipid lysolecithin (lysophosphatidylcholine, LPC) **(Miron et al., 2010, Sheridan and Dev, 2012)**. With this in mind, we first determined if psychosine induce demyelination in cerebellar slices and secondly examined if pFTY720 attenuate this psychosine induced demyelination. Organotypic cerebellar slices were exposed to LPC (0.5 mg/ml) or psychosine (100 nM, 1 μM, 20 μM) in the presence or absence of pFTY720 (0.1 nM, 1nM) for 18 h and treated for a further 30 h with pFTY720 (0.1nM, 1nM) (Figure. 3.6A). In agreement with our previous studies **(Sheridan and Dev, 2012, Pritchard et al., 2014),** pFTY720 attenuated LPC induced demyelination compared with control, as observed by expression of myelin oligodendrocyte glycoprotein (MOG) (Figure. 3.6B) and myelin basic protein (Figure. 3.6C-D). Importantly, the exposure of the slice cultures to psychosine also decreased the expression of MOG (Figure. 3.5B, Supplemental Figure. 3.1), myelin basic protein (MBP) (33.4+/-3.8 vs 12.4+/-2.5, 1 μM psychosine) (Figure. 3.6C-D), and myelin proteolipid protein (PLP) (Supplemental Figure. 3.2), as well as decreasing the expression of neurofilament H (NFH) (29.9+/-5.4 vs 13.4+/-4.6, 1μM psychosine). It is noteworthy, that pFTY720 (0.1 nM, 1nM) prevented psychosine-induced decrease in expression of MOG (Figure. 3.6B, Supplemental Figure. 3.1), MBP (12.43+/-2.5 vs 31.6+/-4.9) and PLP (Supplemental Figure. 3.2), in addition to NFH (13.4+/-4.6 vs 40.7 +/-10.3) (Figure. 3.6C-D). Taken together, therefore, these studies demonstrate that pFTY720 reverses psychosine-induced demyelination and neuronal toxicity in cerebellar slice cultures.

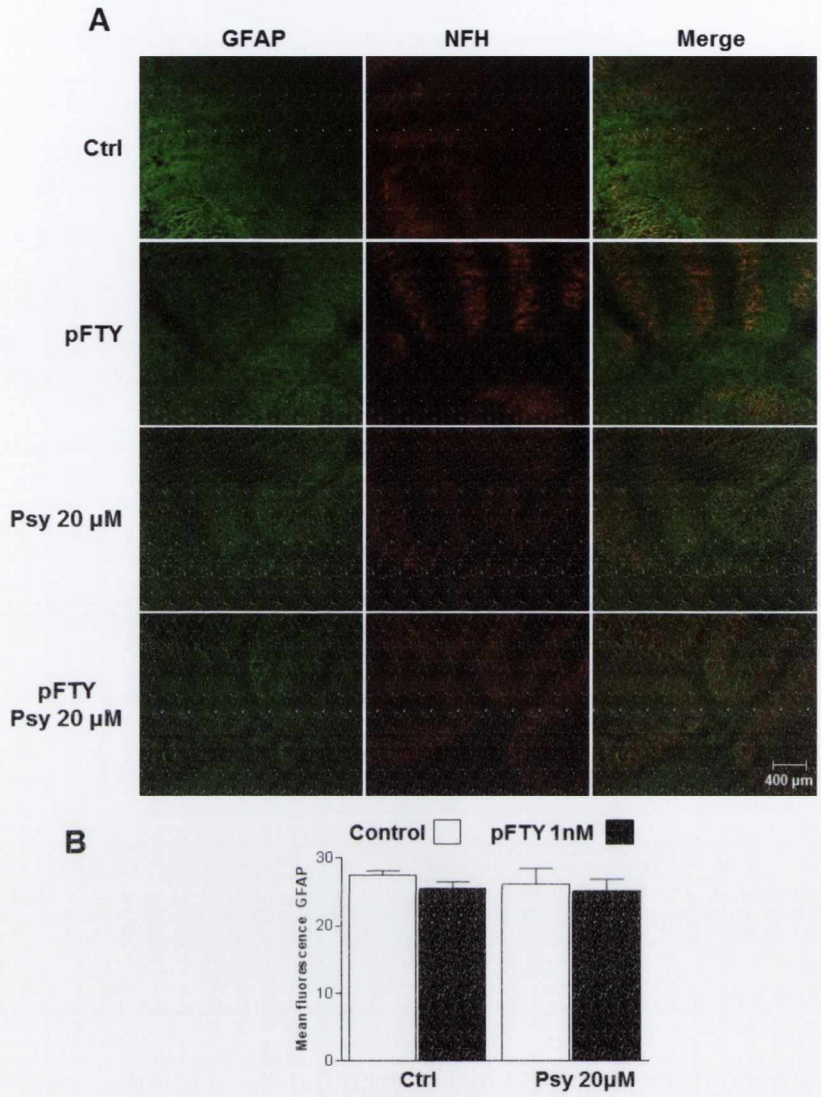

Figure 3.5. Psychosine treatment did not alter GFAP expression in organotypic slice cultures. **(A)** Organotypic slice cultures were prepared from the cerebellum of P10 mice and grown in culture for 12 days. Slices were treated with psychosine (20µM) and/or pFTY for 18 h. The media was then changed and pFTY treatment continued for a further 30 h. Cerebellar culture were then processed for immunocytochemistry. Representative confocal images displaying GFAP (green) and NFH (red) immunostaining under treatment conditions indicated. Confocal images captured at ×10 magnification. The mean fluorescence of GFAP was not altered by psychosine (20µM) treatment. **(B)** Bar graph illustrates GFAP mean fluorescence of psychosine (20µM) +/- *p*FTY (1 nM) treatments. Mean fluorescence was calculated by measuring the fluorescence of the whole captured image in each experiment (Method 2). Data presented as mean +/- SEM (n=3).

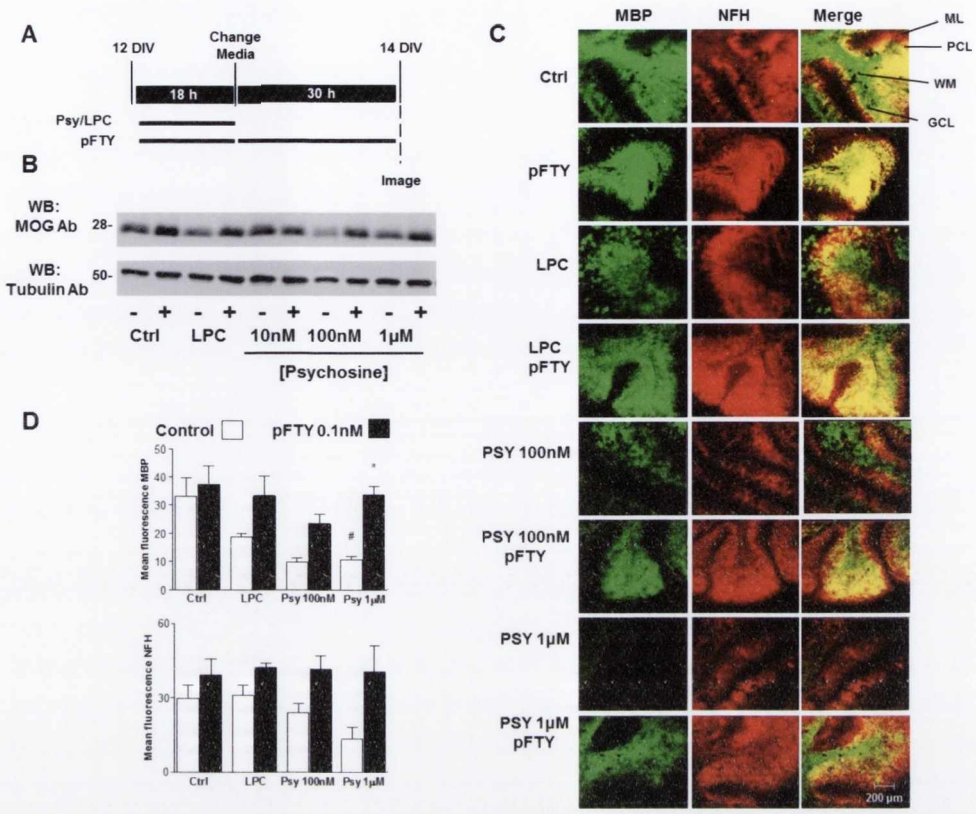

Figure 3.6. pFTY720 treatment inhibits psychosine induced demyelination of cerebellar slices. **(A)** Organotypic slice cultures were prepared from the cerebellum of P10 mice and grown in culture for 12 days. Slices were treated with LPC, psychosine and/or pFTY for 18 h. The media was then changed and pFTY treatment continued for a further 30 h. Cerebellar culture were then processed for Western blotting or immunocytochemistry. **(B)** LPC (0.4mg/ml) and psychosine (100 nM or 1 μM) treatment induced a reduction in MOG expression, which was rescued by pFTY720 (0.1 nM) treatment. **(C)** Representative confocal images displaying MBP (MBP, green) and neurofilament (NFH, red) immunostaining under treatment conditions indicated. Confocal images captured at ×10 magnification. Treatment with pFTY (0.1nm) attenuates LPC (0.4 mg/ml) and psychosine (100 nM or 1 μM) induced demyelination. ML (molecular layer), WM (white matter), PCL (Purkinje cell layer) and GCL (granule cell layer). **(D)** Bar graph illustrates changes in MBP and NFH staining after LPC (0.4mg/ml) and psychosine (100 nM, 1 μM) +/- *p*FTY (0.1 nM) treatments. Mean fluorescence was calculated using a total of 25-36 independent ROI observations in each experiment, (Method 1). Data presented as mean +/- SEM (n=3), one-way ANOVA and Newman-Keuls multiple comparison post-test *$p < 0.05$; # $p < 0.05$ comparing control +/- psychosine.

2.6 Psychosine induced demyelination in cerebellar slices occurs independently of pro-inflammatory cytokines

The involvement of pro-inflammatory cytokines in the pathogenesis of demyelination has been previously investigated **(di Penta et al., 2013)** and a model where S1PR activation may reduce demyelination via a mechanism involving attenuation of cytokine/chemokine release has been proposed **(Sheridan and Dev, 2012)**. Hence we investigated whether psychosine treatment would induce the release of the pro-inflammatory cytokines IL6, TNFα and IL1β from organotypic cerebellar slices. As with the above protocol, organotypic cerebellar slices were exposed to LPC (0.5 mg/ml) or psychosine (100 nM) in the presence or absence of pFTY720 (0.1 nM) for 18 h and treated for a further 30 h with pFTY720 (0.1 nM). After the 30 h incubation the media was collected and analysed by ELISA. LPC induced at least a 4-fold increase of IL6 (136.2+/-61.5 pg/ml vs. 1543.2+/- 89.4 pg/ml), TNFα (15.0+/-4.6 pg/ml vs. 61.9+/-12.3 pg/ml) and IL1β (0.6+/-0.6 pg/ml vs. 178.8+/-32.7 pg/ml), compared with controls (Figure. 3.7A-C). Notably pFTY720 treatment attenuated the LPC induced release of IL-6 (1543.2+/-89.4 pg/ml vs. 1273.1+/-22.1 pg/ml) (Figure. 3.7A), TNFα (61.94+/-12.3 pg/ml vs. 42.32+/-11.2 pg/ml) and IL1β (178.8+/-32.7 pg/ml vs. 14.0+/-14.1 pg/ml) (Figure. 3.7C). Interestingly, psychosine (100 nM) treatment did not induce the release of IL6, TNFα or IL1β, in agreement with our data showing the treatment of mouse astrocytes with psychosine alone had little effect on the release of IL6 (Figure. 3.4C and E), TNFα (Figure. 3.4B and F) and IL1β (*data not shown*). Furthermore, we did not observe significant effects of psychosine on Ionized calcium binding adaptor molecule 1 (Iba1) (microglia) staining nor did BV2 microglia cells treated with psychosine show enhanced levels of IL6 cytokine release (Supplemental Fig. 3.3). Taken together, these results suggest that, in organotypic cerebellar slices, psychosine-induced demyelination occurs via a mechanism that is likely independent from the release of pro-inflammatory cytokines. Moreover, it is important that pFTY720 inhibits this type of demyelination that appears to have a mode of action independent of these conventional pro-inflammatory cytokines.

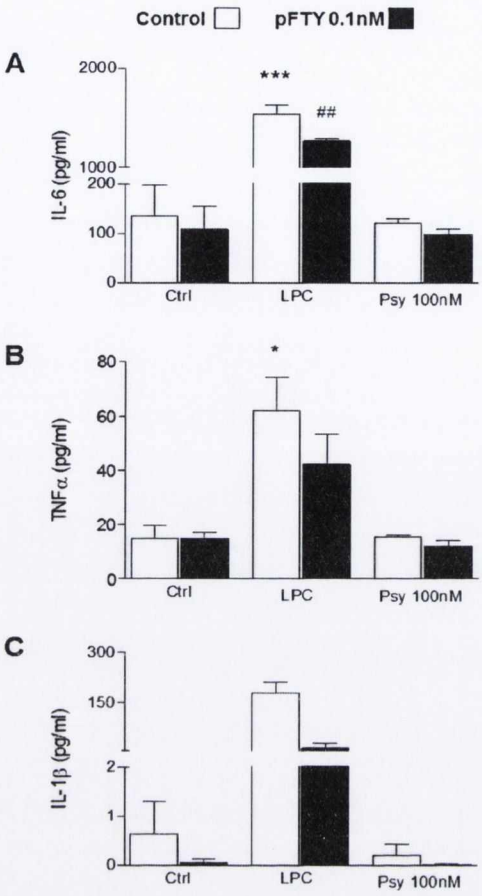

Figure 3.7. Psychosine treatment did not induce the release of pro-inflammatory cytokines from cerebellar slice cultures. Organotypic slice cultures prepared from the cerebellum of P10 mice were grown in culture for 12 days before treatment with LPC (0.4 mg/ml), psychosine (100 nM) and/or pFTY (0.1 nM) for 18 h. Media was then changed and pFTY treatment continued for a further 30 h. The media was collected and cytokine analysis performed by ELISA. Psychosine treatment did not induce the release of **(A)** IL6, **(B)** TNFα and **(C)** IL1β from cerebellar slice cultures. In contrast, treatment with LPC induced the release of all three cytokines analysed, where pFTY attenuated this LPC-induced release of **(A)** IL6 (n=3), **(B)** TNFα (n=3) and **(C)** IL1β (n=2). Data is presented as mean +/- SEM, one-way ANOVA and Newman-Keuls multiple comparison post-test *$p < 0.05$, ***$p < 0.001$.

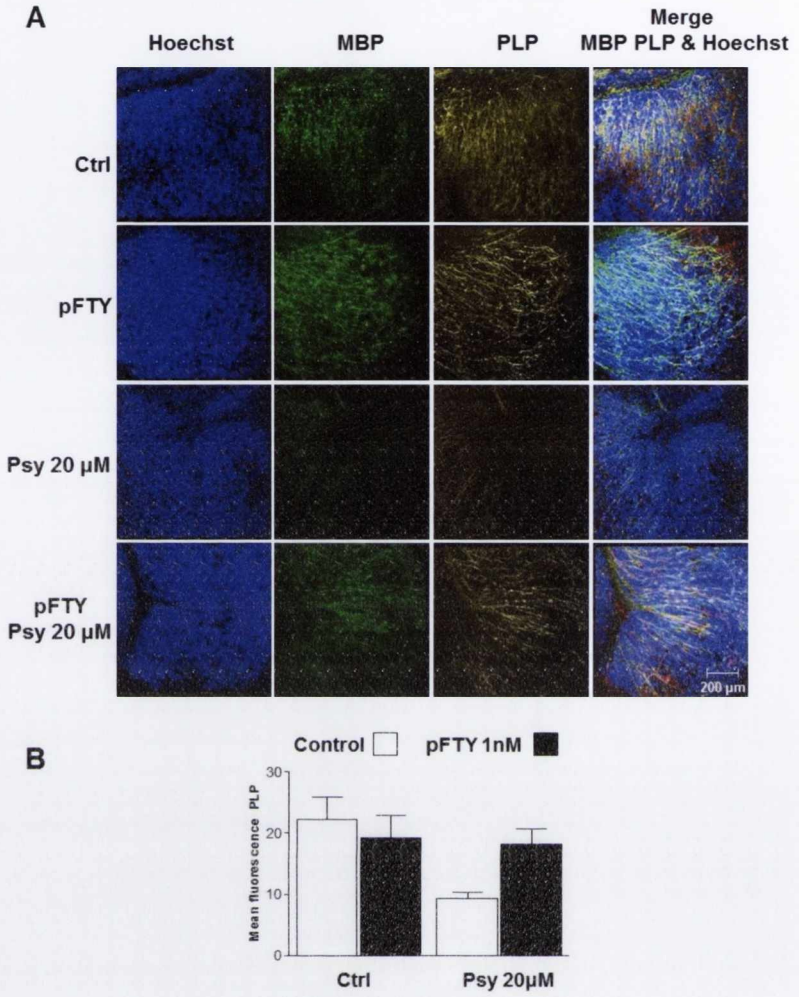

Supplemental Figure 3.1: pFTY720 rescues psychosine-induced reduction in PLP expression in organotypic slice cultures. (A) Organotypic slice cultures were prepared from the cerebellum of P10 mice and grown in culture for 12 days. Slices were treated with psychosine (20µM) and/or pFTY for 18 h. The media was then changed and pFTY treatment continued for a further 30 h. Cerebellar culture were then processed for immunocytochemistry. Representative confocal images displaying Hoescht (blue), MBP (green) and PLP (yellow) immunostaining under treatment conditions indicated. Confocal images captured at ×20 magnification. Treatment with pFTY (1nM) attenuates psychosine (20µM) induced demyelination. **(B)** Bar graph illustrates changes in PLP staining after psychosine (20µM) +/- *p*FTY (1 nM) treatments. Mean fluorescence was calculated by measuring the fluorescence of the whole captured image in each experiment (Method 2). Data presented as mean +/- SEM (n=3).

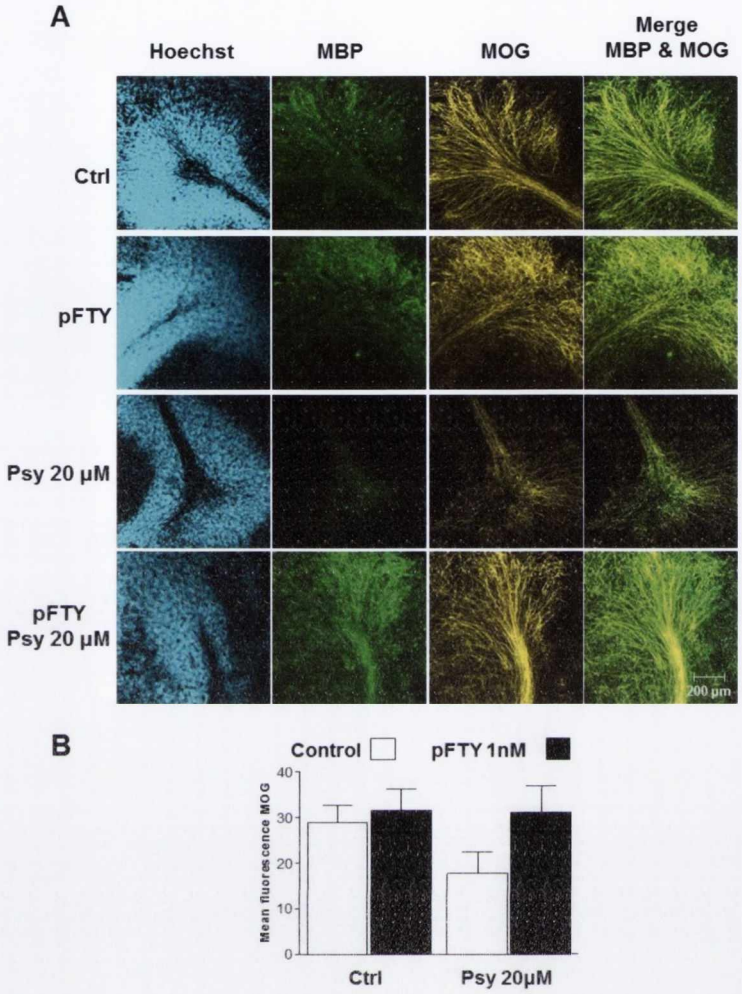

Supplemental Figure. 3.2: Psychosine-induced reductions in MOG expression is attenuated by pFTY720 (A) Organotypic slice cultures were prepared from the cerebellum of P10 mice and grown in culture for 12 days. Slices were treated with psychosine (20µM) and/or pFTY for 18 h. The media was then changed and pFTY treatment continued for a further 30 h. Cerebellar culture were then processed for immunocytochemistry. Representative confocal images displaying Hoescht (blue), MBP (green) and MOG (yellow) immunostaining under treatment conditions indicated. Confocal images captured at ×20 magnification. Treatment with pFTY (1nM) attenuates psychosine (20µM) induced demyelination. **(B)** Bar graph illustrates changes in MOG staining after psychosine (20µM) +/- *p*FTY (1 nM) treatments. Mean fluorescence was calculated by measuring the fluorescence of the whole captured image in each experiment (Method 2). Data presented as mean +/- SEM (n=4).

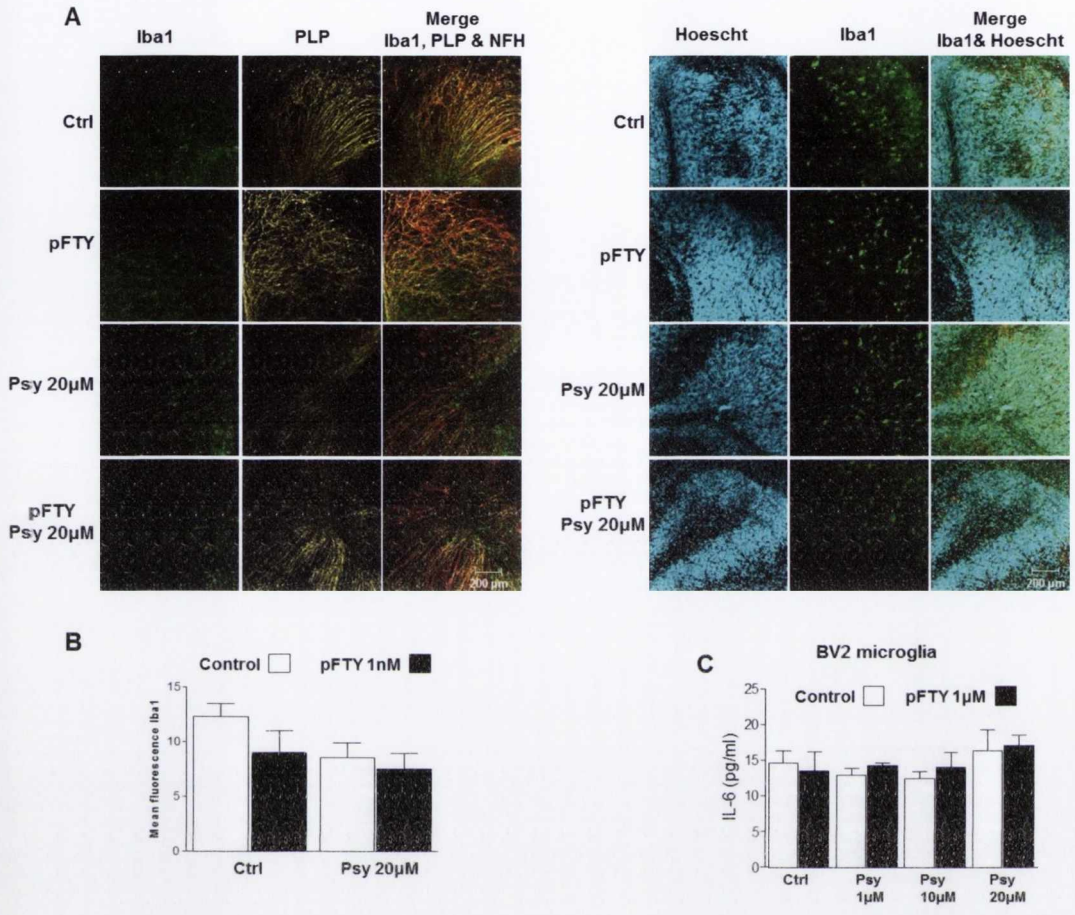

Supplemental Figure 3.3: Psychosine-induced demyelination occurs independently of microglia cell response (A) Organotypic slice cultures were prepared from the cerebellum of P10 mice and grown in culture for 12 days. Slices were treated with psychosine (20µM) and/or pFTY for 18 h. The media was then changed and pFTY treatment continued for a further 30 h. Cerebellar culture were then processed for immunocytochemistry. Representative confocal images displaying Hoescht (blue) and Iba1 (green) immunostaining under treatment conditions indicated. Confocal images captured at ×20 magnification. **(B)** Bar graph illustrates no changes in Iba1staining after psychosine (20µM) +/- *p*FTY (1 nM) treatments. Mean fluorescence was calculated using a total of 25-36 independent ROI observations in each experiment. **(C)** BV2 microglia were serum starved for 3 h and pre-treated with pFTY (1µM) for 1 h. Cells were then treated for 18 h with psychosine (1µM, 10µM and 20µM) and the supernatant collected for ELISA. Data presented as mean +/- SEM (n=4).

3. Discussion

3.1 Summary of Findings

Accumulation of psychosine, propagation of pro-inflammatory cytokines, demyelination and the widespread loss of oligodendrocytes are all hallmarks of the KD brain (**Suzuki, 1998, Wenger et al., 2001**). To date, most studies have focused on the cytotoxic effects of psychosine on oligodendrocytes, however little is known about the effects of psychosine on astrocytes. Here we investigated the effect of the cytotoxic lipid metabolite psychosine on cultures of human astrocytes. Psychosine caused a time- and concentration- dependent decrease in astrocyte cell numbers as previously reported **(Sugama et al., 1990, Giri et al., 2002)**. In agreement with the current literature (**Haq et al., 2003, Davenport et al., 2011, Jatana et al., 2002**), this astrocytic cell death induced by psychosine appeared to occur via an apoptotic process as suggested by our JC-1 studies, which showed psychosine induces mitochondrial dysfunction. Importantly, pFTY720 attenuated psychosine-induced cell death as well as restoring mitochondrial dysfunction and increasing cell viability caused by psychosine. Moreover, we found that while psychosine itself did not induce increased levels of pro-inflammatory cytokines in mouse astrocytes, it did enhance LPS-mediated release of IL6, TNFα and IL1β, and these effects were again reduced by pFTY720. Although psychosine treatment of cerebellar slice cultures did not alter the levels of GFAP expression, we report here, for the first time, that direct application of psychosine to organotypic slice cultures induces demyelination in a manner that does not include enhanced pro-inflammatory cytokine release. These data corroborate the idea that psychosine in the brains of KD patients may directly induce demyelination. In these set of experiments, pFTY720 attenuated LPC induced demyelination which was shown to include enhanced levels of pro-inflammatory cytokines as we have reported before **(Sheridan and Dev, 2012)**. Of most interest, pFTY720 also reduced the demyelination caused by psychosine, in a manner that did not include enhanced levels of IL6, TNFα and IL1β. Overall, these studies suggest that S1PRs may regulate myelination state in both inflammatory and non-inflammatory paradigms.

3.2 Psychosine induces astrocyte cell toxicity

Inflammatory processes have been implicated as a major driving force behind the pathogenesis of KD (**Claycomb et al., 2013**). Several studies have reported the expression of pro-inflammatory cytokines both *in vitro* and in the twi/twi mouse brain (**LeVine and Brown, 1997, Haq et al., 2006, Giri et al., 2002**). However, the mechanism governing psychosine-mediated cell toxicity and the direct role of pro-inflammatory cytokines in the degeneration of astrocytes and/or oligodendrocytes is still not fully understood. In the present study we found psychosine treatment itself did not alter pro-inflammatory cytokine levels, and as such is unlikely to explain the decrease in astrocyte cell numbers we observed after psychosine treatment. Instead, psychosine may induce astrocyte cell death by altering mitochondrial function and electron transport as determined by increased JC1 levels in the cytosol. In agreement with this idea, previous studies have demonstrated that psychosine alters mitochondrial function and electron transfer, likely via a mechanism involving changes in the lipid environment of the membrane (**Tapasi, 1998, Cooper et al., 1993**). Moreover, studies have also reported that pFTY720 can stabilise mitochondrial function, supporting our findings that pFTY720 rescues mitochondrial dysfunction induced by psychosine. Interestingly, in this current study, while psychosine alone had no effect on pro-inflammatory cytokine levels, it

augmented the LPS-induced release of IL6 from mouse astrocytes, with a similar trend for the levels of TNFα and IL1ß. This finding is comparable to those reported previously where psychosine potentiated LPS-induced production of TNFα, IL6, IL1ß and NO in primary rat astrocytes, which in turn was suggested to induce oligodendrocyte cell death (**Giri et al., 2002, Giri et al., 2006**). These enhanced levels of cytokines were reduced by pFTY720, in agreement with previous studies from our and other groups demonstrating that S1PR's play a role in regulating the levels of cytokines in a number of immune and glial cells **(Sheridan and Dev, 2012, Choi et al., 2011, Wang et al., 2007, Zhang et al., 2008b)**. Thus, in astrocytes, it appears that psychosine directly modulates mitochondrial function to induce cell death, while in parallel enhancing cytokine levels under conditions of LPS-induced inflammation and that pFTY720 can attenuate these effects of psychosine.

3.3 pFTY720 attenuates psychosine-induced demyelination

Profound demyelination and almost complete loss of oligodendrocytes are two of the major pathological features of KD. The hypothesis that supraphysiologic levels of psychosine kill oligodendrocytes and result in widespread demyelination is now widely accepted. Recent studies are now emerging that directly implicate astrocytes and microglia in the etiology of KD (**Ijichi et al., 2013, Mohri et al., 2006**). Importantly, S1PRs are known to play many roles in the regulation of differentiation, cell survival and apoptosis of oligodendrocytes, astrocytes and microglia (**Dev et al., 2008, Miron et al., 2008b**). Therefore, we utilised organotypic slice cultures as a more complex cellular model to investigate the effect of psychosine on demyelination. Here, for the first time, we showed that psychosine can directly induce a concentration dependent demyelination, as expressed by a decrease in the levels of MOG and MBP and that pFTY720 can attenuate these effects. These findings are in agreement with our and other previous reports, demonstrating that pFTY720 rescues myelination state (**Jung et al., 2007, Coelho et al., 2007, Miron et al., 2008b, Miron et al., 2008a, Mattes et al., 2010, Sheridan and Dev, 2012**). Interestingly, unlike LPC, psychosine treatment alone did not induce the release of IL6, TNFα or IL1β from cerebellar slices, which was in agreement with our astrocyte data. These findings suggest that psychosine induces demyelination independent from the release of pro-inflammatory cytokines and most importantly that pFTY720 can inhibit demyelination independent from the regulation of pro-inflammatory cytokines. Of note, psychosine also induced a reduction in NFH fluorescence, although this did not reach significance. Interestingly, psychosine accumulation has been reported to increase PP1, PP2A and GSK3β activity, which dephosphorylates neurofilaments and inhibits fast axonal transport **(Cantuti-Castelvetri et al., 2012, Cantuti-Castelvetri et al., 2013)**. If this is the case, the demyelination seen here may not be a direct effect of psychosine on oligodendrocytes, but instead could stem from (i) initial damage to the neurons or (ii) demyelination and neurofilament damage may participate in a cycle in which they augment one another. Importantly, pFTY720 has been shown to have direct effects on neuronal function and in the preservation of axonal integrity **(Slowik et al., 2015)**. Further experiments however, are needed to address the direct effect of psychosine on neurofilaments. While recent clinical data demonstrating a lack of efficacy for pFTY720 in progressive forms of multiple sclerosis has been disappointing, our cellular studies here suggest that S1PRs may be useful targets in demyelinating illnesses such as KD.

3.4 Further discussion and limitations

Some of the limitations observed during this study are worthy of mention. (**1**) In our astrocyte cell culture studies we noted the toxicity of psychosine differed between batches purchased and required optimisation before use. In addition, whether the psychosine concentrations we used *in vitro* reflect those found *in vivo* remains to be clarified. (**2**) We utilized the change in astrocyte cell shape induced by psychosine as one of the assays to measure cell death. There are a number of other, more conventional, cell death assays available such as the MTT assay, TUNEL assay, calcein and propidium iodide stains (Live/Dead assay) and LDH cytotoxicity detection method. There are also assays that specifically detect apoptosis such as DNA fragmentation detection, caspase activation, mitochondrial stains and protease activity assays. There are a number of reasons however, why we believe using cell shape as a method to measure cell death was acceptable for this particular experiment. Firstly, the drastic effect psychosine had on the astrocyte cells was clearly visible using a microscope. Secondly, astrocytes grow in a monolayer stuck firmly to the bottom of the culture dish and dead astrocytes will detach and float off. Therefore, the images could clearly capture psychosine inducing cell death as the astrocytes would first round up and then 'pop off' the bottom of the dish and float in the media and this could be quantified using image J software. In addition to this 'cell shape method' we also used the MTT assay to confirm our findings and utilised the JC-1 assay to indicate the method of cell death was apoptosis. (**3**) FCCP should have been used as a control when running the JC-1 experiment. (**4**) We have used the immunolabeling of MBP, PLP and MOG as an indication of myelination state, however, these proteins are also present in nonmyelinating oligodendrocytes and cell debris and hence can often result in an overestimation of myelin. In addition, this method does not address the thickness or compaction of the myelin sheath. With this in mind, the use of electron microscopy to further validate our findings would be warranted. Another, perhaps more readily available, option would be the immunolabeling of the oligodendroglial protein neurofascin (NFC-155) or its binding partner Caspr in addition to MBP **(Jarjour et al. 2012)**. (**5**) The cerebellar slice experiment was not blinded and this may have introduced bias. To analysis the cerebellar slice experiments (Figure 3.5) we initially used a method in which a total of 25-36 independent ROI observations were made of each 10x slice image and the mean fluorescence was then calculated for each independent experiment. This involved selecting the ROI's and hence may lead to bias. To minimize this, we removed the need to select ROIs and instead measured the fluorescence of the full slice image captured at 20x. Although this may have improved the integrity of the data, in order to remove all bias the slice experiments and analysis should be done blinded.

Chapter 4. The dual S1PR1/5 drug BAF312 (Siponimod) attenutes psychosine induced demyelination in organotypic slice cultures.

Chapter Aims

- To investigate the effect of the S1PR1/5 agonist, BAF312, on ERK and AKT phosphorylation in human and mouse astrocytes.

- To examine the relative importance of S1PR1, S1PR3 and S1PR5 in BAF312 and pFTY720 induced-phosphorylation of ERK and AKT in both mouse and human astrocytes.

- To determine whether the S1PR1/5 selective agonist, BAF312, induces internalisation of the S1PR1.

- To investigate the effect of BAF312 on Ca^{2+} signalling in human astrocytes and to investigate the role of the S1PR1 receptor in Ca^{2+} signalling using the S1PR1 antagonist NIBR-0213.

- To examine the role of S1PRs in regulating levels of IL6 in astrocytes and microglia.

- To determine if BAF312 is protective against LPC and psychosine induced demyelination.

Abstract

BAF312 (Siponimod), a second generation sphingosine-1 phosphate receptor (S1PR) modulator, is a dual agonist at the S1PR1 and S1PR5 subtypes. This drug is currently undergoing clinical trials for secondary progressive multiple sclerosis (MS). Here we investigated the effects of BAF312 on isolated astrocyte and microglia cultures as well as in slice culture models of demyelination. BAF312 modulated pERK, pAKT and Ca^{2+} signaling pathways as well as inducing S1PR1 internalization in astrocytes. We noted the coupling of S1PR1 and S1PR3 subtypes to pERK and pAKT differed in mouse and human astrocytes. In particular, S1PR1, compared to S1PR3, appeared to play a central role in mouse astrocytes while both S1PR1 and S1PR3 were equally coupled to pERK and pAKT in human astrocytes. During our studies, we also observed that BAF312 had moderate effects on LPS or TNFα/IL17-induced increases in IL6 when using astrocyte or microglia cell cultures. In organotypic slice cultures, however, BAF312 attenuated LPC-induced levels of IL6 as well as demyelination. The toxic lipid metabolite psychosine, which accumulates in the brains of patients with Krabbe disease (KD), also induced demyelination in organotypic slice cultures. This demyelination was not associated with changes in the levels of IL6 and importantly, was also attenuated by BAF312. Overall, this current study suggests that BAF312 can modulate glial cell function and attenuate demyelination, highlighting this drug as a further potential therapy in demyelinating disorders such as KD.

1. Introduction

The family of spingosine-1-phosphate receptors (S1PR) have been rapidly gaining attention as important mediators of many cellular processes, including cell differentiation, migration, survival, angiogenesis, calcium homeostasis, inflammation and immunity **(Fyrst and Saba, 2010)**. These receptors are G-protein coupled and are known targets for the drug Gilenya® (pFTY720), an oral therapy used in patients with multiple sclerosis (MS) **(Kappos et al., 2010)**. The phosphorylated version of FTY720 (pFTY720) acts on four of the five S1PRs (S1PR1, S1PR3, S1PR4 and S1PR5) and acts as a functional antagonist at the S1PR1 subtype by causing S1PR1 internalisation, thereby inhibiting lymphocyte egress from lymph nodes to the periphery and central nervous system (CNS) **(Adachi and Chiba, 2008)**. FTY720 can also cross the blood brain barrier, where it is then phosphorylated and likely regulates neuronal and glial cells **(Jackson et al., 2011b, Choi et al., 2011)**. S1PR expression is cell type dependent and these receptors are known to play a role in, for example, astrocyte migration, oligodendrocyte myelination state and neurite outgrowth and neurogenesis. **(Dev et al., 2008, Choi et al., 2011, Sheridan and Dev, 2012, Miron et al., 2010, Mattes et al., 2010)**.

Since the development of pFTY720 and its demonstrated clinical efficacy in MS, there have been ongoing efforts to develop more selective S1PR agonists and antagonists **(Pan et al., 2013)**. These compounds have focused primarily on creating selectivity for S1PR1 and/or S1PR5, with limited activity for S1PR3. Reasons for this, in most part, are due to suggestions that S1PR1 regulates inflammatory response **(Chae et al., 2004)**, that S1PR1 and S1PR5 can promote myelination state **(Ishii et al., 2004, Jaillard et al., 2005, Im et al., 2000, Jackson et al., 2011b)**, but that S1PR3 activation induces bradycardia **(Pan et al., 2013, Forrest et al., 2004)**. Siponimod (BAF312) ((*E*) -1- (4- (1- (((4- cyclohexyl–3- (trifluoromethyl) benzyl)oxy) imino) ethyl)- 2-ethylbenzyl)azetidine-3-carb oxylic acid)), is a S1PR1/S1PR5 dual agonist that has been developed by modification of the hydrophobic alkyl chain in FTY720 and replacement of the *n*-octyl moiety with a substituted benzyloxy oxime moiety **(Pan et al., 2013)**. Further replacement of an amino phosphate moiety of FTY720 by amino carboxylic acids has provided BAF312 with shorter elimination half-lives *in vivo* and with the added benefit of developing a 'non' pro-drug **(Gergely et al., 2012).** In rat models of experimental autoimmune encephalomyelitis (EAE), BAF312 supresses preclinical symptoms **(Gergely et al., 2012)**. Interestingly, however, despite sparing S1PR3 activity, BAF312 still causes bradycardia in humans however, this can be mitigated using a novel dose titration scheme (up to 2-10mg over 9/10 days) **(Pan et al., 2013, Gergely et al., 2012, Legangneux et al., 2013)**. BAF312 has successfully undergone Phase II clinical trials for relapsing remitting MS warranting further Phase III trials **(Selmaj et al., 2013)**.

Here we investigate the effects of BAF312 on receptor trafficking, signalling, and pro-inflammatory cytokine levels in astrocytes, as well as its effects on demyelination in organotypic slices cultures. We also demonstrate the effects of BAF312 in a demyelination slices culture model of globoid cell leukodystrophy (Krabbe disease, KD) using the toxic lipid metabolite psychosine.

2. Results

2.1 Activation of S1PR1/5 promotes pERK and pAKT signalling in mouse and human astrocytes

The Ras/Raf/MEK/ERK and PI3K/PTEN/AKT signalling cascades are key signalling pathways involved in the regulation of cell survival and proliferation of numerous cell types. Activation of the S1PRs is known to induce potent ERK phosphorylation in astrocytes **(Osinde et al., 2007)** and AKT phosphorylation in various mammalian cells **(Lee et al., 2001, Liu et al., 2009).** Induction of pERK is known to be a transient response with maximal induction of signalling seen between 10-30 min of treatment **(Osinde et al., 2007)**. Here we investigated the effect of the S1PR1/5 agonist, BAF312, on ERK and AKT phosphorylation in human and mouse astrocytes. Cultured human and mouse astrocytes were serum starved for 4 h and then treated with increasing concentrations of BAF312 (1nM, 10nM, 100nM and 1μM) for 10 min (pERK) or 30 min (pAKT) and the samples prepared for Western blotting. As expected, the treatment of astrocytes with BAF312 for 10 min and 30 min induced ERK and AKT phosphorylation respectively, in a concentration dependent manner in both mouse and human astrocytes (Figure 4.1). It is noteworthy that species differences in S1PR1 and S1PR3 function, in particular between human and mouse, has been observed, where the initial bradycardia experienced after pFTY720/BAF312 treatment is reported. Next, therefore we aimed to determine if S1PRs were differentially coupled to pERK and pAKT in mouse and human astrocytes.

2.2 Differential roles for S1PR1 and S1PR3 in pERK signalling in mouse and human astrocytes

Given that astrocytes express S1PR1, S1PR3 and S1PR5, we examined further the role of these individual receptors to induce pERK and pAKT using selective agonists and antagonists. In mouse astrocytes, AUY954 treatment (S1PR1 agonist) induced significant pERK signaling, with a limited effect observed for CYM5541 treatment (S1PR3 agonist) (Tocris bioscience, 4897) and no effect seen with a selective S1PR5 agonist, herein called BLA241 (compound 1L, Mattes et al 2010) (Figure 4.2Ai). Pretreatment with NIBR-0213 (S1PR1 antagonist) (1μM) fully inhibited BAF312-induced pERK (Figure 4.2Aii). The data also showed that pretreatment with NIBR-0213 (S1PR1 antagonist), but not TY52156 (S1PR3 antagonist), partially blocked pFTY720-mediated effects (Figure 4.2Aiii). In human astrocytes, AUY954 (S1PR1 agonist) and CYM5541 (S1PR3 agonist) induced pERK signaling to a similar extent, while BLA241 (S1PR5 agonist) treatment had no effect (Figure 4.2Bi). Pre-treatment with NIBR-0213 (S1PR1 antagonist) completely inhibited effects of BAF312 (Figure 4.2Bii), while pre-treatment with NIBR-0213 (S1PR1 antagonist) or TY52156 (S1PR3 antagonist) modestly decreased the effects of pFTY720 on levels of pERK (Figure 4.2Biii). Together, these observations suggest S1PR1 activation, and to a lesser extent S1PR3, increases levels of pERK in mouse astrocytes. In contrast, the activation of S1PR1 or S1PR3 promote equally pERK signalling in human astrocytes.

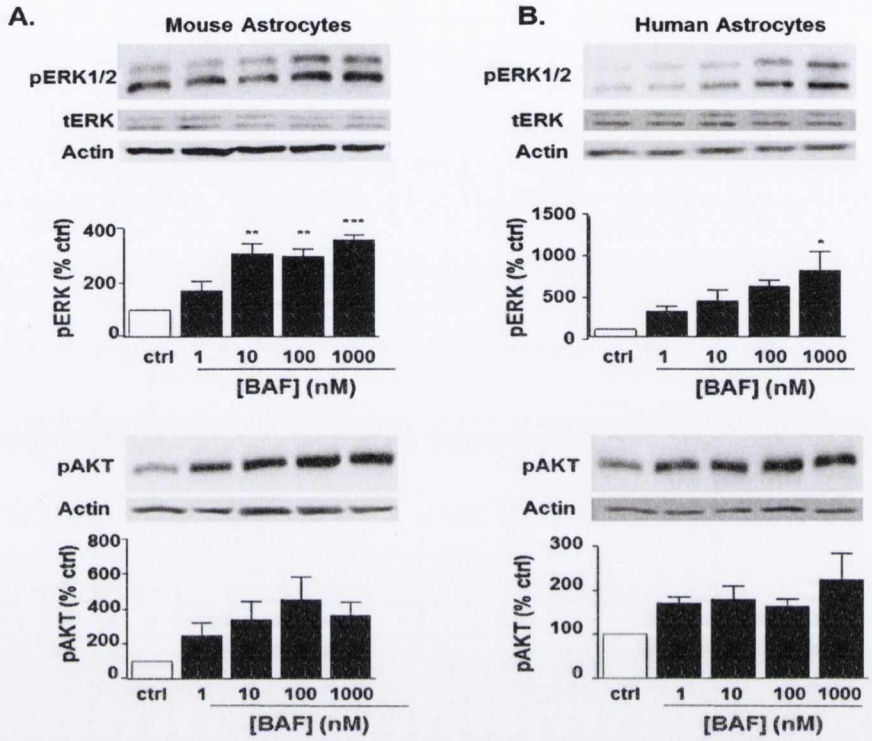

Figure 4.1: Activation of S1PR1/5 promotes pERK and pAkt signaling in mouse and human astrocytes. BAF312 at concentrations shown induced pERK after 10 min (n=3) and pAKT after 30 min treatments (n=4). **(A)** in mouse astrocytes and **(B)** in human astrocytes. Data presented as +/- SEM (n=3-4), one-way ANOVA and Newman-Keuls multiple comparison post-test * $p < 0.05$, ** $p < 0.01$, *** $p < 0.001$.

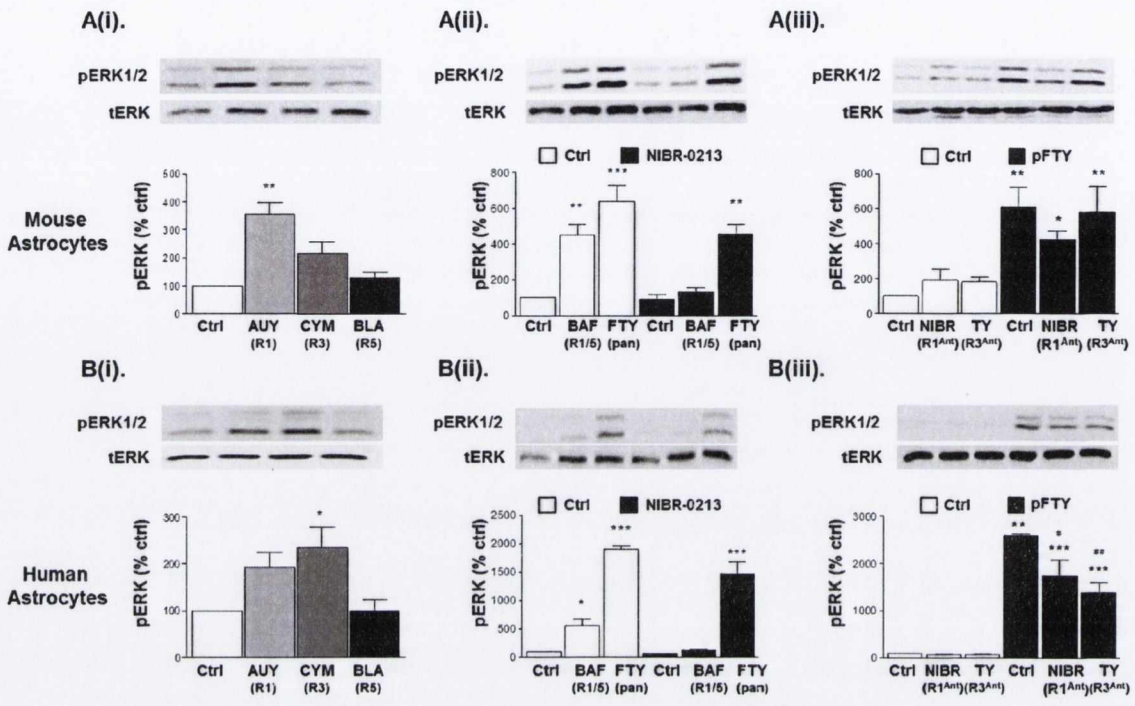

Figure 4.2: Differential roles for S1PR1 and S1PR3 in pERK signalling in mouse and human astrocytes. Astrocytes were serum starved for 4 h before all treatments. All treatment with agonists were for 10 min and pretreatment with antagonists were at 1μM for 1 h. **(Ai)** AUY954 (S1PR1 agonist, 1μM), but not CYM5541 (S1PR3 agonist, 1μM) or BLA214 (S1PR5 agonist,1μM) induced pERK signaling in mouse astrocytes. **(Bi)** Similar treatments with AUY954 or CYM5541, but not BLA214, induced pERK signaling in human astrocytes. Pre-treatment with NIBR-0213 (S1PR1 antagonist) fully blocked BAF312 (100nM)-induced pERK, while partially attenuating pFTY720 (100nM)-mediated effects in **(Aii,iii)** mouse and **(Bii,iii)** human astrocytes. Pre-treatment with TY52156 (S1PR3 antagonist) showed no effect on pFTY720-mediated increase of pERK in **(Aiii)** mouse astrocytes, while **(Biii)** partially attenuating pFTY720 (100nM)-mediated effects in human astrocytes. Data presented as +/- SEM (n=3-6), one-way ANOVA and Newman-Keuls multiple comparison post-test compared to non-treated control *$p < 0.05$, **$p < 0.01$, ***$p < 0.001$, # $p < 0.05$, ## $p < 0.001$ compared to FTY720. (R1); S1PR1, (R3); S1PR3, (R5); S1PR5, (pan); S1PR pan agonist, ($R1^{Ant}$); S1PR1 antagonist, ($R3^{Ant}$); S1PR3 antagonist.

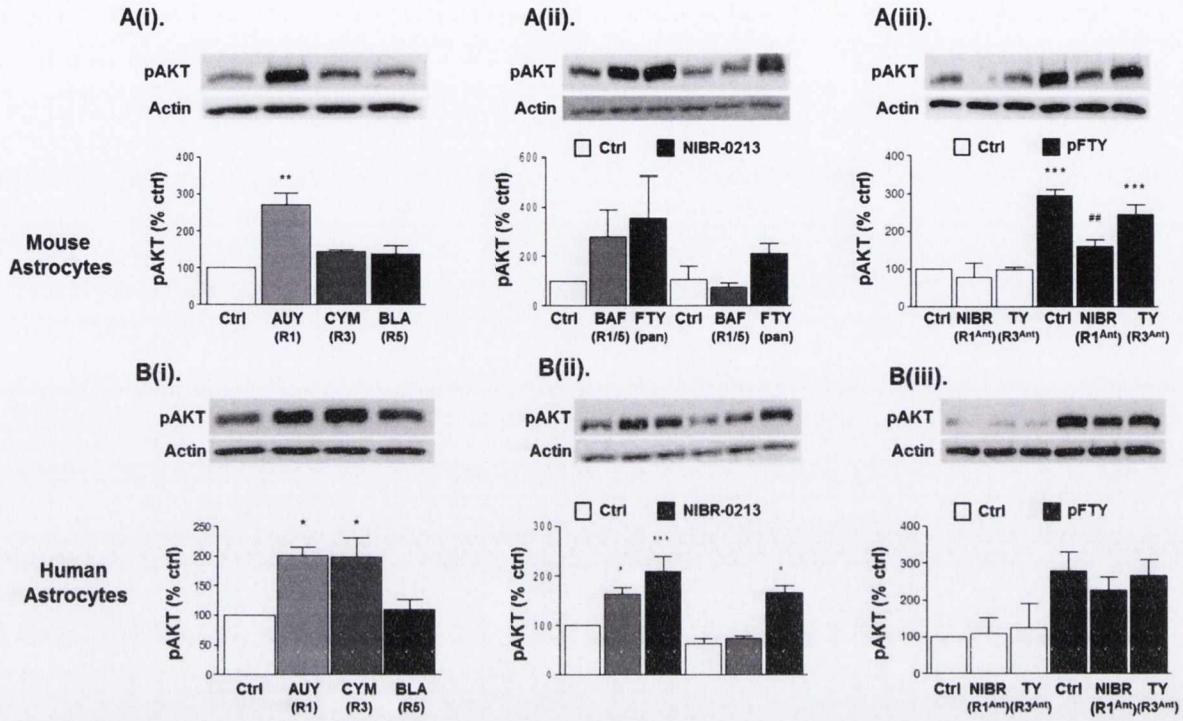

Figure 4.3: Differential roles for S1PR1 and S1PR3 in pAKT signalling in mouse and human astrocytes. Astrocytes were serum starved for 4 h before all treatments. All treatment with agonists were for 30 min and pretreatment with antagonists were at 1μM for 1 h. **(Ai)** AUY954 (S1PR1 agonist, 1μM), but not CYM5541 (S1PR3 agonist, 1μM) or BLA214 (S1PR5 agonist,1μM) induced pAKT signaling in mouse astrocytes. **(Bi)** Similar treatments with AUY954 or CYM5541, but not BLA214, induced pAKT signaling in human astrocytes. Pre-treatment with NIBR-0213 (S1PR1 antagonist) blocked BAF312 (100nM) in **(Aii)** mouse and **(Bii)** human astrocytes, whereas pFTY720 (100nM)-induced pAKT were blocked in **(Aii, iii)** mouse but not **(Bii, iii)** human astrocytes. Pre-treatment with TY52156 (S1PR3 antagonist) showed no effect on pFTY720 (100nM)-mediated increase of pAKT in **(Aiii)** mouse astrocytes or **(Biii)** human astrocytes. Data presented as +/- SEM (n=3-6), one-way ANOVA and Newman-Keuls multiple comparison post-test compared to non-treated control *$p < 0.05$, **$p < 0.01$, ***$p < 0.001$, ## $p < 0.001$ compared to FTY720. (R1); S1PR1, (R3); S1PR3, (R5); S1PR5, (pan); S1PR pan agonist, ($R1^{Ant}$); S1PR1 antagonist, ($R3^{Ant}$); S1PR3 antagonist.

2.5 BAF312 induces an increase in $_{i}Ca^{2+}$ levels in human astrocytes

The endoplasmic reticulum is the major store of Ca^{2+} in astrocytes **(Parpura and Verkhratsky, 2012)** and activation of S1PRs by pFTY720 and AUY954 is known to evoke Ca^{2} signalling in astrocytes **(Healy et al. 2013, Mullershausen et al. 2007)**. Here we investigated the effect of the dual S1PR1/5 agonist BAF312 on Ca^{2+} signaling in human astrocytes. Human astrocytes were serum starved and loaded with Fluo-8 AM prior to stimulation with increasing concentrations of BAF312 (10nM, 100nM, and 1μM). In these studies, BAF312 (100nM and 1μM) was observed to elicit an increase in $_{i}Ca^{2+}$ levels. We also noted a minority of cells showing Ca^{2+} oscillations (*data not shown*). The effect of BAF312 was attenuated by pre-treatment with the S1PR1 antagonist NIBR-0213 suggesting a role for the S1PR1 subtype (Figure 4.5).

2.6 S1PR does not robustly attenuate levels of IL6 in astrocytes.

Previous studies from our and other groups have demonstrated that S1PR's play a role in regulating the levels of cytokines in a number of immune cell cultures and in organotypic slice cultures **(Sheridan and Dev, 2012, Choi et al., 2011, Wang et al., 2007, Zhang et al., 2008b)**. Here we investigated the modulatory effect of BAF312 on LPS- or TNFα/IL17-induced levels of the cytokine IL6 using isolated mouse and human astrocytes respectively. Cultured human and mouse astrocytes were serum starved for 4h and pre-treated with BAF312 (1nM, 10nM, 100nM and 1μM) for 1 h. Mouse astrocytes were then treated with lipopolysaccharide (LPS) (100 ng/mL) for 18 h while human astrocytes were treated with TNFα/IL17 (10ng/ml, 50ng/ml) for 18 h. The supernatants were then analysed by ELISA (Figure 4.6A). LPS treatment of mouse astrocytes resulted in the increase of IL6 which, in our hands, was only modestly attenuated by either pFTY720 or BAF312 (Figure 4.6B). Human astrocytes treated with TNFα/IL17 also resulted in the increase of IL6, which was also not noticeably altered by either pFTY720 or BAF312 treatment (Figure 4.6C). We additionally investigated these effects in mouse microglia cultures and similarly found that LPS induced significant levels of IL6, however these effects were again only modestly attenuated by pFTY720 or BAF312 (Figure 4.6D, E). These data demonstrate that modulation of S1PR by BAF312 or pFTY720 does not strongly alter the levels of IL6 in astrocytes and microglia, at least in isolated cell cultures.

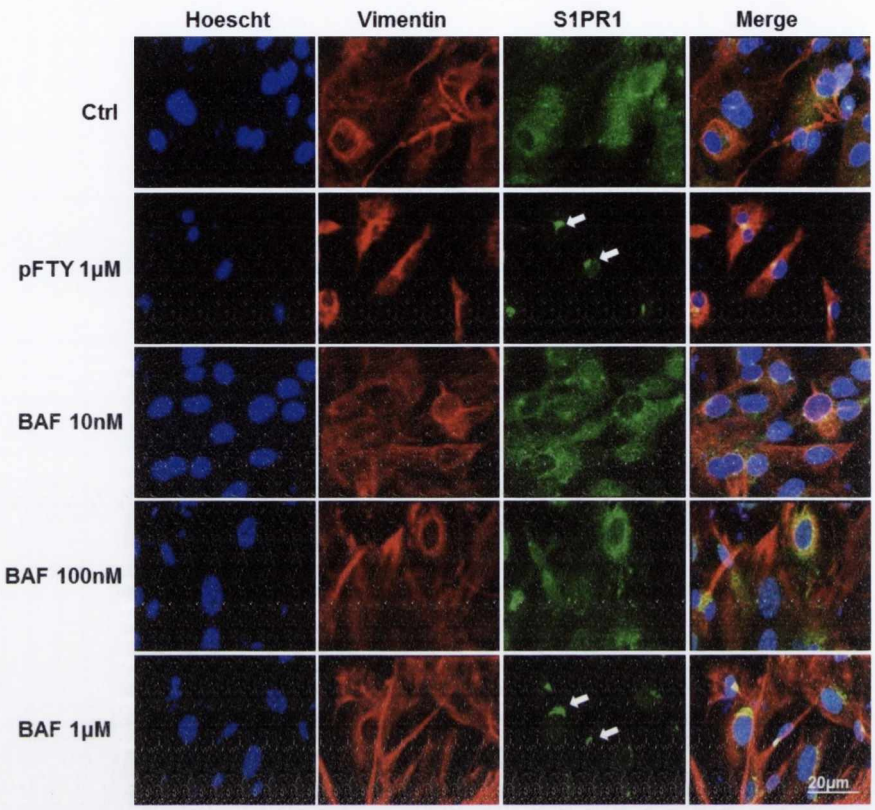

Figure 4.4: BAF312 induces internalisation of the S1PR1. Mouse astrocytes were serum starved for 4 h and then treated for 1 h with BAF312 (10nM, 100nM, 1µM) or pFTY (1µM). BAF312 at 1µM concentration induced internalisation of S1PR1.

2.5 BAF312 induces an increase in $_i Ca^{2+}$ levels in human astrocytes

The endoplasmic reticulum is the major store of Ca^{2+} in astrocytes **(Parpura and Verkhratsky, 2012)** and activation of S1PRs by pFTY720 and AUY954 is known to evoke Ca^{2} signalling in astrocytes **(Healy et al. 2013, Mullershausen et al. 2007)**. Here we investigated the effect of the dual S1PR1/5 agonist BAF312 on Ca^{2+} signaling in human astrocytes. Human astrocytes were serum starved and loaded with Fluo-8 AM prior to stimulation with increasing concentrations of BAF312 (10nM, 100nM, and 1μM). In these studies, BAF312 (100nM and 1μM) was observed to elicit an increase in $_i Ca^{2+}$ levels. We also noted a minority of cells showing Ca^{2+} oscillations (*data not shown*). The effect of BAF312 was attenuated by pre-treatment with the S1PR1 antagonist NIBR-0213 suggesting a role for the S1PR1 subtype (Figure 4.5).

2.6 S1PR does not robustly attenuate levels of IL6 in astrocytes.

Previous studies from our and other groups have demonstrated that S1PR's play a role in regulating the levels of cytokines in a number of immune cell cultures and in organotypic slice cultures **(Sheridan and Dev, 2012, Choi et al., 2011, Wang et al., 2007, Zhang et al., 2008b)**. Here we investigated the modulatory effect of BAF312 on LPS- or TNFα/IL17-induced levels of the cytokine IL6 using isolated mouse and human astrocytes respectively. Cultured human and mouse astrocytes were serum starved for 4h and pre-treated with BAF312 (1nM, 10nM, 100nM and 1μM) for 1 h. Mouse astrocytes were then treated with lipopolysaccharide (LPS) (100 ng/mL) for 18 h while human astrocytes were treated with TNFα/IL17 (10ng/ml, 50ng/ml) for 18 h. The supernatants were then analysed by ELISA (Figure 4.6A). LPS treatment of mouse astrocytes resulted in the increase of IL6 which, in our hands, was only modestly attenuated by either pFTY720 or BAF312 (Figure 4.6B). Human astrocytes treated with TNFα/IL17 also resulted in the increase of IL6, which was also not noticeably altered by either pFTY720 or BAF312 treatment (Figure 4.6C). We additionally investigated these effects in mouse microglia cultures and similarly found that LPS induced significant levels of IL6, however these effects were again only modestly attenuated by pFTY720 or BAF312 (Figure 4.6D, E). These data demonstrate that modulation of S1PR by BAF312 or pFTY720 does not strongly alter the levels of IL6 in astrocytes and microglia, at least in isolated cell cultures.

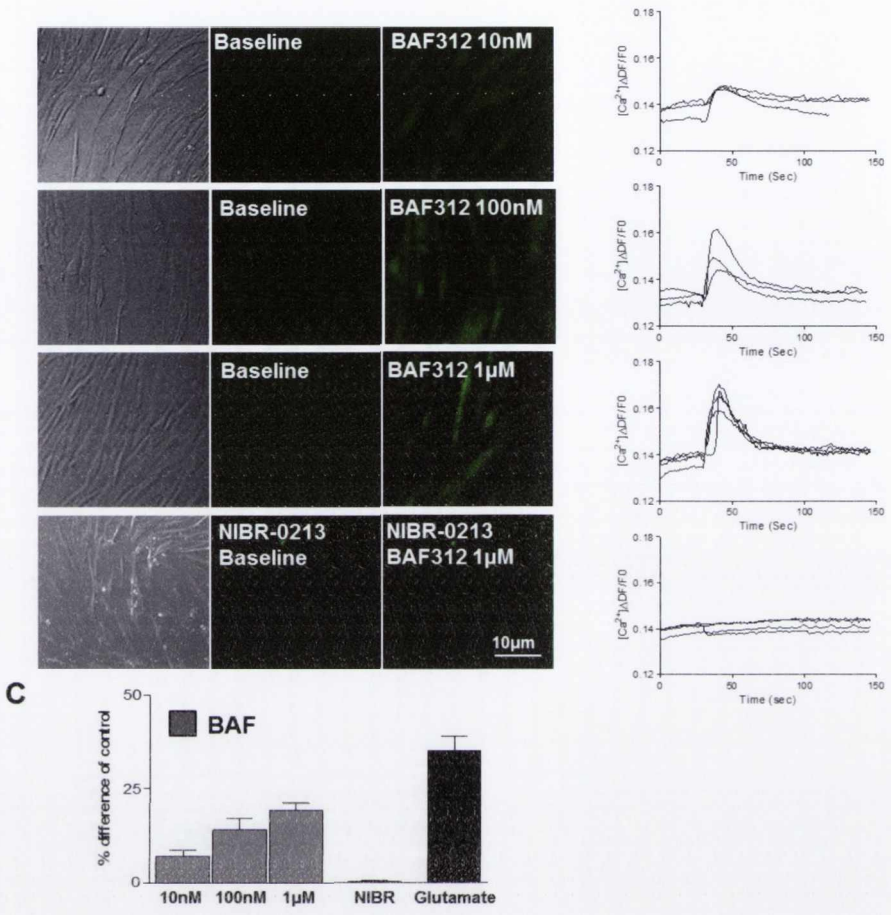

Figure 4.5. BAF312 induces an increase in $_{i}Ca^{2+}$ levels in human astrocytes. Stimulation of human astrocytes with the S1P1/S1P5 receptor agonist BAF312 increases $_{i}Ca^{2+}$ levels in Fluo-8AM loaded human astrocytes. **(A)** Representative images taken from time-lapse series at baseline and after addition of BAF312 (30 sec) is shown. All cells were stimulated and responded to 3 µM glutamate (150 sec) (*not shown*). **(B)** Analysis showing traces of 4 separate experiments. **(C)** Average data showing BAF312 significantly promotes $_{i}Ca^{2+}$ levels in human astrocytes, which is attenuated by the S1PR1 slective antagonist NIBR-0213 (n=4).

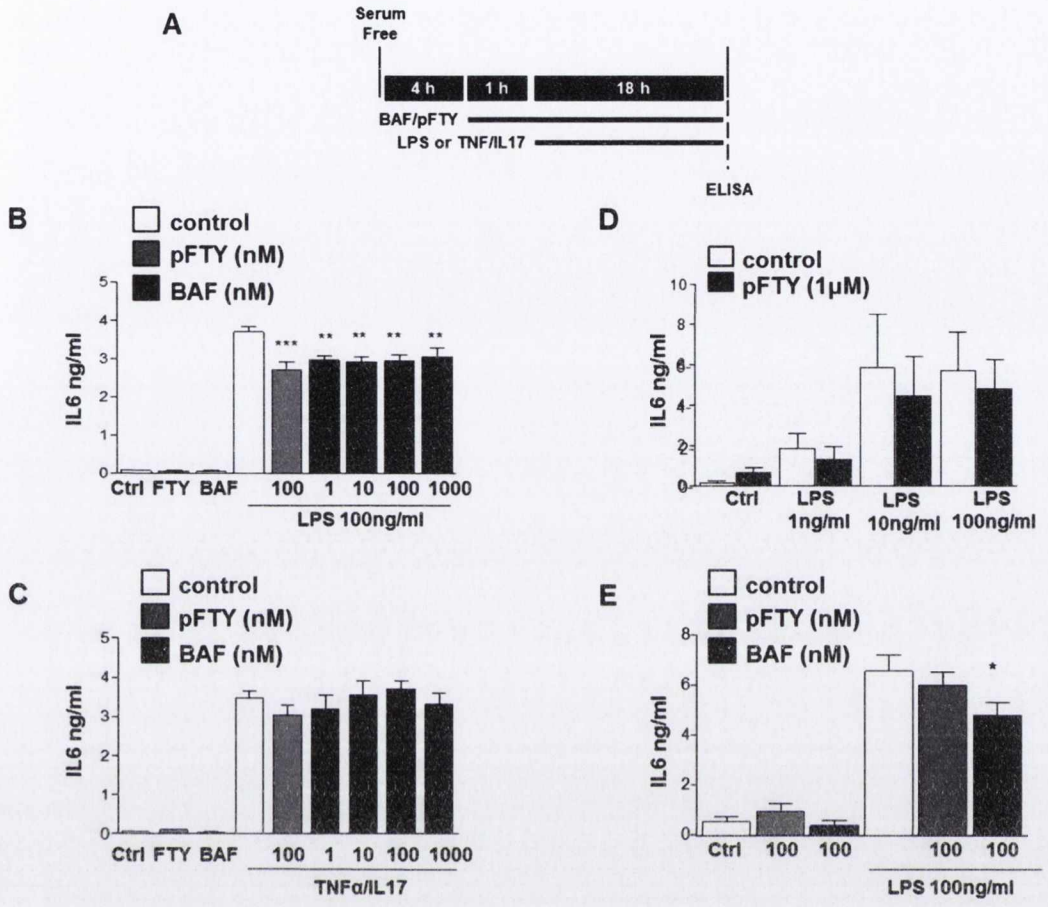

Figure 4.6. S1PR modulation selectively attenuates TLR4, but not TNFR/IL17R, mediated increase in levels of IL6 in astrocytes. (A) Astrocytes or microglia were serum starved for 4 h, pre-treated with indicated concentrations of BAF312 and then treated with LPS (1-100 ng/ml) or TNFα/IL17. **(B)** Mouse astrocytes treated with LPS increased levels of IL6, which was modestly attenuated by BAF312 (n=7). **(C)** Human astrocytes treated with LPS did not increase levels of IL6 (data not shown). In agreement with our previous studies, IL17/TNFα increased levels of IL6, however these were not inhibited by BAF312 or FTY720 (n=4). **(D & E)** Mouse microglia treated with LPS (1-100ng/ml) increased IL6 levels in a concentration dependent manner. pFTY720 and BAF312 moderately attenuated the LPS-induced increases in IL6. Data presented as +/- SEM (n=3-7), one-way ANOVA and Newman-Keuls multiple comparison post-test * $p < 0.05$, ** $p < 0.01$, *** $p < 0.001$.

2.7 BAF312 attenuates LPC-induced demyelination in mouse organotypic cerebellar slice cultures.

pFTY720 promotes remyelination as well as limits demyelination induced by the bioactive lipid lysolecithin (lysophosphatidylcholine, LPC) **(Miron et al., 2010, Sheridan and Dev, 2012)**. The high expression of S1PR5 on oligodendrocytes suggests this receptor may also have roles in myelination. Therefore we exposed organotypic cerebellar slice cultures to LPC (0.5 mg/ml) in the presence or absence of BAF312 (10nM) for 18 h and treated for a further 30 h with BAF312 (10nM) (Figure 4.7A). Similar to our previous studies demonstrating the protective effects of pFTY720 **(Sheridan and Dev, 2012, Pritchard et al., 2014)**, the LPC-induced demyelination in the cerebellar slice cultures was attenuated by treatment with BAF312 (Figure 4.7B). To determine further whether *BAF312* attenuated the levels IL6, the media from these organotypic slice cultures was analysed by ELISA. LPC induced at least a 60-fold increase of IL6 after 18h (24.6+/- 14.6pg/ml vs. 1514 +/- 314.9pg/ml) compared with controls. Notably, in contrast to its effects in isolated astrocyte or microglia cell cultures, BAF312 (10nM) treatment attenuated the LPC-induced levels of IL6 after 18h (1.1 +/- 0.4 ng/ml vs 0.4 +/- 0.04 ng/ml) respectively (Figure 4.7C). These effects were transient, where IL6 returned to high levels after 48h (*not shown*). Taken together, these findings in slice cultures may be explained by direct effects of pFTY720 and BAF312 on immune cells rather than on astrocytes or microglia as we have previously discussed **(Sheridan and Dev, 2012, Pritchard et al., 2014)**.

2.8 BAF312 attenuates demyelination effects of the Krabbe disease metabolite, psychosine, in organotypic cerebellar slice cultures.

Rapid and complete loss of myelin and the myelin forming oligodendrocytes is one of the main pathological features of KD **(Davenport et al., 2011)**. This illness is believed to be caused by the progressive accumulation of the toxic lipid metabolite, psychosine, in the brains of patients **(Davenport et al., 2011)**. Recently, we have shown that pFTY720 significantly attenuates psychosine-induced demyelination in cerebellar slices **(O'Sullivan and Dev, 2015)**. Here, to corroborate these findings, we examined whether BAF312 could also attenuate psychosine-induced demyelination. Organotypic cerebellar slice cultures were exposed to psychosine (20μM) in the presence or absence of BAF312 (10nM) for 18 h and treated for a further 30 h with BAF312 (10nM) (Figure 4.8A). We noted that psychosine induced a modest, although not significant, decrease in the levels of neurofilament H (NFH). More importantly, psychosine induced significant demyelination, as measured by the loss of MBP staining, which was significantly attenuated by BAF312 (10nM) (Figure 4.8B). We again measured the levels of IL6 by ELISA in these experiments, after the initial 18h treatment. In this case, unlike LPC, psychosine did not induce an increase in the levels of IL6 (Figure 4.8C). We suggest, therefore, that the modulation of S1PR1/S1PR5 by BAF312 is sufficient to rescue demyelination associated with or without changes in cytokines induced by toxins such as LPC and psychosine, respectively.

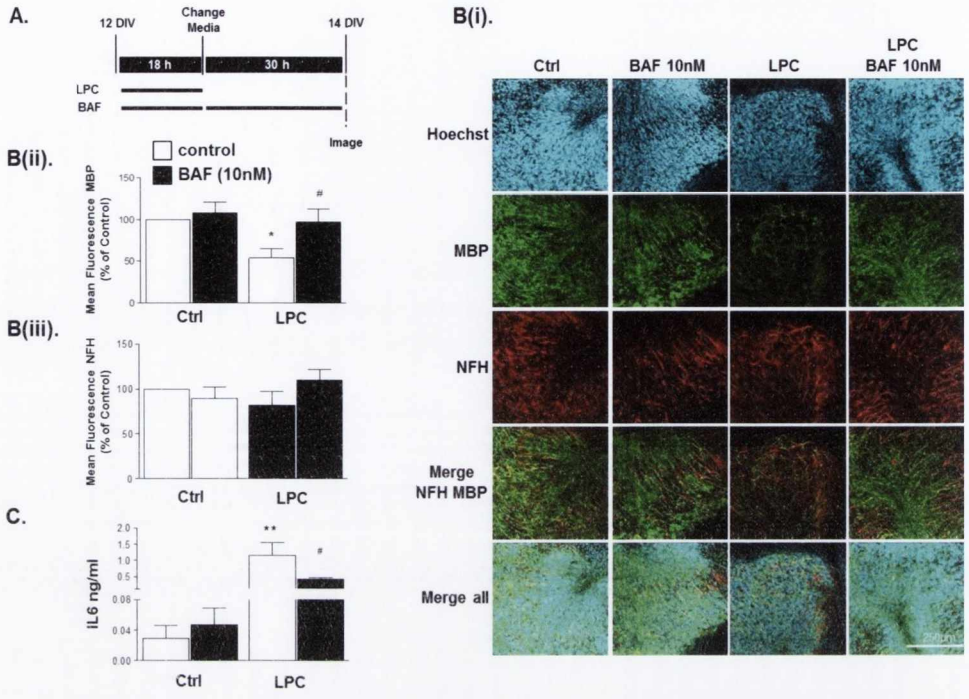

Figure 4.7. BAF312 attenuates LPC induced demyelination and IL-6 levels in mouse organotypic cerebellar slice cultures. (A) Experimental timeline is shown, as previoulsy described (Sheirdan et al 2012). Organotypic cerebellar slice cultures were treated with LPS (0.5 mg/ml) for 18h in the presence or absence of BAF312, and then treated with BAF213 alone for an additional 30h (totalling 48h) after which slices were processed for immunostaining. **(Bi)** Representative images show BAF312 attenuates LPC-induced demyelination as measured by MBP immunostaining, with limited effects on NFH immuoreactivity. **(Bii,iii)** Data analysis of 3 separate experiments, demonstrating effects of BAF312 on LPC-induced changes in MBP and NFH immunostaining. Mean fluorescence was calculated by measuring the fluorescence of the whole captured image in each experiment (Method 2) **(C)** Organotypic cerebellar slice cultures were treated with LPS (0.5 mg/ml) for 18h in the presence or absence of BAF312, and the media was processed for ELISA. Treatment with BAF312 attenuated the levels of IL6. Data presented as +/- SEM (n=3-4), one-way ANOVA and Newman-Keuls multiple comparison post-test * $p < 0.05$, ** $p < 0.01$, # $p < 0.05$ compared to LPC.

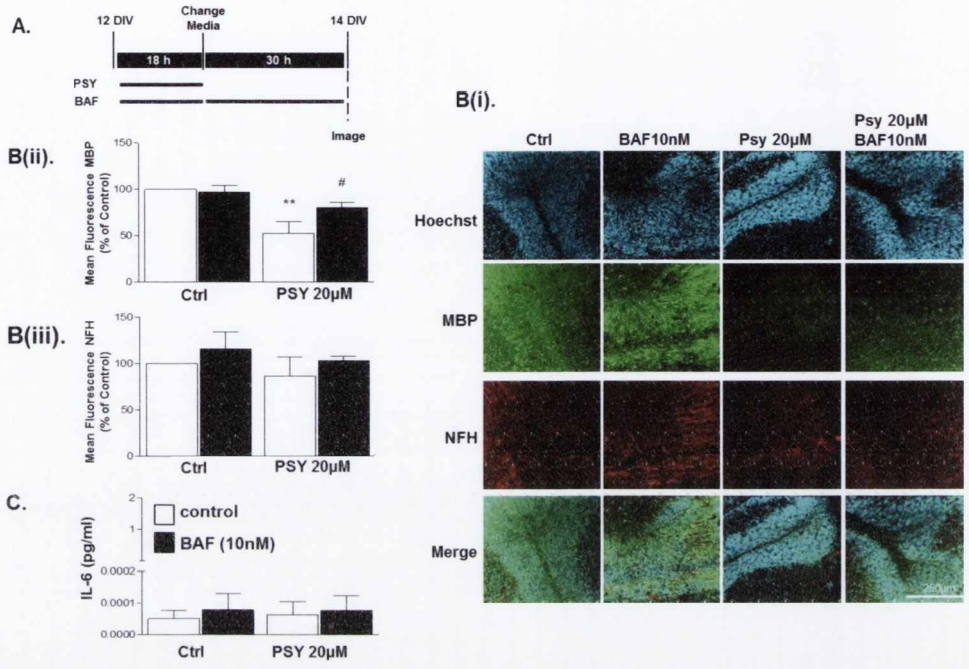

Figure 4.8. BAF312 attenuates psychosine induced demyelination in mouse organotypic cerebellar slice cultures. (A) Experimental timeline is shown. Organotypic cerebellar slice cultures were treated with psychosine (20µM) for 18h in the presence or absence of BAF312, and then treated with BAF213 alone for an additional 30h (totalling 48h) after which slices were processed for immunostaining. **(Bi)** Representative images show BAF312 attenuates psychosine-induced decrease in MBP immunostaining, with limited effects on NFH immuoreactivity**. (Bii,iii)** Data analysis of 4 separate experiments, demonstrating effects of BAF312 on pyschosine-induced changes in MBP and NFH immunostaining. Mean fluorescence was calculated by measuring the fluorescence of the whole captured image in each experiment (Method 2). **(C)** Organotypic cerebellar slice cultures were treated with pyschosine (20µM) for 18h in the presence or absence of BAF312, and the media was processed for ELISA. Treatment with pyschosine, with or without BAF312, showed no chanages in the levels of IL6. Data presented as +/- SEM (n=4).

3. Discussion

3.1 Summary of Findings

In this study, we investigated the role S1PR1 and S1PR5 in astrocyte function by using the S1PR3-sparing drug BAF312 (Siponimod), which is currently in Phase II clinical trials for secondary progressive MS. Similar to pFTY720 **(Healy et al., 2013, Osinde et al., 2007)**, we found BAF312 induced levels of pERK, as well as pAKT, in a concentration dependent manner in both human and mouse astrocytes. Furthermore we demonstrated that the selective S1PR1 agonist, AUY954, induces pERK and pAKT signalling in both human and mouse astrocytes, the S1PR3 agonist, CYM5541, induces pERK and pAKT only in human astrocytes and the S1PR5 agonist, BLA214, does not induce ERK or AKT phosphorylation in either mouse or human astrocytes. The S1PR1 specific antagonist, NIBR-0213 **(Quancard et al., 2012)**, inhibited the effects of BAF312 on pERK and pAKT signalling in human and mouse astrocytes. This suggests that BAF312-induced phosphorylation of ERK and AKT is mediated via the S1PR1 subtype. Using the S1PR1 and S1PR3 antagonists, NIBR-0213 and TY52156, we show that S1PR1 may play a more critical role in regulating pAKT signalling compared to pERK in mouse astrocytes and that both S1PR1 and S1PR3 play a role in pERK and pAKT signalling in human astrocytes. BAF312 also stimulated levels of Ca^{2+} in human astrocytes, which was attenuated by NIBR-0213, indicating further an importance of the S1PR1 subtype. Similar to pFTY720 **(Adachi and Chiba, 2008)** the treatment of astrocytes with BAF312 induced S1PR1 internalisation in a concentration dependent manner. In our hands neither pFTY720 nor BAF312 greatly attenuated the release of IL6 from LPS- or TNFα/IL17-stimulated mouse and human astrocytes, respectively. In addition, pFTY720 did not attenuate IL6 levels from LPS stimulated mouse microglial cultures. We also report here that BAF312 attenuated both LPC- and psychosine-induced demyelination in organotypic slice cultures. The effects of BAF312 in LPC-induced demyelination was accompanied by a decrease in the induced levels of IL6, in agreement with our previous study **(Sheridan and Dev, 2012)**. Of most interest, the effect of BAF312 in the psychosine-induced demyelination was not associated with changes in the levels of IL6. Overall, these studies suggest that BAF312 may regulate myelination state in both inflammatory and non-inflammatory models of demyelination.

3.2 Differential coupling of S1PR subtypes to pERK and pAKT in mouse and human astrocytes.

The signalling molecules pERK and pAKT are both associated with activating pro-survival pathways and moreover S1PRs are known to modulating these pathways **(Coelho et al., 2007, Miron et al., 2008b, Jung et al., 2007)**. To further delineate the relative contributions of S1PR1, 3 or 5 to modulate ERK and AKT phosphorylation in astrocytes, we used the selective agonists AUY954 (S1PR1), CYM5541 (S1PR3) and BLA214 (S1PR5) to stimulate human and mouse astrocytes. We found that S1PR5 is not coupled to pERK and pAKT in mouse or human astrocytes. In contrast the S1PR1 agonist, AUY954, induced ERK and AKT phosphorylation in both human and mouse astrocytes indicating that S1PR1 plays a central role in the induction of pERK and pAKT. Interestingly, the S1PR3 agonist, CYM5541, induced ERK and AKT phosphorylation only in human astrocytes suggesting that S1PR3 may have a greater influence on pERK and pAKT signaling in human astrocytes in comparison to mouse astrocytes. By use of the S1PR1 antagonist, NIBR-0213 and the S1PR3 antagonist, TY52156, we also demonstrated the following rank order of importance for pFTY720 activation of pERK and pAKT in human and

mouse astrocytes: S1PR1>S1PR3 for pERK signalling and S1PR1>>S1PR3 for pAKT signalling in mouse astrocytes; S1PR3≥S1PR1 for pERK signalling and S1PR1=S1PR3 for pAKT signalling in human astrocytes (Figure 4.9). Such species dependent differences between human and mouse S1PR1 and S1PR3 function has been reported before. For example, a variance in S1PR1 and S1PR3 function between human and mouse has been seen previously as the initial bradycardia experienced after pFTY720/BAF312 treatment is reported to be species-dependent **(Pan et al., 2013, Gergely et al., 2012)**. In addition, bone marrow derived mesenchymal stem cells (MSCs) have been shown to express collagen via the activation of S1PR1 and S1PR3 in mouse cells, while collagen expression MSCs is negatively regulated by S1PR1 and S1PR3 in human cells **(Chang et al., 2014)**. In summary, our results suggest that S1PR1, compared to S1PR3, plays a more dominant role in pERK/pAKT signalling in mouse astrocytes, whereas S1PR1 and S1PR3 are equally important in regulating these pathways human astrocytes.

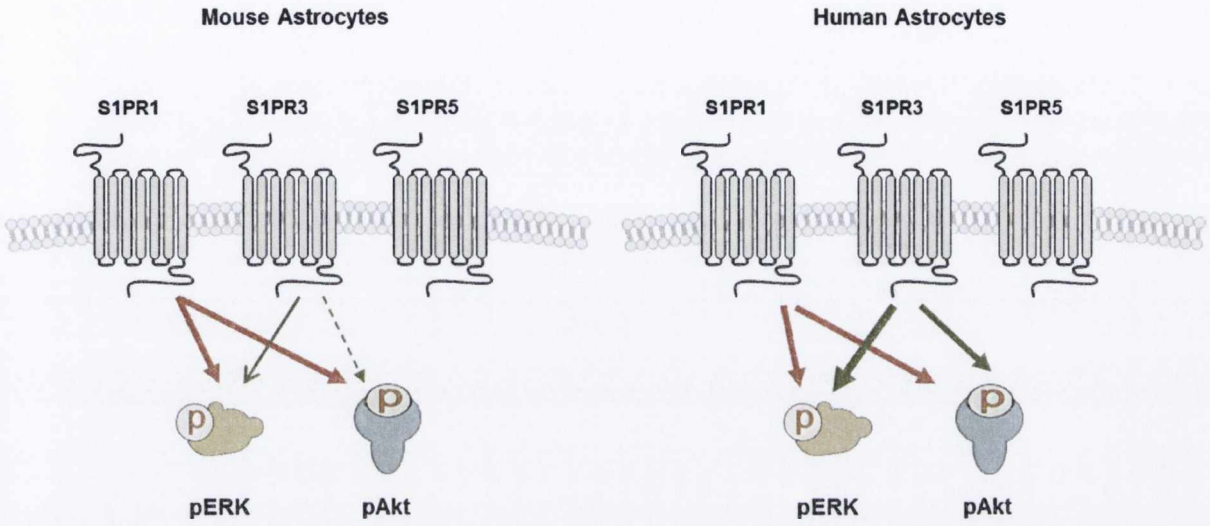

Figure 4.9. Summary figure of S1PR1 and S1PR3 contributions to pERK and pAKT signalling in mouse and human astrocytes. S1PR1>S1PR3 for pERK signalling and S1PR1>>S1PR3 for pAKT signalling in mouse astrocytes; S1PR3≥S1PR1 for pERK signalling and S1PR1=S1PR3 for pAKT signalling in human astrocytes.

3.3 The role of S1PRs in regulating levels of IL6 in microglia and astrocytes

Specific knockout of S1PR1 from astrocytes or pFTY720 treatment reduces the levels of IL1β, IL6 and IL17, which are cytokines increased during the course of EAE **(Choi et al., 2011).** In agreement, pFTY720 also attenuates the levels of cytokines such as IL6, TNFα and IL1β from LPS-activated microglia, in addition to enhancing the levels of BDNF (brain-derived nerve factor) and GDNF (glial-derived nerve factor) **(Noda et al., 2013)**. Here, we showed that while BAF312 and pFTY720 modestly attenuate the levels of IL6 from LPS-stimulated mouse astrocytes, they had no observable effect on TNFα/IL17 stimulated human astrocytes. We also found pFTY720 did not strongly attenuate LPS-induced IL6 in cultured mouse microglia. In contrast, BAF312 attenuated the levels of IL6 levels in organotypic slice cultures treated with LPC, similar to our previous data **(Sheridan and Dev, 2012)**. Unlike isolated cell cultures, organotypic slice cultures preserve the brain architecture and also contain immune cells **(Prodinger et al., 2011, Ling et al., 2008, Sheridan and Dev, 2012)**. Thus, one possible explanation for our findings using cultured astrocytes and microglia, versus organotypic slice cultures, may be the absence or presence of peripheral immune cells, respectively. This is in line with our previous findings demonstrating that MOG-reactive splenocytes can induce demyelination when added to organotypic slice cultures and their treatment with pFTY720 reverses this effect **(Pritchard et al., 2014)**.

3.4 The potential use of S1PRs as drug targets in Krabbe disease

The treatment of organotypic slices with the demyelinating agent lysophosphatidylcholine (LPC) is an established *in vitro* model to study the effects demyelination, where drugs such as pFTY720 have shown to be protective **(Miron et al., 2010, Sheridan and Dev, 2012)**. In the present study, we found BAF312 attenuated both LPC-induced demyelination as well as the levels of IL6 in organotypic slice cultures, similar to that observed for pFTY720 **(O'Sullivan and Dev, 2015)**. We also used the toxic agent psychosine to induce demyelination, which accumulates in the brain of patients with KD causing widespread demyelination and almost complete loss of oligodendrocytes in the white matter **(Davenport et al., 2011)**. Notably, we have found that psychosine induces demyelination in a manner that is not associated with altered levels of cytokines, including IL1β, TNFα and IL6 **(O'Sullivan and Dev, 2015).** In the present study, psychosine induced demyelination that was not associated with altered levels of IL6 as we have previously observed **(O'Sullivan and Dev, 2015)** and most importantly, BAF312 attenuated this psychosine-induced demyelination. As stated in chapter 3, it is important to note that psychosine-induced axon damage may also be cause of demyelination in this experimental paradigm. Although no significant reduction of NFH fluorescence was observed in the current study, further work is required to conclusively determine if psychosine induces demyelination via damage to the oligodendrocytes, axons or indeed both. Importantly S1PR modulation has been shown to preserve axon integrity **(Slowik et al., 2015)**, prevent/reverse pre- and postsynaptic alterations of glutamate transmission seen in EAE mice **(Rossi et al., 2012)** and increase brain derived neurotrophic factor (BDNF) **(Deogracias et al., 2012).** Therefore, as the preservation of axons is frequently linked to remyelination, the neuroprotective effects of S1PR modulation may be an additional avenue through which pFTY720 and BAF312 exerted protection over psychosine-induced demyelination in these organotypic slice cultures. Overall, these studies suggest that S1PR modulation is protective in both inflammatory and non-inflammatory models of demyelination.

3.5 Concluding Remarks

The clinical success of pFTY720 in the treatment of relapsing remitting MS demonstrated the therapeutic potential of S1PR modulation and prompted efforts to develop more specific agonists for these receptors. Modulators with selectivity towards S1PR1 and S1PR5 seemed of particular interest as preclinical observations in mice suggested that S1PR3 may be responsible for the transient bradycardia experienced after the first dose of pFTY720 **(Pan et al., 2013, Forrest et al., 2004)**. Furthermore, S1PR1 modulation plays a key role in lymphocyte migration **(Hla and Brinkmann, 2011)** and S1PR5 is expressed on oligodendrocytes where it plays a role in myelination **(Jaillard et al., 2005, Miron et al., 2010, Mattes et al., 2010)**. This has led to the synthesis of the dual S1PR1/S1PR5 agonist: BAF312 (Siponimod). Similar to pFTY720, BAF312 has been reported to supress pre-clinical symptoms in animal models of EAE. This drug also selectively decreases T cells ($CD4^+$, naive & central memory) and B cells in healthy human volunteers, while sparing effector memory T cells **(Gergely et al., 2012).** In a phase II clinical study for relapsing remitting MS, BAF312 reduced brain MRI lesions up to 80% in comparison with placebo control **(Selmaj et al., 2013).** Bradycardia is also observed with BAF312, but can be mitigated with a dose titration regimen **(Legangneux et al., 2013),** thus providing additional benefits. Importantly, BAF312 is currently undergoing a phase III trial to investigate its efficacy in patients with the chronic secondary progressive MS, a disease in which there is a particular lack of treatments **(Kappos et al., 2014)**. Given that pFTY720 has shown limited beneficial effects in patients with the chronic primary progressive MS **(ClinicalTrials.gov:NCT00731692)** and limited effect in secondary progressive EAE **(Al-Izki et al., 2011)**, the outcome of these clinical trials with BAF312 are highly awaited. In addition to the differences between primary and secondary progressive MS, differential effects of the two drugs on human astrocytes, which are not observed in mouse astrocytes, might influence the clinical outcome of the two drugs in progressive MS.

Here we demonstrated that BAF312 regulates a number of signaling pathways in human and mouse astrocytes. In addition, this compound attenuated demyelination in organotypic slice cultures induced by LPC and by psychosine, a toxic metabolite that accumulates in the brains of patients with KD. These findings suggest the S1PR drugs such as BAF312, may have utility beyond MS, in a range of demyelinating diseases such as KD, for which no therapies currently exist.

3.6 Further discussion and limitations

There are certain limitations observed during this study that are worthy of mention. (**1**) Similar to chapter 3, we have used the immunolabeling of MBP as an indication of myelination state, however, this can often result in an overestimation of myelin as this protein is also present in nonmyelinating oligodendrocytes and cell debris. Furthermore this method does not address the properties of the myelin sheath such as thickness or compaction. With this in mind, the immunolabeling of the oligodendroglial protein NFC-155 or its binding partner Caspr in addition to MBP **(Jarjour et al. 2012)** or preferribly the use of electron microscopy to further validate our findings would be warranted. (**2**) A blinded experimental design would have insured no bias in the capturing of slice images and should be introduced into the protocol for all future organotypic slice experiments. Although a systematic approach of imaging each branch and middle section of every cerebellar slice was used, this does not conclusively rule out bias.

In addition, the method with which the slices were analysed in this chapter (fluorescence of the full slice image measured) was introduced to avoid the need to select ROIs and hence help minimize bias, however a fully blinded experiment would have addressed this concern more effectively.

Chapter 5. Discovery of a novel S1PR interacting protein; Pex14.

Aims

- To create S1PR1 and Pex14 cDNA for biochemical studies
- To confirm interaction between S1PR1 and Pex14
- Determine the site of interaction of Pex14 on the S1PR1
- To express S1PR1 and Pex14 in HEK cells and astrocytes for functional studies
- Investigate if Pex14 alters S1PR1 trafficking +/- pFTY720
- Study the effect of Pex14 overexpression on S1PR1 signaling
- Determine if Pex14 overexpression influences pFTY720 modulation of LPS-induced cytokine release.

Abstract

Sphingosine-1 phosphate receptors (S1PR) are now recognised to be important mediators of many cellular processes in immune, cardiovascular and central nervous systems. These receptors are targets for the drug pFTY720, an oral therapy used in patients with multiple sclerosis (MS). The most well studied of this receptor family is the S1PR1 subtype, which is internalised by pFTY720. While the pFTY720-induced internalisation of S1PR1 underlies clinical efficacy, mechanisms that govern S1PR1 trafficking are not well understood. Thus, knowledge of the structure and physiochemical properties of the S1PR1 subtype is important in understanding trafficking as well as signalling of this receptor and may benefit in the design of new S1PR modulators. In this study, we therefore aimed to identify novel proteins interacting with S1PR1, with the purpose to further understand S1PR1 trafficking and internalisation. Here, we report a previously unknown interaction between the peroxisomal matrix protein Pex14 and S1PR1. Both co-immunoprecipitation and GST pulldown studies confirmed a S1PR1-Pex14 interaction, where the intracellular loop (ICL) 3 and C-terminus (CT) of S1PR1 was found to interact with Pex14. In silco docking analysis further suggested that the coiled-coil motif of Pex14 interacted with S1PR1. Unfortunately, the over-expression of Pex14 did not modulate pFTY720-induced trafficking of S1PR1 in transiently transfected HEK293T cells or mouse astrocytes. Pex14 over-expression also had no significant effect on LPS-induced cytokines in mouse astrocytes either in the absence or presence of pFTY720. Moreover, the transient transfection of Pex14 in mouse astrocytes only moderately increased the phosphorylation of ERK and AKT in both control and pFTY720 treated astrocytes. In summary, although the functional role for this interaction remains tenuous, overall, these studies identify Pex14 as a new S1PR1-interacting protein.

1. Introduction

Sphingosine 1-phosphate (S1P) is a zwitterionic lysophospholipid that has been implicated as a crucial regulator in many physiological and pathophysiological processes. The actions of S1P are primarily mediated via a family of G protein coupled receptors (GPCR) namely the S1P receptors 1-5 (S1PRs). These receptors are expressed and play a role in the immune, cardiovascular and central nervous systems (CNS) **(Dev et al., 2008, Hla and Brinkmann, 2011, Mann, 2012, Nixon, 2009, Iwasaki, 2011)**. Briefly, S1PRs are involved in the transmigration and egress of T cells from lymphoid tissues as well as in the regulation of cytokine release and antibody production from immune cells **(Hla and Brinkmann, 2011)**. In the CNS, S1PRs regulate astrocyte migration, oligodendrocyte myelination state and survival as well as neurite outgrowth and neurogenesis **(Dev et al., 2008)**. Importantly, these receptors are known drug targets for multiple sclerosis (MS), where the S1PR pan-agonist pFTY720 (Fingolimod) is currently used as a therapy for relapsing remitting MS **(Kappos et al., 2010)**.

Of the S1PR subtypes, S1PR1 is the most widely expressed member and is believed to be the main receptor through which pFTY720 confers the majority of its efficacy in the treatment of MS. This receptor couples exclusively with PTX-sensitive $G_{i/o}$ proteins and hence mediates adenylyl cyclase inhibition, Ca^{2+} mobilization, mitogen-activated protein kinase (MAPK) activation, phospholipase C (PLC) activation and Rac and Rho activation **(Ishii et al., 2004)**. The binding of pFTY720 to S1PR1 induces receptor internalisation and renders B and T lymphocytes unresponsive to the S1P gradient, preventing their migration from the periphery to the CNS **(Kappos et al., 2006)**. Hence this drug is often referred to as a 'functional antagonist' **(Choi et al., 2011).** Once internalised by pFTY720, S1PR1s have also been suggested to continue to signal in a process known as 'persistent signaling' **(Mullershausen et al., 2009)**. The mechanism governing S1PR1 internalisation, degradation and sustained signaling remains unclear, but likely involves chaperone and trafficking proteins **(Bockaert et al., 2004).** Here we aimed to identify novel proteins interacting with the S1PR1 in order to further understand its mechanisms of functional antagonism and/or persistent signalling and perhaps association with other genetic disorders.

Peroxisomal disorders, given the prototype name 'Zellweger syndrome', can be grouped into either single peroxisomal enzyme deficiencies or peroxisome biogenesis disorders (PBD). The PBDs are a continuum of disorders that are divided into four types including Zellweger syndrome (ZS), neonatal adrenoleukodystrophy (NALD), infantile Refsum disease (IRD) and rhizomelic chondrodysplasia punctata (RCDP) **(Wanders, 2004, Moser et al., 1995, Steinberg SJ, 2003, Steinberg et al., 2006).** Defects in one particular peroxin, namely, the *PEX14* gene causes PBD complementation group K (PBD-CGK), which arises from a failure of protein import into the peroxisomal membrane or matrix. Pex14 is a component of the docking complex that enables peroxisomal matrix proteins, that are synthesised in the cytosol, to be imported into the peroxisome **(Su et al., 2009)**. Pex 14 interacts with other peroxins including Pex5, Pex13 and Pex19, as well as interacting with tubulin enabling it to play a role in peroxisome motility by serving as a peroxisomal membrane anchor for microtubules **(Neuhaus et al., 2014)**. There is also increasing support for a role of Pex14 in the autophagic degradation of peroxisomes as demonstrated in yeast studies **(Kiel et al., 2006, Williams and Distel, 2006)**. Pex14 has been

identified as the sole peroxin that possess the dual function of peroxisome formation and peroxisome degradation (pexophagy) **(van Zutphen et al., 2008)**.

In this current study, we report a novel interaction between S1PR1 and the protein Pex14, which is mutated in Zellweger syndrome.

2. Results

2.1. Identification of interaction between S1PR1 and Pex14

To identify putative S1PR1 interacting proteins, co-immunoprecipitation studies were performed commercially by LogoPharm (www.logopharm.com). Briefly, S1PR1 antibodies (either Santa Cruz SC-25489, Santa Cruz SC-48356 or R&D Systems MAB2016) were used in affinity purification experiments to isolate S1PR1 interacting proteins from the lysates of cultured HUVEC cells. Subsequent LC-MS/MS analysis was performed on the isolated interacting proteins as previously described **(Müller et al., 2010)**. These experiments identified peptide sequences of Pex14 as a putative protein interacting with S1PR1. In order to further confirm the interaction between S1PR1 and Pex14, co-immunoprecipitation was performed using cell lysates prepared from mouse astrocytes. A mammalian expression vector of Pex14, epitope-tagged at the c-terminal with V5 (pcDNA3.1 Pex14-V5) was subcloned and the plasmid was verified by sequence analysis as well as by restriction enzyme digestion (Figure 5.1A). Expression of the Pex14-V5 protein was confirmed by transient transfection of HEK293T cells and Western blot analysis using a V5 antibody (Abcam, ab27671) (Figure 5.1B). Cell lysates prepared from Pex14-V5-transiently transfected mouse astrocytes were incubated with anti-V5 or anti-S1PR1 (Santa-Cruz, sc-25489) antibodies bound to protein G sepharose beads. A Western blot of these samples demonstrated the immunoprecipitation of Pex14-V5 by the V5 antibody as well as co-immunoprecipitation by the S1PR1 antibody, confirming initial observations of an interaction between Pex14 with S1PR1 (Figure 5.1C).

2.2. Pex14 interacts with ICL 3 and the C-terminus of S1PR1.

In order to identify the Pex14 interaction site on S1PR1, we performed GST pulldown experiments using intracellular fragments of the receptor. GST fusion proteins of the S1PR1 intracellular loops (ICL) and C-terminal (CT) fragments were constructed by cloning into the pGEX4T-1 vector using BamH1 and EcoR1 restriction digest sites (Figure 5.2A). The presence of each ICL and CT fragment of S1PR1 (GST-L1, GST-L2, GST-L3, GST-CT and GST-CT10) was confirmed by sequence analysis and restriction digestions (*data not shown*). In addition, IPTG-induced overexpression of the GST-S1PR1 fragments in transformed BL21 bacteria confirmed protein expression of these S1PR1 GST fragments as demonstrated by bands at ~27kDa (GST-L1), 28kDa (GST-L2), 30kDa (GST-L3), 34kDa (GST-CT) and 27kDa (GST-CT10) (Figure 5.2A). To perform GST-pull down experiments, the S1PR1 GST fusion proteins were coupled to glutathione Sepharose B matrix and incubated with the Pex14-V5 transfected HEK293T cell lysate. Ponceau staining of the membrane after transfer confirmed that equal amounts of each GST protein was present (Figure 5.2B). Western blot with the V5 antibody showed retention of Pex14-V5 by the GST-L3 and the GST-CT, suggesting that Pex14 binds with the ICL3 and CT of S1PR1 (Figure 5.2B).

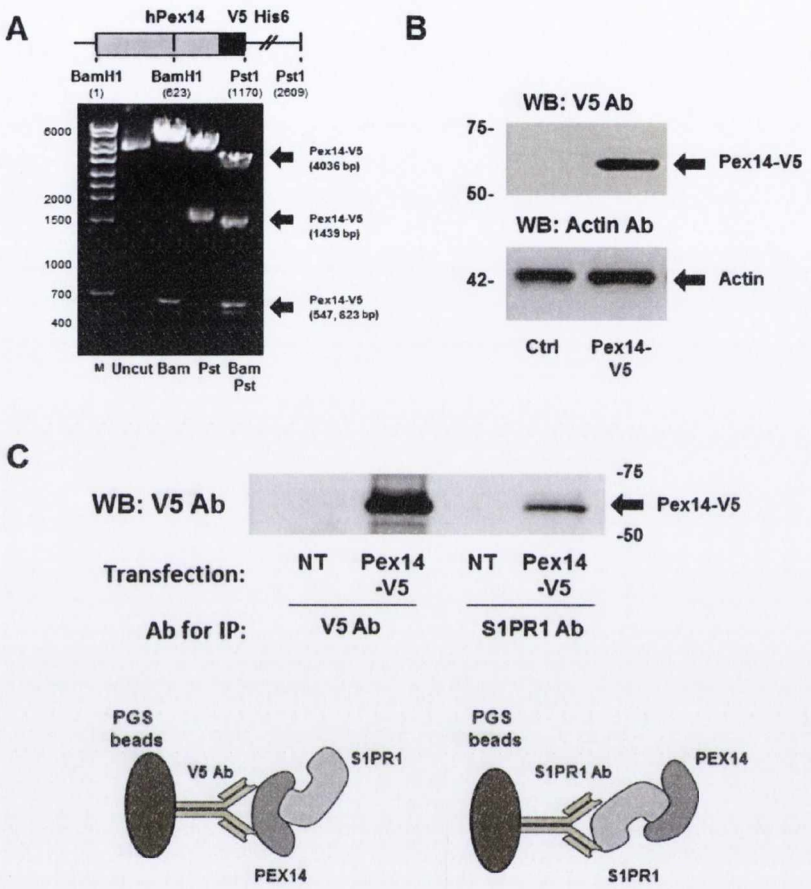

Figure 5.1. PEX14 interacts with S1PR1. (A) Agarose gel shows digestion of Pex14-V5 bands (547bp, 623bp, 1439bp and 4036bp) using BamH1 and Pst1 confirming the presence of the Pex14-V5 construct (Data representative of 5 experiments). **(B)** Western blot shows successful transfection and expression of Pex14-V5 in HEK293T cells (data representative of 3 experiments). **(C)** CO-immnuoprecipitation (IP) assay and western blot analysis. Mouse astrocytes were transiently transfected with Pex-V5 and lysates subjected to a Co-IP assay with an anti-V5 and anti-S1PR1 Ab and were immunoblotted (WB) with anti-V5 Ab. Schematic of Co-IP depicting S1PR1 and Pex14 interaction. (Pex14-V5 construct was obtained from Novartis Institutes for Biomedical Sciences, Basel, Switzerland).

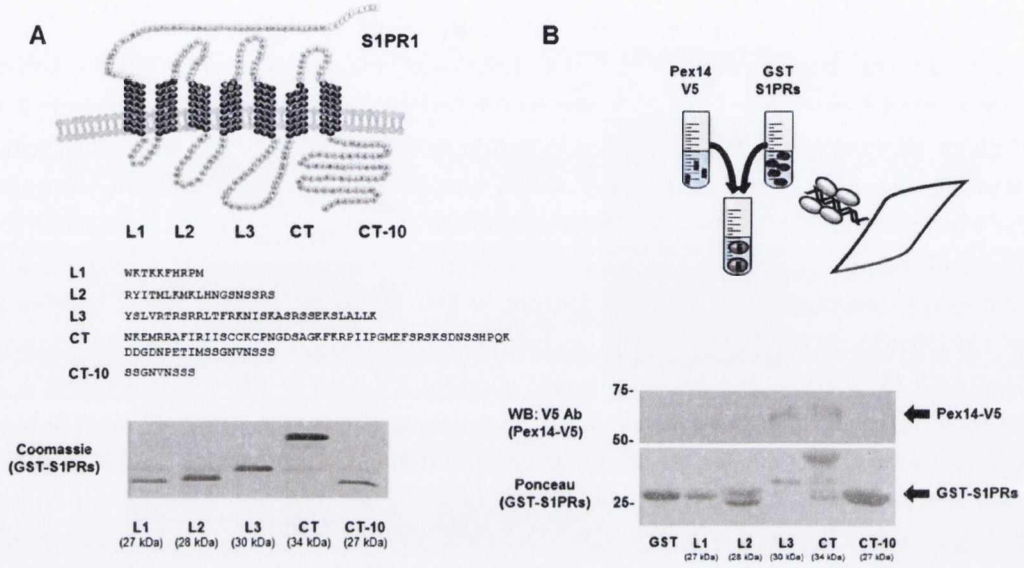

Figure 5.2. PEX14 interacts with ICL 3 and CT of S1PR1. (A) Schematic of S1PR1 showing intracellular loops (ICL) and c-terminal (CT) fragments cloned (**O'Sullivan and Dev 2013**). Below depicts coomassie stain of IPTG-induced GST-S1PR1 fragments: L1 (27kDa), L2 (28kDa), L3 (30kDa), CT (34kDa) and CT-10 (27kDa). **(B)** Diagram shows GST-affinity chromatrography setup. Pex14-V5 was obtained from HEK293T transiently transfected cells while GST-S1PR fragments were purified from BL21 *E.coli*. GST pull-down using GST-S1PR1 fragments and Pex14-V5. Western blot shows Pex14-V5 is retained by GST-S1PR1-L3 and GST-S1PR1-CT (data representative of 3 experiments).

2.3. Domain analysis of Pex14

Pex 14 is a 377 amino acid protein that is evolutionary highly conserved, with small residue differences in mouse, rat and human homologs. Pex 14 contains multiple conserved domains such as the N-terminal, coiled-coil and transmembrane domains **(Su et al., 2010)** (Figure 5.3A). The crystal structure of the N-terminal of Pex14 has recently been determined to a resolution of 1.8-Å **(Su et al., 2009)**. This highly conserved N-terminal domain of Pex14 contains three α helices (α1-α3) with a right-handed twist stabalised by a rigid hydrophobic core formed by interactions between hydrophobic residues in the α helicies **(Su et al., 2010)**. Two concave pockets located at one side of the molecule contain highly conserved residues such as Phe^{35} and Phe^{52} (that are essential for Pex14 function) and also contains an electropositive potential due to several positively charged residues; Arg^{25}, Lys^{34}, Arg^{40}, Lys^{55} and Lys^{56}. **(Su et al., 2009)** (Figure 5.3B). This provides Pex 14 with a suitable surface with which to recognise the WXXXF/Y motif of Pex5 **(Su et al., 2010)**. This N-terminus of Pex14 has also been identified as the binding site for Pex13 and Pex19 **(Itoh and Fujiki, 2006, Neufeld et al., 2009)**. Moreover, this N-terminal domain of Pex14 is believed to contain the tubulin binding motif that interacts with tubulin **(Bharti et al., 2011)**. To further investigate the site of interaction of S1PR1 on Pex14, we performed an inslico docking analysis. The complete S1PR1 and PEX14 proteins were first modeled using Zhang server **(Yang et al., 2015)**. The models obtained from Zhang server for S1PR1 and PEX14 were then docked using the protein-protein docking server ClusPro2.0 **(Kozakov et al., 2013).** The results obtained from all the docked poses showed that the transmembrane domain and the coiled-coil domain of Pex14 binds to the ICL3 and CT of S1PR1 receptor (Figure 5.3C). These findings are in agreement with coiled-coil domains playing important roles in protein-protein interactions and acting as scaffold proteins. Diagram indicates putative binding site of Pex14 with ICL3 and CT of S1PR1 (Figure 5.3D).

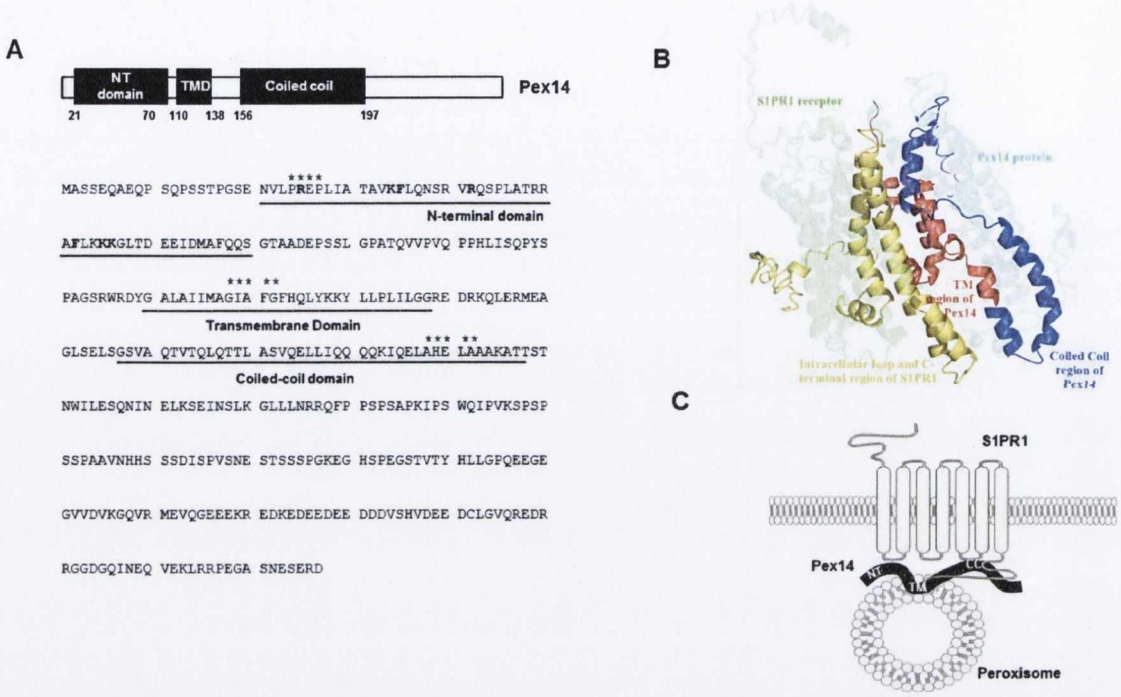

Figure 5.3. Domain analysis of Pex14. (A) Diagram and amino acid sequence of the main domains of Pex14. N-terminal domain, highly conserved domain comprising residues 21-70 and involved in interaction with Pex5p, Pex13p, Pex19p and tubulin (**Su et al., 2009, Su et al., 2010, Bharti et al., 2011**); Transmembrane domain comprising residues 110-138; coiled-coil domain comprising residues 156-197; PXXP, ligand for SH3 domain of Pex13 (**Su et al., 2010**); AXXXA, GXXXG: stabilize high molecular mass complexes after dimerization (**Itoh and Fujiki, 2006**); Phe35 and Phe52 allow for hydrophobic interactions with PXXP (**Itoh and Fujiki, 2006**); Arg25, Lys34, Arg40, Lys55, Lys56 provide electropositive potential and provide surface to recognise WXXXF/Y of Pex5p (**Su et al., 2010**). **(B)** An example of the one of the docked poses of S1PR1 and Pex14 is shown. **(C)** A cartoon of Pex14 and S1PR1 membrane topology. The coiled-coil domain of Pex14 is shown to interact with the ICL3 and CT of S1PR1.

2.4. Pex 14 does not inhibit pFTY720-induced S1PR1 internalisation in HEK293T cells

The ability of pFTY720 to induce internalisation of S1PR1 is central to the efficacy of this drug in the treatment of MS. Here, we investigated if Pex14 overexpression altered pFTY720 induced S1PR1 trafficking in HEK293T cells. Firstly, we demonstrated a pFTY720-induced internalisation of S1PR1. HEK293T cells were transiently transfected with a pLL4.0-myc-S1PR1 construct that had been previously subcloned and sequence verified. After 48-72 h the cells were treated with 1 μM pFTY720 for 1 h and immunocytochemical analysis was performed with a range of S1PR1 antibodies (Santa-Cruz, sc-25489 and Millipore, MABC94) as well as myc tag antibodies (Santa-Cruz, sc-789 and Millipore, 05-419). In agreement with previous studies **(Healy et al., 2013, Mullershausen et al., 2007, Osinde et al., 2007)** pFTY720 induced internalisation of the transiently transfected myc-S1PR1 (Figure 5.4A). Secondly, to examine the role of Pex14 in pFTY720-induced internalisation of S1PR1, expression of native Pex14 as well as Pex14-V5 was examined in control and transiently transfected HEK293T cells. As staining controls, HEK293T cells (control or transiently transfected) showed no immunoflouresence when incubated with primary (anti-V5 or anti-Pex14) or secondary (anti-mouse or anti-rabbit) antibodies (*data not shown*). In addition, non-transfected HEK293T cells exhibited no staining with either V5 or Pex14 antibodies, suggesting both specificity of the Pex14 antibody and that HEK293T cells do not express endogenous Pex14 (Figure 5.4B). Both V5 and Pex14 antibodies also co-localised when used to stain Pex14-V5 transfected HEK293T cells further confirming specificity of the Pex14 antibody (Figure 5.4B). Immunoprecipitation further confirmed the expression of transiently transfected Pex14-V5 as well as specificity of the Pex14 antibody (Figure 5.4C). Thirdly, to examine the effects of Pex14 on pFTY720-induced S1PR1 internalisation, HEK293T cells were transiently co-transfected with myc-S1PR1 and Pex14-V5 and treated for 1 h with 1 μM pFTY720. Treatment with 1 μM pFTY720 induced S1PR1 internalisation as expected, with little or no effect on the expression or localisation of Pex14-V5 (Figure 5.4D). In addition, we observed no effect of Pex14-V5 overexpression on the pFTY720-induced internalisation of S1PR1 (Figure 5.4D).

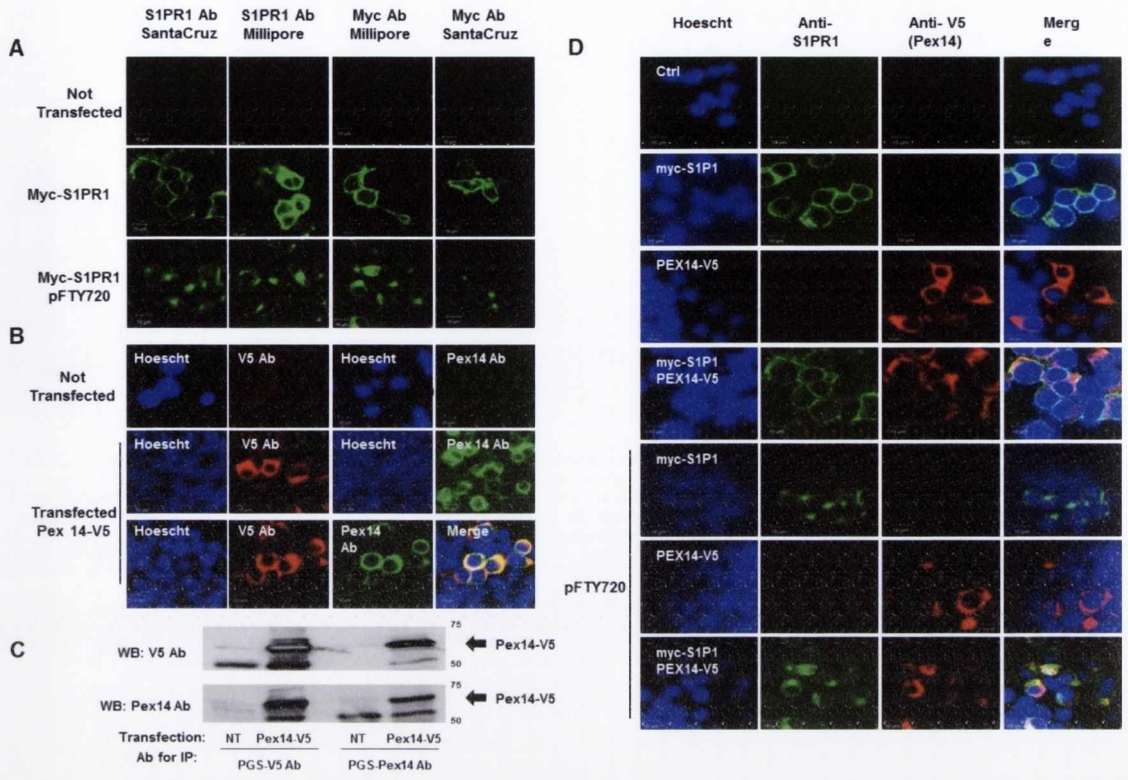

Figure 5.4 Pex 14 does not inhibit pFTY720-induced S1PR1 internalisation in HEK293T cells. (A) S1PR1 and myc tag antibodies (Santa Cruz and Millipore) were used to investigate S1PR1 expression and distribution in transiently transfected HEK293T cells. All antibodies were used to stain non-transfected HEK293T cells, myc-S1PR1 transiently transfected HEK293T cells and pFTY720 (1 μM) treated myc-S1PR1 transfected HEK293T cells (data representative of 3 experiments). pFTY720 induced internalisation of the myc-S1PR1 as expected. **(B)** Pex14 is not endogenously expressed in HEK293T cells. Ctrl and Pex14-V5 transiently transfected HEK293T cells were stained with anti-V5 and anti-Pex14 antibodies. Images show individual staining of V5 and Pex14 as well as co-localisation of V5 and Pex14 in Pex14-V5 transfected HEK293T cells. **(C)** Immunoprecipatition assay of Pex14-V5 transfected HEK293T cells using anti-V5 and anti-Pex14 antibodies. **(D)** HEK293T cells were transiently transfected with myc-S1PR1 and/or Pex14-V5 and treated with 1 μM pFTY720 for 1 h. Cells were then fixed and stained with antibodies against S1PR1 and V5 tag. Co-transfection of myc-S1PR1 and Pex14-V5 had no effect on the expression levels or localisation of either protein. pFTY720 treatment of myc-S1PR1 transfected cells induced receptor internalisation while pFTY720 treatment had no effect on Pex14-V5 distribution in transfected HEK293T cells. pFTY720 treatment of cells expressing both myc-S1PR1 and Pex14-V5 resulted in myc-S1PR1 internalisation, hence Pex14-V5 did not alter the pFTY720-induced internalisation of myc-s1PR1 (Data representative of 3 experiments).

2.5. Effects of Pex14 on pFTY720-induced S1PR1 internalisation in mouse astrocytes

As we found heterologous HEK293T cells to endogenously express little or no S1PR1 or Pex14 (Figure 5.4), we next investigated the possible effect of Pex14 on S1PR1 trafficking in primary mouse astrocytes. Cultured mouse astrocytes were confirmed to be over 95% pure as determined by staining for markers of microglia (Iba1), neurons (βIII tubulin and neurofilament H) and oligodendrocyte progenitors (NG2) (Figure 5.5A). The immunostaining of these cultures confirmed the endogenous expression of both Pex14 and S1PR1, in contrast to HEK293T cells (Figure 5.5B). To investigate the effect of pFTY720 on endogenous Pex14 expression in mouse astrocytes we treated for 1 h with pFTY720 (1μM) and stained for S1PR1 and Pex14. pFTY720, while inducing internalisation of the S1PR1 as expected, did not have any observable effect on the localisation of endogenously expressed Pex14 (Figure 5.5B). While we noted significant expression of endogenous Pex14, we nevertheless examined effects of the overexpression of Pex14 on S1PR1 trafficking. The transient transfection of mouse astrocytes with Pex14-V5 resulted in significant overexpression of the protein as demonstrated by immunostainning with the V5 antibody (Figure 5.5C). This overexpression of Pex14-V5, however, had no effect on S1PR1 localisation and/or levels of expression (Figure 5.5C). Furthermore, overexpression of Pex14 did not alter pFTY720 (1μM) mediated internalisation of S1PR1 in mouse astrocytes (Figure 5.5C). Taken together, these data suggest that Pex14 does not attenuate pFTY720-induced internalisation of S1PR1.

Pex14 overexpression increases pERK1/2 and pAKT signalling in mouse astrocytes

Next, we investigated the effect of Pex14 overexpression on S1PR1 signaling, specifically both ERK and AKT pathways. It has been demonstrated previously that pFTY720 induces ERK phosphorylation in astrocytes and that this promotes astrocyte cell migration **(Mullershausen et al., 2007, Osinde et al., 2007)**. Links between AKT phosphorylation have also been described before as both ERK and AKT can share an upstream activator in Ras **(Mendoza et al., 2011)** and like ERK, AKT is a signaling molecule that is known to be activated downstream of growth factor receptors and GPCRs **(Lee et al., 2001)**. In order to investigate if overexpression of Pex14-V5 would alter pERK or pAKT signaling in mouse astrocytes we first transiently transfected with Pex14-V5 and a vector control. After 48-72 h the transfected astrocytes were serum starved for 4 h before treatment with pFTY720 (100 nM) for 5 or 15 minutes. The cells were then scraped and processed for Western blotting. Data showed significant expression of Pex14-V5 when transiently transfected in mouse astrocytes (Figure 5.6), confirming previous immunocytochemistry data (Figure 5.5C). When compared to control, however, the transfection of Pex14-V5 did not significantly alter pFTY720-mediated increase in the levels of pERK (Figure 5.6A) or pAKT (Figure 5.6B). Notably, we observed that transfection of Pex14-V5 significantly increased the basal levels of both pERK (Figure 5.6A) and pAKT (Figure 5.6B), in comparison to the vector transfected controls. While it appears that Pex14 does not alter pFTY720-induced signaling, at least for pERK or pAKT, the data suggests Pex14 alone may regulate signaling pathways such as pERK and pAKT. From this data, we propose that the overexpression of Pex14 may have only subtle effects on already highly expressed levels of endogenous Pex14.

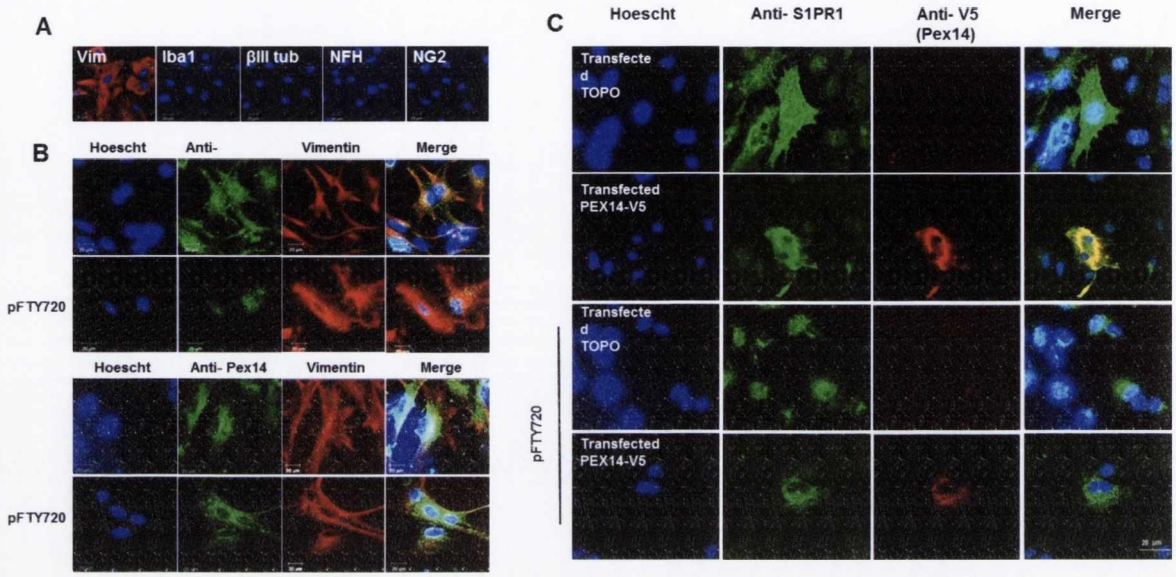

Figure 5.5. Pex14 does not inhibit pFTY720-induced S1PR1 internalisation in astrocytes. (A) Mouse astrocytes were tested for purity with antibodies against vimentin (Vim) Iba1, βIII tubulin, NFH (neurofilament H) and NG2. **(B)** Mouse astrocytes endogenously express S1PR1 and Pex14. Mouse astrocytes were treated with pFTY720 (1 μM) and stained for S1PR1, Pex14 and vimentin. pFTY720 (1 μM) induces internalisation of S1PR1 but had no effect on Pex14 expression or localisation. **(C)** Mouse astrocytes were transiently transfected with Pex14-V5 and treated with 1 μM pFTY720 for 1 h. Cells were then fixed and stained with antibodies against S1PR1 and V5 tag. Transfection with Pex14-V5 had no effect on the expression levels or localisation of S1PR1. pFTY720 treatment induced S1PR1 internalisation and had no effect on Pex14-V5 distribution. (Data representative of 3 experiments)

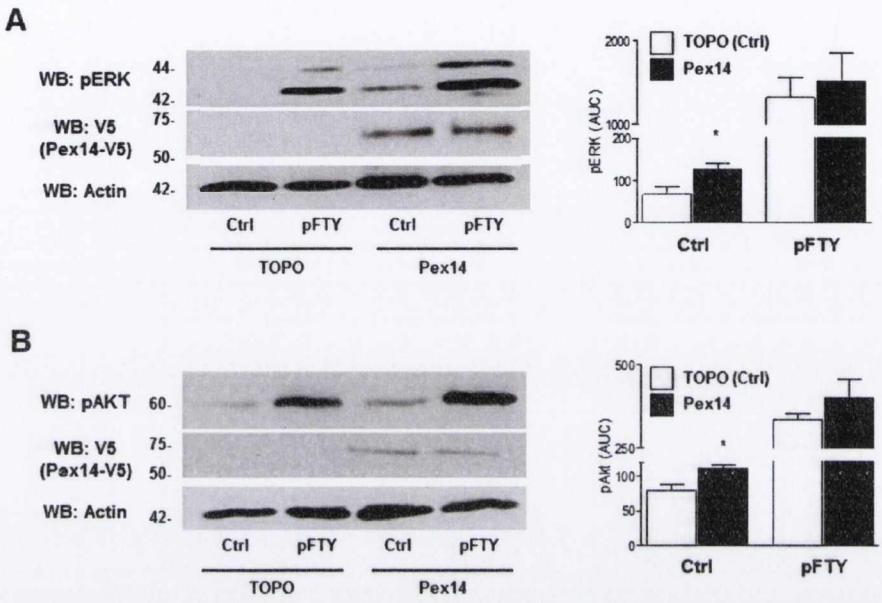

Figure 5.6: Pex14 overexpression increases pFTY720-induced pERK1/2 and pAkt signaling in mouse astrocytes. Mouse astrocytes were transiently transfected with empty vector control or Pex14-V5. Pex14 expression in the astrocytes was confirmed by Western blot using V5 antibody. Transfected astrocytes were then treated with or without pFTY720 (100 nM) for 15 minutes or 5 minutes before processing for Western blotting. **(A)** The Pex14-V5 transfected astrocytes treated with pFTY720 (100 nM) for 15 minutes had an increased level of phosphorylated ERK1/2 in comparison to the empty vector transfected control. **(B)** Pex14-V5 transfected astrocytes treated with pFTY720 (100 nM) for 5 minutes had an increased level of phosphorylated Akt in comparison to the empty vector transfected control. Data presented as +/- SEM (n=4).

2.6. Effects of Pex14 on LPS-induced levels of cytokines in mouse astrocytes.

S1PR's have been shown to play a role in regulating the levels of cytokines in a number of organotypic slice and immune cell cultures **(Sheridan and Dev, 2012, Choi et al., 2011, Wang et al., 2007, Zhang et al., 2008b)**. In addition, specific knockout of astrocytic S1PR1 or pFTY720 treatment reduces the levels of cytokines increased during the course of experimental autoimmune encephalomyelitis (EAE), namely: IL1β, IL6 and IL17 **(Choi et al., 2011)**. In our hands, pFTY720 only moderately attenuates LPS-induced increases in cytokine levels. Here we investigated if Pex14 overexpression may augment this pFTY720 effect and further limit the levels of cytokines induced by LPS. Mouse astrocytes were transiently transfected with Pex-V5 or vector control for 72 h. Cells were then serum starved for 4h and pre-treated for 1 h with pFTY720 (1 μM) before being treated with LPS (100 ng/ml) for a further 18 h (Figure 5.7). ELISAs performed on the supernatants revealed pFTY720 moderately attenuated LPS-induced increases in IL6, TNFα and IL1β as we routinely observe (Figure 5.7). Moreover, we found that Pex14-V5 overexpression did not alter LPS-induced or pFTY720 effects on the levels of cytokines investigated (Figure 5.7).

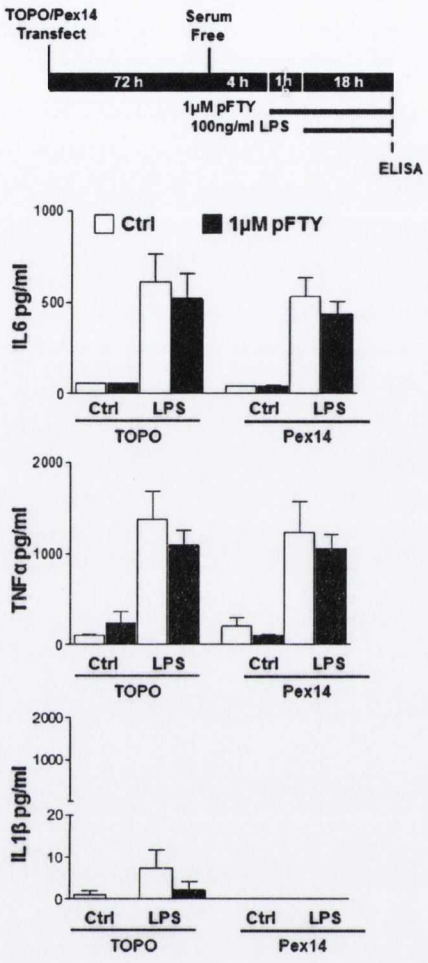

Figure 5.7: Pex14 overexpression does not augment pFTY720-induced attenuation of cytokines in mouse astrocytes. Mouse astrocytes were transiently transfected with Pex-V5 or empty vector control for 72 h. Cells were then serum starved for 4h and pre-treated for 1 h with pFTY720 (1 μM) before being treated with LPS (100 ng/ml) for a further 18 h. The supernatants were then analysed by ELISA. LPS induced an increase in IL6 TNFα and IL1β levels which was moderately attenuated by pFTY720. Overexpression of Pex14-V5 had no effect on the pFTY720 –induced attenuation of these cytokine levels.

3. Discussion

3.1. Summary of Findings

The mechanisms governing S1PR1 internalisation and trafficking have yet to be fully elucidated. In general, however, the fate of receptors following endocytosis is controlled by many factors such as interaction with kinases and chaperone proteins. GPCR's interact with many accessory proteins, which modulate receptor function, signalling, endocytosis, expression at cell surface and recycling **(Bockaert et al., 2004, Bhattacharya et al., 2004, Ferguson, 2007)**. Here, we demonstrated a novel interaction between the peroxin Pex14 and S1PR1. A co-immunoprecipitation assay was initially used to confirm the interaction of Pex14 with endogenously expressed S1PR1 in astrocytes. GST-pull down studies were then used to determine the site of interaction between Pex14 and S1PR1, demonstrating that Pex14 interacts with ICL3 and the CT of S1PR1. In silico analysis suggested that the coiled-coil domain of Pex14 interacted with S1PR1. We hypothesised that the interaction of S1PR1 with Pex14 may alter the trafficking or signalling of this receptor. In our current study the over-expression of Pex14-V5 did not alter pFTY720 induced trafficking or internalisation of S1PR1 in HEK293T or mouse astrocytes. We also investigated the effect of Pex14 overexpression on S1PR1 signaling. While overexpression of Pex14 alone increased the levels of pERK and pAKT, the overexpression of Pex14 did not significantly alter pFTY720-induced phosphorylation of ERK and AKT. pFTY720 is suggested to modulate levels of proinflammatory cytokines in slice culture models and in immune cell cultures **(Sheridan and Dev, 2012, Choi et al., 2011, Wang et al., 2007, Zhang et al., 2008b).** In our group, pFTY720 has been seen to moderately attenuate LPS-induced increases in cytokines such as IL6 from dissociated cultures of mouse astrocytes. Here we investigated if Pex14 overexpression in mouse astrocytes alters pFTY720 mediated modulation of IL6, TNFα or IL1β. Although LPS induced an increase in all three cytokines, Pex14 overexpression did not alter pFTY720-induced effects on the levels of these cytokines. Overall therefore, while this data strongly supports an interaction between S1PR1 and Pex14, the functional role of this interaction as yet remains unclear.

3.2. How does the transmembrane domain of Pex14 bind to S1PR1?

Our protein-protein docking analysis revealed that that transmembrane domain (TMD) of Pex14 may bind the ICL3 and CT of S1PR1. While interacting with the TMD seems unlikely, the exact residues allocated to this domain, together with the overall topological arrangement of mammailian Pex14 in the peroxisomal membrane remains controversial despite numerous mapping studies. For example, proteinase K treatment of intact organelles suggest that the CT-Pex14 is partially exposed to the cytosol **(Will et al., 1999)**. In agreement, a study using a combination of protease protection assays and CNBr cleavage reported that amino acids 130-377 of Pex14 are completely exposed to the cytosol **(Oliveira et al., 2002).** In addition to a cytosolic CT-Pex14, the NT-Pex14 is also reported to be cytosolic **(Shimizu et al., 1999, Jardim et al., 2002)**. Supporting the cytosolic placement of NT-Pex14 are findings that this region is suggested to bind tubulin, Pex5 and Pex19. However, studies against the cytosolic placement of NT-Pex14, include reports that Pex14 only possess one TMD and that the first 130 amino acids of rat Pex14 are protected from proteolytic attack implying this domain faces the peroxisomal lumen. There is apparent discordance in findings that both CT- and NT-Pex14 are cytosolic; that the NT-Pex14 is protected against proteolytic cleavage and can bind tubulin,

Pex5, and Pex19; and that the single TMD-Pex14 can bind S1PR1. Unifying this apparent disparity is the idea that firstly TMD-Pex14 does not entirely cross but instead acts as a reentrant loop similar to that reported for ionotropic glutamate receptor subunits and the transient receptor potentials channels (TRPs) **(Bennett and Dingledine, 1995, Szallasi and Blumberg, 1999)** and, secondly, that NT-Pex14 is embedded close to the membrane and hence is sterically hindered from proteolytic cleavage but is found in the cytosol and can bind tubulin, Pex5 and Pex19 **(Oliveira et al., 2002, Bharti et al., 2011)**.

3.3. The coiled-coil domain of Pex14 binds to S1PR1

Our insilico docking analysis also found that the coiled-coil domain of Pex14 interacted with the ICL3 and CT of S1PR1. Coiled-coil domains consist of two or more α-helices intertwined in a superhelical twist. These motifs provide protein-protein interaction sites for many structurally and functionally diverse multimeric proteins ranging from simple homodimeric transcription factors to heteromultimeric scaffolding clusters **(Strauss and Keller, 2008).** Coiled-coil interactions regulate a diverse range of cellular functions including transcription, dynamic assembly of protein complexes, intracellular trafficking and viral infection **(O'Shea et al., 1992, Rose and Meier, 2004, Gillingham and Munro, 2003, Carr and Kim, 1993)**. Furthermore, due to the large number of roles coiled-coil domains have in both physiological and pathophysiology processes, this motif has since emerged as a potential target for diseases **(Strauss and Keller, 2008)**. Indeed many GPCRs are known to bind with their respective interacting proteins via coiled-coil domains. These reports are in line with findings that the coiled-coil motif in Pex14 mediates a Pex14-Pex14 interaction forming Pex14 homopolymers **(Oliveira et al., 2002)** and with our data that Pex14 interacts with S1PR1. The finding that S1PR1 binds to the coiled-coil domain of Pex14 and that these domains can allow Pex14 homodimerisation may provide a mechanism by which S1PR1s cluster, although we did not observe Pex14 overexpression to induce S1PR1 clustering in our studies.

3.4. The functional roles of peroxins binding GPCRs

Interestingly, the peroxin Pex5 also binds to the somatostatin receptor subtype 5 (SSTR5) **(Wente et al., 2005)**. Pex5 is a cytosolic, and to a lesser extent a peroxisomal membrane bound protein, that recognises peroxisomal targeting signals (PTS1) and sorts these PTS1 motif containing proteins to the peroxisome **(Rucktäschel et al., 2011, Gouveia et al., 2000)**. The PDZ domain of human and mouse SSTR5 was found to interact with Pex5, however, this interaction did not target SSTR5 to the peroxisome but trafficked instead the receptor to the plasma membrane **(Wente et al., 2005)**. From this the authors suggest that either additional factors besides the PTS1 motif are necessary to target a membrane protein to the peroxisomes or that Pex5 participates in additional signalling events **(Wente et al., 2005)**. Investigation into the structure of cargo-loaded Pex5 in a complex with Pex14 using small angle x-ray scattering and static light scattering has revealed that the N-terminus of Pex5 remains extended when bound to cargo and Pex14 **(Shiozawa et al., 2009)**. This may allow for 'Fly casting' mechanism whereby protein binding kinetics influence protein folding. In this phenomenon, proteins in an unfolded state have a greater capture radius and hence can bind weakly to a specific binding site at a large distance. This is then followed by folding as the protein approaches the binding site and is an effective way to recruit protein assemblies **(Shoemaker et al., 2000)**. The unfolded N-terminal of Pex5, when in a complex with Pex14, could therefore play a role in

interactions with lipids and membrane proteins **(Shiozawa et al., 2009)**. The binding of Pex5 to SSTR5 and the discovery that Pex14 binds to tubulin as well as plays a crucial role in the recycling of peroxisomes (pexophagy), indicates that these peroxins may have roles outside the formation of the peroxisomal docking complex. Therefore it is not unsurprising that certain peroxins like Pex5 and Pex14 may bind to receptors including SSTR5 and S1PR1, respectively.

3.5. Why does Pex14 increase pERK and pAKT?

The Ras/Raf/MEK/ERK and PI3K/PTEN/AKT signalling cascades are key signalling pathways involved in the regulation of cell survival and proliferation of numerous cell types. ERK, a member of the evolutionary conserved family of enzymes termed the MAPKs (ERK, p38 and JNK), has been linked to phosphorylation of the AP-1 subunits, transcription of c-fos and activation of Elk-1 and Sp-1 transcription factors **(Monick and Hunninghake, 2003, Janknecht and Hunter, 1997, Shaulian and Karin, 2002)**. The PI3K/AKT pathway is also known to have a pro-survival influence via a number of mechanisms. These include inactivation of factors involved in apoptosis such as Bad and caspase-9 and activation of NFκB and induction of anti-apoptotic factors **(Toker and Newton, 2000, Toker, 2000, Anderson et al., 1999)**. Activation of the S1PRs is known to induce potent ERK phosphorylation in astrocytes **(Osinde et al., 2007)** and AKT phosphorylation in various mammalian cells **(Lee et al., 2001, Liu et al., 2009)**. In the present study over-expressing of Pex14 did not alter pFTY720-mediated increase in ERK and AKT signalling. Interestingly, however, over-expression of Pex14 did increase the basal levels of pERK and pAKT. Given that pERK and pAKT are both pro-survival signals, the moderate increase in these signalling pathways by Pex14, may be due to a slight toxicity induced during the overexpression of this peroxin. In support of this idea, Pex14 has been reported to be involved in both peroxisome formation and selective degradation (pexophagy) **(Zutphen et al., 2008)**.

3.6. Future Studies

While we report an interaction between Pex14 and the ICL3 and CT of S1PR1, the functional importance of this interaction remains elusive. In our studies we investigated the effects of Pex14 on pFTY720-mediated changes in S1PR1 internalisation, as well as pERK and pAKT signalling and cytokine release. Although a functional role for the Pex14-S1PR1 interaction was not found in the current study, it is possible that this interaction may have a role in other cellular processes. For example S1PRs have been reported to regulate Ca^{2+} signaling and astrocyte migration **(Mullershausen et al., 2007, Healy et al., 2013)** where Pex14 may play a role, although this warrants further investigation. In addition, a caveat encountered in these studies was the relatively high levels of Pex14 found endogenously expressed in astrocytes. Thus the further overexpression of Pex14 in our studies may have limited or provided only subtle effects not detected in our studies. In this regard, the use of siRNA to down regulate Pex14 or a knock-out of Pex14 would be necessary in to further investigate the potential role of the Pex14-S1PR1 interaction. It would also be important to demonstrate S1PR1 interaction with endogenous Pex14. Peroxisome function also varies according to the cell type and the specific metabolic needs of each cell type. Hence it is possible that the Pex14-S1PR1 interaction may have cell type dependent roles, for example important roles in HUVEC cells where the interaction was originally isolated compared to astrocytes **(Peraza-Reyes et al., 2011)**. While the S1PR1-Pex14 functional role in astrocytes is not clear, further discovery of S1PR1-interacting proteins will likely provide new insights into the pharmacology, signalling

and subcellular localisation of the S1PR1. Development of mechanisms to either promote or block these events may thus also provide new avenues for the development of novel therapeutic agents.

3.7 Further discussion and limitations

An experiment demonstrating that endogenous Pex14 is associated with SIPR1 would be necessary before any further work is performed on this interaction. Although the co-immunoprecipitation of endogenous Pex14 in HUVEC cells and S1PR1 was performed commercially by LogoPharm (www.logopharm.com), we did not confirm the experiment ourselves with endogenous Pex14 and this is a major limitation of the current study.

Chapter 6. Discussion

6.1. Study overview

The role of S1PRs in a diverse range of autoimmune and neurological diseases has received a great deal of attention since clinical approval of the drug fingolimod (pFTY720) for the treatment of relapsing remitting MS. The functional roles of modulating S1PRs by pFTY720, as well as newly designed pharmacological compounds such as BAF312, are also the subject of intense research in academic, clinical and pharmaceutical sectors. In the CNS, S1PR modulation is currently being investigated as a putative treatment in Alzheimer's disease **(Di Pardo et al., 2014, Hemmati et al., 2013, Deogracias et al., 2012, Estrada-Bernal et al., 2012, Gao et al., 2012)**. Furthermore, elucidation and understanding of the functional roles interacting proteins play in S1PR modulation may provide additional strategies for the development of novel therapeutic agents. This current study set out to examine the effect of S1PR modulation, using pFTY720 and the more selective drug BAF312, as a therapy for the demyelinating disorder Krabbe disease and to also investigate a putative S1PR1 interacting protein called Pex14.

6.2 Summary of Results

Initially, we investigated the ability of psychosine, a pathogenic agent in KD, to directly induce hallmarks of KD and examined if S1PR modulation by pFTY720 was able to reverse these effects. The data showed that psychosine induced concentration- and time-dependent astrocyte cell death, likely via apoptotic mechanisms, and potentiated LPS-induced increases in proinflammatory cytokines. In addition, psychosine was shown to directly induce significant demyelination in mouse organotypic slice cultures in the absence of a proinflammatory milieu. Importantly, modulation of S1PRs with pFTY720 attenuated these psychosine-induced hallmarks of KD, most notably, conferring significant protection against demyelination in cerebellar slice cultures (Figure 6.1) **(Chapter 3 results)**.

Secondly we investigated a next generation S1PR modulator as a potential therapy for KD. Since the development of pFTY720 and its demonstrated clinical efficacy in MS, there have been ongoing efforts to develop S1PR agonists that are selective for S1PR1 and/or S1PR5, with limited activity for the S1PR3 subtype **(Pan et al., 2013)**. One such S1PR modulator is the S1PR1/5 dual agonist, Siponimod (BAF312). Previous research performed using BAF312 has mainly investigated the effects of this compound on immune cells in the periphery **(Gergely et al., 2012, Legangneux et al., 2013, Selmaj et al., 2013)**. Here we investigated the effects of BAF312 on S1PR1 trafficking, signalling, and pro-inflammatory cytokine levels in glial cells, as well as its effects on LPC and psychosine induced demyelination in organotypic slices cultures. BAF312 induced S1PR1 internalisation and also caused ERK and AKT phosphorylation, Ca^{2+} signalling and moderately attenuated IL6 release from glial cells. This drug also attenuated two distinct modes of demyelination, namely LPC induced demyelination that was shown to have an inflammatory component and psychosine induced demyelination, which was independent of increases in the proinflammatory cytokine IL6 (Figure 6.2) **(Chapter 4 results)**.

Finally we report a novel interaction between S1PR1 and the peroxisomal membrane protein Pex14. Co-immunoprecipitation studies, initially performed commercially, identified Pex14 as a putative S1PR1 interacting protein. We then confirmed the interaction with our own co-immunoprecipitation experiments, as well as identified the region of S1PR1 that interacts with Pex14, namely the intracellular loop 3 and the C-terminus of this receptor. Transient

transfection of HEK293T cells and mouse astrocytes with myc tagged S1PR1 and V5 tagged Pex14 enabled us to perform various studies to attempt to elucidate the functional consequences of the Pex14-S1PR1 interaction. The data showed that Pex14 overexpression did not inhibit pFTY720-induced internalisation of transiently transfected S1PR1 in HEK293T cells nor endogenous S1PR1 expressed in astrocytes. Pex14 overexpression also did not impact on the moderate attenuation of LPS-induced proinflammatory cytokines by pFTY720. Finally, while Pex14 did not alter pFTY720-induced increases in pERK and pAKT signalling, the constitutive levels of pERK and pAKT were increased in the Pex14 transfected astrocytes (Figure 6.3) (**Chapter 5 results**).

6.3 Astrocytes and astrogliosis

Altered astrocytic function is believed to be a major contributing factor to the progression of a growing number of neurological disorders, in particular, the pathogenesis of a number of demyelinating disorders **(Claycomb et al., 2013)**. This is unsurprising as astrocytes are responsible for a wide variety of essential and complex functions in the CNS. These cells have impact on neuronal function influencing synaptic function and plasticity by regulating the supply of energy substrates, regulation of blood flow and adjustment of ion homeostasis among many other processes. Reactive astrogliosis (a term used to collectively describe changes in astrocyte biochemistry, morphology and function in response to CNS injury/disease) and glial scar formation are often used as pathological hallmarks of the diseased CNS (**Pekny and Pekna, 2014**). An exact definition of reactive astrogliosis is hard to define as it encompasses a continuum of changes of gene expression and astrocyte morphology that vary with the severity of the insult (**Sofroniew and Vinters, 2010, Pekny and Pekna, 2014**). Three broad categories however have been described to help classify the levels of reactive astrogliosis. These include (i) mild to moderate astrogliosis, generally associated with mild non-contusive trauma and viral infections, includes an up-regulation of GFAP expression, hypertrophy of cell body with little to no astrocyte proliferation (**Sofroniew, 2009**), (ii) severe diffuse reactive astrogliosis found in areas surrounding severe focal lesion or areas responding to chronic neurodegeneration and is characterised by pronounced GFAP up-regulation and hypertrophy as well as astrocyte proliferation and (iii) severe reactive astrogliosis with glial scar formation triggered by penetrating trauma, neoplasm and chronic neurodegeneration and in addition to GFAP up-regulation, hypertrophy and astrocyte proliferation, glial scar formation is also present (**Sofroniew and Vinters, 2010**). In the past reactive astrogliosis and scar formation was viewed as a negative maladaptation that impeded CNS recovery, however, evidence now exists that reactive astrocytes protect CNS tissue and the formation of glial scars are neuroprotective providing physical barriers to infectious agents and inflammatory cells (**Voskuhl et al., 2009, Bush et al., 1999**). It is important to note however that while reactive astrogliosis can have beneficial functions that help protect the CNS, it can also have harmful effects that contribute to CNS disorders. For example, in the centre of lesions or at early times after injury, reactive astrocytes may have a proinflammatory role while at later times and near the borders of lesions, reactive astrocytes may have an anti-inflammatory effect (**Sofroniew and Vinters, 2010**).

6.3 Krabbe disease and astrocytes

Reactive astrogliosis and glial scar formation are known to be involved in traumatic brain and spinal cord injury, stroke, infection, MS, Alzheimer's disease, Parkinson's disease, amyotrophic lateral sclerosis, hepatic encephalopathy, Creutzfeldt–Jakob disease, Niemann-Pick type C, neuropathic pain, Alexander disease and other leukodystrophies **(Sofroniew, 2009, Takano et al., 2009, Semmler et al., 2005, Voskuhl et al., 2009, Zhang et al., 2008a, Brenner et al., 2001, Nagele et al., 2004, Song et al., 2009, Sofroniew and Vinters, 2010)**. Much of the focus in KD to date has been on the myelin producing oligodendrocyte cells and hence the contribution of astrocytes in the pathogenesis of KD still needs to be defined. One study in particular highlighted that the pathology of KD is not solely dependent on oligodendrocytes dysfunction. In this study, transplanted oligodendrocytes from twi/twi mice were capable of myelinating the axons of another demyelinating murine model; the shiverer mice. This data suggested that demyelination in the KD brain may not be entirely attributed to oligodendrocyte cell death and may be dependent on a supportive environment **(Kondo et al., 2005)**. Hence it has been suggested that astrocyte dysfunction in the KD brain may in fact be a primary response to psychosine accumulation and not just a secondary response to demyelination **(Claycomb et al., 2013)**. Therefore it is possible that astrocytes may play a role in the development of KD. Of interest is the expression of the S1PRs on astrocytes, namely S1PR1, as this receptor can be targeted by the recently developed immunomodulatory drug, pFTY720.

6.4 The effect of psychosine on astrocyte cell survival

Due to a deficiency in GALC activity the toxic by-product of galactosylceramide catabolism, namely psychosine, accumulates in the KD brain **(Wenger et al., 2001)**. In the present study it was found that psychosine induced astrocyte cell death both in a concentration and time dependent manner. The cytotoxicity of psychosine has been well documented in oligodendrocytes and several mechanisms have been suggested to account for its damaging effects. In oligodendrocytes the mode of cell death induced by psychosine has been reported by many groups to be apoptosis **(Haq et al., 2003, Giri et al., 2006, Zaka and Wenger, 2004)**. Although many of these studies were not performed in astrocytes, one can infer that some of the mechanisms may be similar in both cell types. In addition, in the current study, JC-1 assays performed on astrocytes treated with psychosine indicate that the mode of cell death here is also likely apoptosis. The severity of the toxic effects of psychosine have also been previously reported to be concentration dependent **(Sugama et al., 1990)**. In addition to this, the study also reports that the TD_{50} (50% toxic dose) of psychosine varies from cell type to cell type. Astrocytes were reported to have a TD_{50} (50% toxic dose) of ~ 20 µg/ml of psychosine. Oligodendrocytes however had a lower TD_{50} of ~8 µg/ml and sensory neurons of the dorsal root ganglia had a TD_{50} of ~30 µg/ml of psychosine **(Sugama et al., 1990)**. This suggests that although all the above cells will succumb to psychosine toxicity, oligodendrocytes may be far more susceptible to its damaging effects **(Sugama et al., 1990)**.

6.5 A putative receptor for psychosine

Interestingly an orphan GPCR known as T cell death-associated gene 8 receptor (TDAG8), has been suggested to be a putative receptor for psychosine **(Im et al., 2001)**. The evidence supporting this suggestion includes experiments investigating changes in intracellular [cAMP] and [Ca^{2+}] which indicated that TDAG8 is activated by psychosine and related lysosphingolipids

(Im et al., 2001). Psychosine treatment of cells expressing TDAG8, that do not endogenously express the receptor resulted in the accumulation of multinucleated cells (characteristic of the KD brain) **(Im et al., 2001)**. In addition, cell lines such as U937 that endogenously express TDAG8 become multinucleated in response to psychosine whereas cells that do not express the receptor do not **(Im et al., 2001, Kanazawa et al., 2000)**. Whether psychosine is in fact a ligand for the TDAG8 receptor however is disputable. Firstly, the Ki value for psychosine in increasing $[Ca^{2+}]$ and decreasing [cAMP] in cells expressing TDAG8 is significantly higher (~3μM) compared to other signalling lipids such as sphingosylphosphorylcholine, which activates OGR1 with a Ki of 30nM. This relatively high Ki value of psychosine hence indicates that it may not be the normal physiological ligand for TDAG8 **(Mitchison, 2001)**. In addition, the levels of psychosine in the normal CNS are practically undetectable as the breakdown of this metabolite by GALC is extremely rapid. Therefore it is unlikely that psychosine has a physiological function that it accomplishes via its own receptor. Secondly, psychosine induces a wide range of pleotropic effects making it unlikely that psychosine-induced toxicity is mediated via a single receptor **(Hawkins-Salsbury et al., 2013)**. One study used enantiomers of psychosine to study the mechanisms of action of this lipid metabolite. An enantiomer of psychosine was found to have an equal or greater toxicity profile as psychosine, indicating that the mechanisms through which psychosine exerts its toxicity are not mediated via a specific receptor (ie. TDAG8) **(Hawkins-Salsbury et al., 2013)**. Thirdly, psychosine mediated oligodendrocyte death was found to be independent of TDAG8 in MO3.13 oligodendrocyte cells **(Giri et al., 2006)** and finally, a study using TDAG8 knock out mice also reported that psychosine-induced toxicity was independent of the TDAG8 receptor **(Radu et al., 2006)**.

6.6 pFTY720 protects against psychosine induced cell toxicity

In all of the studies performed with psychosine, pFTY720 was able to attenuate the cytotoxic damage induced by the toxic lipid metabolite to varying degrees. The mechanisms of action through which it exerts its protective effects against psychosine however are unknown. S1P, the natural ligand of the S1PRs is believed to promote cell survival and proliferation while ceramide favours apoptosis, thus the balance between these two lipids (ceramide/S1P) has been called the "sphingolipid-rheostat" **(Hannun and Obeid, 2008, Van Brocklyn and Williams, 2012)**. The majority of pro-survival effects of S1P are known to be mediated via the five GPCRs, S1PR1-S1PR5 **(Czubowicz et al., 2015)**. Importantly, pFTY720 binds to four of these five receptors (S1PR1, S1PR3, S1PR4 and S1PR5) and hence pFTY720 also has a pro-survival influence on cells. One such anti-apoptotic effect is mediated through MAPK pathways and ERK phosphorylation. pFTY720 is known to be a potent inducer of pERK and increased levels of pERK1/2 have been reported to protect astrocytes from ischemic attack and reduce the number of apoptotic cells **(Mullershausen et al., 2007, Osinde et al., 2007, Healy et al., 2013, Jiang et al., 2003)**. The PI3K/AKT pathway, likewise induced by pFTY720, is also associated with pro-survival effects as S1PR1/3 activation inhibited the apoptosis of granulosa cells that had been subjected to H_2O_2 induced oxidative stress. This protective effect was reported to be mediated by activation of the PI3Kt/AKT pathway **(Nakahara et al., 2012)**. It has also been reported that mitochondria play a role in the neuroprotective effects mediated by S1PR activation. In an *in vitro* model of ischemia S1P activation of the S1PRs reduced both apoptosis and necrosis through a mechanism that involved stabilisation of the mitochondrial membrane potential and by reducing calcium loading **(Agudo-López et al., 2010)**. Moreover, pFTY720 has

been shown to prevent human prion protein peptide from inducing mitochondrial depolarisation as well as prevent the translocation of Bax and the release of cytochrome c from neuronal mitochondria. This pFTY720 conferred protection against mitochondrial dysfunction was reported to be due to blocking the phosphorylation of cJNK **(Moon et al., 2013)**. Many more examples exist in the literature describing the pro-survival and protective effects of S1PR modulation in varies cell types **(Czubowicz et al., 2015, Cipriani et al., 2015, Xu et al., 2015, Di Pardo et al., 2014, Potteck et al., 2010, Safarian et al., 2015)**. Hence, although the exact mechanism by which pFTY720 attenuates psychosine-induced astrocytic cell death in the current study has not been fully elucidated, it is likely to involve activation of the MAPK/ERK pathways, PI3K/AKT pathways and protection against mitochondrial dysfunction. pFTY720 is also a known immunomodulator and hence may attenuate cell damage via the dampening of proinflammatory processes, although we noted such inflammatory responses were not significant in psychosine-mediated astrocyte cell death or demyelination **(Wang et al., 2007)**.

6.7 Astrocyte priming by LPS and psychosine

Cytokines such as IL6 and TNFα have been reported to be increased in the brains of twi/twi mice compared to wildtype controls thus implicating inflammatory processes in the pathogenesis of KD **(LeVine and Brown, 1997)**. The relative contribution of proinflammatory cytokines to the progression of the disease however is still unknown. In the present study, psychosine treatment alone did not increase the levels of IL6, TNFα or IL1β from cultured mouse astrocytes. Interestingly, in the presence of LPS, psychosine treatment did potentiate the LPS-induced increases in IL6 and TNFα levels. These findings are comparable to a study in which psychosine had no effect on the induction of NO or increase in proinflammatory cytokines levels in primary rat astrocytes. When co-treated with LPS however, psychosine potentiated the LPS-induced increase of NO, IL6, TNFα and IL1β in a concentration dependent manner **(Giri et al., 2002)**. This may be an example of astrocytic priming which, similar to microglia priming, results in an exaggerated response to a secondary stimulus due to sensitisation to a first stimulus **(Cunningham et al., 2005)**. Astrocytic priming has been demonstrated *in vitro* and, more recently, *in vivo.* IFNγ-sensitised astrocytes displayed exaggerated responses to subsequent IL1β or LPS challenges while priming with IL1β, LPS and TNFα resulted in exacerbated chemokine and cell adhesion molecules (CAM) in response to a subsequent TLR2 challenge **(Chung and Benveniste, 1990, Henn et al., 2011).** Recently, intrahippocampal administration of IL1β or TNFα to ME7 prion diseased animals and wildtype controls demonstrated that astrocytes in the degenerating brain are also primed to produce exaggerated chemokine responses to acute stimulation with proinflammatory cytokines **(Hennessy et al., 2015)**.

6.8 The role of proinflammatory cytokines in the pathogenesis of KD

The elucidation of the role of inflammatory molecules in the pathogenesis of KD has been further complicated by various studies which have reported conflicting results. For example, one study reported that psychosine decreased the LPS-induced production of iNOS in a BV2 cell line, whereas in a mixed glial culture, psychosine potentiated the LPS-induced induction of iNOS **(Bashir and Haq, 2011)**. In addition, psychosine is a known inhibitor of PKC and PKC is in turn an inducer of IL6 expression in astrocyte cultures **(Cadman et al., 1994)**. Hence,

psychosine might be expected to suppress IL6 expression in astrocytes via inhibition of PKC **(LeVine and Brown, 1997)**. In order to investigate the significance of elevated levels of TNFα in the twi/twi mouse brain, one group generated twi/twi mice that were also deficient for TNF-R1 (the main receptor through which TNFα acts). In comparison to twi/twi controls, TNF-R1 deficient mice displayed no significant difference in either the clinical or pathological course of the disease. However, when mice were administered with an injection of LPS, the twi/twi TNF-R1 deficient mice had a worsened disease course and a shorter life span **(Pedchenko et al., 2000)**. This indicates that TNF-R1 is not sufficiently activated to contribute to the pathology of KD, however, if a secondary insult such as an infection or fever occurs, TNF-R1 does lead to significant worsening of the disease. Furthermore, in the present study, psychosine induced significant demyelination in organotypic slice cultures prepared from the cerebellum of 10 day old mice pups. However, unlike LPC induced demyelination, which was associated with increased levels of proinflammatory cytokines such as IL6, TNFα and IL1β, psychosine did not induce significant changes in these measured cytokines.

6.9 pFTY720 inhibits psychosine-induced demyelination without an inflammatory component.

Overall the role of psychosine in the direct regulation of proinflammatory cytokines is still ambiguous. It is likely however, that psychosine will enhance the levels of proinflammatory cytokines in the presence of an inflammatory milieu such as the environment created by an infection, fever or insult. In this scenario, psychosine in conjunction with NO, IL6, TNFα and other pro-inflammatory mediators may greatly exacerbate the disease pathology. Importantly the immunomodulatory and anti-inflammatory effects of S1PR modulation has received much attention in the past number of years. Activation of S1PR's in resident immune cells of the brain can regulate their ability to produce cytokines **(Wang et al., 2007)**. pFTY720 has been demonstrated to reduce the levels of IL6 in microglia, astrocytes and neurons succeeding a traumatic brain injury **(Zhang et al., 2008b)** and to attenuate LPC-induced NO release **(Jackson et al., 2011a)**. In addition, specific knockout of S1PR1 from astrocytes or pFTY720 treatment was seen to reduce the release of IL1ß, IL6 and IL17 **(Choi et al., 2011)**. In the present study pFTY720 attenuated the psychosine-induced potentiation of LPS-induced IL6 and TNFα from mouse astrocytes. We also investigated the effect of pFTY720 and BAF312 on LPS-induced IL6 in mouse astrocyte and microglia cells. In our hands pFTY720 and BAF312 only moderately attenuated the levels of IL6 induced by LPS in both mouse astrocytes and microglia. In contrast, pFTY720 and BAF312 significantly attenuated the levels of proinflammatory cytokines in organotypic slice cultures treated with the demyelinating agent LPC. Congruent with this result, pFTY720 has been reported to significantly reduce the levels of cytokines and chemokines in LPC treated organotypic slice cultures **(Sheridan and Dev, 2012)**. The disparity in results between isolated cell cultures and the organotypic slice cultures may be due to the presence of peripheral immune cells in these brain slice models. S1PR modulation of immune cells in the slice cultures by pFTY720 or BAF312 may account for the much greater effect of these drugs at attenuating LPC-induced cytokine levels. Notably, unlike LPC-induced demyelination of organotypic slice cultures, psychosine appeared to effectively induce demyelination without inducing a proinflammatory response. This result in particular was somewhat unexpected and interesting as it demonstrated that S1PR modulation can be

protective against two disparate forms of demyelination, namely demyelination associated with and without an inflammatory component.

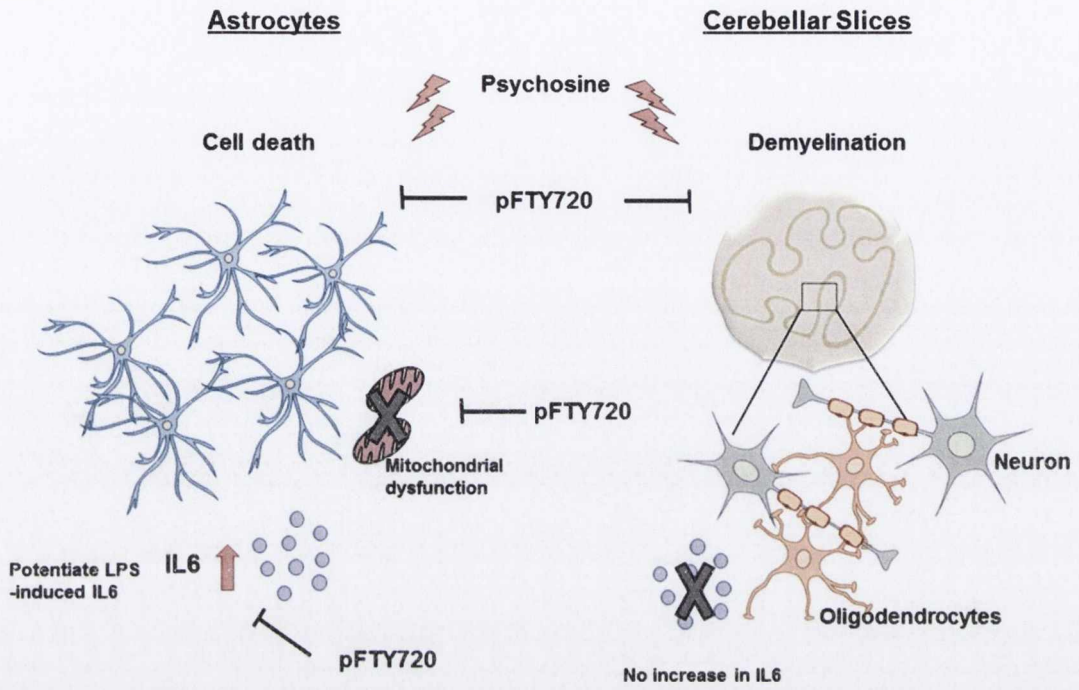

Figure 6.1. Chapter 3 results; Galactosylsphingosine (psychosine) induced demyelination is attenuated by sphingosine 1-phosphate signalling.pFTY720 attenuated psychosine-induced astrocyte cell death, mitochondrial dysfunction and proinflammatory cytokine release. Psychosine also induced wide spread demyelination in cerebellar slice cultures without inducing the release of proinflammatory cytokines. pFTY720 protected the slice cultures from psychosine induced demyelination.

6.10 The effect of psychosine on myelination state in cerebellar slices

Demyelination and oligodendrocyte cell death, induced by the toxic metabolite psychosine, are two major pathological features of the KD brain. Although not fully understood, many proposed mechanisms governing psychosine-induced oligodendrocyte cell death have been described. These include preferential accumulation of psychosine in lipid rafts and resultant inhibition of PKC; mitochondrial damage and cytochrome c release; upregulation of JNK; caspase mediated apoptosis; an increase in $sPLA_2$; and increased levels of proinflammatory cytokines and NO generation **(Davenport et al., 2011)**. In the current study psychosine induced demyelination in organotypic slice cultures prepared from mouse cerebellum as measured by MBP, MOG and PLP immunostaining. Treatment with pFTY720 prevented the psychosine-induced loss of MBP, MOG and PLP observed in these slice cultures. Given our knowledge of S1PRs in regulating oligodendrocyte physiology, we postulate the efficacy of pFTY720 in protecting against psychosine-induced demyelination may be due to direct effects on oligodendrocyte survival and/or maturation as well as attenuating inflammatory or cell death pathways **(Dev et al., 2008, Miron et al., 2008b)**.

6.11 S1PRs enhance myelination via modulation of OPCs

Over a decade ago, S1PRs were reported to regulate Ca^{2+} and MAPK signalling in cultured oligodendrocyte cells **(Fatatis and Miller, 1996, Hida et al., 1999)**. Since then much work on the effect of S1PR activation on oligodendrocytes and myelination in toxin-induced CNS demyelinating models and in the MS EAE animal model have been performed. Treatment with pFTY720 is reported to reduce the degree of initial injury, augment the number of OPCs and enhance remyelination during the recovery phase in a cuprizone model of demyelination (a copper chelator; *bis*-cyclohexanone oxaldihydrazone), although these results remain controversial **(Kim et al., 2011)**. pFTY720 is also reported to modulate process extension, differentiation, and survival in human oligodendrocytes. Enhancing OPC number and function is believed as beneficial as these cells play important roles in remyelination. OPC's respond to chemotactic signals, migrate to lesions, proliferate and differentiate into mature oligodendrocytes, which can then remyelinate axons **(Miron et al., 2011)**. The functional effects of S1PR modulation on oligodendrocytes have been associated with activation of ERK signalling pathways, as observed in rat oligodendroglia lineage cells **(Coelho et al., 2007, Jung et al., 2007)**. Another signalling cascade regulated by S1PRs is the Shh-Pat-Smo-Gli1 pathway (sonic hedgehog protein, Patched receptor, Smoothened and Gli1 transcription factor), which is essential for OPC survival, proliferation, differentiation and subsequent remyelination **(Zhang et al., 2009, Zhang et al., 2015, Ortega et al., 2012)**. Interestingly, treatment of EAE mice with pFTY720 increased the levels of Shh, Smo and Gli1 which coincided with increased OPC proliferation and differentiation **(Zhang et al., 2015)**.

6.12 Glia cells as cellular targets in KD

In addition to the effects of pFTY720 on OPCs and oligodendrocytes, pFTY720 likely prevents demyelination through immunomodulation of glial cells. Many now believe that astrocytes and microglia play a prominent role in myelin dysfunction **(Chew et al., 2013, Yeo et al., 2012)**.
The activation of astrocytes and microglial have also been reported to play important roles in disease progression in the twi/twi mice **(LeVine and Brown, 1997, Mohri et al., 2006, Ijichi et al., 2013)**. Astrocytes and microglia physically communicate via, for example, receptor ligand

interactions such as CD200/CD200R, as well as communication via several connexins **(Claycomb et al., 2013, Koning et al., 2009.)**. Disruption of CD200/CD200R interaction activates microglial suggested to encourage proinflammatory responses in the CNS, whereas dysfunction of connexins 43/47 and 30/32 in astrocytic gap junctions has been implicated in the pathogenesis of several models of demyelinating disease **(Brand-Schieber et al., 2005, Lutz et al., 2009)**. In twi/twi mice, microglia are reported to increase production of hematopoietic prostaglandin synthase (HPGDS) and PGD2, while astrocytes have increased expression of PGD2 receptors, DP1 and DP2 **(Mohri et al., 2006)**. The genetic ablation of DP1 and blockade of HPGDS in the twi/twi mouse resulted in decreased activation of both astrocytes and microglia and significantly less demyelination **(Mohri et al., 2006)**. In this regard, it has been suggested that pFTY720 can promote remyelination via limiting microglial response **(Jackson et al., 2011a)**. Recent studies are now also emerging that implicate directly astrocytes in the etiology of KD **(Ijichi et al., 2013)**. In particular, the expression of matrix metalloproteinase 3 (MMP3) is reported to be increased in astrocytes at the time of disease onset in the twi/twi mouse and also seen to elevate with disease progression **(Ijichi et al., 2013)**. Astrocytic MMP3 is believed to proteolitically target myelin protein and is a major mediator of globoid cell formation **(Ijichi et al., 2013)**. In our studies we did not observe overt microglial activation in our slice cultures or increased levels of IL6 in response to psychosine-induced demyelination. We acknowledge, however, these slice culture studies may differ to *in vivo* settings, where demyelination observed in KD may involve an intricate balance between astrocytes and microglia and where drugs such as pFTY720 may attenuate psychosine-induced demyelination via a multi-cellular mechanism.

6.13 Regulating neuronal dysfunction by pFTY720

Psychosine accumulation has also been reported to increase PP1, PP2A and GSK3β activity, which dephosphorylates neurofilaments and inhibits fast axonal transport **(Cantuti-Castelvetri et al., 2012, Cantuti Castelvetri et al., 2013)**. Importantly, pFTY720 has been shown to have direct effects on neuronal function and in the preservation of axonal integrity. For example, pFTY720 was found to reduce acute axonal damage after acute and chronic cuprizone-induced demyelination **(Slowik et al., 2015)** and also prevented/reversed pre- and postsynaptic alterations of glutamate transmission seen in EAE mice **(Rossi et al., 2012)**. As the preservation of axons is frequently linked to remyelination, the neuroprotective effects of S1PR modulation may be an additional avenue through which pFTY720 and BAF312 exerted protection over psychosine-induced demyelination in organotypic slice cultures. Furthermore, pFTY720 is reported to increase brain derived neurotrophic factor (BDNF) levels through the MAPK pathway and counteract NMDA-induced neuronal death **(Deogracias et al., 2012)**. This may be therapeutically relevant for Rett syndrome in particular as BDNF levels are decreased in the mouse model of Rett syndrome (*MeCP2*-null mice) and correlates with symptom progression **(Deogracias et al., 2012)**.

6.14 Controversy over pFTY720 and its ability to enhance remyelination *in vivo*

Despite the considerable evidence in support of pFTY720 enhancing remyelination *in vitro*, there is controversy in the literature regarding its effect on myelination *in vivo* **(Slowik et al., 2015)**. Treatment with pFTY720 has been reported by a number of independent studies to not enhance remyelination after cuprizone -induced demyelination in mice **(Hu et al., 2011, Kim et**

al., 2011, Slowik et al., 2015, Alme et al., 2015). Furthermore focal demyelination induced by LPC injection in rat spinal cord was also unaffected by pFTY720 treatment **(Hu et al., 2011)**. The discrepant results reported for organotypic slice cultures **(Miron et al., 2010, Sheridan and Dev, 2012)** and *in vivo* cuprizone model **(Slowik et al., 2015, Alme et al., 2015)** are likely caused by the differing experimental paradigms used. In addition the time in which pFTY720 treatment is initiated in the cuprizone mice model may be an important factor and a study addressing this may be beneficial. Overall, however, it is clear that pFTY720, and likely BAF312, exerts beneficial effects beyond an immunomodulatory function, acting directly on OPCs, oligodendrocytes, astrocytes, microglia and neurons.

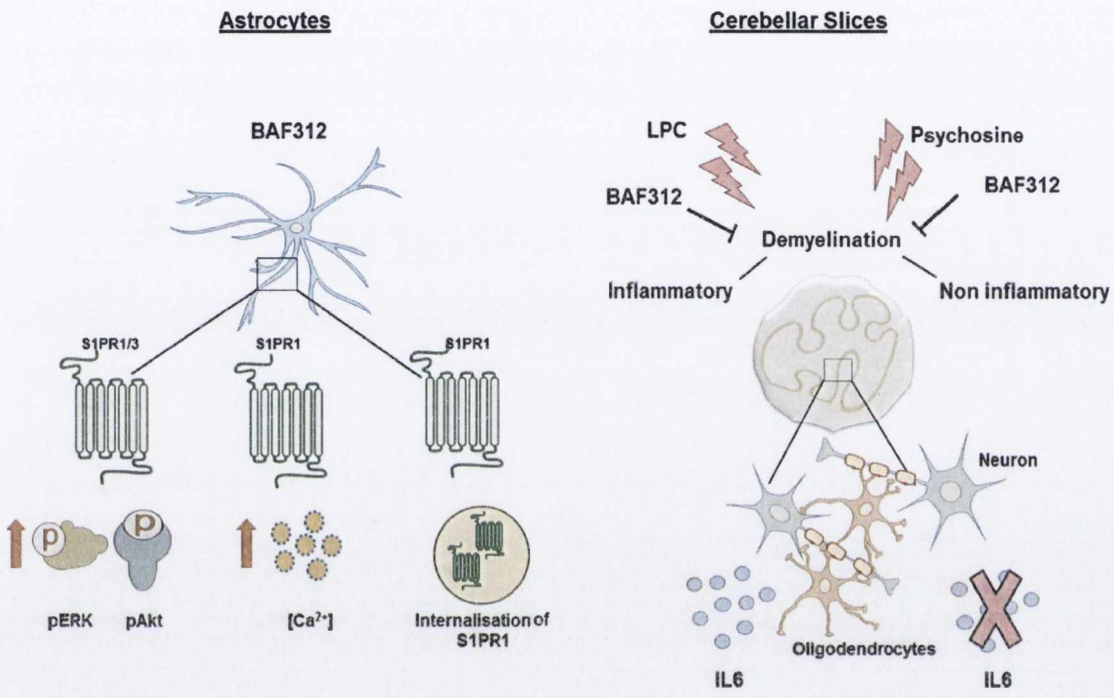

Figure 6.2. Chapter 4 results; BAF312 (Siponimod) attenutes psychosine induced demyelination in organotypic slice cultures. BAF312 induces pERK, pAKT and Ca^{2+} signalling through the S1PR1 subtype and internalisation of S1PR1 in astrocytes. BAF312 also attenuated proinflammatory associated LPC-induced demyelination and proinflammatory independent psychosine-induced demyelination in cerebellar slice cultures.

6.15 S1PR1 interacts with Pex14, a protein mutated in Zellweger syndrome

To date the mechanisms governing processes such as S1PR1 internalisation, degradation and sustained signaling as well as the identity of many of these accessory proteins remains unclear. Studies investigating these interacting proteins may provide new insights into the pharmacology, function and disease relevance of S1PRs and ultimately lead to the development of novel therapeutic agents. Here we identified a biochemical interaction between S1PR1 and the peroxin Pex14 and performed a number of functional studies to identify its role. Although, as yet, the functional role of this interaction remains unclear, it is interesting to note that mutation of Pex14 is linked to the disease Zellweger syndrome (ZS). ZS is an autosomal recessive disorder caused by mutations in *PEX* genes that result in a disruption to the import of matrix proteins to the peroxisome **(Purdue and Lazarow, 2001, Wanders, 2004)**. In the most severe cases of this disease, patients usually die within their first year, suffering from a range of phenotypes including neonatal seizures, neurologic dysfunction, abnormal neuronal migration, dysmyelination or hypomyleination and neuronal degeneration **(Wanders, 2004, Crane, 2014)** . Mutations in *PEX14* accounts for a small number of ZS cases, where to date only two cases with a *PEX14* deficiency have been documented **(Steinberg SJ, 2003)**. In the first reported case a patient homozygous for a nonsense mutation in a putative coiled-coil region of PEX14, c.553C>T (p.Q185X) has been reported **(Shimozawa et al., 2004)**. The second documented case described a novel deletion frameshift mutation in exon 3 of *PEX14* **(Huybrechts et al., 2008)**. While, from our studies the function role of S1PR1-Pex14 interaction remains elusive, these studies highlight the importance of identifying novel S1PR1 interacting proteins for the purpose of exploiting and developing better S1PRs drugs for a range of illnesses.

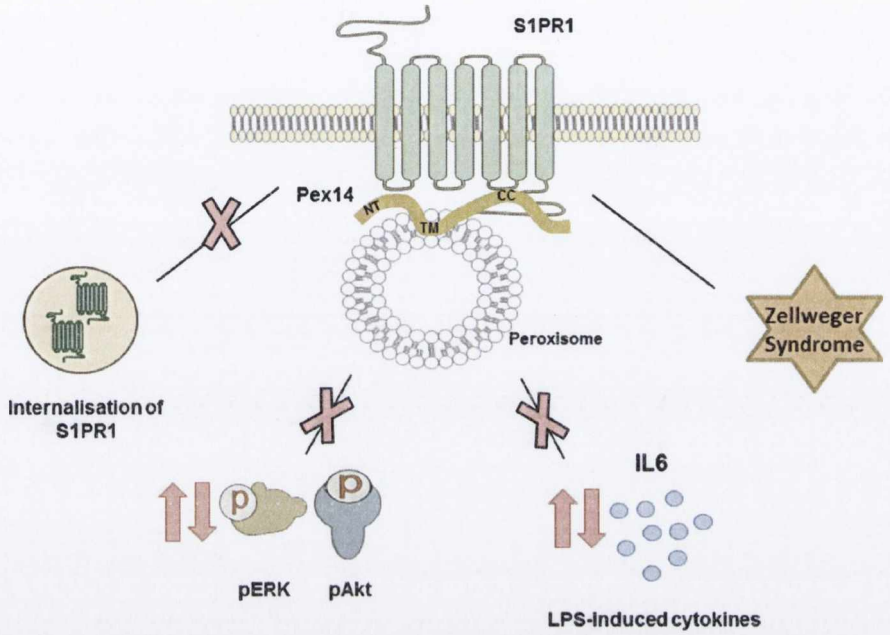

Figure 6.3. Chapter 5 results; Discovery of a novel S1PR interacting protein; Pex14. Mutated Pex14 can cause Zellweger syndrome. The intracellular loop 3 and C terminus of S1PR1 interacts with coiled coil region of Pex14.This interaction does not inhibit pFTY720-induced internalisation of S1PR1, nor does it alter pFTY720 mediated modulation of cytokine levels or pFTY720-induced pERK and pAKT signalling.

6.16 Further Studies and Future directions

The current study demonstrated the protective effects of S1PR modulation over psychosine induced toxicity and demyelination in an *in vitro* setting as well as identified a novel S1PR1 interacting protein (Pex14). Some of the limitations observed during our studies have been detailed at the end of each chapter. A number of findings reported here warrant further investigation. Firstly, it would be of interest to further investigate the effect of psychosine on the axon itself and to determine if this may be a causal factor in the psychosine-induced demyelination observed here. It would also be important to determine the temporal effect of psychosine and elucidate which cell type was first to succumb to psychosine toxicity and hence perpetuate the damage. A second, and most important, part of this work that remains is to examine the effects of pFTY720 and BAF312 in the twi/twi mouse model of KD. Indeed, treatment with pFTY720 or BAF312 either alone or in combination with other tried therapies such as viral mediated gene therapy or BMT would provide support to our cell culture and slice demyelination studies and perhaps support the use of these therapies in clinical trials. Thirdly, an experiment demonstrating the interaction between S1PR1 and endogenous Pex14 would be necessary before any further work on a functional role of this interaction could be performed.

6.16 Concluding remarks

Demyelinating disorders such as KD have devastating effects on the lives of the patient and their family. Although this disease is rare there is still an urgent need to develop more efficacious treatments that will hopefully improve the quality of life for these children. The S1PR modulator, pFTY720, is currently being used as a therapy for relapsing remitting MS however, it is thought that this drug may be beneficial in a number of diseases that exhibit a range of neuroinflammatory and neurodegenerative features. In support of this, the neuroprotective spectrum of pFTY720 has been illustrated in a number of animal models including models of Alzheimer's disease **(Hemmati et al., 2013)**, spinal cord injury **(Lee et al., 2009)**, Rett syndrome **(Deogracias et al., 2012)**, ischaemic stroke **(Liu et al., 2013)** and Huntington's disease **(Di Pardo et al., 2014)**. Another S1PR modulator, BAF312, which targets the S1PR1 and S1PR5 subtypes is also being tested in a clinical setting and has successfully undergone Phase II clinical trials for relapsing remitting MS **(Selmaj et al., 2013)** and is in Phase II clinical trials for secondary progressive MS. In the current study, BAF312 was found to induce pERK, pAKT and Ca^{2+} signalling as well as internalise S1PR1 on astrocyte cells in a similar manner to pFTY720. In addition, pFTY720 attenuated psychosine-induced mitochondrial dysfunction and astrocyte cell death while both pFTY720 and BAF312 successfully attenuated LPC- and psychosine- induced demyelination in cerebellar slice cultures. Furthermore an interaction between SPR1 and a novel binding partner Pex14 was discovered.

Given the data presented in the current study, further investigation into the effects of pFTY720 and BAF312 in the KD animal model, namely, the twitcher mouse, are now warranted. In closing, we suggest that this work and further *in vivo* studies will support the use of pFTY720 and BAF312 as novel therapies for the treatment of KD.

References

ABBOTT, N. J., RONNBACK, L. & HANSSON, E. 2006. Astrocyte-endothelial interactions at the blood-brain barrier. *Nat Rev Neurosci,* 7, 41-53.

ADACHI, K. & CHIBA, K. 2008. FTY720 story. Its discovery and the following accelerated development of sphingosine 1-phosphate receptor agonists as immunomodulators based on reverse pharmacology. *Perspectives in Medicinal Chemistry,* 1, 11-23.

AGUDO-LÓPEZ, A., MIGUEL, B. G., FERNÁNDEZ, I. & MARTÍNEZ, A. M. 2010. Involvement of mitochondria on neuroprotective effect of sphingosine-1-phosphate in cell death in an in vitro model of brain ischemia. *Neuroscience Letters,* 470, 130-133.

AL-IZKI, S., PRYCE, G., JACKSON, S. J., GIOVANNONI, G. & BAKER, D. 2011. Immunosuppression with FTY720 is insufficient to prevent secondary progressive neurodegeneration in experimental autoimmune encephalomyelitis. *Multiple Sclerosis Journal,* 17, 939-948.

ALBERT, R., HINTERDING, K., BRINKMANN, V., GUERINI, D., MÜLLER-HARTWIEG, C., KNECHT, H., SIMEON, C., STREIFF, M., WAGNER, T., WELZENBACH, K., ZÉCRI, F., ZOLLINGER, M., COOKE, N. & FRANCOTTE, E. 2005. Novel Immunomodulator FTY720 Is Phosphorylated in Rats and Humans To Form a Single Stereoisomer. Identification, Chemical Proof, and Biological Characterization of the Biologically Active Species and Its Enantiomer. *J Med Chem,* 48, 5373-5377.

ALME, M. N., NYSTAD, A. E., BØ, L., MYHR, K.-M., VEDELER, C. A., WERGELAND, S. & TORKILDSEN, Ø. 2015. Fingolimod does not enhance cerebellar remyelination in the cuprizone model. *Journal of Neuroimmunology,* 285, 180-186.

ANDERSON, R. A., BORONENKOV, I. V., DOUGHMAN, S. D., KUNZ, J. & LOIJENS, J. C. 1999. Phosphatidylinositol Phosphate Kinases, a Multifaceted Family of Signaling Enzymes. *Journal of Biological Chemistry,* 274, 9907-9910.

ASLE-ROUSTA, M., KOLAHDOOZ, Z., ORYAN, S., AHMADIANI, A. & DARGAHI, L. 2013. FTY720 (Fingolimod) Attenuates Beta-amyloid Peptide (Aβ42)-Induced Impairment of Spatial Learning and Memory in Rats. *Journal of Molecular Neuroscience,* 50, 524-532.

BALATONI, B., STORCH, M. K., SWOBODA, E.-M., SCHÖNBORN, V., KOZIEL, A., LAMBROU, G. N., HIESTAND, P. C., WEISSERT, R. & FOSTER, C. A. 2007. FTY720 sustains and restores neuronal function in the DA rat model of MOG-induced experimental autoimmune encephalomyelitis. *Brain Research Bulletin,* 74, 307-316.

BANKOVICH, A. J., SHIOW, L. R. & CYSTER, J. G. 2010. CD69 suppresses sphingosine 1-phosophate receptor-1 (S1P1) function through interaction with membrane helix 4. *J Biol Chem,* 285, 22328-37.

BARNETT, S. C. & LININGTON, C. 2013. Myelination: Do Astrocytes Play a Role? *The Neuroscientist,* 19, 442-450.

BASHIR & HAQ 2011. Effect of psychosine on inducible nitric-oxide synthase expression under different culture conditions: implications for Krabbe disease. *Eur Rev Med Pharmacol Sci,* 15, 1282-1287.

BASSI, R., ANELLI, V., GIUSSANI, P., TETTAMANTI, G., VIANI, P. & RIBONI, L. 2006. Sphingosine-1-phosphate is released by cerebellar astrocytes in response to bFGF and induces astrocyte proliferation through Gi-protein-coupled receptors. *Glia,* 53, 621-630.

BENNETT, J. A. & DINGLEDINE, R. 1995. Topology profile for a glutamate receptor: Three transmembrane domains and a channel-lining reentrant membrane loop. *Neuron,* 14, 373-384.

BHARTI, P., SCHLIEBS, W., SCHIEVELBUSCH, T., NEUHAUS, A., DAVID, C., KOCK, K., HERRMANN, C., MEYER, H. E., WIESE, S., WARSCHEID, B., THEISS, C. & ERDMANN, R. 2011. PEX14 is required for microtubule-based peroxisome motility in human cells. *Journal of Cell Science,* 124, 1759-1768.

BHATTACHARYA, BABWAH & FERGUSON 2004. Small GTP-binding protein-coupled receptors. *Biochemical Society Transactions* 32, 1040-1044.

BIEBERICH, E. 2011. There is More to a Lipid than just Being a Fat: Sphingolipid-Guided Differentiation of Oligodendroglial Lineage from Embryonic Stem Cells. *Neurochemical Research,* 36, 1601-1611.

BIRGBAUER, E., RAO, T. S. & WEBB, M. 2004. Lysolecithin induces demyelination in vitro in a cerebellar slice culture system. *Journal of Neuroscience Research,* 78, 157-166.

BISWAS, S. & LE VINE, S. M. 2002. Substrate-Reduction Therapy Enhances the Benefits of Bone Marrow Transplantation in Young Mice with Globoid Cell Leukodystrophy. *Pediatr Res,* 51, 40-47.

BLAKEMORE, W. F. & CRANG, A. J. 1989. The relationship between type-1 astrocytes, Schwann cells and oligodendrocytes following transplantation of glial cell cultures into demyelinating lesions in the adult rat spinal cord. *J Neurocytol,* 18, 519-28.

BOCKAERT, J., ROUSSIGNOL, G., BECAMEL, C., GAVARINI, S., JOUBERT, L., DUMUIS, A., FAGNI, L. & MARIN, P. 2004. GPCR-interacting proteins (GIPs): nature and functions. *Biochem Soc Trans,* 32, 851-5.

BRAND-SCHIEBER, E. & WERNER, P. 2004. Calcium channel blockers ameliorate disease in a mouse model of multiple sclerosis. *Exp Neurol,* 189, 5-9.

BRAND-SCHIEBER, E., WERNER, P., IACOBAS, D. A., IACOBAS, S., BEELITZ, M., LOWERY, S. L., SPRAY, D. C. & SCEMES, E. 2005. Connexin43, the major gap junction protein of astrocytes, is down-regulated in inflamed white matter in an animal model of multiple sclerosis. *Journal of Neuroscience Research,* 80, 798-808.

BRENNER, M., JOHNSON, A. B., BOESPFLUG-TANGUY, O., RODRIGUEZ, D., GOLDMAN, J. E. & MESSING, A. 2001. Mutations in GFAP, encoding glial fibrillary acidic protein, are associated with Alexander disease. *Nat Genet,* 27, 117-120.

BROWN, L.-A. & BAKER, A. 2008. Shuttles and cycles: transport of proteins into the peroxisome matrix (Review). *Molecular Membrane Biology,* 25, 363-375.

BRÜCK, W. 2005. Inflammatory demyelination is not central to the pathogenesis of multiple sclerosis. *Journal of Neurology,* 252, v10-v15.

BUSH, T. G., PUVANACHANDRA, N., HORNER, C. H., POLITO, A., OSTENFELD, T., SVENDSEN, C. N., MUCKE, L., JOHNSON, M. H. & SOFRONIEW, M. V. 1999. Leukocyte Infiltration, Neuronal Degeneration, and Neurite Outgrowth after Ablation of Scar-Forming, Reactive Astrocytes in Adult Transgenic Mice. *Neuron,* 23, 297-308.

CADMAN, E. D., WITTE, D. G. & LEE, C.-M. 1994. Regulation of the Release of Interleukin-6 from Human Astrocytoma Cells. *Journal of Neurochemistry,* 63, 980-987.

CANTUTI-CASTELVETRI, L., ZHU, H., GIVOGRI, M. I., CHIDAVAENZI, R. L., LOPEZ-ROSAS, A. & BONGARZONE, E. R. 2012. Psychosine induces the dephosphorylation of neurofilaments by deregulation of PP1 and PP2A phosphatases. *Neurobiology of Disease,* 46, 325-335.

CANTUTI CASTELVETRI, L., GIVOGRI, M. I., HEBERT, A., SMITH, B., SONG, Y., KAMINSKA, A., LOPEZ-ROSAS, A., MORFINI, G., PIGINO, G., SANDS, M., BRADY, S. T. & BONGARZONE, E. R. 2013. The Sphingolipid Psychosine Inhibits Fast Axonal Transport in Krabbe Disease by Activation of GSK3β and Deregulation of Molecular Motors. *The Journal of Neuroscience,* 33, 10048-10056.

CARR, C. M. & KIM, P. S. 1993. A spring-loaded mechanism for the conformational change of influenza hemagglutinin. *Cell,* 73, 823-832.

CHAE, S. S., PROIA, R. L. & HLA, T. 2004. Constitutive expression of the S1P1 receptor in adult tissues. *Prostaglandins Other Lipid Mediat,* 73, 141-50.

CHEN, H., LIU, Z. & HUANG, X. 2010. Drosophila models of peroxisomal biogenesis disorder: peroxins are required for spermatogenesis and very-long-chain fatty acid metabolism. *Human Molecular Genetics,* 19, 494-505.

CHEW, L. J., FUSAR-POLI, P. & SCHMITZ, T. 2013. Oligodendroglial alterations and the role of microglia in white matter injury: relevance to schizophrenia. *Dev Neurosci,* 35, 102-29.

CHIBA, K. & ADACHI, K. 2012. Sphingosine 1-Phosphate Receptor 1 as a Useful Target for Treatment of Multiple Sclerosis. *Pharmaceuticals,* 5, 514-528.

CHOI, J. W. & CHUN, J. 2013. Lysophospholipids and their receptors in the central nervous system(). *Biochim Biophys Acta,* 1831, 20-32.

CHOI, J. W., GARDELL, S. E., HERR, D. R., RIVERA, R., LEE, C. W., NOGUCHI, K., TEO, S. T., YUNG, Y. C., LU, M., KENNEDY, G. & CHUN, J. 2011. FTY720 (fingolimod) efficacy in an animal model of multiple sclerosis requires astrocyte sphingosine 1-phosphate receptor 1 (S1P1) modulation. *Proceedings of the National Academy of Sciences,* 108, 751-6.

CHUNG, I. Y. & BENVENISTE, E. N. 1990. Tumor necrosis factor-alpha production by astrocytes. Induction by lipopolysaccharide, IFN-gamma, and IL-1 beta. *The Journal of Immunology,* 144, 2999-3007.

CIPRIANI, R., CHARA, J. C., RODRÍGUEZ-ANTIGÜEDAD, A. & MATUTE, C. 2015. FTY720 attenuates excitotoxicity and neuroinflammation. *Journal of Neuroinflammation,* 12, 86.

CLAYCOMB, K., JOHNSON, K., WINOKUR, P., SACINO, A. & CROCKER, S. 2013. Astrocyte Regulation of CNS Inflammation and Remyelination. *Brain Sciences,* 3, 1109-1127.

COELHO, R. P., PAYNE, S. G., BITTMAN, R., SPIEGEL, S. & SATO-BIGBEE, C. 2007. The Immunomodulator FTY720 Has a Direct Cytoprotective Effect in Oligodendrocyte Progenitors. *Journal of Pharmacology and Experimental Therapeutics,* 323, 626-635.

COLTON & WILCOCK 2010. Assessing activation states in microglia. . *CNS Neurol Disord Drug Targets.* , April;9, 174-91.

COMPSTON, A. & COLES, A. 2008. Multiple sclerosis. *Lancet,* 372, 1502-17.

COOPER, C. E., MARKUS, M., SEETULSINGH, S. P. & WRIGGLESWORTH, J. M. 1993. Kinetics of inhibition of purified and mitochondrial cytochrome c oxidase by psychosine (beta-galactosylsphingosine). *Biochemical Journal,* 290, 139-144.

CRANE, D. I. 2014. Revisiting the neuropathogenesis of Zellweger syndrome. *Neurochemistry International,* 69, 1-8.

CRANER, M. J., DAMARJIAN, T. G., LIU, S., HAINS, B. C., LO, A. C., BLACK, J. A., NEWCOMBE, J., CUZNER, M. L. & WAXMAN, S. G. 2005. Sodium channels contribute to microglia/macrophage activation and function in EAE and MS. *Glia,* 49, 220-9.

CUNNINGHAM, C., WILCOCKSON, D. C., CAMPION, S., LUNNON, K. & PERRY, V. H. 2005. Central and Systemic Endotoxin Challenges Exacerbate the Local Inflammatory Response and Increase Neuronal Death during Chronic Neurodegeneration. *The Journal of Neuroscience,* 25, 9275-9284.

CYSTER, J. G. & SCHWAB, S. R. 2012. Sphingosine-1-phosphate and lymphocyte egress from lymphoid organs.

CZUBOWICZ, K., CIEŚLIK, M., PYSZKO, J., STROSZNAJDER, J. B. & STROSZNAJDER, R. P. 2015. Sphingosine-1-Phosphate and Its Effect on Glucose Deprivation/Glucose Reload Stress: From Gene Expression to Neuronal Survival. *Molecular Neurobiology,* 51, 1300-1308.

DAVENPORT, WILLIAMSON & TAYLOR 2011. Pathophysiology of Krabbe disease. *Orbit: The University of Sydney undergraduate research journal,* 2, 1-20.

DE GASPERI, R. F., V L PEREZ, G M SENTURK, E WEN, P H KELLEY, K ELDER, G A GAMA SOSA, M A 2004. Transgenic rescue of Krabbe disease in the twitcher mouse. *Gene Therapy, Nature,* 11

1188-1194.

DEOGRACIAS, R., YAZDANI, M., DEKKERS, M. P. J., GUY, J., IONESCU, M. C. S., VOGT, K. E. & BARDE, Y.-A. 2012. Fingolimod, a sphingosine-1 phosphate receptor modulator, increases BDNF levels and improves symptoms of a mouse model of Rett syndrome. *Proceedings of the National Academy of Sciences,* 109, 14230-14235.

DEV, K. K., MULLERSHAUSEN, F., MATTES, H., KUHN, R. R., BILBE, G., HOYER, D. & MIR, A. 2008. Brain sphingosine-1-phosphate receptors: Implication for FTY720 in the treatment of multiple sclerosis. *Pharmacology & Therapeutics,* 117, 77-93.

DI PARDO, A., AMICO, E., FAVELLATO, M., CASTRATARO, R., FUCILE, S., SQUITIERI, F. & MAGLIONE, V. 2014. FTY720 (fingolimod) is a neuroprotective and disease-modifying agent in cellular and mouse models of Huntington disease. *Human Molecular Genetics,* 23, 2251-2265.

DI PENTA, A., MORENO, B., REIX, S., FERNANDEZ-DIEZ, B., VILLANUEVA, M., ERREA, O., ESCALA, N., VANDENBROECK, K., COMELLA, J. X. & VILLOSLADA, P. 2013. Oxidative Stress and Proinflammatory Cytokines Contribute to Demyelination and Axonal Damage in a Cerebellar Culture Model of Neuroinflammation. *PLoS One,* 8, e54722.

DUCHEN, W., EICHER, M., JACOBS, M., SCARAVILLI, F. & TEIXEIRA, F. 1980. HEREDITARY LEUCODYSTROPHY IN THE MOUSE: THE NEW MUTANT TWITCHER. *Brain,* 103, 695-710.

ESCOLAR, M. L., POE, M. D., MARTIN, H. R. & KURTZBERG, J. 2006. A Staging System for Infantile Krabbe Disease to Predict Outcome After Unrelated Umbilical Cord Blood Transplantation. *Pediatrics,* 118, e879-e889.

ESTRADA-BERNAL, A., PALANICHAMY, K., RAY CHAUDHURY, A. & VAN BROCKLYN, J. R. 2012. Induction of brain tumor stem cell apoptosis by FTY720: a potential therapeutic agent for glioblastoma. *Neuro-Oncology,* 14, 405-415.

FANELLI, F. & DE BENEDETTI, P. G. 2011. Update 1 of: computational modeling approaches to structure-function analysis of G protein-coupled receptors. *Chem Rev,* 111, PR438-535.

FATATIS, A. & MILLER, R. J. 1996. Sphingosine and Sphingosine 1-Phosphate Differentially Modulate Platelet-derived Growth Factor-BB-induced Ca Signaling in Transformed Oligodendrocytes. *Journal of Biological Chemistry,* 271**,** 295-301.

FELTS, P. A., WOOLSTON, A.-M., FERNANDO, H. B., ASQUITH, S., GREGSON, N. A., MIZZI, O. J. & SMITH, K. J. 2005. Inflammation and primary demyelination induced by the intraspinal injection of lipopolysaccharide. *Brain,* 128**,** 1649-1666.

FERGUSON, S. S. G. 2007. Phosphorylation-independent attenuation of GPCR signalling. *Trends Pharmacol Sci,* 28**,** 173-179.

FIEGER, C. B., HUANG, M.-C., VAN BROCKLYN, J. R. & GOETZL, E. J. 2005. Type 1 sphingosine 1-phosphate G protein-coupled receptor signaling of lymphocyte functions requires sulfation of its extracellular amino-terminal tyrosines. *The FASEB Journal.*

FISCHER, I., ALLIOD, C., MARTINIER, N., NEWCOMBE, J., BRANA, C. & POULY, S. 2011. Sphingosine Kinase 1 and Sphingosine 1-Phosphate Receptor 3 Are Functionally Upregulated on Astrocytes under Pro-Inflammatory Conditions. *PLoS One,* 6**,** e23905.

FORREST, M., SUN, S.-Y., HAJDU, R., BERGSTROM, J., CARD, D., DOHERTY, G., HALE, J., KEOHANE, C., MEYERS, C., MILLIGAN, J., MILLS, S., NOMURA, N., ROSEN, H., ROSENBACH, M., SHEI, G.-J., SINGER, I. I., TIAN, M., WEST, S., WHITE, V., XIE, J., PROIA, R. L. & MANDALA, S. 2004. Immune Cell Regulation and Cardiovascular Effects of Sphingosine 1-Phosphate Receptor Agonists in Rodents Are Mediated via Distinct Receptor Subtypes. *Journal of Pharmacology and Experimental Therapeutics,* 309**,** 758-768.

FUJIWARA, Y., OSBORNE, D. A., WALKER, M. D., WANG, D. A., BAUTISTA, D. A., LILIOM, K., VAN BROCKLYN, J. R., PARRILL, A. L. & TIGYI, G. 2007. Identification of the hydrophobic ligand binding pocket of the S1P1 receptor. *J Biol Chem,* 282**,** 2374-85.

FYRST, H. & SABA, J. D. 2010. An update on sphingosine-1-phosphate and other sphingolipid mediators. *Nature Chemical Biology,* 6**,** 489-497.

GAO, F., LIU, Y., LI, X., WANG, Y., WEI, D. & JIANG, W. 2012. Fingolimod (FTY720) inhibits neuroinflammation and attenuates spontaneous convulsions in lithium-pilocarpine induced status epilepticus in rat model. *Pharmacology Biochemistry and Behavior,* 103**,** 187-196.

GERGELY, P., NUESSLEIN-HILDESHEIM, B., GUERINI, D., BRINKMANN, V., TRAEBERT, M., BRUNS, C., PAN, S., GRAY, N. S., HINTERDING, K., COOKE, N. G., GROENEWEGEN, A., VITALITI, A., SING, T., LUTTRINGER, O., YANG, J., GARDIN, A., WANG, N., CRUMB JR, W. J., SALTZMAN, M., ROSENBERG, M. & WALLSTRÖM, E. 2012. The selective sphingosine 1-phosphate receptor modulator BAF312 redirects lymphocyte distribution and has species-specific effects on heart rate. *British Journal of Pharmacology,* 167**,** 1035-1047.

GILLINGHAM, A. K. & MUNRO, S. 2003. Long coiled-coil proteins and membrane traffic. *Biochimica et Biophysica Acta (BBA) - Molecular Cell Research,* 1641**,** 71-85.

GIRI, S., JATANA, M., RATTAN, R., WON, J. S., SINGH, I. & SINGH, A. K. 2002. Galactosylsphingosine (psychosine)-induced expression of cytokine-mediated inducible nitric oxide synthases via AP-1 and C/EBP: implications for Krabbe disease. *FASEB J,* 16**,** 661-672.

GIRI, S., KHAN, M., NATH, N., SINGH, I. & SINGH, A. K. 2008. The role of AMPK in psychosine mediated effects on oligodendrocytes and astrocytes: implication for Krabbe Disease. *Journal of Neurochemistry,* 105**,** 1820-1833.

GIRI, S., KHAN, M., RATTAN, R., SINGH, I. & SINGH, A. K. 2006. Krabbe disease: psychosine-mediated activation of phospholipase A2 in oligodendrocyte cell death. *J Lipid Res,* 47**,** 1478-92.

GIUNTI, D., PARODI, B., CORDANO, C., UCCELLI, A. & KERLERO DE ROSBO, N. 2014. Can we switch microglia's phenotype to foster neuroprotection? Focus on multiple sclerosis. *Immunology,* 141**,** 328-339.

GOUVEIA, A. M. M., REGUENGA, C., OLIVEIRA, M. E. M., SÁ-MIRANDA, C. & AZEVEDO, J. E. 2000. Characterization of Peroxisomal Pex5p from Rat Liver: Pex5p IN THE Pex5p-Pex14p MEMBRANE COMPLEX IS A TRANSMEMBRANE PROTEIN. *Journal of Biological Chemistry,* 275**,** 32444-32451.

GROVES, A., Y., K. & CHUN J. 2013. Fingolimod: Direct CNS effects of sphingosine 1-phosphate (S1P) receptor modulation and implications in multiple sclerosis therapy. *Journal of the Neurological Sciences,* 328 9-18.

GUTOWSKI, NEWCOMBE & CUZNER 1999. Tenascin-R and C in multiple sclerosis lesions: relevance to extracellular matrix remodelling. *Neuropathology and Applied Neurobiology,* 25, 207-214.

HALL, S. M., REDFORD, E. J. & SMITH, K. J. 2000. Tumour necrosis factor-α has few morphological effects within the dorsal columns of the spinal cord, in contrast to its effects in the peripheral nervous system. *Journal of Neuroimmunology,* 106, 130-136.

HANNUN & BELL 1987. Lysosphingolipids inhibit protein kinase C: implications for the sphingolipidoses. *Science,* 235, 670-674.

HANNUN, Y. A. & OBEID, L. M. 2008. Principles of bioactive lipid signalling: lessons from sphingolipids. *Nat Rev Mol Cell Biol,* 9, 139-150.

HANSON, M. A., ROTH, C. B., JO, E., GRIFFITH, M. T., SCOTT, F. L., REINHART, G., DESALE, H., CLEMONS, B., CAHALAN, S. M., SCHUERER, S. C., SANNA, M. G., HAN, G. W., KUHN, P., ROSEN, H. & STEVENS, R. C. 2012. Crystal structure of a lipid G protein-coupled receptor. *Science,* 335, 851-5.

HAQ, E., CONTRERAS, M. A., GIRI, S., SINGH, I. & SINGH, A. K. 2006. Dysfunction of peroxisomes in twitcher mice brain: A possible mechanism of psychosine-induced disease. *Biochemical and Biophysical Research Communications,* 343, 229-238.

HAQ, E., GIRI, S., SINGH, I. & SINGH, A. K. 2003. Molecular mechanism of psychosine-induced cell death in human oligodendrocyte cell line. *Journal of Neurochemistry,* 86, 1428-1440.

HAWKINS-SALSBURY, J. A., PARAMESWAR, A. R., JIANG, X., SCHLESINGER, P. H., BONGARZONE, E., ORY, D. S., DEMCHENKO, A. V. & SANDS, M. S. 2013. Psychosine, the cytotoxic sphingolipid that accumulates in globoid cell leukodystrophy, alters membrane architecture. *Journal of Lipid Research,* 54, 3303-3311.

HEALY, L. M., SHERIDAN, G. K., PRITCHARD, A. J., RUTKOWSKA, A., MULLERSHAUSEN, F. & DEV, K. K. 2013. Pathway specific modulation of S1P1 receptor signalling in rat and human astrocytes. *British Journal of Pharmacology,* 169, 1114-1129.

HEMMATI, F., DARGAHI, L., NASOOHI, S., OMIDBAKHSH, R., MOHAMED, Z., CHIK, Z., NAIDU, M. & AHMADIANI, A. 2013. Neurorestorative effect of FTY720 in a rat model of Alzheimer's disease: Comparison with Memantine. *Behavioural Brain Research,* 252, 415-421.

HENN, A., KIRNER, S. & LEIST, M. 2011. TLR2 Hypersensitivity of Astrocytes as Functional Consequence of Previous Inflammatory Episodes. *The Journal of Immunology,* 186, 3237-3247.

HENNESSY, E., GRIFFIN, É. W. & CUNNINGHAM, C. 2015. Astrocytes Are Primed by Chronic Neurodegeneration to Produce Exaggerated Chemokine and Cell Infiltration Responses to Acute Stimulation with the Cytokines IL-1β and TNF-α. *The Journal of Neuroscience,* 35, 8411-8422.

HIDA, H., NAGANO, S., TAKEDA, M. & SOLIVEN, B. 1999. Regulation of Mitogen-Activated Protein Kinases by Sphingolipid Products in Oligodendrocytes. *The Journal of Neuroscience,* 19, 7458-7467.

HLA, T. & BRINKMANN, V. 2011. Sphingosine 1-phosphate (S1P): Physiology and the effects of S1P receptor modulation. *Neurology,* 76, S3-8.

HLA, T. & MACIAG, T. 1990. An abundant transcript induced in differentiating human endothelial cells encodes a polypeptide with structural similarities to G-protein-coupled receptors. *Journal of Biological Chemistry,* 265, 9308-9313.

HOLDSWORTH, G., OSBORNE, D., PHAM, T., FELLS, J., HUTCHINSON, G., MILLIGAN, G. & PARRILL, A. 2004. A single amino acid determines preference between phospholipids and reveals length restriction for activation ofthe S1P4 receptor. *BMC Biochemistry,* 5, 12.

HOOGERBRUGGE, P. M., POORTHUIS, B. J., ROMME, A. E., VAN DE KAMP, J. J., WAGEMAKER, G. & VAN BEKKUM, D. W. 1988. Effect of bone marrow transplantation on enzyme levels and clinical course in the neurologically affected twitcher mouse. *J Clin Invest,* 81, 1790-1794.

HU, Y., LEE, X., JI, B., GUCKIAN, K., APICCO, D., PEPINSKY, R. B., MILLER, R. H. & MI, S. 2011. Sphingosine 1-phosphate receptor modulator fingolimod (FTY720) does not promote remyelination in vivo. *Molecular and Cellular Neuroscience,* 48, 72-81.

HUYBRECHTS, S. J., VAN VELDHOVEN, P. P., HOFFMAN, I., ZEEVAERT, R., DE VOS, R., DEMAEREL, P., BRAMS, M., JAEKEN, J., FRANSEN, M. & CASSIMAN, D. 2008.

Identification of a novel PEX14 mutation in Zellweger syndrome. *Journal of Medical Genetics,* 45, 376-383.

IJICHI, K., BROWN, G. D., MOORE, C. S., LEE, J.-P., WINOKUR, P. N., PAGARIGAN, R., SNYDER, E. Y., BONGARZONE, E. R. & CROCKER, S. J. 2013. MMP-3 mediates psychosine-induced globoid cell formation: Implications for leukodystrophy pathology. *Glia,* 61, 765-777.

IM, D.-S., HEISE, C. E., ANCELLIN, N., O'DOWD, B. F., SHEI, G.-J., HEAVENS, R. P., RIGBY, M. R., HLA, T., MANDALA, S., MCALLISTER, G., GEORGE, S. R. & LYNCH, K. R. 2000. Characterization of a Novel Sphingosine 1-Phosphate Receptor, Edg-8. *Journal of Biological Chemistry,* 275, 14281-14286.

IM, D.-S., HEISE, C. E., NGUYEN, T., O'DOWD, B. F. & LYNCH, K. R. 2001. Identification of a Molecular Target of Psychosine and Its Role in Globoid Cell Formation. *The Journal of Cell Biology,* 153, 429-434.

ISHIBASHI, T., DAKIN, K. A., STEVENS, B., LEE, P. R., FIELDS, R. D., KOZLOV, S. V. & STEWART, C. L. 2006. Astrocytes Promote Myelination in Response to Electrical Impulses. *Neuron,* 49, 823-832.

ISHII, I., FUKUSHIMA, N., YE, X. & CHUN, J. 2004. LYSOPHOSPHOLIPID RECEPTORS: Signaling and Biology. *Annu Rev Biochem,* 73, 321-354.

ITOH, R. & FUJIKI, Y. 2006. Functional Domains and Dynamic Assembly of the Peroxin Pex14p, the Entry Site of Matrix Proteins. *Journal of Biological Chemistry,* 281, 10196-10205.

IWASAKI, T., KITANO, KANDA, SEKIGUCHI, KITANO AND SANO 2011. Role of sphingosine 1-phosphate signaling for the pathogenesis of autoimmune diseases. *Inflammation and Regeneration* Vol. 31.

JACKSON, S., GIOVANNONI, G. & BAKER, D. 2011a. Fingolimod modulates microglial activation to augment markers of remyelination. *Journal of Neuroinflammation,* 8, 1-12.

JACKSON, S. J., GIOVANNONI, G. & BAKER, D. 2011b. Fingolimod modulates microglial activation to augment markers of remyelination. *J Neuroinflammation,* 8, 76.

JAILLARD, C., HARRISON, S., STANKOFF, B., AIGROT, M. S., CALVER, A. R., DUDDY, G., WALSH, F. S., PANGALOS, M. N., ARIMURA, N., KAIBUCHI, K., ZALC, B. & LUBETZKI, C. 2005. Edg8/S1P5: An Oligodendroglial Receptor with Dual Function on Process Retraction and Cell Survival. *The Journal of Neuroscience,* 25, 1459-1469.

JANKNECHT, R. & HUNTER, T. 1997. Convergence of MAP kinase pathways on the ternary complex factor Sap-1a. *The EMBO Journal,* 16, 1620-1627.

JARDIM, A., RAGER, N., LIU, W. & ULLMAN, B. 2002. Peroxisomal targeting protein 14 (PEX14) from Leishmania donovani: Molecular, biochemical, and immunocytochemical characterization. *Mol Biochem Parasitol,* 124, 51-62.

JATANA, M., GIRI, S. & SINGH, A. K. 2002. Apoptotic positive cells in Krabbe brain and induction of apoptosis in rat C6 glial cells by psychosine. *Neuroscience Letters,* 330, 183-187.

JIANG, ZHANG, CHEN, LAM, YANG, XU & YU, C. H. 2003. Apoptosis and Activation of Erk1/2 and Akt in Astrocytes Postischemia. *Neurochemical Research,* 28, 831-837.

JO, E., SANNA, M. G., GONZALEZ-CABRERA, P. J., THANGADA, S., TIGYI, G., OSBORNE, D. A., HLA, T., PARRILL, A. L. & ROSEN, H. 2005. S1P1-selective in vivo-active agonists from high-throughput screening: off-the-shelf chemical probes of receptor interactions, signaling, and fate. *Chem Biol,* 12, 703-15.

JUNG, C. G., KIM, H. J., MIRON, V. E., COOK, S., KENNEDY, T. E., FOSTER, C. A., ANTEL, J. P. & SOLIVEN, B. 2007. Functional consequences of S1P receptor modulation in rat oligodendroglial lineage cells. *Glia,* 55, 1656-1667.

KAMAL, M., MAURICE, P. & JOCKERS, R. 2011. Expanding the Concept of G Protein-Coupled Receptor (GPCR) Dimer Asymmetry towards GPCR-Interacting Proteins. *Pharmaceuticals,* 4, 273-284.

KANAZAWA, T., NAKAMURA, S., MOMOI, M., YAMAJI, T., TAKEMATSU, H., YANO, H., SABE, H., YAMAMOTO, A., KAWASAKI, T. & KOZUTSUMI, Y. 2000. Inhibition of Cytokinesis by a Lipid Metabolite, Psychosine. *The Journal of Cell Biology,* 149, 943-950.

KAPPOS, L., ANTEL, J., COMI, G., MONTALBAN, X., O'CONNOR, P., POLMAN, C. H., HAAS, T., KORN, A. A., KARLSSON, G. & RADUE, E. W. 2006. Oral Fingolimod (FTY720) for Relapsing Multiple Sclerosis. *New England Journal of Medicine,* 355, 1124-1140.

KAPPOS, L., BAR-OR, A., CREE, B., FOX, R., GIOVANNONI, G., GOLD, R., VERMERSCH, P., LAM, E., POHLMANN, H. & WALLSTRÖM, E. 2014. P036 - Siponimod (BAF312) for the treatment of secondary progressive multiple sclerosis: Design of the phase 3 EXPAND trial. *Multiple Sclerosis and Related Disorders,* 3, 752.

KAPPOS, L., RADUE, E.-W., O'CONNOR, P., POLMAN, C., HOHLFELD, R., CALABRESI, P., SELMAJ, K., AGOROPOULOU, C., LEYK, M., ZHANG-AUBERSON, L. & BURTIN, P. 2010. A Placebo-Controlled Trial of Oral Fingolimod in Relapsing Multiple Sclerosis. *New England Journal of Medicine,* 362, 387-401.

KARIN, M. & LIN, A. 2002. NF-kappaB at the crossroads of life and death. *Nature Immunology,* 3, 221-227.

KAYS, J. S., LI, C. & NICOL, G. D. 2012. Expression of sphingosine 1-phosphate receptors in the rat dorsal root ganglia and defined single isolated sensory neurons. *Physiological Genomics,* 44, 889-901.

KHAN, M., HAQ, E., GIRI, S., SINGH, I. & SINGH, A. K. 2005. Peroxisomal participation in psychosine-mediated toxicity: implications for Krabbe's disease. *J Neurosci Res,* 80, 845-54.

KIEL, J. A. K. W., VEENHUIS, M. & VAN DER KLEI, I. J. 2006. PEX Genes in Fungal Genomes: Common, Rare or Redundant. *Traffic,* 7, 1291-1303.

KIM, H. J., MIRON, V. E., DUKALA, D., PROIA, R. L., LUDWIN, S. K., TRAKA, M., ANTEL, J. P. & SOLIVEN, B. 2011. Neurobiological effects of sphingosine 1-phosphate receptor modulation in the cuprizone model. *The FASEB Journal,* 25, 1509-1518.

KIUCHI, M., ADACHI, K., KOHARA, T., MINOGUCHI, M., HANANO, T., AOKI, Y., MISHINA, T., ARITA, M., NAKAO, N., OHTSUKI, M., HOSHINO, Y., TESHIMA, K., CHIBA, K., SASAKI, S. & FUJITA, T. 2000. Synthesis and Immunosuppressive Activity of 2-Substituted 2-Aminopropane-1,3-diols and 2-Aminoethanols1,2. *J Med Chem,* 43, 2946-2961.

KIUCHI, M., ADACHI, K., KOHARA, T., TESHIMA, K., MASUBUCHI, Y., MISHINA, T. & FUJITA, T. 1998. Synthesis and biological evaluation of 2,2-disubstituted 2-aminoethanols: analogues of FTY720. *Bioorg Med Chem Lett,* 8, 101-106.

KOBAYASHI, T., YAMANAKA, T., JACOBS, J. M., TEIXEIRA, F. & SUZUKI, K. 1980. The twitcher mouse: an enzymatically authentic model of human globoid cell leukodystrophy (Krabbe disease). *Brain Research,* 202, 479-483.

KOHNO, T., WADA, A. & IGARASHI, Y. 2002. N-Glycans of sphingosine 1-phosphate receptor Edg-1 regulate ligand-induced receptor internalization. *The FASEB Journal,* 16, 983-992.

KOLYADA, A. Y. & MADIAS, N. E. 2001. Transcriptional regulation of the human iNOS gene by IL-1beta in endothelial cells. *Mol Med,* 7, 329-43.

KONDO, Y., WENGER, D. A., GALLO, V. & DUNCAN, I. D. 2005. Galactocerebrosidase-deficient oligodendrocytes maintain stable central myelin by exogenous replacement of the missing enzyme in mice. *Proc Natl Acad Sci U S A,* 102, 18670-5.

KONING, SWAAB, HOEK & HUITINGA 2009. . Distribution of the immune inhibitory molecules CD200 and CD200R in the normal central nervous system and multiple sclerosis lesions suggests neuron-glia and glia-glia interactions *Journal Neuropathol Exp Neurol.* , Feb;68, 159-67.

KOZAKOV, D., BEGLOV, D., BOHNUUD, T., MOTTARELLA, S. E., XIA, B., HALL, D. R. & VAJDA, S. 2013. How good is automated protein docking? *Proteins: Structure, Function, and Bioinformatics,* 81, 2159-2166.

LAEMMLI, U. K. 1970. Cleavage of structural proteins during the assembly of the head of bacteriophage T4. *Nature,* 227, 680-5.

LEE, M.-J., THANGADA, S., PAIK, J.-H., SAPKOTA, G. P., ANCELLIN, N., CHAE, S.-S., WU, M., MORALES-RUIZ, M., SESSA, W. C., ALESSI, D. R. & HLA, T. 2001. Akt-Mediated Phosphorylation of the G Protein-Coupled Receptor EDG-1 Is Required for Endothelial Cell Chemotaxis. *Molecular Cell,* 8, 693-704.

LEE, W. C., TSOI, Y. K., DICKEY, C. A., DELUCIA, M. W., DICKSON, D. W. & ECKMAN, C. B. 2006. Suppression of galactosylceramidase (GALC) expression in the twitcher mouse model of globoid cell leukodystrophy (GLD) is caused by nonsense-mediated mRNA decay (NMD). *Neurobiology of Disease,* 23, 273-280.

LEGANGNEUX, E., GARDIN, A. & JOHNS, D. 2013. Dose titration of BAF312 attenuates the initial heart rate reducing effect in healthy subjects. *British Journal of Clinical Pharmacology,* 75, 831-841.

LEVINE, S. M. & BROWN, D. C. 1997. IL-6 and TNFα expression in brains of twitcher, quaking and normal mice. *Journal of Neuroimmunology,* 73, 47-56.
LEVINE, S. M., PEDCHENKO, T. V., BRONSHTEYN, I. G. & PINSON, D. M. 2000. L-cycloserine slows the clinical and pathological course in mice with globoid cell leukodystrophy (twitcher mice). *Journal of Neuroscience Research,* 60, 231-236.
LI, P., NIJHAWAN, D., BUDIHARDJO, I., SRINIVASULA, S. M., AHMAD, M., ALNEMRI, E. S. & WANG, X. 1997. Cytochrome c and dATP-Dependent Formation of Apaf-1/Caspase-9 Complex Initiates an Apoptotic Protease Cascade. *Cell,* 91, 479-489.
LI, Z., PAIK, J.-H., WANG, Z., HLA, T. & WU, D. 2005. Role of guanine nucleotide exchange factor P-Rex-2b in sphingosine 1-phosphate-induced Rac1 activation and cell migration in endothelial cells. *Prostaglandins & Other Lipid Mediators,* 76, 95-104.
LIM, H. S., PARK, J. J., KO, K., LEE, M. H. & CHUNG, S. K. 2004. Syntheses of sphingosine-1-phosphate analogues and their interaction with EDG/S1P receptors. *Bioorganic and Medicinal Chemistry Letters,* 14, 2499-2503.
LIN, D., DONSANTE, A., MACAULEY, S., LEVY, B., VOGLER, C. & SANDS, M. S. 2007. Central Nervous System-directed AAV2//5-Mediated Gene Therapy Synergizes with Bone Marrow Transplantation in the Murine Model of Globoid-cell Leukodystrophy. *Mol Ther,* 15, 44-52.
LING, C., VERBNY, Y. I., BANKS, M. I., SANDOR, M. & FABRY, Z. 2008. In Situ Activation of Antigen-Specific CD8+ T Cells in the Presence of Antigen in Organotypic Brain Slices. *The Journal of Immunology,* 180, 8393-8399.
LIU, G., BURNS, S., HUANG, G., BOYD, K., PROIA, R. L., FLAVELL, R. A. & CHI, H. 2009. The receptor S1P1 overrides regulatory T cell-mediated immune suppression through Akt-mTOR. *Nat Immunol,* 10, 769-777.
LIU, J. & LIN, A. 2005. Role of JNK activation in apoptosis: A double-edged sword. *Cell Research, Nature,* 15, 36-42.
LUTTRELL, L. 2008. Reviews in Molecular Biology and Biotechnology: Transmembrane Signaling by G Protein-Coupled Receptors. *Molecular Biotechnology,* 39, 239-264.
LUTZ, S. E., ZHAO, Y., GULINELLO, M., LEE, S. C., RAINE, C. S. & BROSNAN, C. F. 2009. Deletion of Astrocyte Connexins 43 and 30 Leads to a Dysmyelinating Phenotype and Hippocampal CA1 Vacuolation. *The Journal of Neuroscience,* 29, 7743-7752.
MACEYKA, M., HARIKUMAR, K. B., MILSTIEN, S. & SPIEGEL, S. 2012. Sphingosine-1-phosphate signaling and its role in disease. *Trends in Cell Biology,* 22, 50-60.
MAGALHAES, A. C., DUNN, H. & FERGUSON, S. S. G. 2012. Regulation of GPCR activity, trafficking and localization by GPCR-interacting proteins. *British Journal of Pharmacology,* 165, 1717-1736.
MANN, D. L. 2012. Sphingosine 1-Phosphate as a Therapeutic Target in Heart Failure: More Questions than Answers. *Circulation.*
MARKS-KONCZALIK, J., CHU, S. C. & MOSS, J. 1998. Cytokine-mediated Transcriptional Induction of the Human Inducible Nitric Oxide Synthase Gene Requires Both Activator Protein 1 and Nuclear Factor κB-binding Sites. *Journal of Biological Chemistry,* 273, 22201-22208.
MATTES, H., DEV, K. K., BOUHELAL, R., BARSKE, C., GASPARINI, F., GUERINI, D., MIR, A. K., ORAIN, D., OSINDE, M., PICARD, A., DUBOIS, C., TASDELEN, E. & HAESSIG, S. 2010. Design and Synthesis of Selective and Potent Orally Active S1P5 Agonists. *ChemMedChem,* 5, 1693-1696.
MATYSZAK, M. K. & PERRY, V. H. 1995. Demyelination in the central nervous system following a delayed-type hypersensitivity response to bacillus Calmette-Guérin. *Neuroscience,* 64, 967-977.
MENDOZA, M. C., ER, E. E. & BLENIS, J. 2011. The Ras-ERK and PI3K-mTOR pathways: cross-talk and compensation. *Trends Biochem Sci,* 36, 320-328.
MEYER ZU HERINGDORF, D. & JAKOBS, K. H. 2007. Lysophospholipid receptors: Signalling, pharmacology and regulation by lysophospholipid metabolism. *Biochimica et Biophysica Acta (BBA) - Biomembranes,* 1768, 923-940.
MIRON, V. E., HALL, J. A., KENNEDY, T. E., SOLIVEN, B. & ANTEL, J. P. 2008a. Cyclical and Dose-Dependent Responses of Adult Human Mature Oligodendrocytes to Fingolimod. *The American Journal of Pathology,* 173, 1143-1152.
MIRON, V. E., JUNG, C. G., KIM, H. J., KENNEDY, T. E., SOLIVEN, B. & ANTEL, J. P. 2008b. FTY720 modulates human oligodendrocyte progenitor process extension and survival. *Annals of Neurology,* 63, 61-71.

MIRON, V. E., KUHLMANN, T. & ANTEL, J. P. 2011. Cells of the oligodendroglial lineage, myelination, and remyelination. *Biochimica et Biophysica Acta (BBA) - Molecular Basis of Disease,* 1812, 184-193.

MIRON, V. E., LUDWIN, S. K., DARLINGTON, P. J., JARJOUR, A. A., SOLIVEN, B., KENNEDY, T. E. & ANTEL, J. P. 2010. Fingolimod (FTY720) Enhances Remyelination Following Demyelination of Organotypic Cerebellar Slices. *The American Journal of Pathology,* 176, 2682-2694.

MITCHISON, T. J. 2001. Psychosine, Cytokinesis, and Orphan Receptors: Unexpected Connections. *The Journal of Cell Biology,* 153, 1-4.

MOHRI, I., TANIIKE, M., TANIGUCHI, H., KANEKIYO, T., ARITAKE, K., INUI, T., FUKUMOTO, N., EGUCHI, N., KUSHI, A., SASAI, H., KANAOKA, Y., OZONO, K., NARUMIYA, S., SUZUKI, K. & URADE, Y. 2006. Prostaglandin D2-Mediated Microglia/Astrocyte Interaction Enhances Astrogliosis and Demyelination in twitcher. *The Journal of Neuroscience,* 26, 4383-4393.

MONICK, M. M. & HUNNINGHAKE, G. W. 2003. SECOND MESSENGER PATHWAYS IN PULMONARY HOST DEFENSE. *Annu Rev Physiol,* 65, 643-667.

MOON, JEONG, LEE & PARK 2013. FTY720 protects neuronal cells from damage induced by human prion protein by inactivating the JNK pathway. *International Journal of Molecular Medicine,* 32, 1387-1393.

MOSER, A. B., RASMUSSEN, M., NAIDU, S., WATKINS, P. A., MCGUINNESS, M., HAJRA, A. K., CHEN, G., RAYMOND, G., LIU, A., GORDON, D., GARNAAS, K., WALTON, D. S., SKJELDAL, O. H., GUGGENHEIM, M. A., JACKSON, L. G., ELIAS, E. R. & MOSER, H. W. 1995. Phenotype of patients with peroxisomal disorders subdivided into sixteen complementation groups. *The Journal of Pediatrics,* 127, 13-22.

MÜLLER, C. S., HAUPT, A., BILDL, W., SCHINDLER, J., KNAUS, H.-G., MEISSNER, M., RAMMNER, B., STRIESSNIG, J., FLOCKERZI, V., FAKLER, B. & SCHULTE, U. 2010. Quantitative proteomics of the Cav2 channel nano-environments in the mammalian brain. *Proceedings of the National Academy of Sciences,* 107, 14950-14957.

MULLERSHAUSEN, F., CRAVEIRO, L. M., SHIN, Y., CORTES-CROS, M., BASSILANA, F., OSINDE, M., WISHART, W. L., GUERINI, D., THALLMAIR, M., SCHWAB, M. E., SIVASANKARAN, R., SEUWEN, K. & DEV, K. K. 2007. Phosphorylated FTY720 promotes astrocyte migration through sphingosine-1-phosphate receptors. *Journal of Neurochemistry,* 102, 1151-1161.

MULLERSHAUSEN, F., ZECRI, F., CETIN, C., BILLICH, A., GUERINI, D. & SEUWEN, K. 2009. Persistent signaling induced by FTY720-phosphate is mediated by internalized S1P1 receptors. *Nature Chemistry Biology,* 5, 428-434.

NAGELE, R. G., WEGIEL, J., VENKATARAMAN, V., IMAKI, H., WANG, K.-C. & WEGIEL, J. 2004. Contribution of glial cells to the development of amyloid plaques in Alzheimer's disease. *Neurobiology of Aging,* 25, 663-674.

NAKAHARA, T., IWASE, A., NAKAMURA, T., KONDO, M., BAYASULA, KOBAYASHI, H., TAKIKAWA, S., MANABE, S., GOTO, M., KOTANI, T. & KIKKAWA, F. 2012. Sphingosine-1-phosphate inhibits H2O2-induced granulosa cell apoptosis via the PI3K/Akt signaling pathway. *Fertility and Sterility,* 98, 1001-1008.e1.

NEER, E. J. 1995. Heterotrimeric C proteins: Organizers of transmembrane signals. *Cell,* 80, 249-257.

NERI, M., RICCA, A., DI GIROLAMO, I., ALCALA'-FRANCO, B., CAVAZZIN, C., ORLACCHIO, A., MARTINO, S., NALDINI, L. & GRITTI, A. 2011. Neural Stem Cell Gene Therapy Ameliorates Pathology and Function in a Mouse Model of Globoid Cell Leukodystrophy. *Stem Cells (Dayton, Ohio),* 29, 1559-1571.

NEUFELD, C., FILIPP, F. V., SIMON, B., NEUHAUS, A., SCHULLER, N., DAVID, C., KOOSHAPUR, H., MADL, T., ERDMANN, R., SCHLIEBS, W., WILMANNS, M. & SATTLER, M. 2009. Structural basis for competitive interactions of Pex14 with the import receptors Pex5 and Pex19. *EMBO J,* 28, 745-754.

NEUHAUS, A., KOOSHAPUR, H., WOLF, J., MEYER, N. H., MADL, T., SAIDOWSKY, J., HAMBRUCH, E., LAZAM, A., JUNG, M., SATTLER, M., SCHLIEBS, W. & ERDMANN, R. 2014. A Novel Pex14 Protein-interacting Site of Human Pex5 Is Critical for Matrix Protein Import into Peroxisomes. *Journal of Biological Chemistry,* 289, 437-448.

NIXON, G. F. 2009. Sphingolipids in inflammation: pathological implications and potential therapeutic targets. *British Journal of Pharmacology,* 158, 982-993.

NODA, H., TAKEUCHI, H., MIZUNO, T. & SUZUMURA, A. 2013. Fingolimod phosphate promotes the neuroprotective effects of microglia. *Journal of Neuroimmunology,* 256, 13-18.

NOVGORODOV, A. S., EL-ALWANI, M., BIELAWSKI, J., OBEID, L. M. & GUDZ, T. I. 2007. Activation of sphingosine-1-phosphate receptor S1P5 inhibits oligodendrocyte progenitor migration. *The FASEB Journal,* 21, 1503-1514.

O'SHEA, E. K., RUTKOWSKI, R. & KIM, P. S. 1992. Mechanism of specificity in the Fos-Jun oncoprotein heterodimer. *Cell,* 68, 699-708.

O'SULLIVAN, C. & DEV, K. K. 2015. Galactosylsphingosine (psychosine) induced demyelination is attenuated by sphingosine 1-phosphate signalling. *Journal of Cell Science,* Submitted.

OBINATA, H. & HLA, T. 2012. Sphingosine 1-phosphate in coagulation and inflammation. *Semin Immunopathol,* 34, 73-91.

OHNO, Y., ITO, A., OGATA, R., HIRAGA, Y., IGARASHI, Y. & KIHARA, A. 2009. Palmitoylation of the sphingosine 1-phosphate receptor S1P1 is involved in its signaling functions and internalization. *Genes to Cells,* 14, 911-923.

OKAMOTO, H., TAKUWA, N., YATOMI, Y., GONDA, K., SHIGEMATSU, H. & TAKUWA, Y. 1999. EDG3 Is a Functional Receptor Specific for Sphingosine 1-Phosphate and Sphingosylphosphorylcholine with Signaling Characteristics Distinct from EDG1 and AGR16. *Biochemical and Biophysical Research Communications,* 260, 203-208.

OLAH, M., AMOR, S., BROUWER, N., VINET, J., EGGEN, B., BIBER, K. & BODDEKE, H. W. G. M. 2012. Identification of a microglia phenotype supportive of remyelination. *Glia,* 60, 306-321.

OLIVEIRA, M. E. M., REGUENGA, C., GOUVEIA, A. M. M., GUIMARÃES, C. P., SCHLIEBS, W., KUNAU, W.-H., SILVA, M. T., SÁ-MIRANDA, C. & AZEVEDO, J. E. 2002. Mammalian Pex14p: membrane topology and characterisation of the Pex14p–Pex14p interaction. *Biochimica et Biophysica Acta (BBA) - Biomembranes,* 1567, 13-22.

OO, M. L., CHANG, S. H., THANGADA, S., WU, M. T., REZAUL, K., BLAHO, V., HWANG, S. I., HAN, D. K. & HLA, T. 2011. Engagement of S1P-degradative mechanisms leads to vascular leak in mice. *J Clin Invest,* 121, 2290-300.

OO, M. L., THANGADA, S., WU, M. T., LIU, C. H., MACDONALD, T. L., LYNCH, K. R., LIN, C. Y. & HLA, T. 2007. Immunosuppressive and anti-angiogenic sphingosine 1-phosphate receptor-1 agonists induce ubiquitinylation and proteasomal degradation of the receptor. *J Biol Chem,* 282, 9082-9.

ORFI, L., LARIVE, C. & LEVINE, S. 1997. Physicochemical characterization of psychosine by 1H nuclear magnetic resonance and electron microscopy. *Lipids,* 32, 1035-1040.

ORTEGA, M. C., CASES, O., MERCHÁN, P., KOZYRAKI, R., CLEMENTE, D. & DE CASTRO, F. 2012. Megalin mediates the influence of sonic hedgehog on oligodendrocyte precursor cell migration and proliferation during development. *Glia,* 60, 851-866.

OSINDE, M., CLAVAGUERA, F., MAY-NASS, R., TOLNAY, M. & DEV, K. K. 2008. Lentivirus Tau (P301S) expression in adult amyloid precursor protein (APP)-transgenic mice leads to tangle formation. *Neuropathology and Applied Neurobiology,* 34, 523-531.

OSINDE, M., MULLERSHAUSEN, F. & DEV, K. K. 2007. Phosphorylated FTY720 stimulates ERK phosphorylation in astrocytes via S1P receptors. *Neuropharmacology,* 52, 1210-1218.

PALCZEWSKI, K. 2006. G protein-coupled receptor rhodopsin. *Annu Rev Biochem,* 75, 743-67.

PAN, S., GRAY, N. S., GAO, W., MI, Y., FAN, Y., WANG, X., TUNTLAND, T., CHE, J., LEFEBVRE, S., CHEN, Y., CHU, A., HINTERDING, K., GARDIN, A., END, P., HEINING, P., BRUNS, C., COOKE, N. G. & NUESSLEIN-HILDESHEIM, B. 2013. Discovery of BAF312 (Siponimod), a Potent and Selective S1P Receptor Modulator. *ACS Medicinal Chemistry Letters,* 4, 333-337.

PARPURA, V. & VERKHRATSKY, A. 2012. Homeostatic function of astrocytes: Ca(2+) and Na(+) signalling. *Translational neuroscience,* 3, 334-344.

PARRILL, A. L., LIMA, S. & SPIEGEL, S. 2012. Structure of the first sphingosine 1-phosphate receptor. *Sci Signal,* 5, pe23.

PARRILL, A. L., WANG, D.-A., BAUTISTA, D. L., VAN BROCKLYN, J. R., LORINCZ, Z., FISCHER, D. J., BAKER, D. L., LILIOM, K., SPIEGEL, S. & TIGYI, G. 2000. Identification of Edg1 Receptor Residues That Recognize Sphingosine 1-Phosphate. *Journal of Biological Chemistry,* 275, 39379-39384.

PEDCHENKO, T. V., BRONSHTEYN, I. G. & LEVINE, S. M. 2000. TNF-receptor 1 deficiency fails to alter the clinical and pathological course in mice with globoid cell leukodystrophy (twitcher mice) but affords protection following LPS challenge. *Journal of Neuroimmunology,* 110, 186-194.

PEKNY, M. & PEKNA, M. 2014. Astrocyte Reactivity and Reactive Astrogliosis: Costs and Benefits. *Physiological Reviews,* 94, 1077-1098.

PERAZA-REYES, L., ARNAISE, S., ZICKLER, D., COPPIN, E., DEBUCHY, R. & BERTEAUX-LECELLIER, V. 2011. The importomer peroxins are differentially required for peroxisome assembly and meiotic development in Podospora anserina: insights into a new peroxisome import pathway. *Molecular Microbiology,* 82, 365-377.

PETERSON, L. K. & FUJINAMI, R. S. 2007. Inflammation, Demyelination, Neurodegeneration and Neuroprotection in the Pathogenesis of Multiple Sclerosis. *Journal of neuroimmunology,* 184, 37-44.

PHAM, T.-C. T., FELLS SR, J. I., OSBORNE, D. A., NORTH, E. J., NAOR, M. M. & PARRILL, A. L. 2008. Molecular recognition in the sphingosine 1-phosphate receptor family. *Journal of Molecular Graphics and Modelling,* 26, 1189-1201.

PODBIELSKA, M., KROTKIEWSKI, H. & HOGAN, E. 2011. Signaling and Regulatory Functions of Bioactive Sphingolipids as Therapeutic Targets in Multiple Sclerosis. *Neurochemical Research,* 1-16.

POSTMA, J., HENGEVELD, AND MOOLENAAR 1996. Sphingosine-1-phosphate rapidly induces Rho-dependent neurite retraction: action through a specific cell surface receptor. *EMBO Journal* 15, 2388–2392.

POTTECK, H., NIEUWENHUIS, B., LÜTH, A., VAN DER GIET, M. & KLEUSER, B. 2010. Phosphorylation of the Immunomodulator FTY720 Inhibits Programmed Cell Death of Fibroblasts Via the S1P₃ Receptor Subtype and Bcl-2 Activation. *Cellular Physiology and Biochemistry,* 26, 67-78.

PRITCHARD, A. J., MIR, A. K. & DEV, K. K. 2014. Fingolimod Attenuates Splenocyte-Induced Demyelination in Cerebellar Slice Cultures. *PLoS One,* 9, e99444.

PRODINGER, C., BUNSE, J., KRÜGER, M., SCHIEFENHÖVEL, F., BRANDT, C., LAMAN, J., GRETER, M., IMMIG, K., HEPPNER, F., BECHER, B. & BECHMANN, I. 2011. CD11c-expressing cells reside in the juxtavascular parenchyma and extend processes into the glia limitans of the mouse nervous system. *Acta Neuropathologica,* 121, 445-458.

PURDUE, P. E. & LAZAROW, P. B. 2001. PEROXISOME BIOGENESIS. *Annual Review of Cell and Developmental Biology,* 17, 701-752.

QUANCARD, J., BOLLBUCK, B., JANSER, P., ANGST, D., BERST, F., BUEHLMAYER, P., STREIFF, M., BEERLI, C., BRINKMANN, V., GUERINI, D., SMITH, PAUL A., SEABROOK, TIMOTHY J., TRAEBERT, M., SEUWEN, K., HERSPERGER, R., BRUNS, C., BASSILANA, F. & BIGAUD, M. 2012. A Potent and Selective S1P1 Antagonist with Efficacy in Experimental Autoimmune Encephalomyelitis. *Chem Biol,* 19, 1142-1151.

RADU, C. G., CHENG, D., NIJAGAL, A., RIEDINGER, M., MCLAUGHLIN, J., YANG, L. V., JOHNSON, J. & WITTE, O. N. 2006. Normal Immune Development and Glucocorticoid-Induced Thymocyte Apoptosis in Mice Deficient for the T-Cell Death-Associated Gene 8 Receptor. *Molecular and Cellular Biology,* 26, 668-677.

RAFI, M. A., RAO, H. Z., LUZI, P., CURTIS, M. T. & WENGER, D. A. 2012. Extended normal life after AAVrh10-mediated gene therapy in the mouse model of Krabbe disease. *Mol Ther,* 20, 2031-42.

RAJAGOPAL, S., RAJAGOPAL, K. & LEFKOWITZ, R. J. 2010. Teaching old receptors new tricks: biasing seven-transmembrane receptors. *Nat Rev Drug Discov,* 9, 373-86.

RAO, T. S., LARIOSA-WILLINGHAM, K. D., LIN, F.-F., PALFREYMAN, E. L., YU, N., CHUN, J. & WEBB, M. 2003. Pharmacological characterization of lysophospholipid receptor signal transduction pathways in rat cerebrocortical astrocytes. *Brain Research,* 990, 182-194.

REDDY, A. S., KIM, J. H., HAWKINS-SALSBURY, J. A., MACAULEY, S. L., TRACY, E. T., VOGLER, C. A., HAN, X., SONG, S.-K., WOZNIAK, D. F., FOWLER, S. C., KLEIN, R. S. & SANDS, M. S. 2011. Bone Marrow Transplantation Augments the Effect of Brain- and Spinal Cord-Directed Adeno-Associated Virus 2/5 Gene Therapy by Altering Inflammation in the Murine Model of Globoid-Cell Leukodystrophy. *The Journal of Neuroscience,* 31, 9945-9957.

REMINGTON, L. T., BABCOCK, A. A., ZEHNTNER, S. P. & OWENS, T. 2007. Microglial Recruitment, Activation, and Proliferation in Response to Primary Demyelination. *The American Journal of Pathology,* 170**,** 1713-1724.

RIPOLL, C. B., FLAAT, M., KLOPF-EIERMANN, J., FISHER-PERKINS, J. M., TRYGG, C. B., SCRUGGS, B. A., MCCANTS, M. L., LEONARD, H. P., LIN, A. F., ZHANG, S., EAGLE, M. E., ALVAREZ, X., LI, Y. T., LI, S. C., GIMBLE, J. M. & BUNNELL, B. A. 2011. Mesenchymal Lineage Stem Cells Have Pronounced Anti-Inflammatory Effects in the Twitcher Mouse Model of Krabbe's Disease. *STEM CELLS,* 29**,** 67-77.

ROSE, A. & MEIER, I. 2004. Scaffolds, levers, rods and springs: diverse cellular functions of long coiled-coil proteins. *Cellular and Molecular Life Sciences CMLS,* 61**,** 1996-2009.

ROSEN, H. & GOETZL, E. J. 2005. Sphingosine 1-phosphate and its receptors: an autocrine and paracrine network. *Nat Rev Immunol,* 5**,** 560-570.

ROSEN, H., GONZALEZ-CABRERA, P. J., SANNA, M. G. & BROWN, S. 2009. Sphingosine 1-phosphate receptor signaling. *Annu Rev Biochem,* 78**,** 743-68.

ROSSI, S., LO GIUDICE, T., DE CHIARA, V., MUSELLA, A., STUDER, V., MOTTA, C., BERNARDI, G., MARTINO, G., FURLAN, R., MARTORANA, A. & CENTONZE, D. 2012. Oral fingolimod rescues the functional deficits of synapses in experimental autoimmune encephalomyelitis. *British Journal of Pharmacology,* 165**,** 861-869.

ROUACH, N., PÉBAY, A., MÊME, W., CORDIER, J., EZAN, P., ETIENNE, E., GIAUME, C. & TENCÉ, M. 2006. S1P inhibits gap junctions in astrocytes: involvement of Gi and Rho GTPase/ROCK. *European Journal of Neuroscience,* 23**,** 1453-1464.

RUCKTÄSCHEL, R., GIRZALSKY, W. & ERDMANN, R. 2011. Protein import machineries of peroxisomes. *Biochimica et Biophysica Acta (BBA) - Biomembranes,* 1808**,** 892-900.

SAFARIAN, F., KHALLAGHI, B., AHMADIANI, A. & DARGAHI, L. 2015. Activation of S1P1 Receptor Regulates PI3K/Akt/FoxO3a Pathway in Response to Oxidative Stress in PC12 Cells. *Journal of Molecular Neuroscience,* 56**,** 177-187.

SAINI, H. S., COELHO, R. P., GOPARAJU, S. K., JOLLY, P. S., MACEYKA, M., SPIEGEL, S. & SATO-BIGBEE, C. 2005. Novel role of sphingosine kinase 1 as a mediator of neurotrophin-3 action in oligodendrocyte progenitors. *Journal of Neurochemistry,* 95**,** 1298-1310.

SALT, I. P. & PALMER, T. M. 2012. Exploiting the anti-inflammatory effects of AMP-activated protein kinase activation. *Expert Opinion on Investigational Drugs,* 21**,** 1155-1167.

SCHURER, S. C., BROWN, S. J., GONZALEZ-CABRERA, P. J., SCHAEFFER, M. T., CHAPMAN, J., JO, E., CHASE, P., SPICER, T., HODDER, P. & ROSEN, H. 2008. Ligand-binding pocket shape differences between sphingosine 1-phosphate (S1P) receptors S1P1 and S1P3 determine efficiency of chemical probe identification by ultrahigh-throughput screening. *ACS Chem Biol,* 3**,** 486-98.

SELMAJ , LI , HARTUNG, HEMMER, KAPPOS, FREEDMAN, STÜVE , RIECKMANN, MONTALBAN, ZIEMSSEN, AUBERSON, POHLMANN, MERCIER, DAHLKE & WALLSTRÖM 2013. Siponimod for patients with relapsing-remitting multiple sclerosis (BOLD): an adaptive, dose-ranging, randomised, phase 2 study. *Lancet Neurol.,* 2**,** 756-767.

SEMMLER, A., OKULLA, T., SASTRE, M., DUMITRESCU-OZIMEK, L. & HENEKA, M. T. 2005. Systemic inflammation induces apoptosis with variable vulnerability of different brain regions. *Journal of Chemical Neuroanatomy,* 30**,** 144-157.

SHAULIAN, E. & KARIN, M. 2002. AP-1 as a regulator of cell life and death. *Nat Cell Biol,* 4**,** E131-E136.

SHERIDAN, G. K. & DEV, K. K. 2012. S1P1 receptor subtype inhibits demyelination and regulates chemokine release in cerebellar slice cultures. *Glia,* 60**,** 382-392.

SHIMIZU, N., ITOH, R., HIRONO, Y., OTERA, H., GHAEDI, K., TATEISHI, K., TAMURA, S., OKUMOTO, K., HARANO, T., MUKAI, S. & FUJIKI, Y. 1999. The Peroxin Pex14p. cDNA CLONING BY FUNCTIONAL COMPLEMENTATION ON A CHINESE HAMSTER OVARY CELL MUTANT, CHARACTERIZATION, AND FUNCTIONAL ANALYSIS. *J. Biol. Chem.,* 274**,** 12593-12604.

SHIMOZAWA, N., TSUKAMOTO, T., NAGASE, T., TAKEMOTO, Y., KOYAMA, N., SUZUKI, Y., KOMORI, M., OSUMI, T., JEANNETTE, G., WANDERS, R. J. A. & KONDO, N. 2004. Identification of a new complementation group of the peroxisome biogenesis disorders and PEX14 as the mutated gene. *Human Mutation,* 23**,** 552-558.

SHIOZAWA, K., KONAREV, P. V., NEUFELD, C., WILMANNS, M. & SVERGUN, D. I. 2009. Solution Structure of Human Pex5·Pex14·PTS1 Protein Complexes Obtained by Small Angle X-ray Scattering. *Journal of Biological Chemistry,* 284, 25334-25342.

SHOEMAKER, B. A., PORTMAN, J. J. & WOLYNES, P. G. 2000. Speeding molecular recognition by using the folding funnel: The fly-casting mechanism. *Proceedings of the National Academy of Sciences,* 97, 8868-8873.

SLOWIK, A., SCHMIDT, T., BEYER, C., AMOR, S., CLARNER, T. & KIPP, M. 2015. The sphingosine 1-phosphate receptor agonist FTY720 is neuroprotective after cuprizone-induced CNS demyelination. *British Journal of Pharmacology,* 172, 80-92.

SOFRONIEW, M. V. 2009. Molecular dissection of reactive astrogliosis and glial scar formation. *Trends in Neurosciences,* 32, 638-647.

SOFRONIEW, M. V. & VINTERS, H. V. 2010. Astrocytes: biology and pathology. *Acta Neuropathologica,* 119, 7-35.

SOMVANSHI, R. K. & KUMAR, U. 2012. Pathophysiology of GPCR Homo- and Heterodimerization: Special Emphasis on Somatostatin Receptors. *Pharmaceuticals,* 5, 417-446.

SONG, Y. J., HALLIDAY, G. M., HOLTON, J. L., LASHLEY, T., O'SULLIVAN, S. S., MCCANN, H., LEES, A. J., OZAWA, T., WILLIAMS, D. R., LOCKHART, P. J. & REVESZ, T. R. 2009. Degeneration in different parkinsonian syndromes relates to astrocyte type and astrocyte protein expression. *J Neuropathol Exp Neurol,* 68, 1073-83.

SONGZHU, THIEU, WEI, G., O. & J., E. 1997. Identification of cDNAs encoding two G protein-coupled receptors for lysosphingolipids. *FEBS Lett,* 417, 279-282.

SORENSEN, S. D., NICOLE, O., PEAVY, R. D., MONTOYA, L. M., LEE, C. J., MURPHY, T. J., TRAYNELIS, S. F. & HEPLER, J. R. 2003. Common Signaling Pathways Link Activation of Murine PAR-1, LPA, and S1P Receptors to Proliferation of Astrocytes. *Mol Pharmacol,* 64, 1199-1209.

SOSUNOV, A. A., GUILFOYLE, E., WU, X., MCKHANN, G. M. & GOLDMAN, J. E. 2013. Phenotypic Conversions of "Protoplasmic" to "Reactive" Astrocytes in Alexander Disease. *The Journal of Neuroscience,* 33, 7439-7450.

SPOHR, T. C. L. D. S. E., DEZONNE, R. S., NONES, J., DOS SANTOS SOUZA, C., EINICKER-LAMAS, M., GOMES, F. C. A. & REHEN, S. K. 2012. Sphingosine 1-phosphate-primed astrocytes enhance differentiation of neuronal progenitor cells. *Journal of Neuroscience Research,* 90, 1892-1902.

STADELMANN, C., WEGNER, C. & BRÜCK, W. 2011. Inflammation, demyelination, and degeneration — Recent insights from MS pathology. *Biochimica et Biophysica Acta (BBA) - Molecular Basis of Disease,* 1812, 275-282.

STEINBERG, S. J., DODT, G., RAYMOND, G. V., BRAVERMAN, N. E., MOSER, A. B. & MOSER, H. W. 2006. Peroxisome biogenesis disorders. *Biochimica et Biophysica Acta (BBA) - Molecular Cell Research,* 1763, 1733-1748.

STEINBERG SJ, R. G., BRAVERMAN NE, 2003. Peroxisome Biogenesis Disorders, Zellweger Syndrome Spectrum. *GeneReviews™ [Internet].* .

STOFFELS, J. M. J., DE JONGE, J. C., STANCIC, M., NOMDEN, A., VAN STRIEN, M. E., MA, D., ŠIŠKOVÁ, Z., MAIER, O., FFRENCH-CONSTANT, C., FRANKLIN, R. J. M., HOEKSTRA, D., ZHAO, C. & BARON, W. 2013. Fibronectin aggregation in multiple sclerosis lesions impairs remyelination. *Brain,* 136, 116-131.

STRAUSS, H. M. & KELLER, S. 2008. Pharmacological Interference with Protein-Protein Interactions Mediated by Coiled-Coil Motifs. *In:* KLUSSMANN, E. & SCOTT, J. (eds.) *Protein-Protein Interactions as New Drug Targets.* Springer Berlin Heidelberg.

SU, J.-R., TAKEDA, K., TAMURA, S., FUJIKI, Y. & MIKI, K. 2010. Monomer–dimer transition of the conserved N-terminal domain of the mammalian peroxisomal matrix protein import receptor, Pex14p. *Biochemical and Biophysical Research Communications,* 394, 217-221.

SU, J. R., TAKEDA, K., TAMURA, S., FUJIKI, Y. & MIKI, K. 2009. Crystal structure of the conserved N-terminal domain of the peroxisomal matrix protein import receptor, Pex14p. *Proc Natl Acad Sci U S A,* 106, 417-421.

SUGAMA, S., KIM, S. U., IDA, H. & ETO, Y. 1990. Psychosine cytotoxicity in rat neural cell cultures and protection by phorbol ester and dimethyl sulfoxide. *Pediatr Res,* 28, 473-6.

SUZUKI, K. 1998. Twenty five years of the 'Psychosine Hypothesis': A personal perspective of its history and present status. *Neurochemical Research,* 23, 251-259.

SUZUKI, K. 2003. Globoid cell leukodystrophy (Krabbe's disease): update. *Journal of Child Neurology,* 18, 595-603.
SUZUKI, K. & TANIIKE, M. 1995. Murine model of genetic demyelinating disease: the twitcher mouse. *Microsc Res Tech,* 32, 204-14.
SVENNERHOLM, L., VANIER, M. T. & MÅNSSON, J. E. 1980. Krabbe disease: a galactosylsphingosine (psychosine) lipidosis. *Journal of Lipid Research,* 21, 53-64.
SZALLASI, A. & BLUMBERG, P. M. 1999. Vanilloid (Capsaicin) Receptors and Mechanisms. *Pharmacological Reviews,* 51, 159-212.
TAKAHASHI, H. & SUZUKI, K. 1984. Demyelination in the spinal cord of murine globoid cell leukodystrophy (the twitcher mouse). *Acta Neuropathologica,* 62, 298-308.
TAKANO, T., OBERHEIM, N., COTRINA, M. L. & NEDERGAARD, M. 2009. Astrocytes and Ischemic Injury. *Stroke,* 40, S8-S12.
TAPASI, P., SETTY 1998. Effect of psychosine on mitochondrial function. *Indian Journal of Biochemistry Biophysiology,* 35, 161-166.
TAYLOR, CULLEN & MARTIN 2008. Apoptosis: controlled demolition at the cellular level. *Nature Review Molecular Cellular Biology,* 9, 231-241.
THAM, C.-S., LIN, F.-F., RAO, T. S., YU, N. & WEBB, M. 2003. Microglial activation state and lysophospholipid acid receptor expression. *International Journal of Developmental Neuroscience,* 21, 431-443.
THANGADA, S., KHANNA, K. M., BLAHO, V. A., OO, M. L., IM, D.-S., GUO, C., LEFRANCOIS, L. & HLA, T. 2010. Cell-surface residence of sphingosine 1-phosphate receptor 1 on lymphocytes determines lymphocyte egress kinetics. *The Journal of Experimental Medicine.*
TOHYAMA, J., MATSUDA, J. & SUZUKI, K. 2001. Psychosine Is as Potent an Inducer of Cell Death as C6-Ceramide in Cultured Fibroblasts and in MOCH-1 Cells. *Neurochemical Research,* 26, 667-671.
TOKER, A. 2000. Protein Kinases as Mediators of Phosphoinositide 3-Kinase Signaling. *Mol Pharmacol,* 57, 652-658.
TOKER, A. & NEWTON, A. C. 2000. Akt/Protein Kinase B Is Regulated by Autophosphorylation at the Hypothetical PDK-2 Site. *Journal of Biological Chemistry,* 275, 8271-8274.
VAN ANTWERP, D. J., MARTIN, S. J., KAFRI, T., GREEN, D. R. & VERMA, I. M. 1996. Suppression of TNF-alpha-induced apoptosis by NF-kappaB. *Science,* 274, 787-9.
VAN BROCKLYN, J. R., BEHBAHANI, B. & LEE, N. H. 2002. Homodimerization and heterodimerization of S1P/EDG sphingosine-1-phosphate receptors. *Biochimica et Biophysica Acta (BBA) - Molecular and Cell Biology of Lipids,* 1582, 89-93.
VAN BROCKLYN, J. R. & WILLIAMS, J. B. 2012. The control of the balance between ceramide and sphingosine-1-phosphate by sphingosine kinase: Oxidative stress and the seesaw of cell survival and death. *Comparative Biochemistry and Physiology Part B: Biochemistry and Molecular Biology,* 163, 26-36.
VAN DOORN, R., VAN HORSSEN, J., VERZIJL, D., WITTE, M., RONKEN, E., VAN HET HOF, B., LAKEMAN, K., DIJKSTRA, C. D., VAN DER VALK, P., REIJERKERK, A., ALEWIJNSE, A. E., PETERS, S. L. M. & DE VRIES, H. E. 2010. Sphingosine 1-phosphate receptor 1 and 3 are upregulated in multiple sclerosis lesions. *Glia,* 58, 1465-1476.
VAN ZUTPHEN, T., VEENHUIS, M. & VAN DER KLEI, I. J. 2008. Pex14 is the sole component of the peroxisomal translocon that is required for pexophagy. *Autophagy,* 4, 63-66.
VENTER, J. C., ADAMS, M. D., MYERS, E. W., LI, P. W., MURAL, R. J., SUTTON, G. G., SMITH, H. O., YANDELL, M., EVANS, C. A., HOLT, R. A., GOCAYNE, J. D., AMANATIDES, P., BALLEW, R. M., HUSON, D. H., WORTMAN, J. R., ZHANG, Q., KODIRA, C. D., ZHENG, X. H., CHEN, L., SKUPSKI, M., SUBRAMANIAN, G., THOMAS, P. D., ZHANG, J., GABOR MIKLOS, G. L., NELSON, C., BRODER, S., CLARK, A. G., NADEAU, J., MCKUSICK, V. A., ZINDER, N., LEVINE, A. J., ROBERTS, R. J., SIMON, M., SLAYMAN, C., HUNKAPILLER, M., BOLANOS, R., DELCHER, A., DEW, I., FASULO, D., FLANIGAN, M., FLOREA, L., HALPERN, A., HANNENHALLI, S., KRAVITZ, S., LEVY, S., MOBARRY, C., REINERT, K., REMINGTON, K., ABU-THREIDEH, J., BEASLEY, E., BIDDICK, K., BONAZZI, V., BRANDON, R., CARGILL, M., CHANDRAMOULISWARAN, I., CHARLAB, R., CHATURVEDI, K., DENG, Z., FRANCESCO, V. D., DUNN, P., EILBECK, K., EVANGELISTA, C., GABRIELIAN, A. E., GAN, W., GE, W., GONG, F., GU, Z., GUAN, P., HEIMAN, T. J., HIGGINS, M. E., JI, R.-R., KE, Z., KETCHUM, K. A., LAI, Z., LEI, Y.,

LI, Z., LI, J., LIANG, Y., LIN, X., LU, F., MERKULOV, G. V., MILSHINA, N., MOORE, H. M., NAIK, A. K., NARAYAN, V. A., NEELAM, B., NUSSKERN, D., RUSCH, D. B., SALZBERG, S., SHAO, W., SHUE, B., SUN, J., WANG, Z. Y., WANG, A., WANG, X., WANG, J., WEI, M.-H., WIDES, R., XIAO, C., YAN, C., et al. 2001. The Sequence of the Human Genome. *Science,* 291**,** 1304-1351.

VERKHRATSKY & BUTT 2013. Glial physiology and pathophysiology. *Wiley-Blackwell*

VOSKUHL, R. R., PETERSON, R. S., SONG, B., AO, Y., MORALES, L. B. J., TIWARI-WOODRUFF, S. & SOFRONIEW, M. V. 2009. Reactive astrocytes form scar-like perivascular barriers to leukocytes during adaptive immune inflammation of the CNS. *Journal of Neuroscience,* 29**,** 11511-11522.

WALZER, T., CHIOSSONE, L., CHAIX, J., CALVER, A., CAROZZO, C., GARRIGUE-ANTAR, L., JACQUES, Y., BARATIN, M., TOMASELLO, E. & VIVIER, E. 2007. Natural killer cell trafficking in vivo requires a dedicated sphingosine 1-phosphate receptor. *Nat Immunol,* 8**,** 1337-44.

WANDERS, R. J. A. 2004. Metabolic and molecular basis of peroxisomal disorders: A review. *American Journal of Medical Genetics Part A,* 126A**,** 355-375.

WANG, D. A., LORINCZ, Z., BAUTISTA, D. L., LILIOM, K., TIGYI, G. & PARRILL, A. L. 2001. A single amino acid determines lysophospholipid specificity of the S1P1 (EDG1) and LPA1 (EDG2) phospholipid growth factor receptors. *J Biol Chem,* 276**,** 49213-20.

WANG, W., HUANG, M.-C. & GOETZL, E. J. 2007. Type 1 Sphingosine 1-Phosphate G Protein-Coupled Receptor (S1P1) Mediation of Enhanced IL-4 Generation by CD4 T Cells from S1P1 Transgenic Mice. *The Journal of Immunology,* 178**,** 4885-4890.

WENGER, RAFI & LUZI 1997. Molecular genetics of Krabbe disease (globoid cell leukodystrophy): Diagnostic and clinical implications. *Human Mutation,* 10**,** 268-279.

WENGER, D. A., SUZUKI, K., SUZUKI, Y. & SUZUKI, K. 2001. Galactosylceramide lipidosis: globoid cell leukodystrophy (Krabbe disease). *McGraw-Hill; New York***,** 3669-3694.

WENTE, W., STROH, T., BEAUDET, A., RICHTER, D. & KREIENKAMP, H.-J. 2005. Interactions with PDZ Domain Proteins PIST/GOPC and PDZK1 Regulate Intracellular Sorting of the Somatostatin Receptor Subtype 5. *Journal of Biological Chemistry,* 280**,** 32419-32425.

WHITE, A. B., GIVOGRI, M. I., LOPEZ-ROSAS, A., CAO, H., VAN BREEMEN, R., THINAKARAN, G. & BONGARZONE, E. R. 2009. Psychosine Accumulates in Membrane Microdomains in the Brain of Krabbe Patients, Disrupting the Raft Architecture. *The Journal of Neuroscience,* 29**,** 6068-6077.

WIESE, S., KARUS, M. & FAISSNER, A. 2012. Astrocytes as a source for Extracellular matrix molecules and cytokines. *Frontiers in Pharmacology,* 3.

WILL, G. K., SOUKUPOVA, M., HONG, X., ERDMANN, K. S., KIEL, J. A. K. W., DODT, G., KUNAU, W.-H. & ERDMANN, R. 1999. Identification and Characterization of the Human Orthologue of Yeast Pex14p. *Molecular and Cellular Biology,* 19**,** 2265-2277.

WILLIAMS, C. & DISTEL, B. 2006. Pex13p: Docking or cargo handling protein? *Biochimica et Biophysica Acta (BBA) - Molecular Cell Research,* 1763**,** 1585-1591.

XU, H.-L., PELLIGRINO, D. A., PAISANSATHAN, C. & TESTAI, F. D. 2015. Protective role of fingolimod (FTY720) in rats subjected to subarachnoid hemorrhage. *Journal of Neuroinflammation,* 12**,** 16.

YAMADA, H., MARTIN, P. & SUZUKI, K. 1996. Impairment of protein kinase C activity in twitcher Schwann cells in vitro. *Brain Research,* 718**,** 138-144.

YAMAZAKI, K., SATO, TOMURA, SATO, YONEYA, OKAZAKI, OKAJIMA,AND OHTA 2000. Edg-6 as a Putative Sphingosine 1-Phosphate Receptor Coupling to Ca21 Signaling Pathway. *Biochemical and Biophysical Research Communications* 268**,** 583-589

YANG, J., YAN, R., ROY, A., XU, D., POISSON, J. & ZHANG, Y. 2015. The I-TASSER Suite: protein structure and function prediction. *Nat Meth,* 12**,** 7-8.

YEO, Y., MARTÍNEZ GÓMEZ, J., CROXFORD, J., GASSER, S., LING, E.-A. & SCHWARZ, H. 2012. CD137 ligand activated microglia induces oligodendrocyte apoptosis via reactive oxygen species. *Journal of Neuroinflammation,* 9**,** 1-9.

YOUNG, P. P., FANTZ, C. R. & SANDS, M. S. 2004. VEGF disrupts the neonatal blood–brain barrier and increases life span after non-ablative BMT in a murine model of congenital neurodegeneration caused by a lysosomal enzyme deficiency. *Experimental Neurology,* 188**,** 104-114.

YU, N., LARIOSA-WILLINGHAM, K. D., LIN, F.-F., WEBB, M. & RAO, T. S. 2004. Characterization of lysophosphatidic acid and sphingosine-1-phosphate-mediated signal transduction in rat cortical oligodendrocytes. *Glia,* 45, 17-27.

ZAKA, M. & WENGER, D. A. 2004. Psychosine-induced apoptosis in a mouse oligodendrocyte progenitor cell line is mediated by caspase activation. *Neuroscience Letters,* 358, 205-209.

ZASLAVSKY, A., SINGH, L. S., TAN, H., DING, H., LIANG, Z. & XU, Y. 2006. Homo- and hetero-dimerization of LPA/S1P receptors, OGR1 and GPR4. *Biochimica et Biophysica Acta (BBA) - Molecular and Cell Biology of Lipids,* 1761, 1200-1212.

ZHANG, J., LI, Y., ZHANG, Z. G., LU, M., BORNEMAN, J., BULLER, B., SAVANT-BHONSALE, S., ELIAS, S. B. & CHOPP, M. 2009. Bone marrow stromal cells increase oligodendrogenesis after stroke. *Journal of cerebral blood flow and metabolism : official journal of the International Society of Cerebral Blood Flow and Metabolism,* 29, 1166-1174.

ZHANG, J., ZHANG, Z. G., LI, Y., DING, X., SHANG, X., LU, M., ELIAS, S. B. & CHOPP, M. 2015. Fingolimod treatment promotes proliferation and differentiation of oligodendrocyte progenitor cells in mice with experimental autoimmune encephalomyelitis. *Neurobiology of Disease,* 76, 57-66.

ZHANG, M., STRNATKA, D., DONOHUE, C., HALLOWS, J. L., VINCENT, I. & ERICKSON, R. P. 2008a. Astrocyte-only Npc1 reduces neuronal cholesterol and triples life span of Npc1–/– mice. *Journal of Neuroscience Research,* 86, 2848-2856.

ZHANG, Y., DEVRIES, M. E. & SKOLNICK, J. 2006. Structure Modeling of All Identified G Protein–Coupled Receptors in the Human Genome. *PLoS Comput Biol,* 2, e13.

ZHANG, Z., FAUSER, U. & SCHLUESENER, H. J. 2008b. Early attenuation of lesional interleukin-16 up-regulation by dexamethasone and FTY720 in experimental traumatic brain injury. *Neuropathology and Applied Neurobiology,* 34, 330-339.

ZHU, M. & LI, M. 2012. Revisiting the homology modeling of G-protein coupled receptors: [small beta]1-adrenoceptor as an example. *Molecular BioSystems,* 8, 1686-1693.

ZONDAG, P., ETTEN, VERLAAN, MOOLENAAR 1998. Sphingosine 1-phosphate signalling through the G-protein-coupled receptor Edg-1. *Biochemical Journal.,* 330, 605-9.

ZUTPHEN, VEENHUIS & KLEI, V. D. 2008. Pex14 is the sole component of the peroxisomal translocon that is required for pexophagy. *Autophagy,* 4, 63-66.

Appendix 1

1. Sanna, M.G., et al., *Sphingosine 1-Phosphate (S1P) Receptor Subtypes S1P1 and S1P3, Respectively, Regulate Lymphocyte Recirculation and Heart Rate.* Journal of Biological Chemistry, 2004. **279**(14): p. 13839-13848.
2. Brinkmann, V., et al., *The immune modulator FTY720 targets sphingosine 1-phosphate receptors.* Journal of Biological Chemistry, 2002. **277**(24): p. 21453-21457.
3. Lim, H.S., et al., *Syntheses of sphingosine-1-phosphate analogues and their interaction with EDG/S1P receptors.* Bioorganic and Medicinal Chemistry Letters, 2004. **14**(10): p. 2499-2503.
4. Foss Jr, F.W., et al., *Synthesis and biological evaluation of γ-aminophosphonates as potent, subtype-selective sphingosine 1-phosphate receptor agonists and antagonists.* Bioorganic and Medicinal Chemistry, 2007. **15**(2): p. 663-677.
5. Hale, J. J., et al. *A Rational Utilization of High-Throughput Screening Affords Selective, Orally Bioavailable 1-Benzyl-3-carboxyazetidine Sphingosine-1-phosphate-1 Receptor Agonists.* Journal of Medicinal Chemistry, 2004. 47(27): p. 6662–6665.
6. Clemens, J. J., et al. *Synthesis of benzimidazole based analogues of sphingosine-1-phosphate: discovery of potent, subtype-selective S1P4 receptor agonists*. Bioroganic and Medicinal Chemistry Letters, 2004. 14(19): p. 4903-4906.
7. Gergely, P., et al., *The selective sphingosine 1-phosphate receptor modulator BAF312 redirects lymphocyte distribution and has species-specific effects on heart rate.* British Journal of Pharmacology, 2012. **167**(5): p. 1035-1047.
8. Rosen, H., et al., *Rapid induction of medullary thymocyte phenotypic maturation and egress inhibition by nanomolar sphingosine 1-phosphate receptor agonist.* Proceedings of the National Academy of Sciences, 2003. **100**(19): p. 10907-10912.
9. Gonzalez-Cabrera, P.J., et al., *Full Pharmacological Efficacy of a Novel S1P1 Agonist That Does Not Require S1P-Like Headgroup Interactions.* Molecular Pharmacology, 2008. **74**(5): p. 1308-1318.
10. Shimizu, H., et al., *KRP-203, a Novel Synthetic Immunosuppressant, Prolongs Graft Survival and Attenuates Chronic Rejection in Rat Skin and Heart Allografts.* Circulation, 2005. **111**(2): p. 222-229.
11. Pan, S., et al., *A Monoselective Sphingosine-1-Phosphate Receptor-1 Agonist Prevents Allograft Rejection in a Stringent Rat Heart Transplantation Model.* Chemistry & Biology, 2006. **13**(11): p. 1227-1234.
12. Quancard, J., et al., *A Potent and Selective S1P1 Antagonist with Efficacy in Experimental Autoimmune Encephalomyelitis.* Chem Biol, 2012. **19**(9): p. 1142-1151.
13. Sanna, M.G., et al., *Enhancement of capillary leakage and restoration of lymphocyte egress by a chiral S1P1 antagonist in vivo.* Nature Chemical Biology, 2006. **2**(8): p. 434-441.
14. Oo, M.L., et al., *Immunosuppressive and anti-angiogenic sphingosine 1-phosphate receptor-1 agonists induce ubiquitinylation and proteasomal degradation of the receptor.* Journal of Biological Chemistry, 2007. **282**(12)**:** p. 9082-9089.
15. Marsolais, D. and Rosen H., *Chemical modulators of sphingosine-1-phosphate receptors as barrier-oriented therapeutic molecules.* Nature Review Drug Discovovery, 2009. **8**(4): p. 297-307.
16. Foss Jr, F.W., et al., *Synthesis and biological evaluation of γ-aminophosphonates as potent, subtype-selective sphingosine 1-phosphate receptor agonists and antagonists.* Bioorganic and Medicinal Chemistry, 2007. **15**(2): p. 663-677.
17. Davis, M.D., et al., *Sphingosine 1-Phosphate Analogs as Receptor Antagonists.* Journal of Biological Chemistry, 2005. **280**(11): p. 9833-9841.

18. Osada, M., et al., *Enhancement of sphingosine 1-phosphate-induced migration of vascular endothelial cells and smooth muscle cells by an EDG-5 antagonist.* Biochemical and Biophysical Research Communications, 2002. **299**(3): p. 483-487.
19. Ohmori, T., et al., *Sphingosine 1-phosphate induces contraction of coronary artery smooth muscle cells via S1P2.* Cardiovascular Research, 2003. **58**(1): p. 170-177.

Appendix 2

1. Takasugi, N., et al., *BACE1 Activity Is Modulated by Cell-Associated Sphingosine-1-Phosphate.* The Journal of Neuroscience, 2011. **31**(18): p. 6850-6857.
2. He, Z., et al., *Predicting drug-target interaction networks based on functional groups and biological features.* PLoS One, 2010. **5**(3): e9603 p. 1-8.
3. Kimura, A., et al., *Antagonism of Sphingosine 1-Phosphate Receptor-2 Enhances Migration of Neural Progenitor Cells Toward an Area of Brain Infarction.* Stroke, 2008. **39**(12): p. 3411-3417.
4. Jang, S., et al., *Changes in iNOS, GFAP and NR1 Expression in Various Brain Regions and Elevation of Sphingosine-1-phosphate in Serum after Immobilized Stress.* Neurochemical Research, 2008. **33**(5): p. 842-851.
5. Coste, O., et al., *Sphingosine 1-Phosphate Modulates Spinal Nociceptive Processing.* Journal of Biological Chemistry, 2008. **283**(47): p. 32442-32451.
6. Kułakowska, A., et al., *Intrathecal increase of sphingosine 1-phosphate at early stage multiple sclerosis.* Neuroscience Letters, 2010. **477**(3): p. 149-152.
7. Doyle, T., et al., *Sphingosine-1-phosphate acting via the S1P1 receptor is a downstream signalling pathway in ceramide-induced hyperalgesia.* Neuroscience Letters, 2011. **499**(1): p. 4-8.
8. Skoura, A., et al., *Essential role of sphingosine 1–phosphate receptor 2 in pathological angiogenesis of the mouse retina.* J Clin Invest, 2007. **117**(9): p. 2506-2516.
9. Maines, L.W., et al., *Pharmacologic Manipulation of Sphingosine Kinase in Retinal Endothelial Cells: Implications for Angiogenic Ocular Diseases.* Investigative Ophthalmology & Visual Science, 2006. **47**(11): p. 5022-5031.
10. Sabbadini, R.A., *Sphingosine-1-phosphate antibodies as potential agents in the treatment of cancer and age-related macular degeneration.* British Journal of Pharmacology, 2011. **162**(6): p. 1225-1238.
11. Herr, D.R., et al., *Sphingosine 1-Phosphate (S1P) Signalling Is Required for Maintenance of Hair Cells Mainly via Activation of S1P2.* The Journal of Neuroscience, 2007. **27**(6): p. 1474-1478.
12. Ammit, A.J., et al., *Sphingosine 1-phosphate modulates human airway smooth muscle cell functions that promote inflammation and airway remodeling in asthma.* The FASEB Journal, 2001. **15**(17): p. 1212-1214.
13. Cordts, F., et al., *Expression profile of the sphingosine kinase signalling system in the lung of patients with chronic obstructive pulmonary disease.* Life Sciences, 2011. **89**(21–22): p. 806-811.
14. Olivera, A., et al., *Sphingosine kinase 1 and sphingosine-1-phosphate receptor 2 are vital to recovery from anaphylactic shock in mice.* Journal of Clinical Investigation, 2010. **120**(5): p. 1429-1440.
15. Oskeritzian, C.A., et al., *Essential roles of sphingosine-1–phosphate receptor 2 in human mast cell activation, anaphylaxis, and pulmonary edema.* The Journal of Experimental Medicine, 2010. **207**(3): p. 465-474.
16. Spiegel, S. and S. Milstien, *The outs and the ins of sphingosine-1-phosphate in immunity.* Nature Review Immunology, 2011. **11**(6): p. 403-415.
17. Keul, P., et al., *The Sphingosine-1-Phosphate Analogue FTY720 Reduces Atherosclerosis in Apolipoprotein E–Deficient Mice.* Arteriosclerosis Thrombosis and Vascular Biology, 2007. **27**(3): p. 607-613.
18. Deutschman, D.H., et al., *Predicting obstructive coronary artery disease with serum sphingosine-1-phosphate.* American Heart Journal, 2003. **146**(1): p. 62-68.
19. Daum, G., et al, *Sphingosine 1-phosphate: a regulator of arterial lesions.* Arteriosclerosis Thrombosis and Vascular Biology, 2009. **29**(10): p. 1439-43.
20. Knapp, M., et al., *Plasma sphingosine-1-phosphate concentration is reduced in patients with myocardial infarction.* Medical Science Monitor, 2009. **15**(9): p. CR490-493.

21. Sanna, M.G., et al., *Sphingosine 1-Phosphate (S1P) Receptor Subtypes S1P1 and S1P3, Respectively, Regulate Lymphocyte Recirculation and Heart Rate.* Journal of Biological Chemistry, 2004. **279**(14): p. 13839-13848.
22. Means, C.K. and Brown J. H., *Sphingosine-1-phosphate receptor signalling in the heart.* Cardiovascular Research, 2009. **82**(2): p. 193-200.
23. Ikeda, H., et al., *Plasma concentration of bioactive lipid mediator sphingosine 1-phosphate is reduced in patients with chronic hepatitis C.* Clinica Chimica Acta, 2010. **411**(9–10): p. 765-770.
24. Kegeyama, Y., et al., *Antagonism of sphingosine 1-phosphate receptor 2 causes a selective reduction of portal vein pressure in bile duct-ligated rats.* Hepatology, 2012. **56**(4): p. 1427-1428.
25. Whetzel, A.M., et al., *Sphingosine-1 Phosphate Prevents Monocyte/Endothelial Interactions in Type 1 Diabetic NOD Mice Through Activation of the S1P1 Receptor.* Circulation Research, 2006. **99**(7): p. 731-739.
26. Kozian, E., et al., *A Novel Val286Ala Polymorphism in the NPXXY Motif of the Sphingosine-1-Phosphate Receptor S1PR2 Associates with the Incidence and Age of Onset of Diabetes.* Journal of Diabetes & Metabolism, 2010. **1**(113).
27. Stanford, J.C., et al., *Sphingosine-1 phosphate (S1P) regulates glucose-stimulated insulin secretion in pancreatic beta cells.* Journal of Biological Chemistry, 2012. **287**(16): p.13457-13464.
28. Hoofnagle, A., et al., *HDL Lipids and Insulin Resistance.* Current Diabetes Reports, 2010. **10**(1): p. 78-86.
29. Sugita, K., et al., *FTY720 Regulates Bone Marrow Egress of Eosinophils and Modulates Late-Phase Skin Reaction in Mice.* The American Journal of Pathology, 2010. **177**(4): p. 1881-1887.
30. Martino, A., *Sphingosine 1-phosphate as a novel immune regulator of dendritic cells.* Journal of Biosciences, 2007. **32**: p. 1207-1212.
31. Czermak, P., et al., *Membrane-assisted production of S1P loaded SLNs for the treatment of acne vulgaris.* Desalination, 2010. **250**(3): p. 1132-1135.
32. Watson, L., et al., *Increased Serum Concentration of Sphingosine-1-phosphate in Juvenile-onset Systemic Lupus Erythematosus.* Journal of Clinical Immunology, 2012. **32**(5): p.1019-1025.
33. Bollag, W.B., *Potential role of sphingosine 1-phosphate in the pathogenesis of rheumatoid arthritis.* Journal of Lipid Research, 2008. **49**(11): p. 2281-2282.
34. Ishii, M., et al., *Sphingosine-1-phosphate mobilizes osteoclast precursors and regulates bone homeostasis.* Nature, 2009. **458**(7237): p. 524-528.
35. Kitano, M., et al., *Sphingosine 1-phosphate/sphingosine 1-phosphate receptor 1 signalling in rheumatoid synovium: Regulation of synovial proliferation and inflammatory gene expression.* Arthritis & Rheumatism, 2006. **54**(3): p. 742-753.
36. Ryu, J., et al., *Sphingosine 1-phosphate as a regulator of osteoclast differentiation and osteoclast-osteoblast coupling.* The EMBO Journal, 2006. **25**(24): p. 5840-5851.
37. Pyne, N.J. and Pyne S., *Sphingosine 1-phosphate and cancer.* Nature Review Cancer, 2010. **10**(7): p. 489-503.
38. LaMontagne, K., et al., *Antagonism of Sphingosine-1-Phosphate Receptors by FTY720 Inhibits Angiogenesis and Tumor Vascularization.* Cancer Research, 2006. **66**(1): p. 221-231.
39. Ogretmen, B. and Hannun Y. A., *Biologically active sphingolipids in cancer pathogenesis and treatment.* Nature Reviews Cancer, 2004. **4**(8): p. 604-616.
40. Xia, P., et al., *An oncogenic role of sphingosine kinase.* Current Biology, 2000. **10**(23): p. 1527-1530.
41. Visentin, B., et al., *Validation of an anti-sphingosine-1-phosphate antibody as a potential therapeutic in reducing growth, invasion, and angiogenesis in multiple tumor lineages.* Cancer Cell, 2006. **9**(3): p. 225-238.